IL
NUOVO CIMENTO
ORGANO DELLA SOCIETÀ ITALIANA DI FISICA
SOTTO GLI AUSPICI DEL CONSIGLIO NAZIONALE DELLE RICERCHE

VOL. XIII, N. 6 *Serie decima* 16 Settembre 1959

Re-Arrangement Collision Matrix.

G. MOHAN

National Physical Laboratory - New Delhi

(ricevuto il 23 Marzo 1959)

Summary. — A study of the rearrangement collision matrix, under certain asymptotic assumptions is made. It is found that although the « asymptotic states » are non-orthogonal, by a proper choice an orthogonal and complete set of physical states with prescribed asymptotic properties can be constructed. Identity of different expressions of the collision matrix is re-derived. Finally, by the help of the collision matrix the state vector itself is expressed in a form where the incoming and outgoing waves into various channels are explicitly separated without putting any configuration space restrictions.

1. – Introduction.

The theory of rearrangement collisions (1) has been developed on the basis of certain asymptotic assumptions regarding the behaviour of the state vector in the remote past and the future. The possibility of rearrangement collisions in the system requires more than one complete set of basic vectors for an adequate description of the state vector in the initial or final stage. This complicates the construction of the collision matrix because the « asymptotic states » have a non-orthogonal basis. This difficulty has been partly overcome by establishing the existence of complete and orthogonal physical states with prescribed asymptotic behaviour either in the remote past or in the remote future. In the

(1) For some of the recent developments in this subject see R. C. NEWTON: *Ann. Phys.*, **4**, 29 (1958); E. GERJOUY: *Ann. Phys.*, **5**, 58 (1958). The last mentioned contains a good list of references to earlier work.

last section of this paper we express any physical state vector in terms of the collision matrix such that the incoming and outgoing waves into the various channels are explicitly separated out. Co-ordinate representation is not used so that the separation is valid everywhere in an x-representation, if it exists ([2]). It is hoped that this more generally valid relation will further throw some light on the inherent structure of the re-arrangement collision theory irrespective of the nature of the interactions.

2. – The asymptotic states.

We study a two channel multiple particle system. The generalization to multiple channels presents no difficulty. The total Hamiltonian H can be split in two ways:

$$\begin{cases} \mathscr{H} = H_1 + I_1 \\ \mathscr{H} = H_2 + I_2 \end{cases} \tag{1}$$

such that the eigenvectors of H_1 together with those of H_2 are sufficient to describe the asymptotic behaviour of any physical state. The eigenvectors of H_1 or of H_2 alone are insufficient for this purpose although each set by itself forms a complete set of basis vectors. On the other hand not all eigenvectors of H_1 and H_2 are necessary as we shall see presently.

A physical state vector, which is always of the form $\exp[-i\mathscr{H}t]|\Omega\rangle$ is said to make a transition, for example to the channel 1 if the subsequent time development is governed by H_1 in the same manner as it is governed by the total Hamiltonian $\mathscr{H}$. This is essentially a time dependent concept and the fact that at any instant the state vector can always be expressed as a linear superposition of the eigenvectors of H_1 is no guarantee that these eigenvectors will be suitable for the complete formulation of the asymptotic condition.

A time dependent vector $|\omega; t\rangle$ represents a « state » in the channel 1, for example, if its time development is generated by the channel Hamiltonian H_1. If an expansion in the eigenvectors $|\varepsilon_1\alpha\rangle$ of H_1 is made we must have the form (*)

$$|\omega; t\rangle = \int_{\varepsilon_1\alpha} b(\varepsilon_1, \alpha) \exp[-i\varepsilon_1 t]|\varepsilon_1\alpha\rangle = \exp[-iH_1 t]|\omega; 0\rangle\,, \tag{2}$$

where the expansion coefficient b is time independent.

([2]) Compare A. M. LANE and R. G. THOMAS: *Rev. Mod. Phys.*, **30**, 257 (1958).

(*) The symbol $\int_{\varepsilon_1\alpha}$ represents summation or integration on the eigenvalues ε_1, α according as they belong to a discrete or continuous spectrum.

An arbitrary state vector $\exp[-i\mathscr{H}t]|\Omega\rangle$ can always be expressed as a linear superposition of the eigenvectors $|\varepsilon_1\alpha\rangle$ of H_1 or, $|\varepsilon_2\beta\rangle$ of H_2:

$$|\Omega; t\rangle \equiv \exp[-i\mathscr{H}t]|\Omega\rangle = \int_{\varepsilon_1\alpha} a(\varepsilon_1\alpha; t) \exp[-i\varepsilon_1 t]|\varepsilon_1\alpha\rangle\,, \tag{3}$$

where the expansion coefficient

$$a(\varepsilon_1\alpha; t) = \langle\varepsilon_1\alpha|\exp[-i(\mathscr{H}-\varepsilon_1)t]|\Omega\rangle \tag{4}$$

would in general be time dependent. If $|\Omega; t\rangle$ were to represent a state asymptotically going into the channel-1 in the remote future, then the time variation of $a(\varepsilon_1\alpha; t)$ should die down for large t. In other words, the $\lim_{t\to\infty} \langle\varepsilon_1\alpha|\exp[-i(\mathscr{H}-\varepsilon_1)t]|\Omega\rangle$ should exist and must not be identically zero.

Let $|\Omega\rangle$ be an eigenvector of H with the eigenvalue E. Assuming that there does not exist any stable bound state of the entire system, the energy eigenvalue spectrum is a continuum. Under such circumstances the above mentioned limit must yield a Dirac δ-function in energy. It is easily seen that if $\lim_{t\to\infty} \langle\varepsilon_1\alpha|\exp[-i(E-\varepsilon_1)t]|E\rangle$ exists it cannot be different from zero for $E \neq \varepsilon_1$ because of the rapid oscillations for large t. Consequently to give any significant contribution as an integrand this expansion coefficient must have a δ-function singularity at $E = \varepsilon_1$.

As mentioned before not all the eigenvectors $|\varepsilon_1\alpha\rangle$ and $|\varepsilon_2\beta\rangle$ of H_1 and H_2 respectively, are necessary for the description of asymptotic conditions. It is possible that some of the eigenvectors $|\varepsilon_1\alpha\rangle$ under time development generated by the channel Hamiltonian H_1 would behave as « scattering states » going over asymptotically to some $|\varepsilon_2\beta\rangle$. For the complete description of the asymptotic behaviour it would be superfluous to include the above mentioned vectors $|\varepsilon_1\alpha\rangle$ in a set of basis vectors which already contains the corresponding vectors $|\varepsilon_2\beta\rangle$ because the latter will always be sufficient to depict the role of the $|\varepsilon_1\alpha\rangle$ in the remote future. An adequate set of basic vectors, which are capable of constructing all possible situations in the remote future, would be obtained if we selected from the two complete sets $|\varepsilon_1\alpha\rangle$ and $|\varepsilon_2\beta\rangle$ only those members that do not make transitions, asymptotically, into the other channel. In other words we omit $|\varepsilon_1\beta\rangle_\pm$ which have the Lippmann-Schwinger ([3-6]) representation (*)

$$|\varepsilon_1\beta\rangle_\pm = |\varepsilon_2\beta\rangle + \frac{1}{\varepsilon_1 - H_2 \pm i\eta}(H_1 - H_2)|\varepsilon_1\beta\rangle_\pm\,, \tag{5a}$$

([3]) B. A. Lippmann and J. Schwinger: *Phys. Rev.*, **79**, 469 (1950).

([4]) B. A. Lippmann: *Phys. Rev.*, **102**, 264 (1956).

([5]) L. L. Foldy and W. Tobocman: *Phys. Rev.*, **105**, 1099 (1957).

([6]) S. T. Epstein: *Phys. Rev.*, **106**, 598 (1957).

(*) A vector denoted by the form $|\rangle_-$ or $|\rangle_+$ will always be regarded η-dependent. See references ([5]) and ([6]).

and, similarly, omit $|\varepsilon_2\alpha\rangle_\pm$ which have the representation

$$|\varepsilon_2\alpha\rangle_\pm = |\varepsilon_1\alpha\rangle + \frac{1}{\varepsilon_2 - H_1 \pm i\eta}(H_2 - H_1)|\varepsilon_2\alpha\rangle_\pm . \tag{5b}$$

Henceforth $|\varepsilon_1\alpha\rangle$ and $|\varepsilon_2\beta\rangle$ will denote only those members that are left after the above mentioned omission. Since the reduced mixed set $\{|\varepsilon_1\alpha\rangle, |\varepsilon_2\beta\rangle\}$ is capable of describing all possible asymptotic situations it must be a complete set although not an orthogonal set.

There is an alternative way of arriving at this mixed set without making an explicit reference to the Lippmann-Schwinger representation. We have seen before that if an arbitrary state vector $\exp[-E_1t]|E_1\alpha\rangle$ has a non-vanishing probability of going over asymptotically to the state

$$\exp[-iE_2t]|E_2\beta\rangle \quad \text{then} \quad \lim_{t\to\infty} \exp[-i(E_1 - E_2)t]\langle E_2\beta|E_1\alpha\rangle$$

must have a δ-function singularity at $E_2 = E_1$. Our criterion for the selection of the mixed complete set would admit only one state of such pair of states, the other being superfluous. Consequently, all the vectors $|\varepsilon_1\alpha\rangle$ and $|\varepsilon_2\beta\rangle$ admitted into the set would satisfy

$$\lim_{t\to\pm\infty} \exp[-i(\varepsilon_1 - \varepsilon_2)t]\langle\varepsilon_2\beta|\varepsilon_1\alpha\rangle = 0 . \tag{6}$$

This is a more convenient criterion to distinguish the members of the mixed, complete set; and on physical grounds the largest set of members from the original two complete sets that satisfy the above equation should form another complete set. We see that the eq. (6) gives an asymptotically orthogonal basis.

3. – Asymptotic condition.

Another set of basis vectors which are eigenvectors of the total Hamiltonian $\mathscr{H}$ are introduced through the following asymptotic assumption. Corresponding to every $|\varepsilon_1\alpha\rangle$ we have an eigenvector (*) $|E\alpha\rangle_+$ of $\mathscr{H}$ such that in the remote past the state $\exp[-iEt]|E\alpha\rangle_+$ is asymptotically the pure channel-1 state $|\varepsilon_1\alpha\rangle$,

$$\lim_{t\to-\infty} \exp[-i(E - \varepsilon_1')t]\langle\varepsilon_1'\alpha'|E\alpha\rangle_+ = \langle\varepsilon_1'\alpha'|\varepsilon_1\alpha\rangle . \tag{7}$$

(*) Unlike $|\varepsilon_1\alpha\rangle$ the state vector $|E\alpha\rangle_+$ does not represent an eigenvector of certain observables whose eigenvalues are α. In this case α is just a label. In the following we shall always adopt the notation numerically, $\varepsilon_1 = \varepsilon_2 = E$, $\varepsilon_1' = \varepsilon_2' = E'$ and generally $E \neq E'$.

Similarly there are states $\exp[-iEt]|E\beta\rangle_+$ which are, in the remote past, asymptotically the pure channel-2 states $|\varepsilon_2\beta\rangle$,

$$\lim_{t\to-\infty} \exp[-i(E-\varepsilon_2')t]\langle\varepsilon_2'\beta'|E\beta\rangle_+ = \langle\varepsilon_2'\beta'|\varepsilon_2\beta\rangle\,. \tag{8}$$

The totality of $|E\alpha\rangle_+$ and $|E\beta\rangle_+$ must be complete in view of the postulate that $\{|\varepsilon_1\alpha\rangle, |\varepsilon_2\beta\rangle\}$ is complete. They are also effectively orthogonal

$$\begin{aligned} {}_+\langle E'\alpha'|E\beta\rangle_+ &= \left\{\langle\varepsilon_1'\alpha'| + \langle\varepsilon_1'\alpha'|I_1\frac{1}{E'-\mathscr{H}-i\eta}\right\}|E\beta\rangle_+ = \\ &= \langle\varepsilon_1'\alpha'|\left\{|E\beta\rangle_+ - \frac{1}{E-H_1+i\eta}I_1|E\beta\rangle_+\right\} = \frac{i\eta}{E-E'+i\eta}\langle\varepsilon_1'\alpha'|\varepsilon_2\beta\rangle\,, \end{aligned}$$

where we have used the LIPPMANN (4) relation

$$|E\beta\rangle_+ = \frac{i\eta}{E-H_1+i\eta}|\varepsilon_2\beta\rangle + \frac{1}{E-H_1+i\eta}I_1|E\beta\rangle_+\,.$$

So that ${}_+\langle E'\alpha'|E\beta\rangle_+$ is zero everywhere except possibly at $E'=E$ and at this point it is equal to $\langle\varepsilon_1'\alpha'|\varepsilon_2\beta\rangle$ which must be finite and bounded due to equation (6). Since E belongs to a continuous spectrum there cannot be any contribution to an integral from such an isolated point and hence, effectively ${}_+\langle E'\alpha'|E\beta\rangle_+ = 0$.

In a similar manner the state vectors $|E\alpha\rangle_-$ and $|E\beta\rangle_-$ are introduced through the asymptotic condition in the remote future.

4. – The collision matrix.

The collision matrix element between any two basic vectors, say $|\varepsilon_1\alpha\rangle$ and $|\varepsilon_2'\beta\rangle$ gives the probability amplitude of a state asymptotically decaying into the channel-2 state $|\varepsilon_2'\beta\rangle$ when, in the remote past it was asymptotically the channel-1 state $|\varepsilon_1\alpha\rangle$. That is,

$$\begin{cases} \langle\varepsilon_2'\beta|S|\varepsilon_1\alpha\rangle = \lim\limits_{t\to\infty}\exp[-i(E-\varepsilon_2')t]\langle\varepsilon_2'\beta|E\alpha\rangle_+\,, \\ \langle\varepsilon_2'\beta'|S|\varepsilon_2\beta\rangle = \lim\limits_{t\to\infty}\exp[-i(E-E')t]\langle\varepsilon_2'\beta'|E\beta\rangle_+\,. \end{cases} \tag{9}$$

Henceforth we work with the Lippmann-Schwinger representation of the scattering states $|E\alpha\rangle_\pm$ and $|E\beta\rangle_\pm$ so that the asymptotic conditions (7) and (8)

are automatically satisfied,

$$(10)\qquad \begin{cases} |E\alpha\rangle_{\pm} = |\varepsilon_1\alpha\rangle + \dfrac{1}{E - H_1 \pm i\eta} I_1 |E\alpha\rangle_{\pm}\,, \\ |E\beta\rangle_{\pm} = |\varepsilon_2\beta\rangle + \dfrac{1}{E - H_2 \pm i\eta} I_2 |E\beta\rangle_{\pm}\,. \end{cases}$$

By algebraic manipulation we obtain, alternatively

$$(11)\qquad \begin{cases} |E\alpha\rangle_{\pm} = |\varepsilon_1\alpha\rangle + \dfrac{1}{E - \mathscr{H} \pm i\eta} I_1 |\varepsilon_1\alpha\rangle\,, \\ |E\beta\rangle_{\pm} = |\varepsilon_2\beta\rangle + \dfrac{1}{E - \mathscr{H} \pm i\eta} I_2 |\varepsilon_2\beta\rangle\,. \end{cases}$$

As a consequence of the equations (10) and (11) we immediately obtain

$$(12)\qquad \begin{cases} {}_{+}\langle E'\alpha' | E\alpha\rangle_{+} = \left\{\langle \varepsilon_1'\alpha' | + \langle \varepsilon_1'\alpha' | I_1 \dfrac{1}{E' - \mathscr{H} - i\eta}\right\} |E\alpha\rangle_{+}\,, \\ \qquad\qquad = \langle \varepsilon_1'\alpha' | \left\{ |E\alpha\rangle_{+} - \dfrac{1}{E - H_1 + i\eta} I_1 |E\alpha\rangle_{+}\right\} \\ \qquad\qquad = \langle \varepsilon_1'\alpha' | \varepsilon_1\alpha\rangle\,. \end{cases}$$

Similarly

$$(13)\qquad {}_{+}\langle E'\beta' | E\beta\rangle_{+} = \langle \varepsilon_2'\beta' | \varepsilon_2\beta\rangle\,.$$

The collision matrix elements can alternatively be expressed in terms of the eigenvectors of $\mathscr{H}$ only. Keeping in view the Lippmann-Schwinger equation for $|E\beta\rangle_{-}$ we obtain

$$\lim_{t\to\infty} \exp[-i(E - E')t]\{\langle \varepsilon_2'\beta | E\alpha\rangle_{+} - {}_{-}\langle E'\beta | E\alpha\rangle_{+}\} = \\ = \lim_{t\to\infty} \exp[-i(E - E')t]\langle \varepsilon_2'\beta | I_2 \frac{1}{E' - \mathscr{H} + i\eta} |E\alpha\rangle_{+} = 0\,,$$

therefore

$$(14)\qquad \langle \varepsilon_2'\beta | S | \varepsilon_1\alpha\rangle = {}_{-}\langle E'\beta | E\alpha\rangle_{+}\,.$$

Similar relations exist when initial and final states belong to the same channel. These relations together with the orthogonality and completeness of $\{|E\alpha\rangle_{\pm}, |E\beta\rangle_{\pm}\}$ establish the « unitarity » of the S-matrix in a certain sense.

If the state vector $|E'\beta\rangle_{-}$ is expressed in terms of $|\varepsilon_2'\beta\rangle$ through the equation (11) one finds that

$$(15)\qquad |E'\beta\rangle_{-} - |E'\beta\rangle_{+} = 2\pi i\, \delta(E' - \mathscr{H}) I_2 |\varepsilon_2'\beta\rangle\,.$$

This relation enables us to bring out the channel interactions in a convenient form. We have

$$(16)\qquad {}_-\langle E'\beta\,|\,E\alpha\rangle_+ = {}_+\langle E'\beta\,|\,E\alpha\rangle_+ - 2\pi i\,\delta(E'-E)\langle\varepsilon_2'\beta\,|\,I_2\,|\,E\alpha\rangle_+ =$$

$$= \frac{i\eta}{E-E'+i\eta}\langle\varepsilon_2'\beta\,|\,\varepsilon_1\alpha\rangle - 2\pi i\,\delta(E'-E)\langle\varepsilon_2'\beta\,|\,I_2\,|\,E\alpha\rangle_+$$

or, alternatively

$$(17)\qquad {}_-\langle E'\beta\,|\,E\alpha\rangle_+ = {}_-\langle E'\beta\,|\,E\alpha\rangle_- - 2\pi i\,\delta(E'-E)\,{}_-\langle E'\beta\,|\,I_1\,|\,\varepsilon_1\alpha\rangle =$$

$$= \frac{-i\eta}{E-E'-i\eta}\,\langle\varepsilon_2'\beta\,|\,\varepsilon_1\alpha\rangle - 2\pi i\,\delta(E'-E)\,{}_-\langle E'\beta\,|\,I_1\,|\,\varepsilon_1\alpha\rangle\,,$$

and for collisions within a channel

$$(18)\qquad {}_-\langle E'\beta'\,|\,E\beta\rangle_+ = \langle\varepsilon_2'\beta'\,|\,\varepsilon_2\beta\rangle - 2\pi i\,\delta(E'-E)\langle\varepsilon_2'\beta'\,|\,I_2\,|\,E\beta\rangle_+$$

$$= \langle\varepsilon_2'\beta'\,|\,\varepsilon_2\beta\rangle - 2\pi i\,\delta(E'-E)\,{}_-\langle E'\beta'\,|\,I_2\,|\,\varepsilon_2\beta\rangle\,.$$

5. – State vector and the collision matrix.

Next we desire to express a state vector with specified channel for the incoming wave, for example $|E\alpha\rangle_-$, in a manner that explicitly separates out the outgoing waves in different channels. From the Lippmann-Schwinger equation for $|E\alpha\rangle_-$ and equation (14), we obtain

$$(19)\qquad \langle\varepsilon_2'\beta\,|\,E\alpha\rangle_- - \langle\varepsilon_2'\beta\,|\,S^*\,|\,\varepsilon_1\alpha\rangle = \{\langle\varepsilon_2'\beta\,| - {}_+\langle E'\beta\,|\}\,|\,E\alpha\rangle_- =$$

$$= \langle\varepsilon_2'\beta\,|\,\frac{1}{E-H_2+i\eta}\,I_2\,|\,E\alpha\rangle_-$$

and

$$(20)\qquad \langle\varepsilon_1'\alpha'\,|\,E\alpha\rangle_- - \langle\varepsilon_1'\alpha'\,|\,S^*\,|\,\varepsilon_1\alpha\rangle = \langle\varepsilon_1'\alpha'\,|\,\frac{1}{E-H_1+i\eta}\,I_1\,|\,E\alpha\rangle_-\,.$$

Since $|\varepsilon_2'\beta\rangle$ and $|\varepsilon_1'\alpha'\rangle$ form a complete set, from equations (19) and (20) we obtain

$$(21)\qquad |E\alpha\rangle_- - S^*\,|\,\varepsilon_1\alpha\rangle = \left\{P_1\,\frac{1}{E-H_1+i\eta}\,I_1 + P_2\,\frac{1}{E-H_2+i\eta}\,I_2\right\}|\,E\alpha\rangle_-,$$

where P_1 and P_2 are the projection operators on the channels 1 and 2 respectively. Formal expressions for P_1 and P_2 can be obtained. A metric operator g

in the non-orthogonal basis is defined by the relations

$$\langle \varepsilon_1 \alpha | g | \varepsilon_1' \alpha' \rangle = \langle \varepsilon_1 \alpha | \varepsilon_1' \alpha' \rangle ,$$
$$\langle \varepsilon_1 \beta | g | \varepsilon_2' \beta' \rangle = \langle \varepsilon_2 \beta | \varepsilon_2' \beta' \rangle ,$$
$$\langle \varepsilon_1 \alpha | g | \varepsilon_2' \beta \rangle = \langle \varepsilon_2' \beta | g | \varepsilon_1 \alpha \rangle = 0 .$$

One can then verify that

$$P_1 = g \int_{\varepsilon_1 \alpha} | \varepsilon_1 \alpha \rangle \langle \varepsilon_1 \alpha | ,$$

$$P_2 = g \int_{\varepsilon_2 \beta} | \varepsilon_2 \beta \rangle \langle \varepsilon_2 \beta | .$$

However, in practice, the experimental detection devices unambiguously separate the different channels and hence one can ascertain beforehand which of the two terms on the right hand side of eq. (21) is relevant.

If we express $|\varepsilon_1 \alpha\rangle$ in terms of $|E\alpha\rangle_-$ in the eq. (21) we obtain

$$(22) \qquad (S^* - 1) | E\alpha \rangle_- = S^* \frac{1}{E - H_1 - i\eta} I_1 | E\alpha \rangle_- -$$
$$- P_1 \frac{1}{E - H_1 + i\eta} I_1 | E\alpha \rangle_- - P_2 \frac{1}{E - H_2 + i\eta} I_2 | E\alpha \rangle_- .$$

On the right hand side of this equation the incoming and the outgoing waves into different channels are explicitly separated out. One can avoid the projection operators P_1 and P_2 and put the above relation in the form

$$(23) \qquad (1 - Sh) | E\alpha \rangle_- =$$
$$= \frac{1}{E - H_1 - i\eta} I_1 | E\alpha \rangle_- - S \int_{\varepsilon_1' \alpha'} \frac{| \varepsilon_1' \alpha' \rangle \langle \varepsilon_1' \alpha' | I_1 | E\alpha \rangle_-}{E - E' + i\eta} - S \int_{\varepsilon_2' \beta'} \frac{| \varepsilon_2' \beta' \rangle \langle \varepsilon_2' \beta' | I_2 | E\alpha \rangle_-}{E - E' + i\eta} ,$$

where we have used the relation

$$ShS^* = 1 = P_1 + P_2 ,$$

where

$$h = \int_{\varepsilon_1 \alpha} | \varepsilon_1 \alpha \rangle \langle \varepsilon_1 \alpha | + \int_{\varepsilon_2 \beta} | \varepsilon_2 \beta \rangle \langle \varepsilon_2 \beta | .$$

Equations (22) and (23) are our main result. A separation into the various outgoing channels, corresponding to a given incoming wave, is effected without the help of an x-representation. This is important because in relativistic theory an x-representation of an interacting state is not known. Further, the validity of the relation is not restricted to regions far-off from the scattering centre. The only restrictions on the interactions I_1 and I_2 are those that are at the very basis of the concept of the S-matrix so that they can indeed be of quite a general character.

* * *

The author wishes to thank Dr. K. S. KRISHNAN, Director, National Physical Laboratory of India, for permission to publish the present work.

RIASSUNTO (*)

Si studia la matrice di collisione di riordinamento, in determinate condizioni asintotiche. Si trova che, benchè gli « stati asintotici » non siano ortogonali, con una scelta appropriata si può costruire un sistema completo di stati fisici con proprietà asintotiche assegnate. Si rideriva l'identità di differenti espressioni della matrice di collisione. Infine, con l'ausilio della matrice di collisione, il vettore di stato si esprime in una forma in cui le onde entranti e uscenti da vari canali sono separate esplicitamente senza porre alcuna restrizione allo spazio delle configurazioni.

(*) *Traduzione a cura della Redazione.*

IL NUOVO CIMENTO Vol. XIII, N. 6 16 Settembre 1959

The Production of Cosmic Radiation by a Solar Flare on August 31, 1956 (*).

K. G. McCracken (**)

Physics Department, University of Tasmania - Hobart

(ricevuto il 15 Aprile 1959)

Summary. — It is shown that the neutron counting rates observed by three widely separated recorders increased by approximately two percent about half an hour after the observation of an intense solar flare at 1226 U.T. on August 31, 1956. The event, as observed at all three stations, exhibited the abrupt onset, and gradual recovery typical of solar flare effects. The time delay between the first visual sighting of the flare, and the earliest arrival of cosmic radiation at the earth was about 20 min. It is shown that the quantity of cosmic radiation which arrived at the earth was two to three orders of magnitude less than the quantities which arrived during earlier flare effects. Consideration of the temporal dependence of the small flare effect suggests that only a small quantity of cosmic radiation was produced in the solar flare.

1. – Introduction.

Over a period of twenty years, five large, transient increases in the cosmic ray intensity have been observed. Four of these commenced soon after the observation of an intense solar flare ([1,2]). Although a flare was not observed optically at the time of the increase on March 7, 1942, the simultaneous occur-

(*) This work was carried out during tenure of an Australian Atomic Energy Commission studentship, and later, a General Motors Holden Research Fellowship.

(**) Now at Physics Department, Massachusetts Institute of Technology, Cambridge, Mass.

(1) H. Elliot: *Progress in Cosmic Ray Physics* (Amsterdam, 1952), p. 502.

(2) P. Meyer, E. N. Parker and J. A. Simpson: *Phys. Rev.*, **104**, 768 (1956).

rence of ionospheric and magnetic disturbances of the types produced by intense solar flares leaves little doubt that the cosmic ray effect was associated with a large flare on the visible solar hemisphere. The only active centre on the sun at the time was a great sunspot on the west limb, and it seems probable that the flare occurred over this centre. Thus it appears that the five increases were all due to cosmic radiation produced in intense solar flares on the visible solar hemisphere.

Intense solar flares occur fairly frequently, for example, 21 class 3 and 29 class 3+ flares were observed between 1940 and 1948 [3]. Some evidence based on a superimposed epoch analysis has been presented that the majority of intense flares produce some cosmic radiation [4]. This evidence is not universally accepted, some authors holding that the cosmic ray flare effect is an « all or none » process [5,6]. That is, it is suggested that there is a threshold in either the process of generation or process of propagation to the earth, and that there is therefore a minimum quantity of radiation which can gain access to the earth. Clearly, if there is such a threshold, a knowledge of the minimum quantity of cosmic radiation which can reach the earth is highly desirable.

In the present paper, one case in which a flare produced a small quantity of cosmic radiation is reported. The observations indicate that, if there is in fact a threshold, it is much smaller than has been thought previously.

2. – Observations.

The neutron data obtained at Mt. Wellington (Geomagnetic latitude $(\lambda) = 52°$ S, altitude 725 m), near Hobart, on August 31, 1956, are plotted in Fig. 1. The data have been corrected for pressure change. It can be seen that the counting rate suddenly increased at about 1300 U.T., the mean for the hour 1300 to 1400 U.T. being five standard deviations greater than the mean for the previous twelve hours. After 1400 U.T. the counting rate gradually returned to a value below the pre-event level.

The neutron data from Mt. Washington, New Hampshire ($\lambda = 55°$ N, altitude 1900 m) and Climax, Colorado ($\lambda = 49°$ N, altitude 3350 m), kindly supplied by Professors J. A. Lockwood and J. A. Simpson, respectively, are also displayed in Fig. 1. It should be noted that the hourly means for Mt. Washington are centred about the U.T. hour, while those for the other two obser-

---

(3) K. O. Kiepenheuer: *The Sun* (Chicago, 1953), p. 377.
(4) J. Firor: *Phys. Rev.*, **94**, 107 (1954).
(5) T. Gold: *Observatory*, **76**, 47 (1956).
(6) E. N. Parker: *Phys. Rev.*, **107**, 830 (1957).

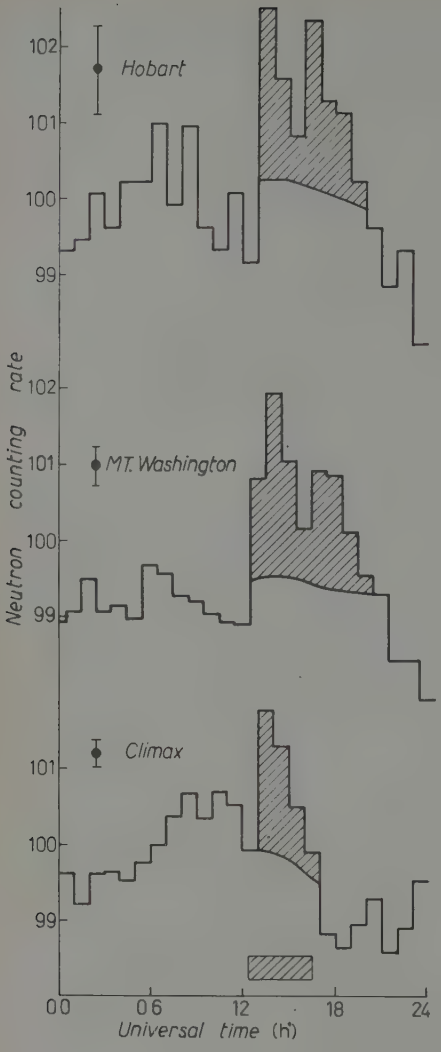

Fig. 1. – The hourly mean, pressure corrected neutron counting rates observed at Hobart, Mt. Washington and Climax on August 31, 1956. Standard deviations are shown. The period during which the solar flare was visible is indicated by the crosshatched rectangle at the bottom of the diagram.

vatories are centred about the U.T. half hour. It is clear that both Mt. Washington and Climax observed events similar to that observed at Hobart, and that the events started at the three observatories at roughly the same time. The observations clearly indicate that there was a sudden, world wide increase in the intensity of the primary cosmic radiation. The events at all three observatories exhibit the rapid increase, and subsequent gradual falling off of intensity characteristic of solar flare effects.

A solar flare of importance 3 was observed to commence at 1226 U.T., the heliographic co-ordinates being about 15° N, 15° E (7). The duration of the flare is indicated in Fig. 1. The maximum intensity of H_α was observed at 1245 U.T., and the maximum line width was 8.1 Å. It is suggested that the increase in cosmic ray intensity was due to the generation of cosmic radiation in this flare.

In Fig. 2 are displayed the positions of the theoretical impact zones at 1300 U.T. Source extensions of 30° in latitude and longitude have been assumed. It can be seen that Mt. Washington was in the 0900 impact zone, while both Hobart and Climax were in the background zones.

The quarter hourly data from Mt. Washington plotted in Fig. 3 show that the event commenced at that observatory between 1243 and 1258 U.T. The fact that the mean counting rates at the other two observatories during the

(7) Intern. Astronomical Union: *Quarterly Bulletin on Solar Activity*, no. 115 (Zurich).

hour 1200 to 1300 U.T. were not abnormal suggests that, at these observatories, the event may have commenced later than at Mt. Washington. This behaviour is consistent with those noticed during the November 19, 1949 and February 23, 1956 events, during which the intensity increased at stations in the impact zones some 10 to 15 minutes earlier than at stations in the background zones ([8]).

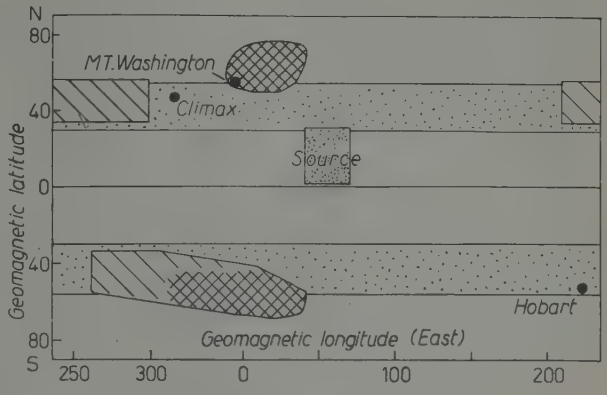

Fig. 2. – The theoretical impact zones at 13 00 U.T. on August 31, 1956. The source dimensions assumed in the preparation of the diagram are shown. The dense crosshatching, the sparse crosshatching, and the sparse dots indicate the 9 00 a.m., 4 00 a.m, and background zones respectively.

From Fig. 3, the fact that the mean intensity for the period 1243 to 1258 U.T. was comparable with that for the subsequent quarter hour suggests that, at Mt. Washington, the intensity enhancement occurred soon after 1243 U.T. Consequently the time delay between the first visual observation of the flare, and the earliest arrival of cosmic radiation was approximately 20 minutes. This is comparable with the 10 minutes and 16 minutes delays observed on

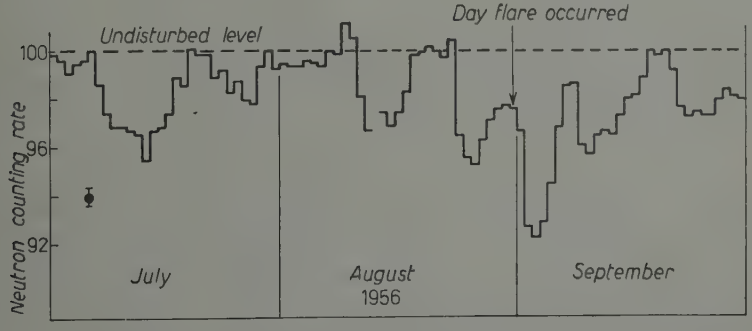

Fig. 3. – The quarter hourly, pressure corrected counting rates observed at Mt. Washington on August 31, 1956. The standard deviation of the data is shown. The 15 min recording periods commenced 2 min before each U.T. quarter hour.

([8]) R. Lüst and J. A. Simpson: *Phys. Rev.*, **108**, 1563 (1957).

the occasions of the February 23, 1956 and November 19, 1949 events, respectively. Furthermore, Fig. 3 indicates that maximum intensity was attained in less than 15 minutes. The earlier events exhibited similar rise times.

Diurnal variations, and the fluctuations occurring during Forbush-type decreases, are about 2.5 times greater in the neutron component than in the meson component. If the August 31, 1956 event were in reality either type of event, an increment of about 0.8% would be expected to be present in the concurrent meson data. Large meson telescopes, for which the standard deviations of the hourly mean counting rates were 0.3%, were operating at Hobart and Mawson, Antarctica, at the time. There is no indication that the meson counting rate increased at either station. This absence of an accompanying effect in the meson component is consistent with the hypothesis that the event in the neutron component was a small solar flare effect, for during other flare effects, the percentage change in the neutron component has been between 50 and 150 times that in the meson component.

Summarizing, the following facts support the view that the event was a small solar flare effect.

1) The event exhibited an abrupt onset, and a gradual recovery to the pre-event level.

2) The event occurred approximately simultaneously at the widely separated longitudes of Australia and the United States of America.

3) The event commenced soon after the observation of a large solar flare.

4) The time delay of about 20 minutes between the first visual sighting of the flare, and the earliest arrival of cosmic radiation, is typical of flare effects.

5) The effect was not observed by high counting rate meson telescopes.

In Fig. 4 are plotted the pressure corrected daily mean neutron intensities observed at Hobart during the period July 1–September 30, 1956. The counting rate appears to have had an « undisturbed » value, below which it was depressed on a number of occasions. A Forbush-type

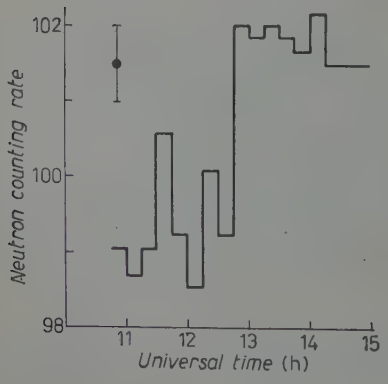

Fig. 4. -- The daily mean, pressure corrected neutron counting rates observed at Hobart prior and subsequent to the small solar flare effect. The standard deviation of the data is shown.

decrease occurred on August 24, and the counting rate was still depressed below the undisturbed value by 2.5 percent when the flare occurred. Thus there was a mechanism reducing the intensity at the earth at the time of the flare, and the solar cosmic radiation must have been affected, to some extent, by this mechanism. In a similar manner, the intensity was depressed prior to the cosmic ray flare effects occurring on February 23, 1956 and March 7, 1942.

3. – Discussion.

Using data from background zone stations at about 50° geomagnetic latitude ([1,2]), and estimating the neutron intensity changes from observed meson changes by multiplication by 100, the neutron intensity changes during all reported flares are listed in Table I. It is clear that the flare of August 31, 1956 was two to three orders of magnitude less effective in the production of an increase in the cosmic ray intensity at the earth than were the earlier events.

TABLE I. – *A summary of the amplitudes of the six observed cosmic ray increases.* The neutron intensity increase was that observed at a background zone station ($\lambda \approx 50°$), or has been estimated from the observed increase in meson intensity at a similarly situated station. The estimates are indicated with asterisks.

Date	Neutron intensity increase
February 28, 1942	100% *
March 7, 1942	1000% *
July 25, 1946	1200% *
November 19, 1949	600%
February 23, 1956	2500%
August 31, 1956	2%

It would therefore seem that either, 1) small quantities of cosmic radiation can be produced in solar flares, and can penetrate to the vicinity of the earth, or 2) on some occasions, while a large quantity of cosmic radiation is produced in a flare, the physical conditions between the sun and the earth are such that only a small quantity can reach the earth.

Consider possibility 2). On August 31, 1956, the rise to maximum intensity was rapid (< 15 minutes), and the time delay between the first visual sighting of the flare and the earliest arrival of cosmic radiation at the earth was comparable with those observed during earlier events. Thus it would appear that on August 31, the physical conditions affecting the cosmic rays

during their passage from the sun to the earth were not appreciably different from those pertaining during earlier flare effects and that possibility 2) can therefore be excluded. Any screening mechanism consisting of a dense, heliocentric diffusing barrier (9), while capable of explaining a reduction in event amplitude, can certainly be excluded, as it would appreciably alter the time scale of the onset of the event at the earth.

The data presented here are believed to be of considerable significance as they show that small flare effects do occur. Further, they show that, if there is a minimum amplitude for such effects, it is not much greater than the threshold of identification applicable to a large neutron monitor. Clearly, even a large meson detector would fail to detect such events.

Any complete theory of the cosmic ray flare effect must explain why only relatively few flares produce a detectable increase in the terrestrial cosmic ray intensity. If a theory satisfies this requirement by predicting that there is a minimum quantity of cosmic radiation which may escape from the sun, then the August 31, 1956 flare will enable a quantitative test of the theory to be made.

* * *

I wish to express my gratitude to Professor J. A. Lockwood and Professor J. A. Simpson, for making the data from their observatories available to me. My thanks also go to Dr. A. G. Fenton for guidance during the course of this investigation.

(9) Y. Sekido and K. Murakami: *Proc. of the Intern. Conference on Cosmic Rays*, Guancajuato, Mexico.

RIASSUNTO (*)

Si dimostra che i conteggi dei neutroni osservati in tre registratori molti distanti fra di loro aumentarono di circa il 2% circa mezz'ora dopo l'osservazione di un intenso brillamento solare alle 12 26 T.U. il 31 Agosto 1956. L'evento osservato nelle tre stazioni ebbe l'inizio brusco e la graduale estinzione tipici degli effetti di brillamento solare. Il ritardo tra il primo avvistamento visuale del brillamento e del primo arrivo della radiazione cosmica alla terra fu di circa 20 min. Si fa notare che la quantità di radiazione cosmica arrivata sulla terra fu di due a tre ordini di grandezza inferiore alle quantità arrivate durante precedenti effetti di brillamento solare. La considerazione della dipendenza temporale del debole effetto di brillamento suggerisce che solo una piccola quantità di radiazione cosmica fu prodotta nel brillamento solare.

(*) *Traduzione a cura della Redazione.*

IL NUOVO CIMENTO Vol. XIII, N. 6 16 Settembre 1959

A Correlation between the Emission of White Light and Cosmic Radiation by a Solar Flare (*).

K. G. McCracken (**)

Physics Department, University of Tasmania - Hobart

(ricevuto il 15 Aprile 1959)

Summary. — It is pointed out that the majority of the solar flares which were observed to produce increases in the terrestrial cosmic ray intensity were also observed in white light. This is interpreted as evidence that it is only the most energetic flares which produce any appreciable quantity of cosmic radiation, and that the rarity of the cosmic ray flare effect is, at least in part, due to the rarity of very energetic solar flares. Evidence is presented that suggest that cosmic radiation produced in a flare on the east limb of the sun is unable to reach the earth.

1. – Observations.

A solar flare is observed as a sudden brightening of the light emitted by a portion of the facular region in the immediate vicinity of a sunspot. For all but the largest flares, the enhanced emission is only appreciable at discrete frequencies such as H_α, H_β, etc. Other phenomena characteristic of large flares are 1) marked broadening of spectral lines, 2) emission of electromagnetic radiation at ultra-violet and radio frequencies, and 3) geophysical phenomena (ionospheric and geomagnetic) attributed to the burst of ultra-violet radiation from the flare. All these phenomena are typical of large 3 or 3+ flares, and do not immediately provide an insight into the reason why relatively very few flares result in an increase in the terrestrial cosmic ray intensity.

Apart from the production of cosmic radiation, there is another phenomenon which sets a few large flares apart from the majority of large flares,

(*) This work was carried out during tenure of a General Motors Holden research fellowship.

(**) Now at Physics Department, Massachusetts Institute of Technology, Cambridge, Mass.

namely, the emission during the flash phase of a continuous visible spectrum of sufficient intensity to be observable against the photospheric background. Such flares will be called « white light » flares. It is conceivable that all large flares emit a continuous spectrum, but that it is only on rare occasions that it is of sufficient intensity to be observed.

Table I lists the cosmic ray and white light producing flares which have occurred during the past 20 years. It will be noticed that the July, 1946;

TABLE I. – *The cosmic ray and white light producing flares which have occurred during the past 20 years.*

The estimated increases in neutron intensity for background zone stations are given ([a]).

Date	Cosmic ray effect (increase in neutron intensity)	White light effect
Feb. 28, 1942	100%	no
Mar. 7, 1942	1000%	Flare not observed
Mar. 5, 1946	nil	yes ([b])
July 25, 1946	1200%	yes ([c])
Nov. 19, 1949	600%	yes ([d])
Feb. 23, 1956	2500%	yes ([e])
Aug. 31, 1956 ([a])	2%	no (*)
Mar. 23, 1958	nil	yes ([f])

([a]) K. G. McCRACKEN: preceding paper.
([b]) M. D'AZAMBUJA: *L'Astronomie*, **61**, 114 (1947).
([c]) M. A. ELLISON: *Mon. Not. Roy. Astr. Soc.*, **103**, 500 (1946).
([d]) M. A. ELLISON and M. CONWAY: *Observatory*, **70**, 77 (1950).
([e]) M. NOTUCKI, T. HATAWAKA and W. UNNO: *Publ. Astr. Soc. Japan*, **8**, 52 (1956).
([f]) M. WALDMEIER: *Zeits. f. Astrophys.*, **46**, 92 (1958). I am indebted to Prof. M. A. ELLISON for bringing this observation to my notice (*).

November, 1949 and February, 1956 flares, all of which produced great cosmic ray increases, were visible in white light. On the other hand, the February 1942 and August 1956 flares, resulting in the two smallest cosmic ray increases, were not observed in white light (*), although the flares were very bright at discrete frequencies.

(*) *Note added in proof.* - Until recently, I had not seen the paper by M. WALDMEIER myself. Gaining access to a copy recently, I notice that he reports that the flare on August 31, 1956 was also visible in white light. Thus, of the five flares which were observed at the time of cosmic ray flare effects, four were « white light » flares. This new information might possibly prevent us from stating that, for those flares producing cosmic rays, the energy invested in the cosmic radiation is a monotonic increasing function of total flare energy. However, the statement that it is only the most energetic flares which produce cosmic radiation still remains valid, and the correspondence between the « white light » and « cosmic ray producing » classes of flares is strengthened.

No cosmic ray increases were reported at the times at which two of the white light flares occurred. In the case of the March, 1946 event, only a few meson detectors were in operation, and it is conceivable that an intensity increase may have escaped detection. However, in the case of the March, 1958 event it is quite certain that no appreciable quantity of cosmic radiation reached the earth, as there have been no reports that any of the extensive network of neutron monitors established during the International Geophysical Year recorded a solar flare effect. It is perhaps significant that the flare occurred on the eastern limb of the sun, and this will be discussed in more detail later.

2. – Discussion.

Assuming that all flares are produced by a single type of mechanism, it is reasonable to conjecture that the total energy released in a solar flare is a monotonic increasing function of the energy released in the visible radiation. The energy released in each of the July 1946, November 1949 and the February 1956 flares was great enough to produce considerable white light emission, and at the same time, large quantities of cosmic radiation were emitted. The flares of February 1942 and August 1956, while still very energetic, were not sufficiently energetic to produce noticeable white light emission, and they produced only relatively small quantities of cosmic radiation. Thus on those occasions when a cosmic ray effect was observed, the quantity of cosmic radiation produced, and consequently the energy invested in the cosmic radiation, was apparently a roughly monotonic increasing function of the total energy dissipated in the flare. This fact suggests that the rarity of the solar flare effect is, at least in part, due to the rarity of very energetic flares.

Considering the white light flare of March 23, 1958, it is suggested that the fact that the flare occurred on the eastern limb of the sun is of some significance. For, if the evidence is accepted that white light flares produce copious quantities of cosmic radiation, it would appear that there must have been a mechanism acting which prevented cosmic radiation produced on the eastern solar limb from reaching the earth. Some support is given to this proposition by the following consideration. Fig. 1 shows the positions on the solar disc at which the six cosmic ray producing flares were observed ([1-3]) and

---

([1]) M. A. Ellison: *Ninth Report on Solar-Terrestrial Relations* (C.I.U.S.).

([2]) K. G. McCracken: previous paper.

([3]) The flare responsible for the March 1942 event was not observed visually. The evidence suggesting the position shown in the diagram has been given in references ([1]) and ([2]).

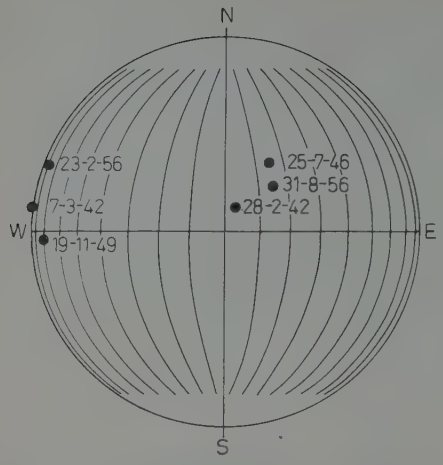

Fig. 1. – The positions on the solar disc at which the solar flares which resulted in cosmic ray increases occurred.

it can be seen that they all occurred to the west of the meridian 15° East of the central solar meridian. If the detection of solar cosmic radiation were independent of the position of a flare on the visible solar disc, the probability that a flare responsible for a cosmic ray increase would not occur to the east of the 15° E meridian is 105/180. Hence the probability that not one of six increases would be produced by a flare to the east of 15 °E is $(105/180)^6 = .039$. This rather small probability suggests that it is not merely a matter of chance that has resulted in no cosmic ray increases being produced by flares on the eastern portion of the solar disc.

3. – Concluding remarks.

GOLD has pointed out ([4]) that whereas a cosmic ray particle by itself would be trapped in the strong magnetic fields in the vicinity of the sunspot group in which the flare occurred, a sufficiently large number could exert sufficient pressure to distort the magnetic fields, and the particles would escape from the sun. Such a mechanism predicts that it is only those flares which invest the greatest energy in cosmic radiation which result in cosmic ray increases at the earth, a prediction which is in accord with the facts presented here. A quantitative test of the Gold mechanism would be the calculation of whether the quantity of cosmic radiation released by the small flare of August 31, 1956 ([2]) could have exerted the necessary pressure. As the estimation of the total energy of the cosmic radiation released by a flare is subject to very considerable error, this calculation will not be attempted in the present paper.

In order to explain some of the features of the cosmic ray solar flare effect, it has been suggested that there are elongated magnetic « bottles » extending from the vicinity of the sun ([5]). Cosmic radiation ejected from a flare into such a bottle would result in a cosmic ray flare effect provided the earth were within the bottle. Radiation travelling along the lines of force would arrive

([4]) T. GOLD: *Observatory*, **76**, 47 (1956).

([5]) G. COCCONI, K. GREISEN, P. MORRISON, T. GOLD and S. HAYAKAWA: *Suppl. Nuovo Cimento*, **8**, 161 (1958).

at the earth quickly, resulting in the sharp initial increase. After a short time, radiation spiralling along the lines of force, and radiation reflected from the sides and ends of the bottle would account for the observed isotropy. The slow diffusion of the radiation out of the bottle would account for the gradual decay of the flare effect. If the earth were outside the bottle, it would only receive the flare radiation after diffusion out of the bottle, and there would be no rapid rise in intensity, and the increase in intensity might not be recognized as a flare effect.

It is further suggested ([5]) that the solar rotation results in the outer portion of the magnetic bottle trailing behind the inner portion. Hence a bottle originating on the eastern solar limb, or on the greater portion of the invisible hemisphere, would not envelop the earth, and hence a cosmic ray increase would not be observed if a flare ejected radiation into the bottle. This would explain the experimental result that flares on the eastern limb of the visible hemisphere, and on the invisible hemisphere, do not result in cosmic ray increases.

RIASSUNTO (*)

Si fa rilevare che i tre brillamenti solari che provocarono forti aumenti dell'intensità dei raggi cosmici terrestri furono osservati in luce bianca, mentre i due brillamenti che provocarono il più piccolo aumento non furono osservati. Ciò si interpreta come prova del fatto che solo i brillamenti di massima energia producono un'apprezzabile quantità di radiazione cosmica e che la rarità dell'effetto di brillamento sui raggi cosmici è dovuta, almeno in parte, alla rarità di brillamenti solari veramente intensi. Si danno prove che suggeriscono che la radiazione cosmica prodotta in brillamenti aventi luogo al lembo orientale del sole non possa raggiungere la terra.

(*) *Traduzione a cura della Redazione.*

IL NUOVO CIMENTO Vol. XIII, N. 6 16 Settembre 1959

Leptonic Decay Modes of K-Mesons and Hyperons.

N. Cabibbo and R. Gatto

Istituto di Fisica e Scuola di Perfezionamento in Fisica Nucleare dell'Università - Roma
Istituto Nazionale di Fisica Nucleare - Sezione di Roma

(ricevuto il 23 Aprile 1959)

Summary. — The decay modes $K \to \pi +$ charged lepton $+ \nu$ and $Y \to N +$ $+$ charged lepton $+ \nu$ are studied by dispersion relation methods. The final spectra for K_3 decays are derived from the solution of an integral equation for the decay amplitude. The methods of solutions for such equations are briefly reviewed.

Introduction.

Goldberger and Treiman have recently applied methods of dispersion theory to evaluate effects of strong interactions on weak processes (1). Though it is rather difficult to judge at present about the success of such methods mainly because of the lack of detailed experimental information, especially on muon capture, this new approach has produced quite consistent results and seems theoretically superior to previous treatments. We apply here dispersion relation techniques to the K_3 decay modes, $K \to \pi +$ charged lepton $+ \nu$, and to the leptonic decays of hyperons $Y \to N +$ charged lepton $+ \nu$. The whole discussion is based on the $A - V$ theory of weak interactions (2), and more specifically on the assumption that leptons interact in the projection $\frac{1}{2}(1+\gamma_5)$ and are emitted from the same space-time point. It is also assumed that parity is conserved in strong interactions. A possible parity non conserving $KK\pi$ vertex would lead to a qualitative difference in the treatment of, for instance $K^+ \to \pi^0 + \mu^+ + \nu$ and $\bar{K}^0 \to \pi^- + \mu^+ + \nu$ because of the appearance of a bound

(1) M. L. Goldberger and S. B. Treiman: *Phys. Rev.*, **111**, 354 (1958); see also reference (6).

(2) R. E. Marshak and E. C. G. Sudarshan: *Padua-Venice Conference on Mesons and Newly Discovered Particles* (Sept. 1957); R. P. Feynman and M. Gell-Mann: *Phys. Rev.*, **109**, 193 (1958).

state contribution in the second reaction. On the hypothesis of parity conservation there is no bound state contribution in any such process.

The dispersion relation techniques that we use are based on subtracted dispersion relations rather than unsubtracted ones. Very little is known at present about the necessity or unnecessity of subtractions in the various cases, and the possibility of a connection with the structure of the original interaction term has also been considered. In the approximations that we adopt unsubtracted dispersion relations would give essentially no probability for the electronic decay modes, a result in direct conflict with present data. We think that this situation illustrates how careful one has to be in using unsubtracted dispersion relations, at least in making practical evaluations.

To determine the decay amplitude we subject it to an integral equation, with a kernel related to the $KK\pi\pi$ — vertex. No direct knowledge is available at present on such vertex, which could possibly be explored by extrapolation procedures on the cross-section for pion production in K-nucleon collisions. We shall make use of the indirect information on such a vertex that can be derived from low-energy K-nucleon scattering. The determination of the two subtraction constants can be accomplished, through the use of the universality hypothesis, from the experimental total rates for K_3 decay into electron and into muon.

The discussion we give of leptonic decays of hyperons is necessarily incomplete because of the absence of detailed information on the amplitudes for associated production in pion-nucleon collisions. Furthermore the question of the presence or absence of the decay mode $\Sigma^+ \to n + l^+ + \nu$ has now become of relevant interest after the recent confirmations of the predictions of the $\Delta T = \frac{1}{2}$ rule in strange particle decays [3].

The Appendix is mainly intended as a review of the methods of solution of the singular integral equations which occur in the applications of dispersion techniques to the determination of physical amplitudes. What we try to do is essentially to produce a unified treatment which allows very simple forms of solutions, whenever this is possible because of analyticity properties of the inhomogeneous term, and leads to more complicated solutions valid in more general cases.

1. – Dispersion relation approach to K_3 decays.

1·1. – We shall consider the decay modes

$$K^+ \to \pi^0 + l^+ + \nu\,, \qquad K^- \to \pi^0 + l^- + \bar{\nu}\,, \tag{1}$$

---

[3] F. S. Crawford, M. Cresti, R. L. Douglas, M. L. Good, G. R. Kalbfleisch, M. L. Stevenson and H. K. Ticho: *Phys. Rev. Lett.*, **2**, 266 (1959).

where $l^{\pm}$ means $e^{\pm}$ or $\mu^{\pm}$. Quite similar considerations apply also to the decay modes

(2) $$K^0 \to \pi^- + l^+ + \nu\,, \qquad \overline{K}^0 \to \pi^+ + l^- + \bar{\nu}\,,$$

(2′) $$K^0 \to \pi^+ + l^- + \bar{\nu}\,, \qquad \overline{K}^0 \to \pi^- + l^+ + \nu\,.$$

We assume that parity is conserved in strong interactions and we define the K-meson to be pseudoscalar. If parity is not conserved in strong interactions there is a qualitative difference in the treatment of processes (1) and (2) on one side and (2′) on the other side arising from the possible existence of a $KK\pi$ vertex, that conserves strangeness but violates parity. In fact one would have a Born term contribution for (1) and (2), corresponding, for instance for the first of reactions (1), to the sequel

$$K^+ \to K^+ + \pi^0 \to \pi^0 + l^+ + \nu\,,$$

while no such term is allowed for (2′) because of strangeness conservation.

We also shall assume the $A-V$ theory of weak interaction [1]. However it should be said that the only assumption on which the treatment rests is that leptons always appear in the interaction in the $\frac{1}{2}(1+\gamma_5)$ projection, and both l and ν are emitted from the same space-time point. The latter assumption in particular implies that we neglect electromagnetic corrections.

12. – To be definite let us consider the first of the reactions (1), and call $p^{(K)}$, $p^{(\pi)}$, $p^{(l)}$ and $p^{(\nu)}$ the momenta of the participating particles. Momentum conservation gives

(3) $$p^{(K)} = p^{(\pi)} + p^{(l)} + p^{(\nu)}\,.$$

In the matrix element $p^{(l)}$ and $p^{(\nu)}$ will only appear in the combination $p^{(l)} + p^{(\nu)}$, because of the assumption that both l and ν are emitted from the same point. Thus one can only dispose of two independent four-vectors, that one can choose, for instance, as $p^{(K)}$ and $p^{(\pi)}$. We call

(4) $$s = -(p^{(K)} - p^{(\pi)})^2\,,$$

the invariant momentum transfer.

The relevant S-matrix element for the decay is given by

(5) $$\langle \pi^0 l^+ \nu;\ \text{out} | K^+;\ \text{in} \rangle\,.$$

If we limit our treatment of weak interactions only to first order we can safely

apply the reduction formula (4) to (5) and write

$$\langle \pi^0 l^+ \nu; \text{out} \,|\, K^+; \text{in} \rangle = \frac{1}{(2\pi)^{\frac{3}{2}}} \bar{u}^{(\nu)} \int \mathrm{d}x \langle \pi^0 l^+; \text{out} \,|\, j(x) \,|\, K^+; \text{in} \rangle \exp[-ip^{(\nu)}x] , \tag{6}$$

where

$$j(x) = \gamma \frac{\partial}{\partial x} \psi^{(\nu)}(x) . \tag{7}$$

We are assuming a normalization $\bar{u}u = (m/E)$ for the spinors and hermitian γ-matrices satisfying $\{\gamma_\mu, \gamma_\nu\} = 2\delta_{\mu\nu}$.

From (7) it follows that $j(x)$ has the form

$$j(x) = \gamma_\mu \boldsymbol{a} \psi^{(l)}(x) J_\mu(x) , \tag{8}$$

where $J_\mu(x)$ is a strangeness non-conserving current. We call $\boldsymbol{a}$ the projection operator $\frac{1}{2}(1+\gamma_5)$. Only the vector part of $J_\mu(x)$ contributes to the decay. In fact from the two independent vectors of the problem one can only form vector covariants to multiply the lepton term $(\bar{u}^{(\nu)} \gamma_\mu \boldsymbol{a} u^{(l)})$.

Since we are treating weak interactions only up to the first order and we are neglecting electromagnetic interactions it is consistent to identify the Heisenberg field $\psi^{(l)}(x)$ with the corresponding « out » field. We can then write for our matrix element

$$\langle \pi^0 l^+ \nu; \text{out} \,|\, K^+; \text{in} \rangle = \tag{9}$$

$$= \frac{1}{(2\pi)^{\frac{3}{2}}} (\bar{u}^{(\nu)} \gamma_\mu \boldsymbol{a} u^{(l)}) \int \mathrm{d}x \langle \pi^0; \text{out} \,|\, J_\mu(x) \,|\, K^+; \text{in} \rangle \exp[-i(p^{(l)} + p^{(\nu)})x] =$$

$$= 2\pi i \, \delta(p^{(K)} - p^{(\pi)} - p^{(l)} - p^{(\nu)}) (\bar{u}^{(\nu)} \gamma_\mu \boldsymbol{a} u^{(l)}) \langle p^{(\pi)} \,|\, J_\mu(0) \,|\, p^{(K)} \rangle , \tag{10}$$

where we have omitted for one-particle states the indications « in » and « out ». We can now again apply the reduction formula to the matrix element of $J_\mu(0)$ and obtain

$$\langle p^{(\pi)} \,|\, J_\mu(0) \,|\, p^{(K)} \rangle = \frac{i}{(2\pi)^3} \int \mathrm{d}x \exp[-ip^{(\pi)}x] (\Box - \mu^2) \langle 0 \,|\, T(\varphi(x) J_\mu(0)) \,|\, p^{(K)} \rangle , \tag{11}$$

where $\varphi(x)$ is the π^0 field and T denotes the chronological product.

To evaluate (11) we use the identity

$$T(\varphi(x) J_\mu(0)) = \varphi(x) J_\mu(0) + \theta(-x) [J_\mu(0), \varphi(x)] . \tag{12}$$

---

(4) H. LEHMAN, K. SYMANZIK and W. ZIMMERMANN: *Nuovo Cimento*, **2**, 425 (1955).

Defining

$$J(x) = (\Box - \mu^2)\varphi(x) \tag{13}$$

we have from (12) and (13)

$$(\Box - \mu^2)T(\varphi(x)J_\mu(0)) = J(x)J_\mu(0) + (\Box - \mu^2)\theta(-x)[J_\mu(0), \varphi(x)]. \tag{14}$$

1·3. – The first term on the right hand side of (14), $J(x)J_\mu(0)$, does not contribute to the decay matrix element. This fact can be seen most easily if one substitutes (14) into (11). One gets a term

$$\int \mathrm{d}x \exp[-ip^{(\pi)}x]\langle 0|J(x)J_\mu(0)|p^{(K)}\rangle = \tag{15}$$

$$= \int \mathrm{d}x \exp[-ip^{(\pi)}x] \sum_z (\Box - \mu^2)\langle 0|\varphi(x)|z\rangle\langle z|J_\mu(0)|p^{(K)}\rangle .$$

By integrating we find $p^{(z)} = p^{(\pi)}$. Thus only the one-pion state can contribute to the sum. However, for such a state, $\langle 0|\varphi(x)|z\rangle$ is the pion wave-function $f(x)$, which satisfies $(\Box - \mu^2)f(x) = 0$.

The second term on the right hand side of (14) is

$$(\Box - \mu^2)\theta(-x)[J_\mu(0), \varphi(x)] = \tag{16}$$

$$= \theta(-t)[J_\mu(0), J(x)] + \dot{\delta}(t)[J_\mu(0), \varphi(x)] + 2\delta(t)[J_\mu(0), \dot{\varphi}(x)].$$

Inserting into (11) one finds a term

$$\frac{i}{(2\pi)^{\frac{3}{2}}}\int \mathrm{d}x \exp[-ip^{(\pi)}x]\theta(-x)\langle 0|[J_\mu(0), J(x)]|p^{(K)}\rangle, \tag{17}$$

which has the form of the Fourier transform of an advanced commutator, and the sum of two other terms which can formally be evaluated since they are expressed through commutators of the Heisenberg fields taken at equal times

$$\frac{1}{(2\pi)^{\frac{3}{2}}} p_0^{(\pi)} \int \mathrm{d}x \exp[-ip^{(\pi)}x]\langle 0|[J_\mu(0), \varphi(x)]|p^{(K)}\rangle\, \delta(t) + \tag{18}$$

$$+ \frac{i}{(2\pi)^{\frac{3}{2}}}\int \mathrm{d}x \exp[-ip^{(\pi)}x]\langle 0|[J_\mu(0), \dot{\varphi}(x)]|p^{(K)}\rangle\delta(t).$$

1·4. – The possible contribution from the two terms (18) will however be included in the subtraction terms of the dispersion relation that we shall write down for the causal amplitude (17). To show this in detail let us assume that

$J_\mu(x)$ contains a term

$$if \frac{\partial \varphi^{(K)}(x)}{\partial x_\mu} \varphi^{(\pi)}(x) + ig\varphi^{(K)}(x) \frac{\partial \varphi^{(\pi)}(x)}{\partial x_\mu}, \tag{19}$$

with f and g constants, that couples the K-field to the π-field and would directly give rise to the decay. For brevity we shall omit consideration of the Z factors that should be included in (19) and that also appear in the equal time commutators, since they are inessential to the formal argument. For such a form of $J_\mu(x)$ we find for the two commutators in (18),

$$[J_\mu(x'), \varphi(x)]\,\delta(t-t') = -ig\varphi^{(K)}(x')\delta(x-x')\delta_{\mu 4},$$

$$[J_\mu(x'), \dot{\varphi}(x)]\,\delta(t-t') = -f\frac{\partial \varphi^{(K)}(x')}{\partial x'_\mu}\delta(x-x') - g\varphi^{(K)}(x')\frac{\partial}{\partial x'_\mu}\delta(x-x')(1-\delta_{\mu 4}).$$

Inserting into (18), after partial integration, one finds

$$\frac{1}{(2\pi)^{\frac{3}{2}}}\langle 0|\varphi^{(K)}(0)|p^{(K)}\rangle(fp_\mu^{(K)} - gp_\mu^{(\pi)}). \tag{20}$$

This is precisely of the form of the subtraction term for the amplitude (17).

We cannot give any reason for the necessity, or lack of necessity, of making a subtraction in the dispersion relation for the causal amplitude (17). It has been pointed out that there may be a deep connection between subtractions and primary couplings in the original Lagrangian ([5]). In their work on form factors in β-decay ([1]) GOLDBERGER and TREIMAN use subtracted dispersion relations for the axial form factor and for the vector form factor, corresponding to the presence of primary couplings for axial and vector β-decay respectively in the original Lagrangian. On the other hand they use a non-subtracted dispersion relation in calculating the $\pi \to \mu + \nu$ decay ([6]), for which one does not have to postulate a primary interaction. According to such a philosophy one would have for the system containing nucleons, pions, gammas, and leptons a complete description of the weak interactions with only the *two* renormalized coupling constants for axial and vector β-decay, apart from the necessary knowledge of the strong interaction amplitudes. In contrast to such a possibility, in the usual perturbation theory approach to renormalization for weak interactions taken only at first order, one has also to introduce two renormalization counterterms, which may be taken to describe the processes $\pi \to l + \nu$ and $\pi \to \pi + l + \nu$. A complete description would thus require *four* weak coupling constants that reduce to three if one adopts the hypothesis of

([5]) M. L. GOLDBERGER: *Proceedings of the Geneva Conference* (1958). Edited by B. FERRETTI, p. 260.

([6]) M. L. GOLDBERGER and S. B. TREIMANN: *Phys. Rev.*, **110**, 1178 (1958).

non-renormalization for the vector part. If one adopts the philosophy that a subtraction is needed any time there is an interaction term in the Lagrangian, one has to make a subtraction in the dispersion relation for $\pi \to \mu + \nu$, and the agreement found in ([6]) has to be regarded as fortuitous. Of course the distinction between terms which are originally introduced in the lagrangian and terms which then arise as renormalization counterterms may be quite ambiguous. It is also quite possible that the two possibilities that we have considered concerning subtractions are both wrong. As far as our problem is concerned a term in the strangeness non-conserving current $J_\mu(x)$ of the form (19) may well exist, and actually very little is known concerning the structure of such a current. Anyway it would presumably appear as a renormalization counterterm in a perturbation theoretical approach with weak interactions taken up to the first order. Apart from such speculations we shall see later that it is unavoidable in our approach to use subtracted dispersion relations. The reason, as it will appear clear later, is the following. In the approximations that we shall adopt the solutions of the set of the non-subtracted dispersion relations would give decay amplitudes for $K \to \pi + l + \nu$ proportional to the lepton mass m_l, and therefore they would give an extremely small branching ratio for decay into an electron, in direct contrast with experiment, which gives a branching ratio of the order of unity ([7]).

2. – Integral equation for the decay amplitude.

2·1. – On invariance arguments the matrix element

$$V_\mu(p^{(\pi)}, p^{(K)}) \equiv \frac{i}{(2\pi)^3}\int \mathrm{d}x \exp[-ip^{(\pi)}x]\theta(-x)\langle 0|[J_\mu(0), J(x)]|p^{(K)}\rangle , \tag{21}$$

can be written in the form

$$V_\mu(p^{(\pi)}, p^{(K)}) = a(s)p_\mu^{(\pi)} + b(s)p_\mu^{(K)} , \tag{22}$$

where the form factors a and b depend on the invariant momentum transfer s. We postulate for the form factors $a(s)$ and $b(s)$ the subtracted dispersion relations

$$a(s) = a(0) + \frac{s}{\pi}\int_0^\infty \frac{\mathrm{Im}\, a(s')}{s'(s' - s - i\varepsilon)}\,\mathrm{d}s' , \tag{23}$$

$$b(s) = b(0) + \frac{s}{\pi}\int_0^\infty \frac{\mathrm{Im}\, b(s')}{s'(s' - s - i\varepsilon)}\,\mathrm{d}s' . \tag{23'}$$

([7]) M. GELL-MANN and A. ROSENFELD: *Ann. Rev. Nucl. Sci.* (Palo Alto, 1957).

From (21) one sees in fact that $V_\mu(p^{(\pi)}, p^{(K)})$ has the form of the Fourier transform of an advanced commutator, suggesting that it should be analytic for $\mathrm{Im}\, E < 0$ in the complex E-plane, where E is the pion energy. In the K rest-system one has the relation

$$s = 2M(E_0 - E)\,, \tag{24}$$

with

$$E_0 = \frac{M^2 + \mu^2}{2M}\,, \tag{24'}$$

where M is the K-meson mass and μ is the pion mass. One is thus led to conclude that $a(s)$ and $b(s)$ are analytic for $\mathrm{Im}\, s > 0$ in the complex s-plane. This property would lead to dispersion relations of the form

$$a(s) = \frac{1}{\pi}\int_0^\infty \frac{\mathrm{Im}\, a(s')}{s' - s - i\varepsilon}\, \mathrm{d}s'\,, \tag{25}$$

$$b(s) = \frac{1}{\pi}\int_0^\infty \frac{\mathrm{Im}\, b(s')}{s' - s - i\varepsilon}\, \mathrm{d}s'\,, \tag{25'}$$

of which (23) and (23′) are the subtracted form.

The imaginary parts in (23) and (23′) are different from zero only for $s > (M+\mu)^2$, since the lowest state contributing is the state containing a K and a π-meson. It will be convenient to introduce also a variable

$$x = \frac{s}{(M+\mu)^2}\,, \tag{26}$$

and the quantity

$$\beta = \left(\frac{M-\mu}{M+\mu}\right)^2. \tag{26'}$$

The physical region for x extends from $m_1^2/(M+\mu)^2$ up to β, which is less than 1. On the other hand the contributions to the imaginary parts start at $x = 1$.

From (21) we find for the absorptive part $A_\mu(p^{(\pi)}, p^{(K)})$ of the amplitude $V_\mu(p^{(\pi)}, p^{(K)})$

$$A_\mu(p^{(\pi)}, p^{(K)}) = \frac{1}{2(2\pi)^{\frac{3}{2}}}\int \mathrm{d}x \exp\left[-ip^{(\pi)}x\right]\langle 0\,|[J_\mu(0), J(x)]\,|\,p^{(K)}\rangle\,. \tag{27}$$

The term $J(x)J_\mu(0)$ from the commutator does not contribute to the matrix

element, as we have already seen in Section 1·3. $A_\mu(p^{(\pi)}, p^{(K)})$ can be written as

$$(28)\quad A_\mu(p^{(\pi)}, p^{(K)}) = \frac{1}{4}(2\pi)^{\frac{5}{2}} \sum_z \langle 0|J_\mu(0)|z;\text{in}\rangle\langle z;\text{in}|J(0)|p^{(K)}\rangle \delta(p^{(K)}-p^{(\pi)}-p^{(z)}) +$$

$$+ \text{same expression with « in » substituted by « out ».}$$

The summations extend over the complete set of « in » and « out » states.

2·2. – The states contributing to the summation will be of the kind $K^+ + \pi^0$, $K^0 + \pi^+$, $K^0 + 2\pi$, $\bar{\Lambda} + N$, $\bar{\Sigma} + N$, etc. Of all such states we shall only keep the $K + \pi$ states. We feel partially justified in the use of such an approximation because we have used subtracted dispersion relations rather than unsubtracted ones. Furthermore the smallness of the effects that we find makes us feel rather confident on the validity of the approximation.

Our second approximation consist in taking a simplified model for the $KK\pi\pi$ vertex, occurring in (28) in the form of the matrix element of $J(0)$ between a one-K state and a $K + \pi$ state. Some direct knowledge about such a vertex would be obtained by extrapolating the measured cross-section for $K + N \to N + K + \pi$ up to the pole corresponding to the virtual process in which a pion propagates from the nucleon to the $KK\pi\pi$ vertex—the procedure would be similar to that proposed by CHEW to determine the $\pi\pi$ interaction ([8]). In the absence so far of any direct evidence on the $KK\pi\pi$ interaction, we shall make use of the analysis by BARSHAY of K-N scattering on the basis of such an interaction ([9]). BARSHAY postulates a direct coupling of the form

$$(29)\qquad \lambda(\varphi^{(K)\dagger}(x)\varphi^{(K)}(x))(\boldsymbol{\varphi}^{(\pi)\dagger}(x)\boldsymbol{\varphi}^{(\pi)}(x))$$

and finds that for $\lambda^2/(4\pi)$ between 1 and 5 one gets a consistent description of K-N scattering. A relevant feature of (29) is that there are no terms in it giving charge exchange processes such as $K^+ + \pi^0 \to K^0 + \pi^+$. This feature is consistent with the observed smallness of the charge exchange K-N scattering. We now insert into (28) the perturbation approximation from the interaction lagrangian (29) for the matrix elements $\langle q^{(K)}, q^{(\pi)}|J(0)|p^{(K)}\rangle$ leading to states $\langle z| = \langle q^{(K)}, q^{(\pi)}|$. For the matrix elements of $J_\mu(0)$ one finds:

$$(30)\qquad \langle 0|J_\mu(0)|q^{(K)}, q^{(\pi)};\text{in}\rangle = V_\mu(-q^{(\pi)}, q^{(K)}),$$

$$(30')\qquad \langle 0|J_\mu(0)|q^{(K)}, q^{(\pi)};\text{out}\rangle = V^*_\mu(-q^{(\pi)}, q^{(K)}),$$

([8]) G. CHEW and F. LOW: UCRL-8427.
([9]) S. BARSHAY: *Phys. Rev.*, **110**, 743 (1958).

where one has made use of the transformation properties of $J_\mu(0)$ under parity and time reversal. The absorptive part of $V_\mu(p^{(\pi)}, p^{(K)})$ can thus be expressed in terms of its dispersive part $D_\mu(p^{(\pi)}, p^{(K)})$

$$(31) \quad A_\mu(p^{(\pi)}, p^{(K)}) = \frac{\lambda}{8\pi^2} \sum_{q^{(K)}, q^{(\pi)}} D_\mu(-q^{(\pi)}, q^{(K)})\, \delta(p^{(K)} - p^{(\pi)} - q^{(K)} - q^{(\pi)}),$$

or

$$(32) \quad A_\mu(p^{(\pi)}, p^{(K)}) = \frac{\lambda}{8\pi^2} \sum_{q^{(K)}, q^{(\pi)}} [-\mathrm{Re}\, a(s) q_\mu^{(\pi)} + \mathrm{Re}\, b(s) q_\mu^{(K)}]\, \delta(p^{(K)} - p^{(\pi)} - q^{(K)} - q^{(\pi)}),$$

where we have used the δ-function to obtain $s' = -(q^{(K)} - (-q^{(\pi)}))^2 = s$. The summation over $q^{(K)}$, $q^{(\pi)}$ can be converted into an integral and the resulting expression is

$$(33) \quad A_\mu(p^{(\pi)}, p^{(K)}) = \frac{\lambda}{32\pi^2} [-\mathrm{Re}\, a(s) G^{(\pi)}(s) + \mathrm{Re}\, b(s)\, G^{(K)}(s)](p^{(K)} - p^{(\pi)})_\mu,$$

where $G^{(\pi)}(s)$ and $G^{(K)}(s)$ have an invariant definition

$$(34) \quad (p^{(K)} - p^{(\pi)})_\mu\, G^{(\pi)}(s) =$$

$$= 4 \int \mathrm{d}q^{(\pi)}\, \delta(q^{(\pi)2} + \mu^2)\, \delta((p^{(K)} - p^{(\pi)} - q^{(\pi)})^2 + M^2)\, \theta(q^{(\pi)})\, \theta(p^{(K)} - p^{(\pi)} - q^{(\pi)}) q_\mu^{(\pi)},$$

$$(34') \quad (p^{(K)} - p^{(\pi)})_\mu\, G^{(K)}(s) =$$

$$= 4 \int \mathrm{d}q^{(K)}\, \delta(q^{(K)2} + M^2)\, \delta((p^{(K)} - p^{(\pi)} - q^{(K)})^2 + \mu^2)\, \theta(q^{(K)})\, \theta(p^{(K)} - p^{(\pi)} - q^{(K)}) q_\mu^{(K)}.$$

The integrals are most easily evaluated in the co-ordinate system where $\boldsymbol{p}^{(K)} = \boldsymbol{p}^{(\pi)}$. The result can then be written in invariant form

$$(35) \quad G^{(\pi)}(s) = \frac{\pi}{s^2}(s - M^2 + \mu^2)[(s - M^2 - \mu^2)^2 - 4\mu^2 M^2]^{\frac{1}{2}},$$

$$(35') \quad G^{(K)}(s) = \frac{\pi}{s^2}(s + M^2 - \mu^2)[(s - M^2 - \mu^2)^2 - 4\mu^2 M^2]^{\frac{1}{2}}.$$

2·3. – It will be convenient to introduce in place of $a(s)$ and $b(s)$ their combinations $v(s)$ and $w(s)$ defined as

$$(36) \quad v(s) = -a(s) + b(s),$$

$$(36') \quad w(s) = a(s) + b(s),$$

so that

$$V_\mu(p^{(\pi)}, p^{(K)}) = v(s)\, p_\mu^{(-)} + w(s) p_\mu^{(+)}\,, \tag{37}$$

with

$$p_\mu^{(\mp)} = \tfrac{1}{2}(p^{(K)} \mp p^{(\pi)})\,. \tag{38}$$

From (33), (37), (35) and (35′) one finds

$$\mathrm{Im}\, v(s) = \frac{\lambda}{32\pi^2}\,[\mathrm{Re}\, v\,(s)\, G^{(+)}(s) + \mathrm{Re}\, w(s)\, G^{(-)}(x)]\,, \tag{39}$$

$$\mathrm{Im}\, w(s) = 0\,, \tag{39′}$$

where

$$G^{(+)}(s) = \frac{2\pi}{s}\,[(s - M^2 - \mu^2)^2 - 4\mu^2 M^2]^{\frac{1}{2}}\,, \tag{40}$$

$$G^{(-)}(s) = \frac{1}{s}\,(M^2 - \mu^2)\, G^{(+)}(s)\,. \tag{40′}$$

Eq. (39′) is a direct consequence of our assumptions for the matrix elements $\langle q^{(K)}, q^{(\pi)} | J(0) | p^{(K)} \rangle$. The dispersion relations (23) and (23′) give

$$w(s) = w(0) = \text{real constant}\,, \tag{41}$$

$$v(s) = v(0) + \frac{\lambda}{32\pi^2}\,\frac{s}{\pi}\int_{(M+\mu)^2}^{\infty} \frac{\mathrm{d}s'\, G^{(+)}(s')}{s'(s' - s - i\varepsilon)}\left[\mathrm{Re}\, v(s') + \frac{1}{s'}\, w(0)(M^2 - \mu^2)\right]\,, \tag{41′}$$

If we had used the non-subtracted dispersion relations (25) and (25′) we would have found with our approximations

$$w(s) = 0\,,$$

because of (39′) which expresses the fact that there is no absorptive term in (33) proportional to $p_\mu^{(+)}$. The S-matrix element for the decay would then be given by

$$\pi i\, \delta(p^{(K)} - p^{(\pi)} - p^{(\,)} - p^{(\nu)})(\bar{u}^{(\nu)} \gamma(p^{(l)} + p^{(\nu)})\, a u^{(l)})\, v(s)\,,$$

which is clearly proportional to the lepton mass m_1, and would give an extremely small branching ratio for decay into an electron, in contradiction with present data, suggesting a branching ratio of the order unity. We think that the above situation illustrates how careful one has to be in the use of unsubtracted dispersion relations.

2·4. – We can reduce the singular integral equation (41′) into standard form by making the substitutions

$$u(x) = \frac{v\left((M+\mu)^2 x\right)}{(M+\mu)^2 x} + w(0)\,\frac{M-\mu}{(M+\mu)^3 x^2}\,, \tag{42}$$

$$f(x) = \frac{v(0)}{(M+\mu)^2 x} + w(0)\,\frac{M-\mu}{(M+\mu)^3 x^2}\,, \tag{42′}$$

$$k(x) = \frac{\lambda}{32\pi^2}\,G^{(+)}\left((M+\mu)^2 x\right)\,. \tag{42″}$$

The variable x has been defined in (26). In terms of such variables equation (41′) becomes

$$u(x) = f(x) + \frac{1}{\pi}\int_1^\infty \frac{\mathrm{d}x'\,k(x')\,\mathrm{Re}\,u(x')}{x'-x-i\varepsilon}\,. \tag{43}$$

From this last equation one finds

$$\mathrm{Im}\,u(x) = k(x)\,\mathrm{Re}\,u(x)\theta(x-1) \tag{44}$$

and substituting again into (43) one finally has

$$u(x) = f(x) + \frac{1}{\pi}\int_1^\infty \frac{\mathrm{d}x'\,h^*(x')\,u(x')}{x'-x-i\varepsilon}\,, \tag{45}$$

where

$$h^*(x) = \frac{k(x)}{1+ik(x)}\,. \tag{46}$$

It will be convenient to introduce a phase $\alpha(x)$ such that

$$k(x) = \mathrm{tg}\,\alpha(x) \tag{47}$$

from which

$$h^0(x) = \sin\alpha(x)\exp\left[-i\alpha(x)\right]. \tag{48}$$

Singular integral equations of the type (45) have been found by many authors and discussed in particular by OMNES [10]. The formal solution reported by OMNES must however be slightly modified before being applied to

[10] R. OMNES: *Nuovo Cimento*, **8**, 316 (1958).

our case. Furthermore it turns out to be convenient to adopt another more direct method of solution which leads to much simpler expressions. The properties and the methods of solution of the singular integral equation (45) are briefly reviewed in the Appendix.

3. – Results and discussion.

3·1. – From (47), (42″), (40) and introducing the quantity defined in (26′), we find

$$\alpha(x) = \operatorname{arctg}\left|\frac{\lambda}{16\pi}\frac{1}{x}(1-x)^{\frac{1}{2}}(\beta-x)^{\frac{1}{2}}\right| . \tag{49}$$

We must therefore choose a subtracted form for the solution of (A.7) since with $\alpha(x)$ as given by (49) the solution (A.8) would not converge. Choosing the form (A.9), which is already convergent, we can write in the whole physical region, where certainly $x < 1$

$$\tau(x+i\varepsilon) = xc(x) , \qquad c(x) = \frac{1}{\pi}\int_1^\infty \frac{\alpha(x')\,\mathrm{d}x'}{x'(x'-x)} . \tag{50}$$

The coefficients a_{-2} and a_{-1} appearing in (A.25) can be determined from the development (A.23), that is easily derived from the (42′)* and from (A.9). Putting

$$\eta = \frac{v(0)}{(M+\mu)^2} , \qquad \eta' = \beta^{\frac{1}{2}}\frac{v(0)}{(M+\mu)^2} , \tag{51}$$

the solution of (45) is

$$u(x) = \left|\frac{\eta - \eta' c(0)}{x} + \frac{\eta'}{x^2}\right| \exp\left[\tau(x+i\varepsilon)\right] . \tag{52}$$

Other solutions of (45) are obtained by addition to (52) of solutions of the homogeneous equation, of the form [10]

$$u^{(0)}(x) = \frac{P(x)}{(x-1)^n} \exp\left[\tau(x+i\varepsilon)\right] , \tag{53}$$

where n is an integer, and $P(x)$ a polynomial. We select (52) on the basis that it is the only solution which in the limit $\lambda \to 0$ reduces to the iterative solution of (45).

To check the consistency of our solution we have to show that the integrals over the circle at infinity in (A.10) and (A.13) vanish. From (A.9) and (49)

it is easy to show that for large z

$$\tau(z) \simeq \frac{1}{\pi} \operatorname{arctg} \frac{\lambda}{16\pi} \log z \,. \tag{54}$$

On the other hand both $f(z)$ and $\varphi(z)$ vanish as z^{-1}, so that the required conditions are certainly satisfied at least for our values of λ.

From the complete solution it is easy to show that $c(x)$ is accurately given from the first order term in its expansion in powers of λ. To show this we note that from (49) $0 \leqslant \operatorname{tg} \alpha(x) \leqslant \lambda/(16\pi)$ and thus

$$0 \leqslant \operatorname{tg} \alpha(x) - \alpha(x) < \frac{1}{3}\left(\frac{\lambda}{16\pi}\right)^2 \operatorname{tg} \alpha(x) \,. \tag{55}$$

From (55) one now obtains

$$c_1(x)\left[1 - \frac{1}{3}\left(\frac{\lambda}{16\pi}\right)^2\right] < c(x) < c_1(x) \,, \tag{56}$$

where

$$c_1(x) = \frac{1}{\pi}\int_1^\infty \frac{\operatorname{tg} \alpha(x')\, \mathrm{d}x'}{x'(x' - x)} \,, \tag{57}$$

is the first order term in the development in powers of λ. One finds

$$c(x) \simeq \frac{\lambda}{16\pi^2}\frac{1}{x}\left[1 + \left(\frac{\beta^{\frac{1}{2}} + \beta^{-\frac{1}{2}}}{2} - \frac{\beta^{\frac{1}{2}}}{x}\right)\log\frac{1+\beta^{\frac{1}{2}}}{1-\beta^{\frac{1}{2}}} + \right.$$
$$\left. + 2\,\frac{(1-x)^{\frac{1}{2}}(\beta - x)^{\frac{1}{2}}}{x}\log\frac{(1-x)^{\frac{1}{2}} + (\beta - x)^{\frac{1}{2}}}{(1-\beta)^{\frac{1}{2}}}\right| . \tag{58}$$

The matrix element $V_\mu(p^{(\pi)}, p^{(K)})$ is given by (37), where $w(s)$ is determined from (41) and $v(s)$ is determined from (42), (52), (51), (50) and (58). The final result is

$$V_\mu(p^{(\pi)}, p^{(K)}) \equiv v(s)p_\mu^{(-)} + w(s)p_\mu^{(+)} = \left| v(0)\exp[xc(x)] + \right.$$
$$\left. + w(0)\left(\beta^{\frac{1}{2}}\frac{1}{x}(\exp[xc(x)] - 1) + \beta^{\frac{1}{2}}c(0)\exp[xc(x)]\right)\right| p_\mu^{(-)} + w(0)p_\mu^{(+)} \,. \tag{59}$$

From this expression and the expression (10) for the matrix element one can calculate the final spectra. In the notations of reference (11) the probability of the final configuration for which the pion has an energy E and the charged

lepton an energy E_1 is given by

$$W_1^{(0)}(EE_1)\,\mathrm{d}E\,\mathrm{d}E_1 = \{m_1^2 X(E^2)(\Delta^2 - p^2 - m_1^2) - 4m_1^2 X(E)\,Y(E)(\Delta - E_1) + \\ + Y(E)^2 M^2 [-(\Delta^2 - p^2 - m_1^2) + 4E_1(\Delta - E_1)]\}\,\mathrm{d}E\,\mathrm{d}E_1\,, \tag{60}$$

where p is the pion momentum and Δ is $M - E$. The relation between $X(E)$, $Y(E)$ and $v(s)$, $w(s)$, which are implicitly defined in (59), is

$$X(E) = \tfrac{1}{2}[v(s) - w(0)]\,, \tag{61}$$

$$Y(E) = v(s)\,, \tag{61'}$$

where we have omitted an unessential multiplicative constant. The relation between s and E is given in (24) and (24'). The polarization of the emitted lepton was also calculated in [11] and can be similarly expressed through $v(s)$ and $w(0)$.

3·2. – The theory of the $\mathrm{K} \to \pi + \mathrm{l} + \nu$ decay derived here contains two unknown parameters $v(0)$ and $w(0)$. The procedure to determine these two parameters consists in calculating from (60) the total decay rates for decay into an electron and into a muon. From the hypothesis of universal interaction $v(0)$ and $w(0)$ must be the same in the two cases. Therefore from the knowledge of the two experimental rates one can determine $v(0)$ and $w(0)$ apart from algebraic ambiguities. We have tried such a procedure numerically using the values of the lifetimes $[\tau(K_{\mu 3})]^{-1} = 3.26 \cdot 10^6\ \mathrm{s}^{-1}$ and $[\tau(K_{e3})]^{-1} = 3.42 \cdot 10^6\ \mathrm{s}^{-1}$ already used in reference [11], that were taken from the review article by GELL-MANN and ROSENFELD [7]. The lepton spectra obtained in this way differ from those given in Fig. 2 of reference [11] by less than 10%. Because of the present almost complete lack of knowledge on such spectra we do not try here any comparison with experiment, hoping that better data will be available soon.

4. – Dispersion relation approach to hyperon leptonic decays.

4·1. – We shall study in this Section the leptonic decays of hyperons by methods similar to those used above. We shall study the decay modes

$$\Sigma^- \to \mathrm{n} + \mathrm{l}^- + \bar{\nu}\,, \tag{62}$$

$$\Sigma^+ \to \mathrm{n} + \mathrm{l}^+ + \nu\,. \tag{62'}$$

[11] R. GATTO: *Phys. Rev.*, **112**, 1926 (1958).

Of course similar considerations apply to the other possible leptonic decay modes of hyperons. It should be remarked that (62′) requires a strangeness non-conserving current with $\Delta S = -\Delta Q$. The existence of such a current would make possible a decay mode $\Xi^- \to n + \pi^-$, not observed. Furthermore (62′) requires that such a current has a component transforming at least as $\Delta T = \frac{3}{2}$. On the other hand preliminary results at Bologna [12] indicate the existence of (62′).

The procedure will be quite similar to that used by GOLDBERGER and TREIMAN in reference [4]. Let us consider for instance reaction (62). The S-matrix element can be written as

$$(63)\qquad \langle n l^- \bar{\nu};\ \text{out}\,|\,\Sigma^-;\ \text{in}\rangle = 2\pi i\,\delta(p^{(\Sigma)} - p^{(n)} - p^{(l)} - p^{(\nu)})(\bar{u}^{(l)}\gamma_\mu a u^{(\nu)})\cdot \cdot(\langle n\,|\,A_\mu(0)\,|\,\Sigma^-\rangle + \langle n\,|\,V_\mu(0)\,|\,\Sigma^-\rangle)\,,$$

where on argument of relativistic invariance

$$(64)\qquad \langle n\,|\,A_\mu(0)\,|\,\Sigma^-\rangle = \frac{1}{(2\pi)^3}(\bar{u}^{(n)}[-a(t)\gamma_\mu\gamma_5 - ib(t)\Delta_\mu\gamma_5 + b'(t)\sigma_{\mu\nu}\Delta_\nu\gamma_5]u^{(\Sigma)}).$$

$$(64')\qquad \langle n\,|\,V_\mu(0)\,|\,\Sigma^-\rangle = \frac{1}{(2\pi)^3}(\bar{u}^{(n)}[c(t)\gamma_\mu - id'(t)\Delta_\mu - id(t)\sigma_{\mu\nu}\Delta_\nu]u^{(\Sigma)})\,,$$

where

$$(65)\qquad \Delta = p^{(\Sigma)} - p^{(n)}\,,\qquad t = -\Delta^2\,.$$

the terms $-ib(t)\Delta_\mu\gamma_5$ and $-id'(t)\Delta_\mu$ give contributions proportional to the lepton mass, and thus they can be neglected for decay into electrons. Applying the reduction formula to the matrix elements (64) and (64′) and neglecting the terms containing equal time commutators we can write

$$(66)\qquad \langle n\,|\,A_\mu(0)\,|\,\Sigma^-\rangle = \frac{i}{(2\pi)^{\frac{3}{2}}}\bar{u}^{(n)}\int \mathrm{d}x\,\exp[-ip^{(n)}x]\langle 0\,|\,[A_\mu(0),\,\psi(x)]\,\theta(-x)\,|\,\Sigma^-\rangle\,,$$

$$(66')\qquad \langle n\,|\,V_\mu(0)\,|\,\Sigma^-\rangle = \frac{i}{(2\pi)^{\frac{3}{2}}}\bar{u}^{(n)}\int \mathrm{d}x\,\exp[-ip^{(n)}x]\langle 0\,|\,[V_\mu(0),\,\psi(x)]\,\theta(-x)\,|\,\Sigma^-\rangle\,,$$

where

$$(67)\qquad \psi(x) = \left(\gamma\frac{\partial}{\partial x} + m\right)\psi^{(n)}(x)\,.$$

These equations show that (66) and (66′) have the structure of Fourier transforms of advanced commutators and one is thus led to assume that they

(12) G. PUPPI: private communication.

are analytic in the lower complex ω-plane, where ω is the neutron energy. In the Σ rest system one has

$$t = 2m_\Sigma(\omega_0 - \omega)\,, \tag{68}$$

with

$$\omega_0 = \frac{m_N^2 + m_\Sigma^2}{2m_\Sigma}\,, \tag{68'}$$

and therefore it would follow that the form factors $a(t)$, $b(t)$, $b'(t)$, $c(t)$, $d'(t)$, $d(t)$ are analytic in the upper complex t-plane. It can also be seen that the terms that we have neglected with equal time commutators give contributions of the same form as those from subtraction terms in the dispersion relations for $a(t)$ and $c(t)$. We therefore postulate subtracted dispersion relations for $a(t)$ and $c(t)$

$$a(t) = G_A + \frac{t}{\pi}\int \mathrm{d}t' \frac{\mathrm{Im}\, a(t')}{t'(t' - t - i\varepsilon)}\,, \tag{69}$$

$$c(t) = G_V + \frac{t}{\pi}\int \mathrm{d}t' \frac{\mathrm{Im}\, c(t')}{t'(t' - t - i\varepsilon)}\,, \tag{69'}$$

and unsubtracted dispersion relations for the remaining form factors $b(t)$, $b'(t)$, $d(t)$, $d'(t)$. For instance for $b(t)$

$$b(t) = \frac{1}{\pi}\int \mathrm{d}t' \frac{\mathrm{Im}\, b(t')}{t' - t - i\varepsilon}\,, \tag{70}$$

G_A and G_V are the renormalized axial and vector coupling constants. Of course they may be quite different from the corresponding renormalized constants of β decay. From (66) and (66') we find for the absorptive parts P_μ, of $\langle n|A_\mu(0)|\Sigma^-\rangle$ and Q_μ of $\langle n|V_\mu(0)|\Sigma^-\rangle$

$$P_\mu = (2\pi)^{\frac{3}{2}}\pi \sum_z \langle 0|A_\mu(0)|z\rangle \bar{u}^{(n)}\langle z|\Psi(0)|\Sigma^-\rangle\, \delta(p^{(\Sigma)} - p^{(n)} - p^{(z)})\,, \tag{71}$$

$$Q_\mu = (2\pi)^{\frac{3}{2}}\pi \sum_z \langle 0|V_\mu(0)|z\rangle \bar{u}^{(n)}\langle z|\Psi(0)|\Sigma^-\rangle\, \delta(p^{(\Sigma)} - p^{(n)} - p^{(z)})\,. \tag{71'}$$

Actually the summation is supposed to be one-half over the complete set of « in » states and one-half over the complete set of « out » states in order to preserve at any stage the reality conditions (1). The states z that contribute are different for Σ^- and Σ^+. In the Σ^- decay one has the states K^-, $K^-\pi^0$, $\bar{K}^0\pi^-$, $\bar{K}+2\pi$, etc. In the Σ^+ decay, there is no bound state contribution, and then one has $\bar{K}^0\pi^+$, $\bar{K}+2\pi$, etc.

4·2. – The bound state contribution in Σ^- decay, can be related to the S-matrix element for $K^- \to l^- + \bar{\nu}$.

$$\langle l^- \bar{\nu}; \text{out} | K^-; \text{in} \rangle = 2i\pi\, \delta(p^{(K)} - p^{(l)} - p^{(\nu)})(\bar{u}^{(l)} \gamma_\mu a u^{(\nu)}) \langle 0 | A_\mu(0) | K^- \rangle . \tag{72}$$

On invariance arguments

$$\langle 0 | A_\mu(0) | K^- \rangle = -\frac{1}{(2\pi)^{\frac{3}{2}}} p_\mu^{(K)} F(p^{(K)^2}) . \tag{73}$$

From (73) the decay probability is

$$\Gamma = \frac{m_l^2 F'^2(-m_K^2)}{\pi m_K} \left(\frac{m_K^2 - m_l^2}{2m_K} \right)^2 . \tag{74}$$

On the other hand

$$(2\pi)^3 \bar{u}^{(n)} \langle K^- | \psi(0) | \Sigma^- \rangle = \sqrt{2}\, g (\bar{u}^{(n)} i\gamma_5 u^{(\Sigma)}) , \tag{75}$$

where g is the renormalized coupling constant for $\Sigma^- \to K^- + n$. The bound state term of P_μ can thus be written as

$$\frac{\pi g F(-m_K^2)}{\Gamma_2 (2\pi)^3} \frac{\Delta_\mu}{2(|\boldsymbol{\Delta}|^2 + m_K^2)^{\frac{1}{2}}} \delta(\Delta^0 - \sqrt{|\boldsymbol{\Delta}|^2 + m_K^2})\, (\bar{u}^{(n)} \gamma_5 u^{(\Sigma)}) . \tag{76}$$

This term contributes only to Im $b(t)$ which becomes

$$\text{Im}\, b(t) = -\sqrt{2}\, \pi g F(-m_K^2) \delta(t - m_K^2) . \tag{77}$$

Substituting into (70) one finds

$$b(t) = g \frac{\sqrt{2} F(-m_K^2)}{t - m_K^2} . \tag{78}$$

There is no contribution to Q_μ from the bound state. From(64) one sees that the bound state contributes an effective pseudoscalar coupling with an energy coupling constant

$$G_p(t) = m_l \frac{\sqrt{2} g F(-m_K^2)}{t - m_K^2} . \tag{79}$$

The magnitude of $F(-m_K^2)$ can be obtained from the K^- lifetime and from its branching ratio for $K \to l + \nu$. From (79) we see that the bound state contribution will be negligible for electronic decays, and thus we limit

our considerations to muonic decays. From the present data one finds

$$m_\mu F(-m_K^2) \cong 3 \cdot 10^{-8} . \tag{80}$$

One also finds that the t dependence in (79) is very weak. In fact in the physical region for t one always has $m_K^2 \gg t$. We take for the factor $(t - m_K)^{-1}$ an average value between its two extremes

$$\overline{(t - m_K^2)^{-1}} \cong -4.9 \cdot 10^{-6} \text{ MeV}^{-2} . \tag{81}$$

From (79), (80) and (81) we find an average value of G:

$$\overline{G_p} = g\, 2.1 \cdot 10^{-13} \text{ MeV}^{-2} , \tag{82}$$

which has to be compared with the value of the unrenormalized Fermi constant $\cong 2.2 \cdot 10^{-11}$ MeV^{-2}. With the present, rather unprecise values of g from associated production, $\overline{G_p}$ is one order of magnitude smaller than the unrenormalized Fermi constant.

We can also evaluate what would be the partial rate of Σ^- decay in $n + \mu^- + \bar{\nu}$, if only this bound state contribution were present. The figure we find is

$$\tau^{-1} \cong 2.8 \cdot 10^{-18} g^2 \text{ MeV} , \tag{83}$$

which has to be compared with the total rate for $\Sigma^- \to n + \mu^- + \bar{\nu}$ calculated assuming an $A-V$ interaction Lagrangian with the same constants as for β decay and neglecting any correction from strong interactions ([2]), which is $\cong 0.9 \cdot 10^{-13}$ MeV. Even allowing for a reduction by a factor ten or twenty in such a rate, as suggested by the recent data ([13]) one has still presumably to do with a small contribution.

4·3. – As to the contribution from the $K\pi$ states we are unfortunately unable to come to definite quantitative conclusions because one would need some analytic continuations of amplitudes for associated production that are not known at present. We therefore limit ourselves in giving the relevant formulae in the hope that some quantitative statement will be possible in a near future. The $K + \pi$ states contribute only to the vector term $\langle n | V_\mu(0) | \Sigma^- \rangle$. The relevant matrix elements are exhibited in (72′). The matrix elements of

([13]) F. S. CRAWFORD, M. CRESTI, M. L. GOOD, G. R. KALBFLEISCH, M. L. STEVENSON and H. K. TYCHO: *Phys. Rev. Lett.*, **1**, 377 (1958); P. NORDIN, J. OREAR, L. REED, A. H. ROSENFELD, F. T. SOLMITZ, H. D. TAFT and R. D. TRIPP: *Phys. Rev. Lett.*, **1**, 380 (1958).

$\langle 0|V_\mu(0)|K\pi\rangle$ can be related to the matrix element $V_\mu(p^{(\pi)}, p^{(K)})$ for $K\to\pi+l+\nu$ defined in (21) and already discussed

$$\langle 0|V_\mu(0)|K^-\pi^0;\,\mathrm{in}\rangle = V_\mu(-p^{(\pi)}, p^{(K)})\,, \tag{84}$$

$$\langle 0|V_\mu(0)|\bar{K}^0\pi^-;\,\mathrm{in}\rangle = V^{(0)}_\mu(-p^{(\pi)}, p^{(K)})\,. \tag{84'}$$

For the other matrix elements one can write

$$\bar{u}^{(n)}\langle K^-\pi^0;\,\mathrm{in}|\Psi(0)|\Sigma^-\rangle = \langle\Sigma^-|\Psi(0)^\dagger\gamma_4 u^{(n)}|K^-\pi^0;\,\mathrm{in}\rangle^*\,. \tag{85}$$

and one can reduce them to analytic continuations of matrix elements for associated production. We define

$$\langle\Sigma^-K^+;\,\mathrm{out}|n\pi^0;\,\mathrm{in}\rangle = i(2\pi)^{\frac{8}{2}}\langle\Sigma^-K^+;\,\mathrm{out}|\Psi(0)^\dagger\gamma_4 u^{(n)}|\pi^0\rangle\cdot \tag{86}$$
$$\cdot\delta(p^{(\pi)}+p^{(n)}-p^{(\Sigma)}-p^{(K)}) = 2\pi i(\bar{u}^{(\Sigma)}[\tfrac{2}{3}\mathcal{F}_{\frac{1}{2}}(p^{(\Sigma)}, p^{(K)}, p^{(\pi)})+$$
$$+\tfrac{1}{3}\mathcal{F}_{\frac{3}{2}}(p^{(\Sigma)}, p^{(K)}, p^{(\pi)})]u^{(n)})\,\delta(p^{(\pi)}+p^{(n)}-p^{(\Sigma)}-p^{(K)})\,,$$

and similarly

$$\langle\Sigma^-K^0;\,\mathrm{out}|n\pi^-;\,\mathrm{in}\rangle = 2\pi i(\bar{u}^{(\Sigma)}\mathcal{F}_{\frac{3}{2}}(p^{(\Sigma)}, p^{(K)}, p^{(\pi)})u^{(n)})\,\delta(p^{(\pi)}+p^{(n)}-p^{(\Sigma)}-p^{(K)}). \tag{86'}$$

Furthermore

$$\langle\Sigma^-|\Psi(0)^\dagger\gamma_4|K^-\pi^0;\,\mathrm{in}\rangle = \tag{87}$$
$$= \frac{i}{(2\pi)^{\frac{3}{2}}}\int \mathrm{d}x\langle\Sigma^-|(\Box-m_K^2)\,T(\varphi^{(K)}(x)\Psi(0)^\dagger)\gamma_4|\pi^0\rangle\exp[ip^{(K)}x],$$

$$\langle\Sigma^-K^+;\,\mathrm{out}|\Psi(0)^\dagger\gamma_4|\pi^0;\,\mathrm{in}\rangle = \tag{87'}$$
$$= \frac{i}{(2\pi)^{\frac{3}{2}}}\int \mathrm{d}x\langle\Sigma^-|(\Box-m_K^2)\,T(\varphi^{(K)}(x)\Psi(0)^\dagger)\gamma_4|\pi^-\rangle\exp[-ip^{(K)}x],$$

which shows that the two matrix elements are related through the substitution $p^{(K)}=-p^{(K)}$. Therefore, using (85), (86) and (86'), we get

$$\bar{u}^{(n)}\langle K^-\pi^0;\,\mathrm{in}|\Psi(0)|\Sigma^-\rangle = \frac{1}{(2\pi)^{\frac{3}{2}}}\bar{u}^{(n)}\left[\frac{2}{3}\gamma_4\mathcal{F}^+_{\frac{1}{2}}(p^{(\Sigma)}, -p^{(K)}, p^{(\pi)})\gamma_4+\right. \tag{88}$$
$$\left.+\frac{1}{3}\gamma_4\mathcal{F}^+_{\frac{3}{2}}(p^{(\Sigma)}, -p^{(K)}, p^{(\pi)})\gamma_4\right]u^{(\Sigma)}\,,$$

$$\bar{u}^{(n)}\langle\bar{K}^0\pi^-;\,\mathrm{in}|\Psi(0)|\Sigma^-\rangle = \frac{1}{(2\pi)^{\frac{3}{2}}}\bar{u}^{(n)}\gamma_4\mathcal{F}^+_{\frac{3}{2}}(p^{(\Sigma)}, -p^{(K)}, p^{(\pi)})\gamma_4 u^{(\Sigma)}. \tag{88'}$$

The resulting expression for Q_μ is

$$(89)\quad Q_\mu = \tfrac{1}{2}\pi\int \mathrm{d}^3p^{(\mathrm{K})}\mathrm{d}^3p^{(\pi)}(4p_0^{(\mathrm{K})}p_0^{(\pi)})^{-1}\,\bar{u}^{(\mathrm{n})}\{\tfrac{2}{3}\gamma_4\mathcal{F}^{\dagger}_{\frac{1}{2}}(p^{(\Sigma)}, -p^{(\mathrm{K})}, p^{(\pi)})\gamma_4 V_\mu(-p^{(\pi)}, p^{(\mathrm{K})}) +$$

$$+\gamma_4\mathcal{F}^{\dagger}_{\frac{3}{2}}(p^{(\Sigma)}, -p^{(\mathrm{K})}, p^{(\pi)})[\tfrac{1}{3}V_\mu(-p^{(\pi)}, p^{(\mathrm{K})}) + V^{(0)}_\mu(-p^{(\pi)}, p^{(\mathrm{K})})]\}\,u^{(\Sigma)},$$

+ a similar contribution from the summation over « out » states, that makes Q_μ real at this stage of approximation.

It is unfortunately impossible at present to push the analysis up to numerical results because of the lack of information on the relevant associated production amplitudes. However, from the smallness of the bound state contribution we are led to suggest a rough description in terms of the two subtraction terms alone, that is neglecting all strong interaction effects apart from renormalization of the constants. In such a case one may use a procedure similar to the one we have used for K-decays. One can calculate the two renormalized coupling constants for $\Sigma^- \to \mathrm{n} + \mathrm{l}^- + \bar{\nu}$ the axial coupling constant and the vector coupling constant, from the measured rates for decay into e^- and into μ^-, and then compute the final spectra of the secondaries.

* * *

We are indebted to Dr. W. Gross for useful discussions on the mathematical aspects of the work.

Appendix

A.1. – The singular integral equations of the form

$$(A.1)\qquad u(x) = f(x) + \frac{1}{\pi}\int_1^\infty \frac{h^*(x')\,u(x')\,\mathrm{d}x'}{x' - x - i\varepsilon}\,,$$

have already been discussed by Omnes [10]. In this Appendix we shall be concerned with the properties of equation (A.1) and the form of its solutions. We shall slightly correct Omnes' solution which cannot literally be applied to our case, and we shall also derive a simpler form for the solution of (A.1), that is valid in practice in most cases, and compare it to the more complicated Omnes solution. We shall also discuss the meaning of the different subtractions as directly applied to equation (A.1). We think that most of the content of this Appendix is perhaps already known to many people. Actually the simpler solution that we find has apparently already been used by Goldberger,

FEDERBUSH and TREIMAN [14] in a particular case. We also do not claim any mathematical rigour in our deductions.

We assume that it is possible to define an analytic continuation for $f(x)$, $f(z)$, that is regular along the cut. The cut goes from 1 to ∞ on the real axis. The more general case including possible poles of $f(z)$ along the cut con also be treated, but for simplicity we limit ourselves to the simpler case. Let us define

$$U(z) = f(z) + \frac{1}{\pi}\int_1^\infty \frac{h^*(x')u(x')\,dx'}{x'-z}\,. \tag{A.2}$$

It follows

$$u(x) = U(x+i\varepsilon) \tag{A.3}$$

and, from (A.2) and (A.3)

$$\log U(x+i\varepsilon) = \log U(x-i\varepsilon) + 2i\alpha(x)\theta(x-1)\,, \tag{A.4}$$

where $\alpha(x)$ is such that

$$h^*(x) = \sin\alpha(x)\exp[-i\alpha(x)]\,. \tag{A.5}$$

With the « ansatz »

$$U(z) = G(z)\exp[\tau(z)]\,, \tag{A.6}$$

where $G(z)$ is assumed to be regular along the cut, (A.4) takes the form

$$\tau(x+i\varepsilon) - \tau(x-i\varepsilon) = 2i\alpha(x)\theta(x-1) \tag{A.7}$$

and can be satisfied with

$$\tau(z) = \frac{1}{\pi}\int_1^\infty \frac{\alpha(x')\,dx'}{x'-z}\,. \tag{A.8}$$

At this point we note that if the last integral does not converge, one may still obtain a convergent solution by repeated subtractions in (A.8). The once-subtracted form is

$$\tau(z) = \frac{z}{\pi}\int_1^\infty \frac{\alpha(x')\,dx'}{x'(x'-z)}\,, \tag{A.9}$$

and so on.

---

[14] P. FEDERBUSH, M. L. GOLDBERGER and S. B. TREIMAN: *Phys. Rev.*, **112**, 642 (1958).

A.2. – A solution $G(z)$ that is regular along the cut is

$$q(z) = f(z)\exp[-\tau(z)] - \frac{1}{2\pi i}\int_C \frac{f(\zeta)\exp[-\tau(\zeta)]\,d\zeta}{\zeta - z}, \tag{A.10}$$

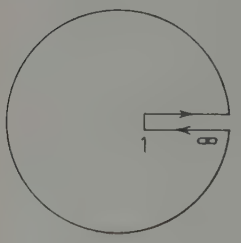

Fig. 1.

with the integration path C as given in Fig. 1. In fact, assuming that the integral on the circle at infinity goes to zero, one finds

$$G(z) = f(z)\exp[-\tau(z)] - \tag{A.11}$$

$$-\frac{1}{2\pi i}\int_1^\infty \frac{f(x)\,dx}{x - z}\left(\exp[-\tau(x + i\varepsilon)] - \exp[-\tau(x - i\varepsilon)]\right),$$

with ε infinitesimal, from which

$$G(x + i\varepsilon) - G(x - i\varepsilon) = 0\,. \tag{A.12}$$

We next show that $G(x)\exp[\tau(x+i\varepsilon)]$ is actually a solution. Let us first evaluate the integral

$$\frac{1}{2\pi i}\int_C \frac{G(z)\exp[\tau(z)]\,dz}{z - z_0} = \frac{1}{2\pi i}\int_{C'} \frac{f(z)\,dz}{z - z_0} - \tag{A.13}$$

$$-\frac{1}{2\pi i}\int_{C'} \frac{dz}{z - z_0}\exp[\tau(z)]\,\frac{1}{2\pi i}\int_C \frac{f(\zeta)\exp[-\tau(\zeta)]\,d\zeta}{\zeta - z},$$

where the integration path C' is internal but infinitesimally close to C, and z_0 is internal to C'. On the right hand side of (A.13) the first integral reduces to an integral over the circle at infinity because $f(z)$ is supposed to be regular on the cut, and we assume it is zero. The second integral gives

$$-\frac{1}{2\pi i}\exp[\tau(z_0)]\int_C \frac{f(\zeta)\exp[-\tau(\zeta)]\,d\zeta}{\zeta - z_0}, \tag{A.14}$$

since there are no other singularities of the integrand. Therefore

$$\frac{1}{2\pi i}\int_C \frac{G(z)\exp[\tau(z)]\,dz}{z - z_0} = (\text{A.14}) = G(z_0)\exp[\tau(z_0)] - f(z_0)\,, \tag{A.15}$$

the last step following directly from (A.10). The integral on the left-hand side of (A.15) can be written as

$$\frac{1}{2\pi i}\int_1^\infty \frac{G(x)\,dx}{x - z_0}\left(\exp[\tau(x + i\varepsilon)] - \exp[\tau(x - i\varepsilon)]\right)dx\,, \tag{A.16}$$

assuming that the contribution from the circle at infinity goes to zero.

Using (A.7) and (A.5) one finds from this last expression

$$G(z_0)\exp[\tau(z_0)] - f(z_0) = \frac{1}{\pi}\int_1^\infty \frac{h^*(x')G(x')\exp[\tau(x'+i\varepsilon)]}{x'-z_0}\,, \tag{A.17}$$

and comparing with (A.1) we find that $G(x)\exp[\tau(x+i\varepsilon)]$ is indeed a solution $u(x)$.

A.3. – To put the solution in the form given by Omnes, let us evaluate $G(z)\exp[\tau(z)]$ from (A.10). We find using (A.7) and (A.5)

$$G(z)\exp[\tau(z)] = f(z) + \frac{1}{\pi}\exp[\tau(z)]\int_1^\infty \frac{\mathrm{d}x'\, f(x')h(x')\exp[-\tau(x'-i\varepsilon)]}{x'-z}\,. \tag{A.18}$$

From (A.18) one can derive a formula for $u(x)$

$$u(x) = G(x)\exp[\tau(x+i\varepsilon)] = \Big[f(x)\cos(\alpha(x)\theta(x-1)) + \\ + \frac{1}{\pi}\exp[\varrho(x)]P\int_1^\infty \frac{\mathrm{d}x'\, f(x')\sin\alpha(x')\exp[-\varrho(x')]}{x'-x}\Big]\exp[i\alpha(x)\theta(x-1)]\,,$$

with

$$\varrho(x) = \frac{1}{\pi}P\int_1^\infty \frac{\alpha(x')\,\mathrm{d}x'}{x'-x}\,, \tag{A.20}$$

which coincides with that given by Omnes for all $x > 1$. To the solution (A.19) one can always add a solution of the omogeneous equation. This additional term must be specified in such a way that the solution has the wanted behaviour at infinity and at $x = 1$; (A.19) however, is the only solution which in the limit $\lambda \to 0$ coincides with the iteration solution of eq. (A.1).

A.4. – It was essential in all our considerations to assume the vanishing of integrals on the circle at infinity. It is convenient to check these assumptions for any particular case. If $f(z)$ does not vanish rapidly enough at infinity one may formally use a subtraction procedure applied directly to (A.1). Let us write formally

$$u(x) - u(0) = f(x) - f(0) + \frac{x}{\pi}\int_1^\infty \frac{h^*(x')u(x')\,\mathrm{d}x'}{x'(x'-x-i\varepsilon)}\,. \tag{A.21}$$

Putting $u_1(x) = x^{-1}u(x)$, (A.21) takes the form

$$u_1(x) = f_1(x) + \frac{1}{\pi}\int_1^\infty \frac{h^*(x')u_1(x')\,\mathrm{d}x'}{x'-x-i\varepsilon}\,, \tag{A.22}$$

where $f_1(x) = x^{-1}[f(x) - f(0) + u(0)]$. If $f(x) \to x^n$ as $x \to \infty$, then $f_1(x) \to x^{n-1}$ and the procedure can be continued until one is left with an inhomogeneous term $f_{n+1}(x)$ going like x^{-1}.

A.5. – The complicated form of the solution (A.18), which contains a double integration, makes its use often unpractical. It is therefore more convenient to try to evaluate $G(z)$ directly from (A.10). This is certainly always possible if $f(z)$ has a finite number of isolated poles inside C. Suppose, as it happens in our case, that $f(z)$ has a single pole at $z = 0$, and specifically

$$f(z) \exp[-\tau(z)] = \frac{a_{-2}}{z^2} + \frac{a_{-1}}{z} + \text{regular terms} . \tag{A.23}$$

To evaluate the integral in (A.10) one needs the residui of the integrand at its two poles, at the origin $\zeta = 0$ and $\zeta = z$. The residuum at the latter pole cancels the first term on the right hand side of (A.10), while the residuum at $\zeta = 0$ again originates the non-regular terms of (A.23). Then

$$G(z) = \frac{a_{-2}}{z^2} + \frac{a_{-1}}{z} , \tag{A.24}$$

from which

$$u(x) = \left(\frac{a_{-2}}{x^2} + \frac{a_{-1}}{x} \right) \exp[\tau(x + i\varepsilon)] , \tag{A.25}$$

where $\tau(z)$ is given either by (A.8) or, if necessary, by a subtracted form of (A.8), such as (A.9)..

Provided the assumptions on the vanishing of the integrals at infinity are satisfied, the solution (A.25) coincides with that obtained with the Omnes method. For instance, for the case considered in the text, it is very easy to check that such assumptions are verified, as shown briefly in A.3. The example illustrates clearly the advantage of starting directly from (A.10), whenever it is possible to reduce the integration to the evaluation of residui, instead of going through the much more complicated explicit representation (A.18).

RIASSUNTO

I modi di decadimento K -> π + leptone carico + ν e Y -> N + leptone carico + ν vengono studiati con tecniche di relazione di dispersione. Gli spettri finali per i decadimenti K_3 sono ricavati dalla soluzione di una equazione integrale per l'ampiezza di decadimento. I metodi di soluzione per tali equazioni vengono esposti brevemente.

IL NUOVO CIMENTO Vol. XIII, N. 6 16 Settembre 1959

On a Relation between Scattering and Production Amplitudes (*).

J. Sucher and T. B. Day

University of Maryland - College Park, Md.

(ricevuto il 15 Maggio 1959)

Summary. — An integral equation is derived which exhibits directly the relation between an amplitude for production, including all interactions, and the corresponding amplitude for complete scattering between the initial particles alone, and between the final particles alone. The only non-measurable quantity involved in this relatively simple relation is shown to be an amplitude for « pure production » in which intermediate states with either the initial particles or the final particles are excluded.

1. – Introduction.

The importance of « final state » interaction in many processes involving the production of elementary particles is well known. There exist, however, reactions in which the *initial* particles may also interact strongly, and in which the complementary concept of « initial state » interaction may play an equally important role. We have in mind particularly the K^--p reactions, *e.g.*, $K^- + p \to \Sigma + \pi$.

We would like to consider the following question: given complete information concerning the scattering interaction between the initial particles, as well as between the final particles, what can be said about the production process complete with all interactions?

(*) This research was supported in part by the United States Air Force through the Air Force Office of Scientific Research of the Air Research and Development Command.

More precisely, we consider the following problem: let the three physical processes

$$\text{A} + \text{B} \to \text{A} + \text{B} \tag{1a}$$

$$\text{A} + \text{B} \to \text{C} + \text{D} \tag{1b}$$

$$\text{C} + \text{D} \to \text{C} + \text{D} \tag{1c}$$

have the matrix elements M_{ii}, M_{fi}, and M_{ff} respectively for scattering between initial particles A and B, production of final particles by initial particles, and scattering between final particles C and D. Let P_{fi} denote the value that M_{fi} would have if there were no final state or initial state interactions, *i.e.*, if, in the production process, no intermediate state appeared in which there were either particles A and B together or particles C and D together. Thus P_{fi} is a quantity which may be simply related to an effective « production potential » for the process (1*b*), and might be calculated directly (cf. Fig. 1).

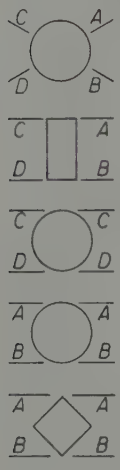

Fig. 1. – Component amplitudes used in the derivation of equation (13).

Then we ask: does there exist a relation such that knowledge of the physical amplitudes M_{ii} and M_{ff} determines M_{fi}; if not, is the additional knowledge, say from calculation, of the non-physical « pure production » amplitude P_{fi}, enough to determine M_{fi}; or must still further information be supplied?

Section 2 answers these questions by deriving a relatively simple relation, which holds rigorously between M_{ii}, M_{ff}, M_{fi}, and P_{fi} alone. Section 3 discusses this result.

2. – Integral equation for production amplitude.

The matrix element for the process (1*b*) is given by

$$M_{fi} = M_{fi}(q_{\text{C}}, q_{\text{D}}; q_{\text{A}}, q_{\text{B}}) = \langle q_{\text{C}}, q_{\text{D}} | T | q_{\text{A}}, q_{\text{B}} \rangle , \tag{2}$$

where, for example, q_{A} denotes the quantum numbers associated with a plane wave state of particle A. As usual, T satisfies

$$T = H_1 + H_1 G T , \tag{3}$$

with

$$G = (E - H_0 + i\varepsilon)^{-1} . \tag{4}$$

We note that the « pure-production » amplitude may be written as

$$P_{fi} = \langle q_C, q_D | T_P | q_A, q_B \rangle , \tag{5}$$

where T_P is a « pure production » operator satisfying

$$T_P = H_1 + H_1 G_P T_P , \tag{6}$$

and

$$G_P = G(1 - \Lambda_{f,i}) . \tag{7}$$

Here $\Lambda_{f,i}$ is a projection operator with the properties

$$\begin{cases} \Lambda_{f,i} | q'_A, q'_B \rangle = | q'_A, q'_B \rangle , \\ \Lambda_{f,i} | q'_C, q'_D \rangle = | q'_C, q'_D \rangle , \end{cases} \tag{8a}$$

and

$$\Lambda_{f,i} | \rangle = 0 , \tag{8b}$$

for $|\rangle$ any other eigen-state of H_0.

Now define a quantity

$$s_i = \langle q'_A, q'_B | T_s | q_A, q_B \rangle , \tag{9}$$

where

$$T_s = H_1 + H_1 G_s T_s , \tag{10}$$

with

$$G_s = G(1 - \Lambda_f) . \tag{11}$$

Here Λ_f is another projection operator satisfying

$$\Lambda_f | q'_C, q'_D \rangle = | q'_C, q'_D \rangle , \tag{12}$$

and Λ_f is zero acting on other eigenstates of H_0.

Then, the expression obtained for M_{fi} is

$$M_{fi} = P_{fi} + M_{ff} \cdot P_{fi} + P_{fi} \cdot s_i + M_{ff} \cdot P_{fi} \cdot s_i . \tag{13}$$

The « dot » multiplication is illustrated by the example

$$M_{ff}\cdot P_{fi}=\sum_{n=(q'_C,\,q'_D)}\frac{M_{ff}(q_C,\,q_D;\,q'_C,\,q'_D)P_{fi}(q'_C,\,q'_D;\,q_A,\,q_B)}{E-E_n+i\varepsilon}\,. \tag{14}$$

Equation (13) is shown graphically in Fig. 2, where the circles mean that all possible intermediate states are included, the upright rectangle means that

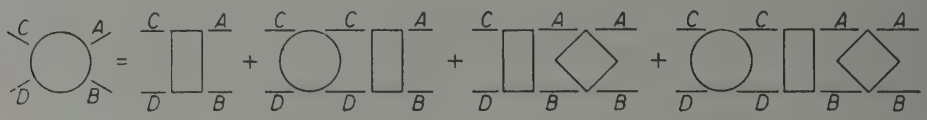

Fig. 2. – Graphical display and proof of equation (13).

intermediate states of the form $|q'_A, q'_B\rangle$ *or* $|q'_C, q'_D\rangle$ are excluded and the tilted square means that only states of the form $|q'_C, q'_D\rangle$ are excluded as intermediate states (these components of Fig. 2 are illustrated in Fig. 1). This graphical representation may be taken as a proof of equation (13) when it is realized that every (time ordered) Feynman diagram which contributes to M_{fi} is contained exactly once in the diagrams as grouped on the right hand side of the graph equality sign. (It is clear that a non-graphical proof will involve only straightforward algebraic manipulation of propagators.)

We now seek to eliminate from equation (13) the non-physical amplitude s_i in favour of the physical one M_{ii}.

If we define two quantities M_{if} and P_{if} entirely analogous to M_{fi} and P_{fi}, only describing the *inverse* production process

$$\mathrm{C}+\mathrm{D}\to\mathrm{A}+\mathrm{B}\,, \tag{16'}$$

then we can see immediately that

$$M_{ii}=s_i+P_{if}\cdot M_{fi}+s_i\cdot P_{if}\cdot M_{fi}\,. \tag{15}$$

This equation is written graphically in Fig. 3, which again constitutes a proof.

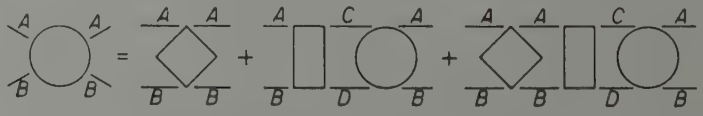

Fig. 3. – Graphical display and proof of equation (15).

If we substitute s_i from equation (15) into equation (13), and manipulate the result into a form where equation (13) may be used again to remove the

remaining terms involving s_i, we get as our result

$$M_{fi} = P_{fi} + P_{fi} \cdot M_{ii} + M_{ff} \cdot P_{fi} + M_{ff} \cdot P_{fi} \cdot M_{ii} - M_{fi} \cdot P_{if} \cdot M_{fi} . \tag{16}$$

Thus, the non-physical amplitude s_i has been eliminated. This result is displayed in Fig. 4.

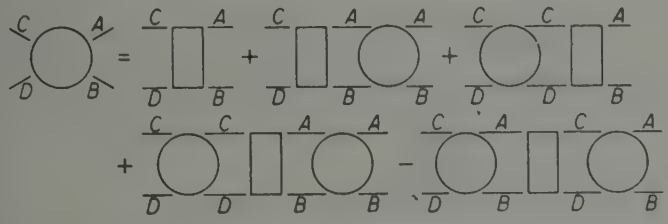

Fig. 4. – Graphical display of equation (16).

Equation (16) now represents a relation between the physical production and scattering amplitudes, with only one non-physical amplitude involved, the pure-production amplitude P_{fi}. It should be noted that

$$P_{if} = (P^*_{fi})_{\varepsilon \to -\varepsilon} . \tag{17}$$

If we regard M_{ii}, M_{ff}, and P_{fi} as known, then equation (16) represents a non-linear integral equation for the determination of M_{fi}. A closed but formal expression for M_{fi} may be obtained from equation (16), in terms of the inhomogeneous part Q_{fi},

$$Q_{fi} = P_{fi} + P_{fi} \cdot M_{ii} + M_{ff} \cdot P_{fi} + M_{ff} \cdot P_{fi} \cdot M_{ii} , \tag{18}$$

and the «kernel» P_{if}. Upon expansion one obtains the iteration solution:

$$M_{fi} = \tfrac{1}{2} \sum_{n=1}^{\infty} a_n [Q_{fi} \cdot P_{if} \cdot Q_{fi} \cdot P_{if} \ldots \cdot Q_{fi}] , \tag{19}$$

where the n-th term contains n factors Q_{fi} and a_n is defined by

$$(1 + 4x)^{\frac{1}{2}} - 1 = \sum_{n=1}^{\infty} a_n x^n . \tag{20}$$

The closed form may be inferred from (19) and (20). The result (19) may be useful in certain cases.

3. – Discussion.

Equation (16) is the desired result. It exhibits a relation between the amplitudes involved in the production process in such a way that all amplitudes except one have a direct physical meaning (and are, in principle, measurable). It should be emphasized that equation (16) is rigorously true, independent of perturbation theory or of the form of the interaction.

In order to use equation (16), the quantity P_{fi}, must somehow be calculated. Once this is done, equation (16) may be used as a consistency check, if all other quantities are measured and suitably extended off the energy shell. Or, it may be used to calculate a physically measurable quantity from measurements of the other amplitudes.

In the above we have assumed that no bound states can be formed. Complications of this type may be considered elsewhere. At present we are studying the possibility of applying equation (16) to a situation in which such complications are not important, in particular, the $K^- + p \to \Sigma + \pi$ reaction in flight.

* * *

This investigation was initiated as a result of some questions put to the authors by Professor G. A. Snow. We wish to thank Professor Snow and Professor S. Oneda for several stimulating discussions.

RIASSUNTO (*)

Si deriva un'equazione integrale che mostra direttamente la relazione tra una ampiezza di produzione, comprendente tutte le interazioni, e la corrispondente ampiezza di scattering completo tra le sole particelle iniziali e tra le sole particelle finali. Si dimostra che la sola grandezza non misurabile comparente in questa relazione relativamente semplice è un'ampiezza di « produzione pura » nella quale sono esclusi stati intermedi sia con le particelle iniziali che con le particelle finali.

(*) *Traduzione a cura della Redazione.*

IL NUOVO CIMENTO Vol. XIII, N. 6 16 Settembre 1959

Note on Anomalous K^+-Decay Events.

K. Hiida

Research Institute for Fundamental Physics, Kyoto University - Kyoto

(ricevuto il 18 Maggio 1959)

Summary. — The π^+-energy spectrum for the radiative θ^+-decay mode is calculated and it is shown that that π^+-energy spectrum has no peak at ~ 60 MeV. Therefore there is no strong evidence to assert that two anomalous K^+-decay events (with a π^--secondary of about 60 MeV) are due more probably to the radiative θ^+-decay mode than to a two body decay mode: $K^+ \to \pi^+ + X^0$, where X^0 is a neutral boson with a mass of (500 ± 5) times the electron mass.

Two years ago the Columbia nuclear emulsion group (1) has found an anomalous K^+-decay event with a π^+-secondary of (60 ± 1) MeV which exceeds the 53.3 MeV upper limit for the τ'^+-decay mode and is less than the 107.7 MeV of the θ^+-decay mode. They propose this event as the first observed case of the possible decay mode: $K^+ \to \pi^+ + \pi^0 + \gamma$. The main reasons why they arrive at this conclusion are as follows: Assuming a direct electric dipole or magnetic dipole transition (2) from the K^+-state to the $(\pi^+ + \pi^0)$-state, the π^+-energy spectrum for the radiative θ^+-decay mode has a broad peak at ~ 60 MeV. For the π^+-secondary of 60 MeV, the emitted photon energy is greater than 55 MeV. The contribution which comes from the mechanism of internal bremsstrahlung (2) decreases rapidly with the photon energy. Therefore they have concluded that this contribution might be negligible in the energy region of their event.

Recently a similar event has been found in Bristol and analysed in

---

(1) G. Harris, J. Lee, J. Orear and S. Taylor: *Phys. Rev.*, **108**, 1561 (1957).
(2) R. H. Dalitz: *Phys. Rev.*, **99**, 915 (1955).

Los Angeles [3]. The reported value of the energy of a π^+-secondary is (61.7 ± 1.5) MeV. Because of the broad peak of the π^+-energy spectrum at ~ 60 MeV for the radiative θ^+-decay mode, PROWSE and EVANS [3] have concluded that both events are due more probably to the radiative θ^+-decay mode than to a two body decay mode: $K^+ \to \pi^+ + X^0$, where X^0 is a neutral boson with a mass of (500 ± 5) times the electron mass. The purpose of this note is to point out that for the radiative θ^+-decay mode the contribution which comes from the mechanism of internal bremsstrahlung is not negligible even in the energy region of these events and that the π^+-energy spectrum has no peak at ~ 60 MeV.

Assuming that the spin of the K-particle is zero and the parity is not conserved in weak decay interactions, then we have the following matrix elements for the θ^+- and the radiative θ^+-decay mode respectively.

$$(1)\qquad \begin{cases} \mathcal{M} = (2\pi)^4 G(p, p_1, p_2)\, \delta(p - p_1 - p_2) \\ \text{and} \\ \mathcal{M}_R = (2\pi)^4 \sqrt{4\pi\alpha}\, \delta(p - p_1 - p_2 - k) \cdot \\ \cdot \left\{ G(p, p_1 + k, p_2) \dfrac{(\boldsymbol{p}_1 \cdot \boldsymbol{\epsilon})}{p_1 \cdot k} + \dfrac{(\boldsymbol{p}_1 \cdot \boldsymbol{\epsilon})}{\Lambda^2} f_1(p, p_1, k) + \dfrac{([\boldsymbol{p}_1 \times \boldsymbol{k}] \cdot \boldsymbol{\epsilon})}{\Lambda^3} f_2(p, p_1, k) \right\}, \end{cases}$$

where p, p_1, p_2 and k are momenta of the K^+, π^+, π^0 and the photon respectively, ε is the polarization vector of the photon, $1/\Lambda$ is the range in which the direct electric dipole and magnetic dipole transitions occur and a special gauge, $p \cdot \varepsilon = 0$, is used. Denoting the masses of the K^+, π^+, π^0 and electron by M_{K^+}, M_{π^+}, M_{π^0} and M_e respectively, and the energy of the π^+ by E^+, and cutting the lower limit of the emitted photon momentum by $2M_e$, the corresponding transition probabilities per unit time and unit volume, w and w_R, are given by

$$(2)\qquad w = M_{\pi^+} M_{\pi^0} |G|^2 \frac{\sqrt{(m_K^2 + 1 - m_0^2)^2 - 4m_K^2}}{m_K^2}$$

(momentum dependence of G was neglected)

and

$$(3)\qquad w_R = \frac{\alpha}{\pi} M_{\pi^+} M_{\pi^0} \int_1^H dE \left\{ A(E) |G(E)|^2 + B(E) \frac{G(E) f_1^*(E) + G^*(E) f_1(E)}{2\lambda^2} + \right.$$
$$\left. + C(E) \frac{|f_1(E)|^2}{\lambda^4} + D(E) \frac{|f_2(E)|^2}{\lambda^6} \right\},$$

[3] D. J. PROWSE and D. EVANS: *Nuovo Cimento*, **8**, 856 (1958).

where

$$
\left\{
\begin{aligned}
& m_k = \frac{M_{K^+}}{M_{\pi^+}}, \qquad m_0 = \frac{M_{\pi^0}}{M_{\pi^+}}, \qquad m_e = \frac{M_e}{M_{\pi^+}}, \qquad E = \frac{E^+}{M_{\pi^+}}, \qquad \lambda = \frac{\Lambda}{M_{\pi^+}}, \\
& A(E) = \frac{4}{X(E)}\left\{E\,Y(E) - 2\sqrt{E^2-1}\right\}, \\
& B(E) = \frac{2}{m_K}\left\{Y(E) + [X(E) + m_0^2]\,Z(E) - 2m_K\sqrt{E^2-1}\right\}, \\
& C(E) = X(E)\left\{(m_K - E)\,Z(E) - 2\sqrt{E^2-1}\right\}, \\
& D(E) = \frac{\sqrt{E^2-1}}{2}\,\frac{X^3(E)}{[X(E)+m_0^2]}\left\{\frac{(m_K-E)^2}{[X(E)+m_0^2]} - \frac{2}{3}\,\frac{(E^2-1)}{[X(E)+m_0^2]} - 1\right\}, \\
& H = \frac{m_K^2 + 1 - m_0^2}{2m_K} - \\
& \quad - m_e\left\{\frac{\sqrt{(m_K^2+1-m_0^2)^2 - 4m_K^2}}{m_K^2+1-m_0^2} + \frac{m_K^2 - 1 + m_0^2}{m_K^2}\right\} + 0(m_e^2), \\
& X(E) = m_K^2 + 1 - m_0^2 - 2m_K E, \\
& Y(E) = \log\frac{E + \sqrt{E^2-1}}{E - \sqrt{E^2-1}} \\
& \text{and} \\
& Z(E) = \log\frac{m_K - E + \sqrt{E^2-1}}{m_K - E - \sqrt{E^2-1}}.
\end{aligned}
\right. \tag{4}
$$

From the same gauge invariance arguments for (1) as in the case of the radiative τ-decay mode given by DALITZ [2], we have

$$|G| \simeq |f_1|\,. \tag{5}$$

From these arguments we can not get any information about the magnitude of f_2 (*). However we will assume to be $\lambda \simeq m_K$, then we get

$$\frac{A(E)\lambda^6}{D(E)} \approx \begin{cases} 6.7\cdot 10^3 & \text{for } E^+ - M_{\pi^+} = 60 \text{ MeV}, \\ 2.9\cdot 10^4 & \text{for } E^+ - M_{\pi^+} = 80 \text{ MeV}, \end{cases}$$

(*) A cut-off perturbation calculation with a cut-off radius equal to Λ would gives $|f_1| \approx |f_2|$.

and the last term in (3) may be neglected. Fig. 1 shows the π^+-energy spectrum for the radiative θ^+-decay mode omitting the E-dependence of $G(E)$ and $f_1(E)$. As is shown by Fig. 1, the π^+-energy spectrum has no broad peak at ~ 60 MeV and the contribution which comes from the mechanism of the internal bremsstrahlung is dominant ($> 90\,\%$) even in the energy region of two anomalous K^+-decay events provided that $\lambda \geqslant m_K$ (*). The error which comes from neglecting the E-dependence on $G(E)$, has the same order of magnitude as the contribution of the electric dipole transition.

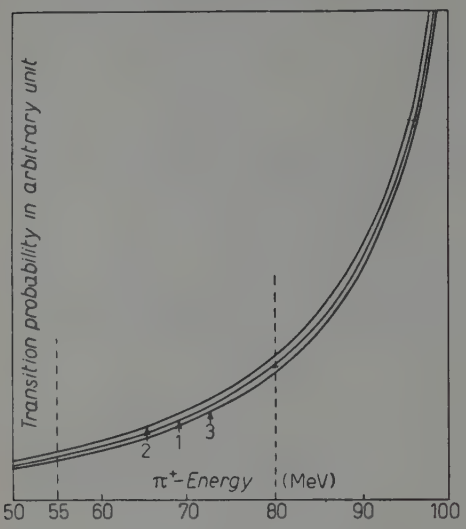

Fig. 1. – The π^+-energy spectrum for the decay mode: $K^+ \to \pi^+ + \pi^0 + \gamma$. Line 1 shows the contribution which comes from the mechanism of internal bremsstrahlung alone. Lines 2 and 3 are obtained by the following conditions: $2 - \lambda = m_K$ and $f_1 = -G$, $3 - \lambda = m_K$ and $f_1 = G$. The E-dependence of G and f_1 is omitted.

The possibility of the existence of X^0-particles ($\sim 500\ M_e$), therefore, results slightly higher than that resulting from the before mentioned two analyses ([1,3]). Now we shall assume that two anomalous events (2 anomalous events in about 1400 normal θ^+-decays) are due to the decay mode $K^+ \to \pi^+ + X^0$, then we may evaluate the rough magnitude of the baryon-X^0 coupling constant, $g_X^2/4\pi$,

$$(6) \qquad \frac{g_X^2}{4\pi} \approx \frac{m_0\sqrt{(m_K^2+1-m_0^2)^2-4m_K^2}}{700\, m_X\sqrt{(m_K^2+1-m_X^2)^2-4m_K^2}} \frac{g^2}{4\pi} \approx 1.6\cdot 10^{-2} \approx 2\alpha\,,$$

where $g^2/4\pi$ is the strong coupling constant between the baryon and the pion, $m_X = M_X/M_{\pi^+}$, M_X is the mass of the X^0-particle and α is the fine structure constant.

Next we shall assume that two anomalous events are due to the radiative decay mode. When the energy of the secondary π^+ is smaller than 55 MeV or larger than 80 MeV, it is difficult to distinguish the radiative θ^+-decay events from the τ'^+ or the θ^+-events ([3]). For this reason we shall evaluate the relative decay ratio of the radiative θ^+-decay in which the energy of the secon-

(*) Even in the case $\lambda = 1$, the π^+-energy spectrum has no broad peak at ~ 60 MeV and monotonically increases with E provided that the E-dependences of $G(E)$, $f_1(E)$ and $f_2(E)$ are neglected and $|G| \approx |f_1| \approx |f_2|$.

dary π^+ lies between 55 MeV and 80 MeV to the normal θ^+-decay, R:

$$R = \frac{1}{1540} \text{ (*)},$$

which is obtained by the first term in (3) alone. This value is not inconsistent with the observed value ($R \simeq 1/700$). The error which comes from the direct electric dipole transition is smaller than 8% provided that $|G| = |f_1|$ and $\lambda = m_K$ The other possibilities to explain these two anomalous events have been discussed by HARRIS *et al.* [1] (**) and are very small.

We can not conclude whether two anomalous K^+-decay events are due to the radiative θ^+-decay mode or to the decay mode $K^+ \to \pi^+ + X^0$, from only two events. In order to get this conclusion and to know whether there exists a neutral 500 M_e particle or not, we must await further work to confirm the unique π^+-energy in the 60 MeV region and to search for other phenomena related to this X^0-particle.

* * *

The author would like to thank Professor S. HAYAKAWA and Dr. S. FRAUTSCHI for helpful discussions.

(*) The relative decay ratio of the total radiative θ^+-decay (the energy of the emitted photon is larger than $2M_e$) to the normal θ^+-decay is $1/144 \approx \alpha$.

(**) There is another possibility to explain these anomalous events. K^+ decays into π^+ state and $(\pi^0 + \pi^0)$ bound state, which decays finally into 2γ states. This possibility is pointed out by Prof. S. HAYAKAWA.

RIASSUNTO (*)

Si calcola lo spettro di energia del π^+ per il modo di decadimento radioattivo θ^+, e si dimostra che tale spettro non ha alcun picco a ~ 60 MeV. Non si hanno quindi elementi validi per affermare che i due eventi anomali di decadimento K^+ (con un π^- secondario di circa 60 MeV) siano dovuti con maggiore probabilità al modo di decadimento radiativo θ^+ piuttosto che al modo di decadimento in due particelle: $K^+ \to \pi^+ + X^0$, dove X^0 è un bosone neutro di massa (500 ± 5) volte la massa dell'elettrone.

(*) *Traduzione a cura della Redazione*

IL NUOVO CIMENTO Vol. XIII, N. 6 16 Settembre 1959

The Renormalization of Dirac-Maxwell Equations.

P. Sen (*)

National Physical Laboratory - New Delhi

(ricevuto il 27 Maggio 1959)

Summary. — A previous hypothesis, that the free energy projection of the interaction term of the Dirac-Maxwell equations combines with the bare electron to form the true experimental electron and that such reformulated Dirac-Maxwell equations in terms of the experimental electron are already renormalized, is shown to be true by constructing an explicit analytic representation for the free energy operator, but it is found that a convergent quantum electrodynamics is a necessary prerequisite for its validity. Such quantum electrodynamics can be constructed with the help of the Feynman cut off or with a non local interaction term in which the structure of the Dirac-Maxwell equations is maintained. The additional result that the charge renormalization is unity is obtained.

1. – Introduction.

In Dyson's renormalization program [1], the renormalizing quantities are removed at the end of every intermediate step of the calculation and this results in its complexity when the total renormalization constants are evaluated [1,2], so that it is difficult to establish a relation between the original

(*) Now at l'Istituto di Fisica dell'Università, Torino.

(1) F. J. Dyson: *Phys. Rev.*, **75**, 486, 1736 (1949); A. Salam: *Phys. Rev.*, **82**, 217 (1951).

(2) J. C. Ward: *Phys. Rev.*, **78**, 182 (1950); G. Källén: *Helv. Phys. Acta*, **25**, 417 (1952); *Dan. Mat. Phys. Medd.*, **27**, no. 12 (1953); H. Lehmann: *Nuovo Cimento*, **11**, 342 (1954); M. Gell-Mann and F. Low: *Phys. Rev.*, **95**, 1300 (1954); Y. Nambu: *Phys. Rev.*, **101**, 1182 (1956); I. Ya. Pomerančuk, V. V. Sudakov and K. A. Ter-Martirosyan: *Phys. Rev.*, **103**, 784 (1956).

Dirac-Maxwell equations and Dyson's renormalized Dirac-Maxwell equations. Hence in order to obtain an analytic formulation of the renormalization program a hypothesis ([3]) was suggested that the interaction term of the Dirac-Maxwell equations may be written as a sum of its free energy projection and the remainder, which was called the principle energy projection, that the free energy projection may combine with the bare particle parts of the Dirac-Maxwell equations to give the experimental electron and photon, and that these reformulated Dirac-Maxwell equations were already renormalized. But no attempt to prove it was made, and from qualitative reasoning several already renormalized Dirac-Maxwell equations, whose subtracted terms resembled Dyson's renormalization terms and which were derived from partly analytic considerations, were given.

We should like to prove it now by giving the free energy operator an analytic definition, by writing the interaction term as the sum of free and principle energy projections, then by showing that the free energy projections can be combined with the bare particles to form the experimental electron and photon and then by showing that the principle energy projections do not contribute to the mass and charge and that furthermore now the electron and photon wavefunctions remain renormalized during the course of the calculations by the usual Feynman procedure ([4]). The charge of the electron is found to remain unaltered and we obtain the equality of the bare and the experimental charge, which has also been derived for Dyson's renormalization program ([1,2]). Here the renormalization terms found in the original Dirac-Maxwell equations are removed by the subtraction procedure contained within the principle projection of the interaction term and so the actual calculations are similar to Dyson's but are obtained from a considerably simpler procedure.

To obtain the renormalized Dirac-Maxwell equations an anlytic representation of the free energy operator is constructed and the δ functions, whose definitions have been generalized to include improper integrands, are found to have the necessary properties for such assignments also. We note that although the physical parts of the second order Feynman graphs have the usual values and thus the second order contributions to the Lamb Retherford shift and the magnetic moment of the electron remain unaltered, the present scheme differs from the others ([1,3]) in an essential way, that is that due to its analytic procedure there are no longer rules for the evaluation of the higher order Feynman graphs.

Then since the irreducible Feynman graphs contained within a higher order Feynman graph cannot now be treated separately and their renormalization

---

([3]) P. Sen: *Nuovo Cimento*, **4**, 270 (1956).

([4]) R. P. Feynman: *Phys. Rev.*, **76**, 749, 769 (1949).

constants cannot be removed independently of the rest of the Feynman graph, the renormalization constants of the lower order graphs sometimes appear in the physical part of the higher order graph. Finite values for these constants have been obtained, from the cut off procedures ([5]) as well as from structurally unaltered non-local Dirac-Maxwell equations. ([6]) The experimental evidence ([7]) for Dyson's renormalization scheme is as yet uncertain.

2. – The free energy projections.

Since some reformulation of the earlier notation ([3]) will be found necessary, in this section we shall briefly state the notation and introduce the energy projections again. The Dirac-Maxwell equations for the wawe functions and the corresponding Feynman Schwinger propagation operators in the absence of external fields are ([6])

$$(1)\quad \begin{cases} (H_0(1) - i\lambda_0 a'(1))\psi'(1) = 0\,, & \overline{\psi}'(1)(\overline{H}_0(1) + i\lambda_0 a'(1)) = 0\,, \\ H_0(1) = \gamma_\mu \dfrac{\partial}{\partial 1_\mu} + \varkappa_0\,, & \overline{H}_0(1) = \gamma_\mu \dfrac{\partial}{\partial 1_\mu} - \varkappa_0\,, \\ m_0 c = \hbar \varkappa_0\,, & e_0 = \lambda_0 \hbar c\,, \end{cases}$$

$$(2)\quad \begin{cases} \Box^2 A'_\mu(1) = -\dfrac{1}{c} j'_\mu(1) = i e_0 c \lambda_0 \displaystyle\int \pi_{\mu\nu}(1,2)\, A'_\nu(2)\, \mathrm{d}2\,, \\ \pi_{\mu\nu}(1,2) = \mathrm{Tr}\, \gamma_\mu \overset{c}{K}'(1,2)\, \gamma_\nu K'(2,1)\,, \\ \dfrac{\partial}{\partial 1_\mu} A'_\mu(1) = 0\,, \end{cases}$$

$$(3)\quad (H_0(1) - i\lambda_0 a'(1))\, K'(1,2) = i\,\delta(12)\,, \qquad K'(1,2)(\overline{H}_0(2) + i\lambda_0 a'(2)) = -i\,\delta(12)\,,$$

$$(4)\quad \Box(1)\, L_{\mu\nu}(1,2) = i\hbar c\, \delta_{\mu\nu}\, \delta(12) + i\hbar c \lambda_0^2 \int \pi_{\mu\alpha}(1,3)\, L'_{\alpha\nu}(3,2)\, \mathrm{d}3\,,$$

$$(5)\quad \psi'(1) = \psi_0(1) + \lambda_0 \int K'(1,2)\, a'(2) \psi_0(2)\, \mathrm{d}2\,,$$

([5]) R. P. Feynman: *Phys. Rev.*, **74**, 1430 (1948); W. Pauli and F. Villars: *Rev. Mod. Phys.*, **21**, 434 (1949).

([6]) P. Sen: *Nuovo Cimento*, **3**, 390 (1956); **6**, 400 (1957).

([7]) D. R. Yennie, M. M. Levy and D. G. Ravenhall: *Rev. Mod. Phys.*, **29**, 144 (1957).

$$K'(1,2) = K_0(12) + \lambda_0 \int K_0(13)\, a'(3)\, K'(3,2)\, \mathrm{d}3\,, \tag{6}$$

$$A'_\mu(1) = A_\mu(1) + \lambda_0^2 \iint L'_{\mu\alpha}(1,3)\, \pi_{\alpha\beta}(3,4)\, A_\beta(4)\, \mathrm{d}3\, \mathrm{d}4\,, \tag{7}$$

$$L'_{\mu\nu}(1,2) = L_{\mu\nu}(12) + \lambda_0^2 \iint L_{\mu\alpha}(13)\, \pi_{\alpha\beta}(3,4)\, L'_{\beta\nu}(4,2)\, \mathrm{d}3\, \mathrm{d}4\,, \tag{8}$$

where m_0 and e_0 denote the bare electron mass and charge.

The free energy operators $\mathscr{E}_0(1)$ and $\mathscr{E}_{0\pi}(1)$ of the electron and photon wavefunctions respectively, whose projections are intepreted as mass and charge renormalizations are defined by

$$\mathscr{E}_0(1)\, X(1) = \frac{1}{(2\pi)^4} \int \exp\left[ip \cdot 1\right] \mathscr{E}_0(p)\, X(p)\, \mathrm{d}^4(p)\,, \tag{9}$$

$$\mathscr{E}_0(1)\, X(1)\, Y(1) = \frac{1}{(2\pi)^8} \iint \exp\left[ip \cdot 1\right] \mathscr{E}_0(p)\, X(p-k)\, Y(k)\, \mathrm{d}^4 p\, \mathrm{d}^4 k\,, \tag{10}$$

$$\mathscr{E}_{0\pi}(1)\, Y(1) = \frac{1}{(2\pi)^4} \int \exp\left[ip \cdot 1\right] \mathscr{E}_{0\pi}(p)\, Y(p)\, \mathrm{d}^4 p\,, \tag{11}$$

where $X(1)$ and $Y(1)$ are arbitrary functions. Let

$$X(p) = \sum_{-\infty}^{\infty} \alpha_n (i\gamma p + \varkappa)^n\,, \qquad Y(p) = \sum_{-\infty}^{\infty} \beta_n p^{2n}\,, \tag{12}$$

where α_n and β_n are constants and $\varkappa$ is the experimental mass of the electron. Then we further define

$$\mathscr{E}_0(p)\, X(p) = \sum_{-\infty}^{0} \alpha_n (i\gamma p + \varkappa)^n = \mathscr{E}_0(p)\, \mathscr{E}_0(p)\, X(p)\,, \tag{13}$$

$$\mathscr{E}_{0\pi}(p)\, Y(p) = \sum_{-\infty}^{0} \beta_n p^{2n} = \mathscr{E}_{0\pi}(p)\, \mathscr{E}_{0\pi}(p)\, Y(p)\,, \tag{14}$$

and the corresponding principle energy projections by

$$\mathscr{P}_0(1) X(1) = (1 - \mathscr{E}_0(1)) X(1)\,, \tag{15}$$

$$\mathscr{P}_{0\pi}(1)\, Y(1) = (1 - \mathscr{E}_{0\pi}(1))\, Y(1)\,. \tag{16}$$

Although it is not essential to the argument we shall now obtain explicitly analytic representations for the free energy operators by extending the definitions of the δ functions to include improper integrands. Let the function $f(p_0)$ be proper at $p_0 = \xi$. Then ([8])

$$\int f(p_0)\,\delta(p_0-\xi)\,\mathrm{d}p_0 = \oint_{c_+} \frac{f(p_0)}{p_0-\xi}\,\mathrm{d}p_0\,, \tag{17}$$

where c_+ is a closed contour around $p_0 = \xi$, and we define for $n > 0$

$$\int \frac{f(p_0)}{(p_0-\xi)^n}\,\delta(p_0-\xi)\,\mathrm{d}p_0 = \frac{1}{2\pi i}\oint_{c_+} \frac{f(p_0)}{(p_0-\xi)^{n+1}}\,\mathrm{d}p_0\,, \tag{18}$$

$$\int \frac{f(p_0)}{(p_0-\xi)^n}\,\delta^2(p_0-\xi)\,\mathrm{d}p_0 = \frac{1}{2\pi i}\oint_{c_+} \frac{f(p_0)}{(p_0-\xi)^{n+2}}\,\mathrm{d}p_0\,. \tag{19}$$

Then we have ([4])

$$\int \frac{1}{(p^2+\varkappa^2)^n}\,\mathrm{d}^4p = -\int\oint_{c^+} \frac{1}{(p^2+\varkappa^2)^n}\,\mathrm{d}p\,\mathrm{d}p_0\,, \tag{20}$$

where c_+ is the closed anticlockwise contour around $p_0 = \xi = \sqrt{p^2+\varkappa^2}$, and

$$\int \frac{1}{(p^2+\varkappa^2)^n}\,(p^2+\varkappa^2)\,\delta\,(p^2+\varkappa^2)\,\mathrm{d}^4p = \frac{1}{2\pi i}\int\oint_{c^+} \frac{1}{(p^2+\varkappa^2)^n}\,\mathrm{d}p\,\mathrm{d}p_0\,, \tag{21}$$

$$\int \frac{1}{(p^2+\varkappa^2)^n}\,(p^2+\varkappa^2)^2\,\delta^2(p^2+\varkappa^2)\,\mathrm{d}^4p = \frac{1}{2\pi i}\int\oint_{c_+} \frac{1}{(p^2+\varkappa^2)^n}\,\mathrm{d}p\,\mathrm{d}p_0\,, \tag{22}$$

where

$$\delta(p^2+\varkappa^2) = \frac{1}{2\xi}\,(\delta(p-\xi)+\delta(p+\xi))\,. \tag{23}$$

Due to the equality of (20) and (21) for improper integrands and the result

$$\int (p^2+\varkappa^2)\,\delta(p^2+\varkappa^2)\,\mathrm{d}^4p = 0\,, \tag{24}$$

([8]) W. Heitler: *The Quantum Theory of Radiation*, 3rd ed. (Oxford, 1954).

for the proper integrands we can now represent the projections in equations (13) and (14) by the analytic relations

$$\mathscr{E}_0(p)X(p) = -2\pi i(p^2+\varkappa^2)\delta_+(p^2+\varkappa^2)X(p) + \tag{25}$$
$$+ \left(X(p) + 2\pi i\,(p^2+\varkappa^2)\delta_+(p^2+\varkappa^2)X(p)\right)_{ip+\varkappa=0},$$

$$\mathscr{E}_{0\pi}(p)\,Y(p) = -2\pi i p^2\delta_+(p^2) + \left(Y(p) + 2\pi i p^2\delta_+(p^2)\,Y(p)\right)_{p^2=0}. \tag{26}$$

3. – The renormalized Dirac-Maxwell equations.

We may now reformulate the equations (1) and (2) by writing the interaction term as the sum of its free and principle energy projections and the equation (1) becomes

$$\left(H_0(1) - i\lambda_0\mathscr{E}_0(1)\,a'(1) - i\lambda_0\mathscr{P}_0(1)\,a'(1)\right)\psi'(1) = 0\,. \tag{27}$$

Then let $\varkappa_0$ be so defined that

$$-i\lambda_0\mathscr{E}_0(1)\,a'(1)\,\psi'(1) = \mathscr{E}_0(1)H_0(1)\psi'(1) = (\varkappa-\varkappa_0)\psi'(1)\,, \tag{28}$$

and we obtain the renormalized Dirac equations

$$\left(H(1) - i\lambda_0\mathscr{P}_0(1)\,a'(1)\right)\psi'(1) = 0\,, \qquad H(1) = \gamma_\mu\frac{\partial}{\partial 1_\mu} + \varkappa\,. \tag{29}$$

The reformulated Maxwell equations are obtained similary and even more simply since the mass renormalization for the photon vanishes due to the Lorentz condition, and are

$$\Box(1)\,A'_\mu(1) + \frac{1}{c}\,\mathscr{P}_{0\pi}(1)\,j'_\mu(1) = 0\,. \tag{30}$$

We note that the more general definition

$$-\mathscr{E}_0(1)H_0(1)\psi'(1) = (\varkappa-\varkappa_0)\psi'(1) + i(\lambda_0-\lambda)\,\mathscr{P}_0(1)a'(1)\psi'(1)\,, \tag{31}$$

in place of (28) is ruled out because it is known that in the right hand side of the expression

$$\psi'(p) = \psi_0(p) + \sum_{-\infty}^{-1}\alpha_n(i\gamma p+\varkappa)^n\psi_0(p) + \alpha_0\psi_0(p) + \sum_{1}^{\infty}\alpha_n(i\gamma p+\varkappa)^n\psi_0(p)\,, \tag{32}$$

the third term only contributes to the charge renormalization and $(i\gamma p+\varkappa_0)\psi_0(p)$ vanishes.

The equations (29) and (30) are similar to the renormalized equations which were proposed earlier [3], and do not contain mass or charge renormalization terms and we, therefore conclude

$$e_0 = e\,, \tag{33}$$

where e is the experimental charge of the electron. Then by making the transformations

$$\lambda_0\psi'(1)\to\lambda_1\psi'(1)\,,\qquad \lambda_0 A'_\mu(1)\to\lambda_2 A'_\mu(1)\,, \tag{34}$$

the Dirac-Maxwell equations become

$$(H_0(1)-i\lambda_2 a'(1))\,\psi'(1)=0\,,\qquad \Box A'_\mu(1)+\frac{1}{c}\frac{\lambda_1^2}{\lambda_2}f'_\mu(1)=0\,, \tag{35}$$

and we note that charge and wave function renormalizations are mutually related and one is accompanied by the other [9]. From the above mentioned absence in (29) and (30) of terms which could be interpreted as either charge or wave function renormalizations and from the equality of the bare and experimental charges we conclude that, by suppressing the terms which have been generally interpreted as charge renormalizations and which may be attributed as well to wave function renormalizations, the principle energy projection maintains the wave functions renormalized during the course of calculations.

Let us now introduce the external fields $A_{e,\mu}(1)$ and $j_{e,\mu}(1)$, so that the Dirac-Maxwell equations become

$$(H_0(1)-i\lambda a'(1)-i\lambda a_e(1)(\psi'(1)=0\,, \tag{36}$$

$$\Box A'_\mu(1)+\frac{1}{c}j'_\mu(1)+\frac{1}{c}j_{e,\mu}(1)=0\,, \tag{37}$$

where $\lambda\hbar c=e$. Then

$$\mathscr{E}_0(1)\,\overline{\psi}(1)\,a_e(1)\,\psi'(1)= \tag{38}$$

$$=\frac{1}{(2\pi)^8}\iint\exp\left[i(p-k_0)\cdot 1\right]\overline{\psi}'(p)\,A_{e,\mu}(k_0)\,\mathscr{E}_0(p,k_0)\,X(p,k_0)\,\psi(p-k_0)\,\mathrm{d}^4p\,\mathrm{d}^4k_0\,,$$

---

[9] R. Karplus and N. M. Kroll: *Phys. Rev.*, **77**, 536 (1950).

where $k_{\mu,0}$ represents the momentum of $A_{e,\mu}(1)$. But the external field must contribute only to the physically observable terms and not to the renormalization terms and therefore we must redefine the free energy operator $\mathscr{E}(1)$ in the momentum representation as

$$\mathscr{E}(p, k_0)\, X_\mu(p, k_0) = \mathscr{E}_0(p)\, X(p, 0)\,. \tag{39}$$

that is when evaluating the free energy projection the momentum of the external field is set equal to zero. Then correspondingly the principle energy projection becomes

$$\mathscr{P}(1) X(1) = (1 - \mathscr{E}(1)) X(1)\,. \tag{40}$$

We note that all the previous remarks remain unaltered and we finally obtain the renormalized equations

$$(H(1) - i\lambda \mathscr{P}(1) a'(1) - i\lambda a_e(1))\, \psi'(1) = 0\,, \tag{41}$$

$$\Box(1) A'_\mu(1) + \frac{1}{c} \mathscr{P}_\pi(1) j'_\mu(1) + \frac{1}{c} j_{e,\mu}(1) = 0\,, \tag{42}$$

$$K'(1, 2) = K(12) + \lambda \int K(13)\, \mathscr{P}(3)\, a'(3)\, K'(3, 2)\, d3\,, \tag{43}$$

$$L'_{\mu\nu}(1, 2) \quad L_{\mu\nu}(12) + \lambda^2 \iint L_{\mu\alpha}(13)\, \mathscr{P}_\pi(3)\, \pi_{\alpha\beta}(3, 4)\, L'_{\beta\nu}(4, 2)\, \mathrm{d}3\, \mathrm{d}4\,. \tag{44}$$

4. – Calculation of the Feynman graphs.

To illustrate the procedure we shall now evaluate some simple Feynman graphs and note that its essential difference from the previous renormalization schemes ([5,3]) is the complete absence of any rules for their calculation, which is due to its analytic approach. The contribution of the second order self energy Feynman graph in momentum representation is

$$\begin{cases} \psi^{(2)}(p) = K(p)\, \mathscr{P}(p)\, \Sigma^{(2)}(p)\, \mathscr{P}(p)\, \psi(p)\,, \\ \qquad\quad = (1 - \mathscr{E}_0(p))\, K(p)\, \Sigma^{(2)}(p)\, \psi(p)\,, \end{cases} \tag{45}$$

where

$$\begin{cases} K(p)\, \Sigma^{(2)}(p) = \dfrac{\lambda^2 \hbar c}{(2\pi)^4} \int K(p) \gamma_\mu K(p - k) L(k) \gamma_\mu \, \mathrm{d}^4 k\,, \\ \qquad\qquad = \displaystyle\sum_{-1}^{\infty} \alpha_n (i\gamma p + \varkappa)^n. \end{cases} \tag{46}$$

Therefore the free energy projection is equal to the renormalization terms obtained from the Dyson procedure ([1,9]). The contribution of the second order vertex graph is

$$(47)\qquad \begin{cases} V^{(2)}(p, k_0) = \overline{\psi}(p) A_{e,\mu}(k_0) \mathscr{P}(p) \Lambda_\mu^{(2)}(p, k_0) \mathscr{P}(p - k_0) \psi(p - k_0) , \\ \qquad\qquad = \overline{\psi}(p) A_{e,\mu}(k_0) \left(\Lambda_\mu^{(2)}(p, k_0) - \mathscr{E}_0(p) \Lambda_\mu^{(2)}(p, 0)\right) \psi(p - k_0) , \end{cases}$$

where

$$(48)\qquad \Lambda_\mu^{(2)}(p, k_0) = \frac{\lambda^2 \hbar c}{(2\pi)^4} \int \gamma_\nu K(p - k) \gamma_\mu K(p - k - k_0) L(k) \gamma_\nu \, \mathrm{d}^4 k ,$$

and the free energy projection is again equal to Dyson's charge renormalization for the second order vertex graph.

The contribution of the fourth order self energy Feynman graph which is obtained by joining two second order self-energy graphs exhibits the absence of rules and the difference from other renormalization schemes and we obtain for it

$$(49)\qquad \begin{cases} \psi^{(4a)}(p) = \left(1 - \mathscr{E}_0(p)\right) K(p) \Sigma^{(2)}(p) K(p) \Sigma^{(2)}(p) \psi(p) , \\ \qquad\qquad = \Big\{ \sum_{m=2}^{\infty} \sum_{n=-1}^{\infty} \alpha_m \alpha_n (i\gamma p + \varkappa)^{m+n} + \alpha_{-1} \sum_{2}^{\infty} \alpha_n (i\gamma p + \varkappa)^n + \\ \qquad\qquad\qquad + \alpha_0 \sum_{1}^{\infty} \alpha_n (i\gamma p + \varkappa)^n + \alpha_1 \sum_{0}^{\infty} \alpha_n (i\gamma p + \varkappa)^n \Big\} \psi(p) . \end{cases}$$

Thus the renormalization constants α_0 and α_{-1} of the second order self-energy graphs occur in $\psi^{(4a)}(p)$ which is already renormalized.

Therefore we find that our conclusions are valid only for a convergent quantum electrodynamics and that the renormalization terms can be described by an analytic free energy projection only for Dirac-Maxwell equations with Feynman cut-off ([5]), and for non-local Dirac-Maxwell equations ([6]) which preserve the structure of the original local Dirac-Maxwell equations and in which the electron has internal degrees of freedom and hence a « radius ». In the non-local electrodynamics these internal degrees of freedom remain undefined and their magnitudes can be chosen to agree with the experimental results. Recent experimental evidence ([7]) is not yet conclusive but seems to indicate the need for the revision of Dyson's renormalization scheme.

To illustrate our procedure for the evaluation of more complicated Feynman graphs we shall evaluate the fourth order overlapping self-energy graph.

Since

$$\frac{1}{(p-k_1-k_2)^2+\varkappa^2} = \frac{(p-k_1)^2+\varkappa^2}{(p-k_1)^2+(p-k_2)^2+2\varkappa^2}\cdot\frac{1}{k_1^2-2k_1(p-k_2)} + \tag{50}$$

$$+\frac{(p-k_2)^2+\varkappa^2}{(p-k_1)^2+(p-k_2)^2+2\varkappa^2}\cdot\frac{1}{k_2^2-2k_2(p-k_1)} + \frac{1}{((p-k_1-k_2)^2+\varkappa^2)_R},$$

where

$$\frac{1}{((p-k_1-k_2)^2+\varkappa^2)_R} = ((p-k_1)^2+\varkappa^2)((p-k_2)^2+\varkappa^2)\cdot \tag{51}$$

$$\cdot(2k_1(p-k_2)+2k_2(p-k_1)-k_1^2-k_2^2)/((p-k_1)^2+(p-k_2)^2+2\varkappa^2)\cdot$$

$$\cdot(k_1^2-2k_1(p-k_2))(k_2^2-2k_2(p-k_1))((p-k_1-k_2)^2+\varkappa^2),$$

we obtain

$$\left\{\begin{aligned}\psi^{(4b)}(p) &= \frac{\lambda^4(\hbar c)^2}{(2\pi)^8}\iint \mathscr{P}_0(p)\,\mathscr{P}_0(p-k_1)\,\mathscr{P}_0(p-k_2)\,K(p)\gamma_\mu K(p-k_1)\gamma_\nu\cdot\\ &\cdot\frac{-i\gamma(p-k_1-k_2)+\varkappa}{(p-k_1-k_2)^2+\varkappa^2}\,\gamma_\mu K(p-k_2)\gamma_\nu L(k_1)\,L(k_2)\,\psi(p)\,\mathrm{d}^4k_1\,\mathrm{d}^4k_2,\\ &= \frac{\lambda^4(\hbar c)^2}{(2\pi)^8}\iint \mathscr{P}_0(p)\,K(p)\gamma_\mu K(p-k_1)\gamma_\nu\frac{-i\gamma(p-k_1-k_2)+\varkappa}{((p-k_1-k_2)^2+\varkappa^2))_R}\cdot\\ &\cdot K(p-k_2)\gamma_\nu L(k_1)\,L(k_2)\,\psi(p)\,\mathrm{d}^4k_1\,\mathrm{d}^4k_2.\end{aligned}\right. \tag{52}$$

5. – Conclusion.

Our work may be summed up here: first a non-local convergent quantum electrodynamics (6) was constructed in which all the properties of the original local Dirac-Maxwell equations were preserved and which was therefore considered to be preferable to them (10), then the possibility of an analytic formulation of the renormalization program for the original local Dirac-Maxwell equations (3) was suggested, and now we conclude that the non-local Dirac Maxwell equations (6) describe the experimental electron and photon fully and therefore the electron has a radius. We also note that the procedure followed here is analytic and therefore perhaps unique, that it is free from assumptions, that the equality of bare and experimental charge is obtained in a simple manner, and that the second order Feynman graphs have the usual values.

(10) See also H. YUKAWA: *Phys. Rev.*, **91**, 415, 416 (1953); P. SEN: *Nuovo Cimento*, **3**, 612 (1956); **8**, 407 (1958).

The internal degrees of freedom of the electron remain undefined and their equations, for instance the Yukawa auxiliary conditions ([10]), or their values, which occur in some of the higher order Feynman graphs, are undetermined, and to assign a magnitude to them, if $\varkappa_0$ is put equal to $\varkappa$, then renormalization may be attributed to the use of the Born approximation. The validity of Dyson's renormalization program is still undecided ([7]) and even if the experimental evidence is in agreement with it for the fourth order Feynman graphs we note that it certainly will not contradict the results obtained from the non-local Dirac-Maxwell equations due to the still undetermined magnitudes within them.

* * *

The author is very grateful to Professor G. Wataghin for helpful correspondence and discussion.

— —

RIASSUNTO (*)

Per dimostrare vera la precedente ipotesi che la proiezione dell'energia libera del termine di interazione delle equazioni di Dirac-Maxwell si combina con l'elettrone nudo a formare il vero elettrone sperimentale e che le equazioni di Dirac-Maxwell riformulate in termini dell'elettrone sperimentale sono già rinormalizzate, si costruisce una rappresentazione analitica esplicita per l'operatore dell'energia libera; si trova però che per la validità di quanto precede premessa necessaria è un'elettrodinamica quantistica convergente. Una simile elettrodinamica può essere costruita con l'ausilio del taglio di Feynmann o con un termine d'interazione non locale nel quale sia conservata la struttura delle equazioni di Dirac-Maxwell. Si ottiene inoltre il risultato che la rinormalizzazione della carica è l'unità.

(*) *Traduzione a cura della Redazione.*

IL NUOVO CIMENTO Vol. XIII, N. 6 16 Settembre 1959

Dislocations and their Effect on X-Ray Diffraction.

L. F. Vassamillet

Mellon Institute - Pittsburgh, Pa.

(ricevuto il 29 Maggio 1959)

Summary. — The problem of understanding the effect of dislocations on the diffraction of X-rays still remains largely unresolved. The treatments by Wilson (1) and Suzuki and Willis (2) have not been verified experimentally. However it is possible to show that the line profile derived from an exact treatment is qualitatively in agreement with that obtained by the Stokes-Wilson approximation (4). The approximate treatment can be extended to the case of an edge dislocation. When this is done, it is found that the « tail » of the line profile is not dependent on the dislocation type or orientation. It is also possible to show that the integral breadth, which is also obtained with the approximate treatment, is strongly dependent on the boundary conditions assumed for the cylindrical crystal. Consequently, the results obtained from a consideration of a single isolated dislocation would not appear applicable to an aggregate of dislocations in a real crystal.

1. – Introduction.

The problem of understanding the effect of dislocations on the diffraction of X-rays still remains largely unresolved. Only the treatments by Wilson(1) and Suzuki and Willis (2) on long cylindrical crystals containing an axial dislocation may be considered exact. Wilson derived the equations for the intensity distribution in reciprocal space for the case of the axial screw dislocation, but did not attempt to obtain profiles of the corresponding Debye-Scherrer lines. Suzuki and Willis published the results of their calculations

(1) A. J. C. Wilson: *Acta Cryst.*, **5**, 318 (1952).
(2) T. Suzuki and B. T. M. Willis: *Nature*, **177**, 712 (1956).

plus the direct observation of the optical diffraction pattern of a two dimensional grating representing the crystal using a Lipson diffractometer.

In an approximate treatment, WILSON [3] derived the shape of the line profile for the case of the axial screw dislocation. This work is based on a study by STOKES and WILSON [4] of strain broadening in which strain gradients are neglected. All of the above results predict a ring-shaped intensity pattern in reciprocal space. In the two papers by WILSON [1,3] the integral breadths have been determined as well.

In Section **2** of this paper the intensity distribution and line profiles for the case of an axial screw dislocation in a long cylindrical crystal are presented. These have been obtained by a numerical integration of the equations derived by WILSON [1]. Because of the general qualitative agreement of the exact and approximate treatments, the latter has been extended, in Section **3**, to the case of an axial edge dislocation. The shape of the diffraction tail is obtained as well as the integral breadth of the $(h00)$ and $(0k0)$ reflections. In Section **4** the limitations of the Stokes-Wilson approximate treatment are discussed.

2. – Line profiles for screw dislocation.

WILSON [1] has shown that the amplitude of the diffracted wave from a crystal containing an axial screw dislocation is

$$G = 2\pi i^{nl} FZC^{-1} \int_0^A J_{nl}(2\pi\varrho r) r \, \mathrm{d}r \,, \tag{1}$$

which may be put into the form

$$G = i^m FZ\pi A^2 C^{-1} K_m(x) \,, \tag{2}$$

with the help of the following equalities: $\zeta = 2\pi\varrho r$, $x = 2\pi\varrho A$, $m = nl$ and $K_m(x) = (2/x^2)\int_0^x \zeta J_m(\zeta)\,\mathrm{d}\zeta$. J_{nl} is the Bessel function of order nl, A is the radius of the cylinder containing the axial screw dislocation. ϱ, l, F, C and Z are defined by WILSON [1]. The diffracted intensity is equal to the product of the amplitude and its complex conjugate:

$$H_m(x) = G_m G_m^* = F^2 Z^2 \pi^2 A^4 C^{-2} [K_m(x)]^2 . \tag{3}$$

[3] A. J. C. WILSON: *Nuovo Cimento*, **1**, 277 (1955).
[4] A. R. STOKES and A. J. C. WILSON: *Proc. Phys. Soc. London*, **56**, 174 (1944).

WILSON ([1,3]) subsequently determined the integral breadth of the diffraction line as a function of m, but did not show the line profile itself. This, however, can be obtained by a numerical integration of $K_m(x)$.

Since only the first maximum of the Bessel function makes an appreciable contribution, the summation processes for values of $K_m(x)$ can be terminated when the values of the arguments $x = 6$, 8, 10 for $m = 1$, 2, 3 respectively. The right side of Fig. 1 shows the intensity distribution calculated for $m = 1$, 2,

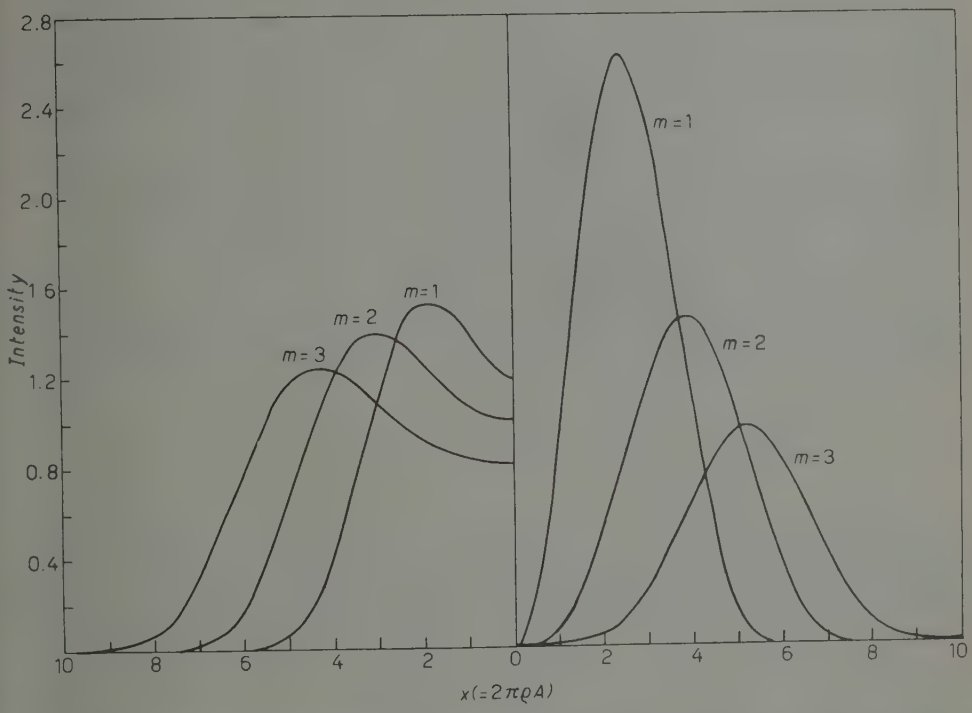

Fig. 1. – Radial intensity functions for the diffraction rings $K_m^2(x)$ (right) and the corresponding line profiles (left) for $m = 1$, 2, 3 as a function of $x = 2\pi\rho A$. The foreshortening effect has not been taken into account in the line profiles.

and 3. The line is symmetrical about the point $x = 0$; that is, about the reciprocal vector $\boldsymbol{s} = h\boldsymbol{a}^* + k\boldsymbol{b}^* + l\boldsymbol{c}^*$. The above integration for $H(x)$ has been performed numerically. The results for each of the intensity distributions are shown on the left hand half of Fig. 1. Whereas the intensity distribution is zero at the nodal point $x = 0$, the line profile is not. The zero value of the distribution function at $x = 0$ has been discussed by FRANK ([5]).

([5]) F. L. FRANK: *Research Lond.*, **2**, 542 (1949).

A close inspection of Fig. 1 shows that the intensity distribution function may be closely approximated either by the Gaussian function

$$H_m(x) \simeq H \exp[-a(x-x_0)]^2 \tag{4a}$$

or the sinusoidal function

$$H_m(x) \simeq H \sin^2 \frac{\pi x}{2x_0} . \tag{4b}$$

(4*a*) differs slightly from $H_m(x)$ for small x, ($x < 1$), whereas (4*b*) differs somewhat from $H_m(x)$ for $x > 4$ ($m = 1$). x_0 is that value of x which corresponds to the maximum value of $H_m(x)$ and depends on m.

The general shape of the line profile was predicted by WILSON [3] who used the Stokes-Wilson approximation [4]. An inspection of Fig. 1 shows that the tail of the line profile does not follow an inverse cube law.

For any real crystal containing a distribution of dislocations, the line profile would depend on some distribution function $f(A)$, *i.e.*, the number of dislocations enclosed in cylinders of radius A. The corresponding line profile can be expressed as

$$I(\varrho) = \int_0^\infty f(A) H_m(2\pi\varrho A) \, \mathrm{d}A . \tag{5}$$

In addition, the integral breadths of the line profiles can be obtained by graphical integration. The straight line relationship found by WILSON [3] and FRANK (op. cit.) is verified, but with a slightly different value of the slope:

$$\beta_l = \beta_0(1 + .973l) . \tag{6}$$

The difference in the value of the slope is probably not significant, since the « foreshortening factor » (mentioned by WILSON, op. cit.) has not been included.

3. – Line profiles and integral breadths of crystals containing a dislocation.

Because of the generally satisfactory agreement between the Stokes-Wilson approximation when applied to integral breadths and the results obtained by the evaluation of (3), it seems worth-while to extend this approach to the case of an edge dislocation lying along the axis of a cylindrical crystal of radius A. The tensile strain in the hkl direction at the point r is

$$\varepsilon_{hkl} = |\boldsymbol{s}|^{-2} \boldsymbol{s} \cdot \nabla \boldsymbol{u} \cdot \boldsymbol{s} , \tag{7}$$

where $\boldsymbol{s} = h\boldsymbol{a}^* + k\boldsymbol{b}^* + l\boldsymbol{c}^*$ is the position vector in reciprocal space and $\boldsymbol{u}$ is the displacement vector at the point r. If the dislocation line is parallel to the $\boldsymbol{c}$ direction and its Burgers vector is along the $\boldsymbol{c}$ direction, then in rectangular co-ordinates $\boldsymbol{u}$ has the form [6]

$$(8) \qquad \boldsymbol{u} = \frac{b}{2}\left\{\left[\mathrm{tg}^{-1}\frac{y}{x} + \beta\frac{xy}{x^2+y^2}\right]\boldsymbol{a} + \left[\gamma \log (x^2+y^2) - \frac{\beta}{2}\left(\frac{x^2-y^2}{x^2+y^2}\right)\right]\boldsymbol{b}\right\},$$

where $\beta = 1/2(1-\mu)$, $\gamma = -(1-2\nu)/4(1-\nu)$ and ν is Poisson's ratio. The general form for ε_{hh} is

$$(9) \qquad \varepsilon_{hh} = \frac{b}{2\pi s^2(x^2+y^2)}\Big[y(2k^2 - \gamma h^2) + xhk(2\gamma+1) + \\ + h\beta(kx - hy)\left(\frac{x^2-y^2}{x^2+y^2}\right) - 2\beta kxy\left(\frac{hy-kx}{x^2+y^2}\right)\Big].$$

The exact form of the lines of constant strain amplitude depends not only on the particular (hkl) plane but also on the value chosen for ν. However it can be shown that for the $(h\,0\,0)$ and $(0\,k\,0)$ reflection ε_{hh} has the form

$$(10) \qquad \varepsilon_{hh} = \mp \text{ const}\,\frac{\beta}{r}\sin\varphi\,(\cos^2\varphi \pm \varkappa) = \frac{c}{r}g(\varphi),$$

where $\varkappa = (1-2\nu)/2$, $r = (x^2+y^2)^{\frac{1}{2}}$, $\varphi = \mathrm{tg}^{-1}\,y/x$.

The upper signs in eqn. (10) correspond to the case of the $(h\,0\,0)$ reflection while the lower signs correspond to the $(0\,k\,0)$ reflection. The form of these curves is shown in Fig. 2*a* and 2*b* for $\nu = 0.3$.

The line profile as a function of distance in radians from the center of the line is given as (STOKES and WILSON, op. cit.)

$$(11) \qquad \frac{I(-e\,\mathrm{tg}\,\theta)}{I(0)} = \frac{\varphi_{hkl}(\varepsilon)}{\varphi(0)},$$

where $\varphi_{hkl}(\varepsilon)\,\mathrm{d}\varepsilon$ is the fraction of the crystal for which the tensile strain in the hkl direction lies between ε and $\varepsilon + \mathrm{d}\varepsilon$. The exact form of $\varphi_{hkl}(\varepsilon)\,\mathrm{d}\varepsilon$ will depend upon the function $g(\varphi)$ and on the boundary conditions. However, if E is the largest value of the strain attained on the periphery of the crystal, then the form of $\varphi(\varepsilon)\,\mathrm{d}\varepsilon$ for $\varepsilon > E$ is easily obtained.

---

[6] W. T. READ jr.: *Dislocation in Crystals* (New York, 1953).

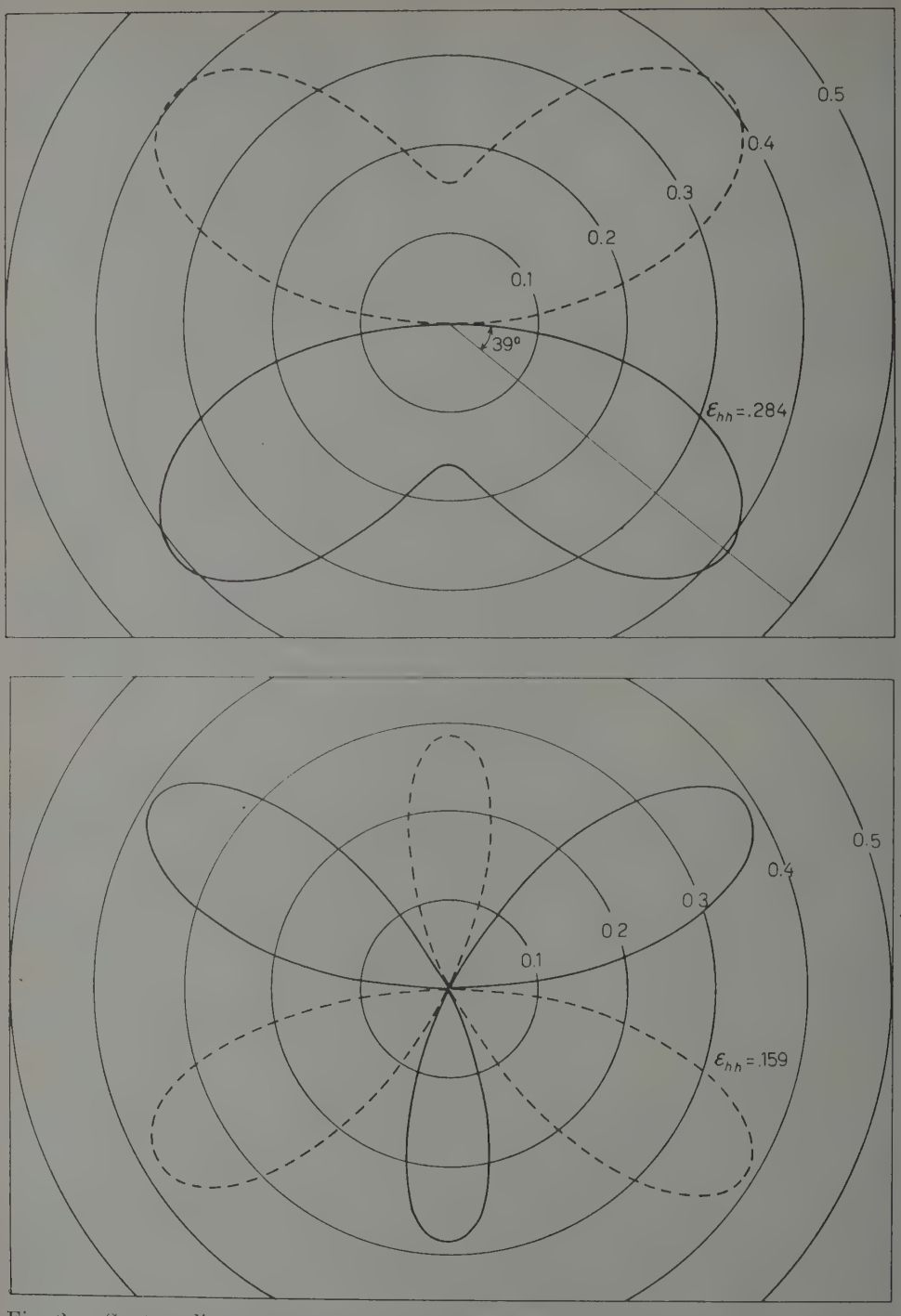

Fig. 2. Contour lines for constant tensile strain ε_{hh} in the hkl direction at the point r, φ (eq. (10)). The radial scale is in units of b. *a*) (h00); *b*) (0k0). The particular values of ε_{hh} correspond to cylinders of nearly the same radii.

The area included within any contour for which the strain ε on that contour is greater than E will be proportional to r^2 where r is the distance from the origin to some particular point on the curve:

$$S = \alpha r^2 , \tag{12}$$

and the value of α will depend on the point chosen. It follows from (10) that the change in r corresponding to a change $\mathrm{d}\varepsilon$ in the direction φ_p is

$$\mathrm{d}r = \frac{c}{\varepsilon_{hkl}} g(\varphi_p)\,\mathrm{d}\varepsilon . \tag{13}$$

Similarly the increase in area is

$$\mathrm{d}S = 2\alpha r\,\mathrm{d}r = \frac{2\alpha c^2 g^2(\varphi_r)\,\mathrm{d}\varepsilon}{\varepsilon^2} . \tag{14}$$

Now if φ_p corresponds to that direction where $g(\varphi)$ is a maximum, then from (10)

$$cg(\varphi_p) = EA \tag{15}$$

and

$$\varphi_{hkl}(\varepsilon)\,\mathrm{d}\varepsilon = \frac{\mathrm{d}S}{\pi A^2} = \frac{2\alpha E^2}{\varepsilon^3}\,\mathrm{d}\varepsilon .$$

Thus it is seen that the tail of diffraction line will tend to zero as the inverse cube of the distance from the center of the line regardless of whether the dislocation is of the screw or edge type, and regardless of the particular diffracting planes chosen, provided that the Stokes-Wilson approximation which neglects strain gradients is used. The only condition necessary is that the contours of constant strain have a form which varies in size inversely as the strain. Inspection of (9) shows that this is true for all (hkl).

The expression for $\varphi(\varepsilon)$ for $\varepsilon < E$ has not been obtained. However, in contrast to the behavior of $\varphi(\varepsilon)$ for $\varepsilon > E$, the form of $\varphi(\varepsilon)$ will probably depend on the particular form of $g(\varphi)$. Fortunately the profile $\varphi(\varepsilon)$ for $\varepsilon < E$ is not needed. The value of $\varphi(0)$ is sufficient since it determines the integral breadth (Stokes and Wilson, op. cit.)

$$\beta = 2\,\mathrm{tg}\,\theta/\varphi(0) . \tag{17}$$

$\varphi(0)$ can be obtained in a straightforward manner. The contour lines for small values of E lie very close to one or several tangent lines. By definition $\varphi(\varepsilon)\,\mathrm{d}\varepsilon$ is that fraction of the cross-sectional area of the crystal in which the

strain lies between ε and $\varepsilon+\mathrm{d}\varepsilon$. Therefore, $\varphi(0)\,\mathrm{d}\varepsilon$ is the area included between the tangent line and the contour line $\varepsilon=\mathrm{d}\varepsilon$. This area can be found as follows: Using the relation between strain and position

$$\varepsilon = f(x, y)\,, \tag{18}$$

one can find $\mathrm{d}\varepsilon/\mathrm{e}y)_{y=0}$, provided that the tangent line is assumed to be the line $y=0$. The desired area is

$$\int_{-A}^{A} \left(\frac{\mathrm{d}y}{\mathrm{d}\varepsilon}\right)_{y=0} \mathrm{d}x \tag{19}$$

and

$$\varphi(0) = \frac{\displaystyle\int_{-A}^{A} \left(\frac{\mathrm{d}y}{\mathrm{d}\varepsilon}\right)_{y=0} \mathrm{d}x}{\pi A^2}\,. \tag{20}$$

If the tangent line is not parallel to $y=0$, then it is necessary to rotate the to-ordinate system in order to satisfy this condition. Carrying out steps (18) chrough (20) on equation (10) gives the result

$$\varphi(0) = \frac{2}{3\pi E}\cdot\frac{g(\varphi_p)}{1+\varkappa}\,. \tag{21}$$

In the case of the $(0k0)$ reflection, the contour line passes through the origin three times, parallel to three tangent lines. It happens that the values of $\varphi(0)$ are the same for all three cases, therefore the correct values of $\varphi(0)$ will be three tiines that for one such line. Taking $\nu=0.3$, $\varkappa=0.2$; the corresponding values of $\varphi(0)$ are listed in the Table below:

hkl	φ_p	$g(\varphi_p)$	$\varphi(0)\cdot\frac{3\pi E}{2}$
100	$-39°$	.506	.422
010	31°	.275	1.032 $(=3\cdot.344)$

The present approximate treatment predicts, therefore, that the integral breadth of the reflection from the (100) planes (the planes which are parallel to the extra half-plane of the dislocation) is nearly $2\frac{1}{2}$ times larger than that from the (010) planes (which are parallel to the slip planes) (*). On the other

(*) This result is qualitatively in agreement with that of Suzuki and Willis (op. cit.) who report that the $(h01)$ reflection is both broader and weaker than the $(0k1)$ reflection.

hand, NYE (7) has shown that the curvature K of the lattice planes resulting from the presence of a density ϱ of dislocations of Burgers' vector $\boldsymbol{b}$ on a given slip system is given by

$$K = \varrho b \cos\theta ,$$

where θ is the angle between the lattice plane and the slip plane. On a geometrical basis, line broadening is proportional to curvature. Consequently these two treatments give different results. It should be borne in mind however, that the two models on which broadening is estimated are quite different and consequently there is little basis for a comparison.

4. – Conclusions.

WILSON (3) suggested that the shape of the line profile in the region where ε is less than E may be « ... an artifact generated by the approximations made in the Stokes-Wilson treatment. » However, it seems equally likely that the tails of the line profile, which are found to decrease as the inverse cube of the distance from the center of the line, are even more dependent on the approximations implicit in this type of derivation. Two results support the present conclusion:

a) The shape of the tail is independent of the dislocation type (edge or screw). For the edge dislocation it is also not dependent on the orientation of the diffracting planes with respect to the orientation of the dislocation line.

b) The shape of the tail obtained by direct calculation (for a screw dislocation) shows that the curve does not fall off as the inverse cube, but in fact decreases more rapidly.

The above treatment casts some doubt on the validity of the Stokes-Wilson treatment. Either the shapes of the diffraction tails are not related to the regions of high distortion near the dislocation axis or the approximations made to derive the line profiles are too severe. The latter seems more probable.

What may be said about the values of the integral breadths that have been derived in the course of the preceding treatment? Assuming that treatment to be valid, it becomes readily apparent that the integral breadths are strongly dependent on the boundary conditions on the surface of the cylinder. Consequently the approximation of a large crystal of low dislocation density by a collection of « isolated » cylindrical crystals each with an axial dislocation

(7) J. F. NYE: *Acta Met.*, **1**, 153 (1953).

is not permissible. In any real crystal containing many dislocations, the contours of zero strain would not only be those tangent lines through the dislocation center, but also, in many instances, the loci of points lying equidistant between dislocations (of opposite sign). Thus the integral breadth should depend as much on the relative orientation of the dislocations as on their number.

Finally it should be noted that the results of the approximate treatment of an axial edge dislocation can be compared with the exact results of SUZUKI and WILLIS (op. cit.) with respect to only one point: the relative breadths and intensities of the $(h01)$ and $(0k1)$ reflection, and concerning this effect both approaches are in qualitative agreement. Of the other four effects listed no comparison can be made.

* * *

The author wishes to thank Professor A. J. C. WILSON for his helpful suggestions and Dr. T. B. MASSALSKI for numerous invaluable discussions.

RIASSUNTO (*)

Il problema di comprendere l'effetto delle dislocazioni sulla diffrazione dei raggi X è ancora largamente insoluto. Le trattazioni di WILSON (1), SUZUKI e WILLIS (2) non sono state verificate sperimentalmente. È tuttavia possibile dimostrare che il profilo lineare dedotto da una precisa trattazione, è in accordo, qualitativamente, con quella ricavata dalla approssimazione di Stokes-Wilson (4). La trattazione approssimata si può estendere al caso di una dislocazione « edge ». Fatto ciò, si trova che la coda del profilo lineare non dipende dal tipo di dislocazione nè dalla orientazione. È pure possibile dimostrare che la larghezza integrale, che si ottiene anche con la trattazione approssimata, è strettamente dipendente dalle condizioni al contorno, assunte per il cristallo cilindrico. Di conseguenza, i risultati ottenuti considerando una singola dislocazione isolata, sembrerebbero applicabili a un aggregato di dislocazioni in un cristallo reale.

(*) *Traduzione a cura della Redazione.*

IL NUOVO CIMENTO Vol. XIII, N. 6 16 Settembre 1959

Pion-Hyperon Scattering. Influence of Non-Symmetric Λ and Σ Interaction.

D. Amati (*), A. Stanghellini (**) and B. Vitale (***)

CERN - Geneva

(ricevuto il 30 Maggio 1959)

Summary. — A field theoretical model is developed in order to study the low-energy pion scattering on Λ or Σ hyperons, taking into account the Λ-Σ mass difference and possible inequality of the coupling constants. From the results it is possible to study the corrections to the prediction of a theory in which Λ and Σ are considered degenerate with respect to pion interactions. These corrections are of the order of the hyperon mass difference over the pion energy and can shift the possible resonances in an appreciable way. It is also briefly discussed which states can present resonances for particular choices of the coupling constants. The relations of the previous results to the K^--N absorption are discussed from a qualitative point of view.

1. – Introduction.

In this paper we shall deal with the low-energy scattering of pions by the Λ or Σ hyperons (which we shall call Y).

The main reason for our interest in such phenomena is that the Y scattering is suitable for theoretical speculation on the validity of global symmetry [1].

The field theoretical model will consist of a fixed Y which can appear either as Λ or Σ, interacting with the π and K meson fields, treated in the one-meson approximation.

(*) On leave from: Istituto di Fisica dell'Università - Roma.

(**) On leave from: Istituto di Fisica dell'Università - Bologna.

(***) On leave from: Istituto di Fisica Teorica dell'Università - Napoli.

(1) M. Gell-Mann: *Phys. Rev.*, **106**, 1297 (1957).

The soundness of the fixed source model ([2]), as applied to the πN scattering and the validity of the one-meson approximation was clarified by the dispersive approach ([3]), and is essentially due to the fact that high-energy phenomena (as inelastic processes and pair effects) are damped by large energy denominators. Moreover, the kinematical recoil corrections do not change the main features of the static model. We therefore feel justified in applying to our case a method which gives a reasonable picture of the analogous problem of πN scattering.

Following such an approach we shall be able to obtain the πY scattering as function of the physical masses, renormalized coupling constants and cut-off parameters. As for the values of those parameters, they would be determined by comparison with future experiments if no other hypothesis (such as global symmetry) is introduced into the theory.

Let us now see how the heavy mesons enter into the game. They give essentially three contributions: mass and charge renormalization, and physical intermediate states in which they are present. Our method allows us to deal automatically with the renormalization effects, because only the observed masses and renormalized coupling constants appear in our equations. The effects due to intermediate K-mesons would enter through physical amplitude for the process like

$$Y + \pi \to \overline{K} + N .$$

The threshold for such a process is of the same order as the one for two-pion production. We shall therefore disregard those contributions which would in any way be less important (*) than the two-pion production which has already been neglected in the spirit of the one-meson approximation.

In the limit of no mass and coupling constant differences, our scattering matrices coincide with the global symmetric ones. However, in this case, or rather in the case where the symmetry is limited to only Λ and Σ hyperons (limited symmetry or l.s.), such results could be obtained in a more simple way. It is sufficient to consider the scattering amplitudes as a combination of the amplitudes $a_{\frac{1}{2}}$, $a_{\frac{3}{2}}$ in the representation in which the Y are taken as isospinors ([4]), and write them as function of the coupling constant and the cut-off parameters in complete analogy with the πN scattering. When all the baryons are degenerate, those parameters coincide with the πN ones in

---

([2]) G. F. CHEW and F. E. LOW: *Phys. Rev.*, **101**, 1570 (1956).

([3]) G. F. CHEW, M. L. GOLDBERGER, F. E. LOW and Y. NAMBU: *Phys. Rev.*, **106**, 1337 (1957).

(*) There have been given reasons to believe that the strength of K interaction is less effective than that of the pion ([1]).

([4]) D. AMATI and B. VITALE: *Nuovo Cimento*, **9**, 895 (1958).

the global symmetry. The influence of mass and coupling constant differences should give an insight on the corrections to the limited symmetric results.

The technique we shall use to solve our model is similar to that developed by BOSCO, FUBINI and STANGHELLINI (5) which leads to the same results as the Chew and Low formalism for the pion-nucleon scattering.

The reason for using such a method, even if it is less general, lies in its simplicity; it allows besides straightforward calculation of matrix elements of other processes in which the πY state is present as final or intermediate (for instance: $\overline{K}N$ absorption and $\overline{K}N$ scattering). We note in passing that in the « pology » philosphy (6) the πY scattering can be measured by a suitable extrapolation of the cross-section for the process $N+Y \to N+Y+\pi$.

We shall treat Λ and Σ as having the same parity. There is not yet any clear experimental justification of that fact (7); however, we note that in the case of opposite parities the l.s. would have no meaning at all.

2. – We start from the hypothesis that the physical $|\Lambda\rangle$ and $|\Sigma_i\rangle$ are eigenstates of the total Hamiltonian, which also contains the K interactions. This total H is normalized to be

$$(1) \qquad \begin{cases} H|\Lambda\rangle = 0 \\ H|\Sigma_i\rangle = \Delta|\Sigma_i\rangle . \end{cases}$$

The scattering states $|\pi Y\rangle$ are given by the following « Ansatz »:

$$(2) \qquad |\pi_q Y\rangle = \Sigma_{q'} a^+_{q'}|\Sigma\rangle X_1(\underline{q}'\underline{q}) + \Sigma_{q'} a^+_{q'}|\Lambda\rangle X_2(\underline{q}'\underline{q}) + |\Sigma\rangle C_1 + |\Lambda\rangle C_2 ,$$

where X and C are matrices in the spin and isospin spaces of the Y's and in the isospaces of the π's. The two constants C_1 and C_2 are determined by the orthogonality between the scattering states and the $|Y\rangle$ states

$$(3) \qquad \begin{cases} \langle\Sigma|Y\pi\rangle = 0 , \\ \langle\Lambda|Y\pi\rangle = 0 . \end{cases}$$

The correct scattering states satisfy the equation

$$(4) \qquad (H-\omega)|\pi_q Y\rangle = 0 ,$$

where ω is the total energy of the state.

(5) B. BOSCO, S. FUBINI and A. STANGHELLINI: *Nucl. Phys.*, **10**, 663 (1959).

(6) G. F. CHEW and F. E. LOW: *Phys. Rev.* **113**, 1640 (1959).

(7) See, for instance, D. AMATI and B. VITALE: *Strong interaction of strange particles*, to appear in *Forts. d. Phys.*

By a variational method ([8]) we choose the approximate states (2) which better satisfy equation (4). This goal is reached if the following two conditions are fulfilled:

$$(5) \qquad \begin{cases} \langle \Sigma | a_{q'}(H-\omega)|\pi_q Y\rangle = 0\,, \\ \langle \Lambda | a_{q'}(H-\omega)|\pi_q Y\rangle = 0\,. \end{cases}$$

These conditions are in the form of two coupled integral equations for the functions X. The solutions of the integral equations determine the scattering state and are simply related to the scattering matrix.

The advantage of having the scattering state directly, and not only the scattering matrix, lies in the possible straightforward calculation of matrix elements where this state is present (as in the case of K^- absorption and scattering).

Let us now say something about the « Ansatz » (2) for the πY state vector. This is constructed in analogy to the πN state vector ([8]). It has the right asymptotic behaviour and it is orthogonal to the ground states. BFS ([5]) have shown that it corresponds to the one-meson approximation of CHEW and LOW ([2]), if one takes the $|Y\rangle$ and the $|\pi Y\rangle$ as intermediate states in the calculation of the kernels. This means that we neglect correction due to physical inelastic processes where more mesons are involved.

It is preferable to have the $|\pi Y\rangle$ state as an eigenstate of the total isotopic spin right from the beginning than to diagonalize the X functions at the end. So we have to deal with three πY states corresponding to $T = 0, 1, 2$ (due to the indipendence of X and C on T_3, we have choosen those components which are most suitable for calculations):

$T = 0$ $T_3 = 0$	$\|\pi_q Y\rangle^0 = \Sigma_{q'i} \dfrac{1}{\sqrt{3}} a^+_{q'i} \|\Sigma_i\rangle X^0(q'q) + \|\Lambda\rangle C_0\,,$
$T = 1$ $T_3 = 0$	$\|\pi_q Y\rangle^1 = \Sigma_{q'} a^+_{q'3} \|\Lambda\rangle X^1_1(q'q) + \Sigma_{q'jk} \dfrac{i}{\sqrt{2}} \varepsilon_{3jk} a^+_{q'j} \|\Sigma_k\rangle X^1_2(q'q) + \|\Sigma_3\rangle C_1\,,$
$T = 2$ $T_3 = 2$	$\|\pi_q Y\rangle^2 = \Sigma_{q'} a^+_{q'+} \|\Sigma_+\rangle X^2(q'q)\,,$

([8]) R. STROFFOLINI: *Phys. Rev.*, **104**, 1146 (1956); M. H. FRIEDMAN, T. D. LEE and R. CHRISTIAN: *Phys. Rev.*, **100**, 1496 (1955).

where X and C are matrices in spin space and ijk indicate the various types of π's and Σ's. $T=0$ and $T=2$ contain only one X and so are very similar to the πN case. The $T=1$ state vector contains two X due to the fact that one can find the Λ and Σ asymptotically; we shall give here some details of the determination of the X's in this less trivial case.

From Eq. (3) we have

$$C = -\Sigma_{q''}\left\{\langle\Sigma_3|a^+_{q''3}|\Lambda\rangle X_1 + \frac{i\varepsilon_{3ji}}{\sqrt{2}}\langle\Sigma_3|a^+_{q''i}|\Sigma_j\rangle X_2\right\}. \tag{6}$$

The two conditions (5) can be written with the introduction of the Ansatz for the scattering state:

$$\left\{\begin{aligned}
&\Sigma_{q''}\langle\Lambda|a_{q'3}(H-\omega)a^+_{q''3}|\Lambda\rangle X_1(q''q) + \langle\Lambda|a_{q'3}(H-\omega)|\Sigma_3\rangle C + \\
&\qquad + \Sigma_{q''}\langle\Lambda|a_{q'3}(H-\omega)a^+_{q''i}|\Sigma_j\rangle X_2(q''q)\frac{i}{\sqrt{2}}\varepsilon_{3ji} = 0, \\
&\Sigma_{q''}\frac{-i}{\sqrt{2}}\varepsilon_{3\varrho\sigma}\langle\Sigma_\varrho|a_{q'\sigma}(H-\omega)a^+_{q''3}|\Lambda\rangle X_1(q''q) - \frac{i}{\sqrt{2}}\varepsilon_{3\varrho\sigma}\langle\Sigma_\varrho|a_{q'\sigma}(H-\omega)|\Sigma_3\rangle C + \\
&\qquad + \Sigma_{q''}\frac{-i}{\sqrt{2}}\varepsilon_{3\varrho\sigma}\langle\Sigma_\varrho|a_{q'\sigma}(H-\omega)a^+_{q''i}|\Sigma_j\rangle\frac{i\varepsilon_{3ji}}{\sqrt{2}}X_2(q''q) = 0.
\end{aligned}\right. \tag{7}$$

Now we take the creation operator from the right to the left and vice versa for the destruction operator, making use of the identity

$$[a_i,[H,a^+_j]] = \omega_i\delta_{ij},$$

which is a consequence of the linearity in the meson field of the interaction Hamiltonian. (9) The commutation relations of the field operators and the use of the normalization of the Hamiltonian lead to:

$$\begin{aligned}
&(\omega'-\omega)X_1(q'q) - \Sigma_{q''}\langle\Lambda|a^+_{q''3}(H+\omega)a_{q'3}|\Lambda\rangle X_1(q''q) - \\
&-\Sigma_{q''}\langle\Lambda|a^+_{q''i}(H+\omega-\Lambda)a_{q'3}|\Sigma_j\rangle X_2(q''q)\frac{i}{\sqrt{2}}\varepsilon_{3ji} + (\Lambda-\omega)\langle\Lambda|a_{q'3}|\Sigma_3\rangle C = 0,
\end{aligned} \tag{8}$$

$$\begin{aligned}
&(\omega'-\Lambda-\omega)X_2(q'q) - \\
&\qquad - \Sigma_{q''}\frac{-i}{\sqrt{2}}\varepsilon_{3\varrho\sigma}\langle\Sigma_\varrho|a^+_{q''i}(H-\omega-2\Lambda)a_{q'\sigma}|\Sigma_j\rangle X_2(q''q)\frac{i}{\sqrt{2}}\varepsilon_{3ji} + \\
&\qquad + \Sigma_{q''}\frac{i}{\sqrt{2}}\varepsilon_{3\varrho\sigma}\langle\Sigma_\varrho|a^+_{q''3}(H+\omega-\Lambda)a_{q'\sigma}|\Lambda\rangle X_1(q''q) + \\
&\qquad + \frac{-i}{\sqrt{2}}(\Lambda-\omega)\varepsilon_{3\varrho\sigma}\langle\Sigma_\varrho|a_{q'\sigma}|\Sigma_3\rangle C = 0.
\end{aligned} \tag{8'}$$

(9) We wish to emphasize that an explicit form of the Hamiltonian is not needed. So our results are independent of the detailed origin of the mass differences and coupling constants renormalization.

We now introduce the hyperons Λ and Σ in (8) and (8′) as intermediate states. Making use of the following identity where $V^+_{qj}=[a_{qj}, H']$

$$\langle \Sigma_i | a_{qj} | \Lambda \rangle = -\frac{1}{\Lambda+\omega_q} \langle \Sigma_i | V^+_{qj} | \Lambda \rangle ,$$

$$\langle \Sigma_i | a_{qj} | \Sigma_k \rangle = -\frac{1}{\omega_q} \langle \Sigma_i | V^+_{qj} | \Sigma_k \rangle ,$$

and the complex conjugate ones, Eqs. (8) and (8′) can be rewritten as

$$(9)\quad \begin{cases} (\omega-\omega')X_1(q'q) = -\Sigma_{q''}K_{11}(\omega\, q'q'')X_1(q''q) - \Sigma_{q''}K_{12}(\omega q'q'')X_1(q''q) , \\ K_{11} = \dfrac{\Lambda+\omega}{(\Lambda+\omega'')(\Lambda+\omega')} \langle \Lambda | V_{q''3} | \Sigma_3 \rangle \langle \Sigma_3 | V^+_{q'3} | \Lambda \rangle - \\ \qquad - \dfrac{(\omega-\Lambda)}{(\omega'-\Lambda)(\omega''-\Lambda)} \langle \Lambda | V^+_{q'3} | \Sigma_3 \rangle \langle \Sigma_3 | V_{q''3} | \Lambda \rangle , \\ K_{12} = \dfrac{\omega}{\omega'(\omega''+\Lambda)} \langle \Lambda | V_{q''i} | \Sigma_i \rangle \langle \Sigma_i | V^+_{q'3} | \Sigma_j \rangle \dfrac{i}{\sqrt{2}} \varepsilon_{3ji} - \\ \qquad - \dfrac{(\omega-\Lambda)}{(\omega'-\Lambda)\omega''} \langle \Lambda | V^+_{q'3} | \Sigma_3 \rangle \langle \Sigma_3 | V_{q''i} | \Sigma_j \rangle \dfrac{i}{\sqrt{2}} \varepsilon_{3ji} , \end{cases}$$

$$(9')\quad \begin{cases} (\omega-\omega'-\Lambda)X_2(q'q) = -\Sigma_{q''}K_{22}(\omega q'q'')X_2(q''q) - \Sigma_{q''}K_{21}(\omega q'q'')X_1(q''q) , \\ K_{22} = \left(\dfrac{\omega'-2\Lambda}{(\omega''-\Lambda)(\omega'-\Lambda)} + \dfrac{\omega-\Lambda}{\omega''\omega'} \right) \langle \Sigma_\varrho | V_{q''i} | \Lambda \rangle \langle \Lambda | V^+_{q'\sigma} | \Sigma_j \rangle \dfrac{\varepsilon_{3\varrho\sigma}\varepsilon_{3ji}}{2} - \\ \qquad - \dfrac{\omega-\Lambda}{\omega'\omega''} \langle \Sigma_\varrho | V^+_{q'\sigma} | \Sigma_3 \rangle \langle \Sigma_3 | V_{q''i} | \Sigma_j \rangle \dfrac{\varepsilon_{3\varrho\sigma}\varepsilon_{3ji}}{2} , \\ K_{21} = \dfrac{-i}{\sqrt{2}} \varepsilon_{3\varrho\sigma} \left(\dfrac{\omega}{\omega''(\omega'-\Lambda)} \langle \Sigma_\varrho | V_{q''3} | \Sigma_\sigma \rangle \langle \Sigma_\sigma | V^+_{q'\sigma} | \Lambda \rangle - \right. \\ \qquad \left. - \dfrac{\omega-\Lambda}{\omega'(\omega''-\Lambda)} \langle \Sigma_\varrho | V^+_{q'\sigma} | \Sigma_3 \rangle \langle \Sigma_3 | V_{q''3} | \Lambda \rangle \right) . \end{cases}$$

The kernels of the two coupled integral equations (9) and (9′) depend only on the mass difference and on the renormalized coupling constants. In fact, the coupling constant renormalization is simply given by the definition

$$(10)\qquad \langle \Lambda | V_{qk} | \Sigma_k \rangle = i f_\Lambda \sqrt{\frac{2\pi}{\omega_q}}\, u_\Lambda(q)\boldsymbol{\sigma q} ,$$

and

$$\langle \Sigma_i | V_{qk} | \Sigma_j \rangle = f_\Sigma \sqrt{\frac{2}{\omega_q}}\, u_\Sigma(q)\boldsymbol{\sigma q}\varepsilon_{ijk} .$$

This means that the interaction of a pseudoscalar π with a physical Λ and Σ with equal relative parity is determined completely, due to the invariance under rotation and reflection in ordinary space and rotation in isospace of the matrix elements (10) by two constants, the renormalized couplings, the reality of which is given by the time reversal invariance. $u_\Lambda(q)$ and $u_\Sigma(q)$ are the cut-off functions introduced in order to show explicitly the low-energy validity of our model.

The part of the kernels coming from an intermediate πY state can be calculated in terms of πY scattering itself. Such contributions can be taken into account by iteration. These corrections are of the same nature as those of the crossing corrections in the πN case. They turn out to be small ([2-5]) and will be neglected in this paper.

We substitute the explicit form of the matrix elements (10) in (9) and (9′). The integral equations in the total angular momentum representation are:

$$(\omega-\omega'-\Delta\delta_{i2})X_i(\omega,\omega')=-\int K_{ij}(\omega,\omega',\omega'')\,X_j(\omega,\omega'')\,\mathrm{d}\omega''\,.$$

$J=\frac{3}{2}$

$$(11)\quad\begin{cases} K_{11}=\dfrac{2f_\Lambda^2}{3\pi}\sqrt{q'^3q''^3}\,\dfrac{\omega+\Delta}{(\omega'+\Delta)(\omega''+\Delta)}\,u_\Lambda(q')u_\Lambda(q''), \\ K_{12}(\omega',\omega'')=-\dfrac{2\sqrt{2}}{3\pi}f_\Lambda f_\Sigma\sqrt{q'^3q''^3}\,\dfrac{\omega}{\omega'(\omega''+\Delta)}\,u_\Lambda(q')u_\Sigma(q'')=K_{21}(\omega'',\omega'), \\ K_{22}=\dfrac{2}{3\pi}\sqrt{q'^3q''^3}\left(f_\Lambda^2\,\dfrac{\omega-2\Delta}{(\omega'-\Delta)(\omega''-\Delta)}\,u_\Lambda(q')u_\Lambda(q'')-f_\Sigma^2\,\dfrac{\omega-\Delta}{\omega'\omega''}\,u_\Sigma(q')u_\Sigma(q'')\right), \end{cases}$$

$J=\frac{1}{2}$

$$(11')\quad\begin{cases} K_{11}=\dfrac{-f_\Lambda^2}{3\pi}\sqrt{q'^3q''^3}\left(\dfrac{\omega+\Delta}{(\omega'+\Delta)(\omega''+\Delta)}+3\,\dfrac{\omega-\Delta}{(\omega'-\Delta)(\omega''-\Delta)}\right)u_\Lambda(q')\,u_\Lambda(q''), \\ K_{12}(\omega',\omega'')=-\dfrac{\sqrt{2}}{3\pi}f_\Lambda f_\Sigma\sqrt{q'^3q''^3}\left(3\,\dfrac{\omega-\Delta}{(\omega'-\Delta)\omega''}-\dfrac{\omega}{(\omega''+\Delta)\omega'}\right)u_\Lambda(q')\,u_\Sigma(q'')= \\ \qquad\qquad =K_{21}(\omega'',\omega'), \\ K_{22}=-\dfrac{1}{3\pi}\sqrt{q'^3q''^3}\cdot \\ \qquad\cdot\left(7f_\Sigma^2\,\dfrac{\omega-\Delta}{\omega'\omega''}\,u_\Sigma(q')\,u_\Sigma(q'')-f_\Lambda^2\,\dfrac{\omega-2\Delta}{(\omega'-\Delta)(\omega''-\Delta)}\,u_\Lambda(q')u_\Lambda(q'')\right). \end{cases}$$

These integral equations have separable kernels and so they can be reduced to the solution of a system of linear equations.

It is convenient to solve the integral equations with stationary boundary conditions and to get the K matrix, which is defined as:

$$\left.\begin{aligned} K_{\Lambda\Lambda} &= -\pi \lim_{\omega\to\omega'} (\omega-\omega') X_1(\omega'\omega) \\ K_{\Lambda\Sigma} &= -\pi \lim_{\omega\to\omega'+\Delta} (\omega-\omega'-\Delta) X_2(\omega'\omega) \end{aligned}\right| \begin{aligned} &\text{with the following stationary boundary conditions:} \\ X_1 &= \delta(\omega-\omega') + \frac{P}{\omega-\omega'}\cdots, \\ X_2 &= \frac{P}{\omega-\omega'-\Delta}\cdots, \end{aligned}$$

$$\left.\begin{aligned} K_{\Sigma\Sigma} &= -\pi \lim_{\omega\to\omega'+\Delta} (\omega-\omega'-\Delta) X_2(\omega'\omega) \\ K_{\Sigma\Lambda} &= -\pi \lim_{\omega\to\omega'} (\omega-\omega') X_1(\omega'\omega) \end{aligned}\right| \begin{aligned} X_1 &= \frac{P}{\omega-\omega'}\cdots, \\ X_2 &= \delta(\omega-\omega'-\Delta) + \frac{P}{\omega-\omega'-\Delta}\cdots. \end{aligned}$$

We do not have $\Lambda\Sigma$ transition for $T=0$ and $T=2$, so the K matrix is simply reduced to the tangent of a real phase-shift. The results are collected here:

$J=\frac{3}{2}$

(12)

$$\left\{\begin{aligned}
&T=0 \\
&\quad \operatorname{tg}\delta_3^0 = \frac{2}{3}\frac{q^3}{D_3^0}\left\{\frac{f_\Lambda^2}{\omega-2\Delta}[1+4f_\Sigma^2 I\Delta] - \frac{2f_\Sigma^2}{\omega-\Delta}[1+2f_\Lambda^2 I\Delta]\right\}, \\
&\quad\quad D_3^0 = 1+2(2f_\Sigma^2-f_\Lambda^2)I\omega + 4(f_\Lambda^2-f_\Sigma^2)I\Delta, \\
&T=1 \\
&\quad K_{\Lambda\Lambda}^3 = \frac{2}{3}\frac{f_\Lambda^2\bar{q}^3}{D_3^1(\omega+\Delta)}\{1+2(f_\Sigma^2+f_\Lambda^2)I\omega + 2(3f_\Lambda^2-f_\Sigma^2)I\Delta + 0(\Delta^2)\}, \\
&\quad K_{\Lambda\Sigma}^3 = -\frac{2\sqrt{2}}{3}\frac{f_\Lambda f_\Sigma\sqrt{q^3}}{D_3'\omega}\{1-2(3f_\Lambda^2-f_\Sigma^2)I\Delta + 0(\Delta^2)\}\sqrt{\bar{q}^3}, \\
&\quad K_{\Sigma\Sigma}^3 = \frac{2}{3}\frac{q^3}{D_3^1}\left\{\frac{f_\Sigma^2[1-6f_\Lambda^2 I\Delta]+0(\Delta^2)}{\omega-\Delta} - \right. \\
&\qquad\qquad \left. - \frac{f_\Lambda^2[1-2(f_\Lambda^2+f_\Sigma^2)I\omega - 2(f_\Lambda^2-f_\Sigma^2)I\Delta]+0(\Delta^2)}{\omega-2\Delta}\right\}, \\
&\quad\quad D_3^1 = 1-2f_\Sigma^2 I\omega - 2(3f_\Lambda^2-f_\Sigma^2)I\Delta - 4f_\Lambda^2(f_\Lambda^2+f_\Sigma^2)I^2\omega^2 + \\
&\qquad\qquad + 4f_\Lambda^2 I^2\Delta\omega + 4f_\Lambda^2(2f_\Lambda^2-f_\Sigma^2)I^2\Delta^2, \\
&T=2 \\
&\quad \operatorname{tg}\delta_3^2 = \frac{2}{3}\frac{q^3}{D_3^2}\left\{\frac{f_\Lambda^2}{\omega-2\Delta}[1-2f_\Sigma^2 I\Delta] + \frac{f_\Sigma^2}{\omega-\Delta}[1+2f_\Lambda^2 I\Delta]\right\}, \\
&\quad\quad D_3^2 = 1-2(f_\Lambda^2+f_\Sigma^2)I\omega + 2(2f_\Lambda^2+f_\Sigma^2)I\Delta,
\end{aligned}\right.$$

where q ($\bar{q}$) is the π momentum when Σ (Λ) is present in the final state.

$J=\frac{1}{2}$

$T=0$

$$\operatorname{tg}\delta_1^0=-\frac{q^3}{3D_1^0}\left\{\frac{f_\Lambda^2}{\omega-2\Delta}[1-2(-9f_\Lambda^2+f_\Sigma^2)I\Delta+\right.$$
$$\left.+\frac{9f_\Lambda^2}{\omega}[1-2(f_\Lambda^2-f_\Sigma^2)I\Delta]-\frac{2f_\Sigma^2}{\omega-\Delta}[1+8f_\Lambda^2I\Delta]\right\},$$

$T=1$

$$K_{\Lambda\Lambda}^1=-\frac{f_\Lambda^2\bar{q}^3}{3D_1^1}\cdot$$
$$\cdot\left\{\frac{1+(7f_\Sigma^2-f_\Lambda^2)I\omega-(7f_\Sigma^2+4f_\Lambda^2)I\Delta-2f_\Lambda^2(11f_\Sigma^2-3f_\Lambda^2)I^2\Delta\omega+0(\Delta^2)}{\omega+\Delta}+\right.$$
$$+\frac{3[1+(7f_\Sigma^2-f_\Lambda^2)I\omega-(7f_\Sigma^2-4f_\Lambda^2)I\Delta-2f_\Lambda^2(7f_\Sigma^2-7f_\Lambda^2)I^2\Delta\omega+0(\Delta^2)]}{\omega-\Delta}-$$
$$\left.-8f_\Sigma^2(1+4f_\Lambda^2I\Delta)I\right\},$$

$$K_{\Lambda\Sigma}^1=-\frac{\sqrt{2}}{3}\frac{f_\Lambda f_\Sigma\sqrt{q^3}}{D_1^1}\cdot$$
$$\cdot\left\{\frac{3[1+(7f_\Sigma^2-f_\Lambda^2)I\omega-(7f_\Sigma^2-4f_\Lambda^2)I\Delta-2f_\Lambda^2(7f_\Sigma^2-7f_\Lambda^2)I^2\Delta\omega+0(\Delta^2)]}{\omega-\Delta}-\right.$$
$$-\frac{1+(7f_\Sigma^2-f_\Lambda^2)I\omega-7f_\Sigma^2I\Delta-2f_\Lambda^2(f_\Sigma^2-f_\Lambda^2)I^2\omega\Delta+0(\Delta^2)}{\omega}-$$
$$\left.-2(7f_\Sigma^2-f_\Lambda^2)(1+4f_\Lambda^2I\Delta)I\right\}\sqrt{q^3},$$

$$K_{\Sigma\Sigma}^1=-\frac{q^3}{3D_1^1}\left\{\frac{7f_\Sigma^2}{\omega-\Delta}[1+4f_\Lambda^2I\omega+4f_\Lambda^2(f_\Sigma^2-f_\Lambda^2)I^2\Delta\omega-f_\Lambda^2I\Delta+0(\Delta^2)]-\right.$$
$$-\frac{f_\Lambda^2}{\omega-2\Delta}[1+4f_\Lambda^2I\omega+24f_\Lambda^2f_\Sigma^2I^2\Delta\omega+(7f_\Sigma^2-2f_\Lambda^2)I\Delta+0(\Delta^2)]-$$
$$\left.-4f_\Lambda^2f_\Sigma^2[2-(7f_\Sigma^2+f_\Lambda^2)I\Delta]\right\},$$

$$D_1^1=1+(7f_\Lambda^2+3f_\Lambda^2)I\omega-7f_\Sigma^2I\Delta+4f_\Lambda^2(5f_\Sigma^2-f_\Lambda^2)I^2\omega^2-$$
$$-2f_\Lambda^2(9f_\Sigma^2-5f_\Lambda^2)I^2\omega\Delta-4f_\Lambda^2(f_\Sigma^2+f_\Lambda^2)I^2\Delta^2,$$

(12′)

$T=2$

$$\operatorname{tg}\delta_1^2=-\frac{1}{3}\frac{q^3}{D_1^2}\left\{\frac{f_\Lambda^2}{\omega-2\Delta}[1+f_\Sigma^2I\Delta]+\frac{f_\Sigma^2}{\omega-\Delta}[1-f_\Lambda^2I\Delta]\right\},$$
$$D_1^2=1+(f_\Lambda^2+f_\Sigma^2)I\omega-(2f_\Lambda^2+f_\Sigma^2)I\Delta.$$

$O(\Delta^2)$ are terms of the order $(\Delta/\Omega)^2$, where $\Omega\simeq 1/f^2I$ is essentially the re-

sonant energy as explained in the next section:

$$I(\omega) = \frac{1}{3\pi}\int \mathrm{d}\omega' \frac{q'^3 u^2(q')}{\omega'^2(\omega' - \omega)} .$$

In the solution of the system of linear equations we have put $\Delta = 0$ in the integrals of the type I. This approximation gives corrections of the order of $\Delta/\omega_{\text{cut-off}}$. Global symmetry and physical intuition suggests that the cut-off energies are of the order of the baryon masses. So any corrections to I due to the mass differences and to possible different cut-off energies will always be of the order of Δ/M_Y. Also, those corrections are consistent with the effective range approximation which one usually does in the πN scattering (I independent of ω) and are quite smaller than the Δ-correction we shall find below.

3. – We shall now discuss which corrections come from the difference of hyperon masses and the inequality of the coupling constants (c.c.). In the l.s. scheme, both corrections are due to renormalization effect of heavy mesons. The mass difference Δ is known from experiments ($\Delta \simeq 75$ MeV); if the renormalization effect on the c.c. is of the same order of magnitude, we can expect $\delta = f_\Lambda^2 - f_\Sigma^2$ to be rather small, perhaps such that $\Delta/M_Y \sim \delta/f_Y^2 Y$.

The first thing to note from (12) is that a resonant phenomenon analogous to the 33 resonance in πN scattering can be present in the states with $J = \frac{3}{2}$ and $T = 1$ or $T = 2$ as was clearly to be expected from global symmetric considerations. It is important to note that for each value of T and J the K matrices for the different reactions have the same denominator for the same value of the total energy. This means that if π-Λ is resonant, π-Σ is also resonant just at the same total energy (different π energies). Then, for instance, in K^-N absorption, the final state is just as near or far from a resonance, disregarding if there is a Λ or a Σ in it.

From the straightforward analysis of (12) is appears that the effect of Δ is essentially of two types. The first one is already present in the Born approximation and is due to the fact that the hyperon mass difference can change the kinetic energy of the intermediate states. In general those corrections are of the order Δ/ω. The second type of corrections, appearing in the rescattering terms, can change the position of the possible resonance and the energy dependence. Putting for simplicity $\delta = 0$, D_1^3 and D_2^3 are given by

$$D_1^3 = [1 + 2f_Y^2 I(\omega - \Delta)]\,[1 - 4f_Y^2 I(\omega + \tfrac{1}{2}\Delta)] ,$$

$$D_2^3 = 1 - 4I(\omega - \tfrac{3}{2}\Delta) .$$

One then easily sees that $\Omega = 1/4 f_Y^2 I$ being the resonant energy in the l.s. approximation, the Δ corrections shift the resonance in different directions for the two different states, *i.e.*

$$\Omega - \tfrac{1}{2}\Delta = \omega_{r,1} ,$$

$$\Omega + \tfrac{3}{2}\Delta = \omega_{r,2} .$$

It would be tempting to associate Ω with the 33 πN resonance energy; this would mean essentially a global symmetry hypothesis of equal π-baryon coupling constants and equal cut-offs for all the baryons. In such a case $\Omega = 290$ MeV, so $\omega_{r,1} \simeq 250$ MeV, and this implies that no πY resonance can be excited in K^-N absorption. Nevertheless, we think that such an association is not very justifiable, the cut-off energies and pion coupling constant being essentially independent parameters. Besides, physical intuition suggests that the corrections to global symmetry should be of the order of the mass difference between nucleons and hyperons. Such corrections are of the same order of magnitude (20%) as those we have discussed in this paper, *i.e.* Δ/Ω, and might spoil the considerations made by associating Ω to the πN resonant energy. As for the shape of the energy dependence of the matrix elements, the corrections are of the order Δ/Ω.

A particularly interesting case is that of $\pi\Sigma \to \pi\Sigma$ for $T = 1$, $J = \frac{3}{2}$. In l.s. the Born approximation for such a process vanishes; this fact can be easily understood in the doublet representation for hyperons from the particular combination of the $I = \frac{1}{2}$ and $\frac{3}{2}$ amplitudes ([1]) of the pion-hyperon doublet scattering. This fact brings a rather different energy behaviour of $K_{\Sigma\Sigma}$ (as compared with $K_{\Lambda\Lambda}$ and $K_{\Sigma\Lambda}$) also in the presence of rescattering. However, the correction to this l.s. result brings on a non-zero Born term of the order Δ or δ.

It is clear that the Δ corrections are important at low energies and become less effective as the energy increases. There is a similar occurrence in pion-nucleon scattering where the pion mass difference spoils the charge independence symmetry at very low energies.

Regarding the δ corrections, these are of the order δ/f_Y^2; however, it is senseless to analyse them in detail without knowing either δ or f_Y^2.

If the coupling constants would be somewhat different (no l.s. at all), we could see by direct inspection of (12) that resonances can appear in states other than those previously discussed ([10]). For instance if $f_\Lambda^2 \gg f_\Sigma^2$ (this is the

([10]) Similar results have been recently obtained by M. NAUENBERG (*Phys. Rev. Letters* **2**, 351 (1959)). We thank Dr. NAUENBERG for having sent us his results prior to publication.

only meaningful drastic inequality because it allows for Λ and Σ processes) resonances could appear in the $T=0$, $J=\frac{3}{2}$ or $T=1$, $J=\frac{1}{2}$ states. As pointed out before, no true meaning can be assigned to these conclusions, *i.e.* no resonance can be really predicted along these lines. But if a resonance of that sort turns out to be found experimentally, there is certainly room for it in our model by suitable choice of the parameters. We note that the state with $T=2$, $J=\frac{1}{2}$ is the only one for which there is no place for a resonance for all choices of the coupling constants.

4. – The results obtained in the previous paragraphs could be of some utility for the study of the $\overline{\mathrm{K}}$-nucleon interactions using a model consistent with that here discussed for the pion-hyperon interaction.

Let us take, for instance, the K^- absorption on nucleon with production of a pion and a hyperon. The matrix elements involved are:

$$\langle N | V_K | \pi Y \rangle ,$$

where V_K represents the K-meson current.

For the $|\pi Y\rangle$ states one can use those derived in the preceeding paragraphs, which implies to treat the K interaction at the lowest order.

Let us assume again, for simplicity, that the Λ and Σ have the same parity. The matrix elements for the different isotopic spin and angular momentum channels will be related very directly to the integrals over the pion-hyperon scattering states which we have already calculated (11).

It is clear that this model allows corrections of the order of Δ/ω to the branching ratios for K^- absorption, as calculated for instance in the limited symmetry theory (4). It could permit also to connect the behaviour of the absorption cross-sections with that of the pion-hyperon ones. In particular, resonances as those predicted on the basis of the global symmetry hypothesis could give raise to an enhancement in the P wave K-nucleon cross-sections.

The assumptions on which this model is based are still too speculative and the number of *a priori* independent parameters too large to permit any quantitative and numerical result to be already reliable. It is our feeling however that, should some light be thrown by independent experiment on the values of such parameters, then our model could give some useful information on the behaviour of the K^--nucleon interaction.

(11) The procedure is very analogous to that followed in (5) for the photopion production.

* * *

We are grateful to Professor S. FUBINI for his kind interest in this investigation; we would also like to thank Professors M. FIERZ and J. PRENTKI for useful discussions.

RIASSUNTO

Si sviluppa un modello per studiare la diffusione a bassa energia di pioni su iperoni Λ e Σ, tenendo conto della differenza di massa Λ — Σ e di eventuali differenze tra le costanti di accoppiamento. I risultati così ottenuti permettono di studiare quali sono le correzioni da introdurre in una teoria nella quale i due iperoni sono degeneri rispetto all'interazione con i pioni. Queste correzioni sono dell'ordine della differenza di massa diviso la energia del pione e possono spostare eventuali risonanze in modo apprezzabile. È anche possibile discutere quali stati presentano risonanze per particolari valori delle costanti di accoppiamento. Il legame di questo lavoro con il trattamento dell'assorbimento di K^- da parte di nucleoni è anche brevemente discusso da un punto di vista qualitativo.

IL NUOVO CIMENTO Vol. XIII, N. 6 16 Settembre 1959

Final State Interaction in $^5He_\Lambda$ Decay.

R. Ammar, R. Levi Setti and W. E. Slater (*)

The Enrico Fermi Institute for Nuclear Studies
The University of Chicago - Chicago, Ill.

S. Limentani, P. E. Schlein (**) and P. H. Steinberg (***)

Northwestern University - Evanston, Ill.

(ricevuto il 3 Giugno 1959)

Summary. — The distribution of certain kinematic quantities defined in the decay $^5He_\Lambda \to \pi^- + p + {}^4He$ are interpreted as being due to the presence of a strong final state interaction. In particular the data are discussed with reference to two simple theories, one of which takes into account the specific p-^{4}He nuclear interaction. The experimental evidence, although not conclusive, is consistent with the expectation that the p-^{4}He $p_{\frac{3}{2}}$ resonance plays an important role in determining the final state configurations.

1. – Introduction.

Zielenski (1), examining a sample of various mesonic hyperfragments, pointed out that a marked asymmetry arises in their decay by the mode π-p-recoil. This asymmetry is in particular noted in the distribution of the cosine, y, of the angle between $\boldsymbol{P}_{\pi p}$ (the vector sum of the laboratory pion and

(*) Research supported by the U.S. Air Force Office of Scientific Research, Contract no. AF 49(638)-209.

(**) Now at the Enrico Fermi Institute for Nuclear Studies, University of Chicago, Chicago, Illinois.

(***) Research supported by the National Science Foundation and by the U. S. Atomic Energy Commission through Argonne National Laboratory subcontract.

(1) P. Zielinski: *Nuovo Cimento*, **3**, 1479 (1956).

proton momenta) and the momentum of the pion in the π-proton c.m. system. This effect was fully born out by the larger body of data contained in the EFINS survey ([2]). It was then suggested by DALITZ ([3]) that such an asymmetry could be due to a final state interaction among the decay products.

The data from the EFINS-NU collaboration experiment ([4]) afford the possibility of studying this effect, with fair statistics, for a specific hypernuclide, *i.e.*, $^5He_\Lambda$.

2. – Experimental results.

The sole known decay mode of $^5He_\Lambda$ is

$$^5He_\Lambda \to \pi^- + p + {}^4He \,. \tag{1}$$

Its investigation is however complicated by the fact that such decays cannot always be distinguished from events due to

$$^4He_\Lambda \to \pi^- + p + {}^3He \,. \tag{2}$$

This distinction becomes impossible for recoil ranges shorter than ~ 3 μm, corresponding to recoil momenta $P_{\pi p} \leqslant 80$ MeV/c. Table I, in which the

TABLE I. – *Numbers of events considered for the study of the final state interaction in* $^5He_\Lambda$.

Hypernuclide	EFINS	NU	EFINS Survey	Total
$^5He_\Lambda$	35	25	17	77
$^{4,5}He_\Lambda$	27	20	12	59
$^4He_\Lambda$	8	5	8	21

available material from Refs ([2]) and ([4]) is summarized, covers for this reason also non-unique $^{4,5}He_\Lambda$ and unique $^4He_\Lambda$ events. As it is seen, the latter two categories form a sizeable fraction of the total. In the distributions of the various kinematic quantities presented hereafter, we have for this reason

([2]) R. LEVI SETTI, W. E. SLATER and V. L. TELEGDI: *Suppl. Nuovo Cimento*, **10**, 68 (1958).

([3]) R. H. DALITZ: private communication, reported by V. L. TELEGDI: *Proc. of the Seventh Annual Rochester Conf. on High Energy Physics* (New York, 1957), VIII-8.

([4]) R. AMMAR, R. LEVI SETTI, S. LIMENTANI, P. E. SCHLEIN, W. E. SLATER and P. H. STEINBERG: *Proc. of the 1958 Annual Intern. Conf. on High Energy Physics at CERN*; M. F. KAPLON and R. H. DALITZ: *Reports*, pp. 181 and 200.

included events belonging to these two categories wherever it was considered useful to cover the entire range of $P_{\pi p}$ (0 to 240 MeV/c). The area corresponding to unique $^4He_\Lambda$ events, otherwise not pertinent to the problem at hand, may guide in estimating the $^4He_\Lambda$ « contamination » in the region ($P_{\pi p} \leqslant 80$ MeV/c) of non-unique assignment (*).

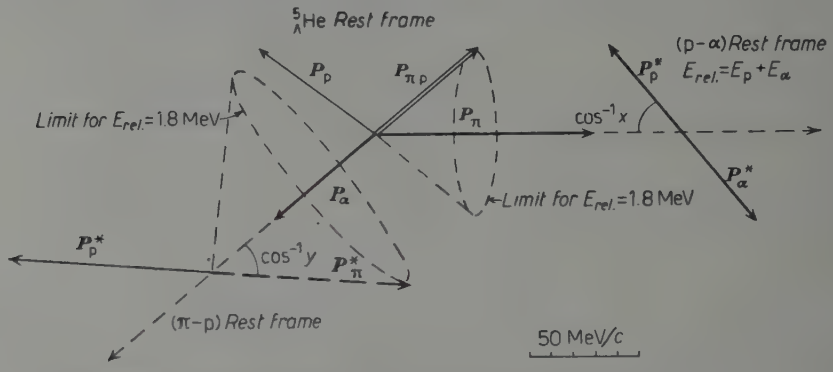

Fig. 1. – Illustration of the kinematical quantities relevant to the study of the decay properties of $^5He_\Lambda$.

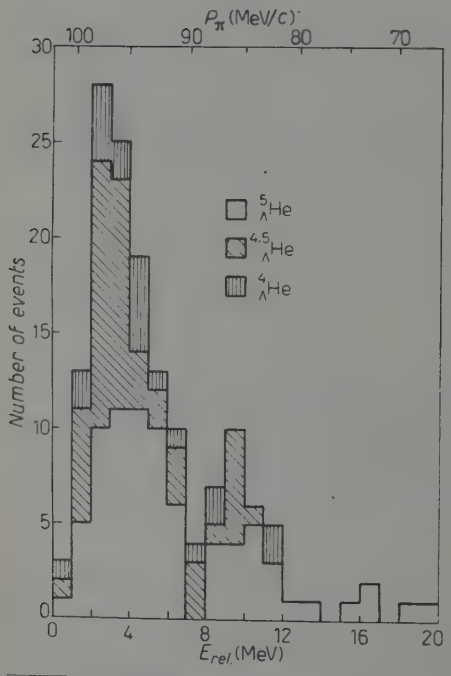

Fig. 2. - Histogram of the distribution of E_{rel}. The histogram also represents the distribution of P_π, by using the upper scale.

Fig. 1 illustrates the relationships between the various kinematical quantities of interest.

Fig. 2 shows a histogram of the distribution of E_{rel}, the energy of relative motion of proton and recoil nucleus in their c.m. system. This distribution, with most events lying below 10 MeV, is peaked at $E_{rel} \simeq 3$ MeV. Since E_{rel} is kinematically related to P_π, the pion momentum in the laboratory, a scale for P_π is also indicated in Fig. 2. The corresponding peak in the P_π distribution occurs at about 97 MeV/c.

(*) From the average B_Λ's of $^5He_\Lambda$, $^4He_\Lambda$ as well as that of the group of ambiguous He_Λ events, the contamination of $^4He_\Lambda$ in the region $P_{\pi p} < 80$ MeV/c is estimated as $\leqslant (26 \pm 22)\%$.

Fig. 3 is a histogram of the distribution of x, the cosine of the angle between the momentum of the proton-recoil system and the proton momentum (in the proton-recoil c.m. system). The peaking of non-unique events in this histo-

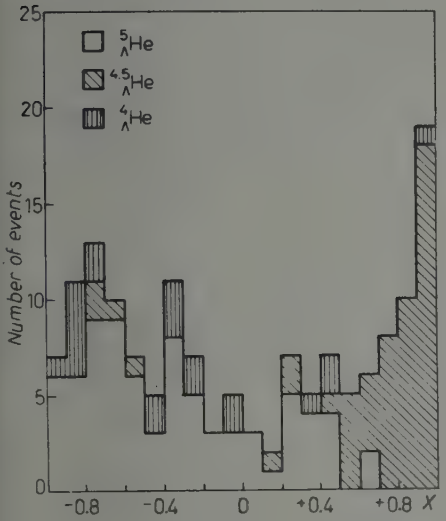

Fig. 3. – Histogram of the distribution of x.

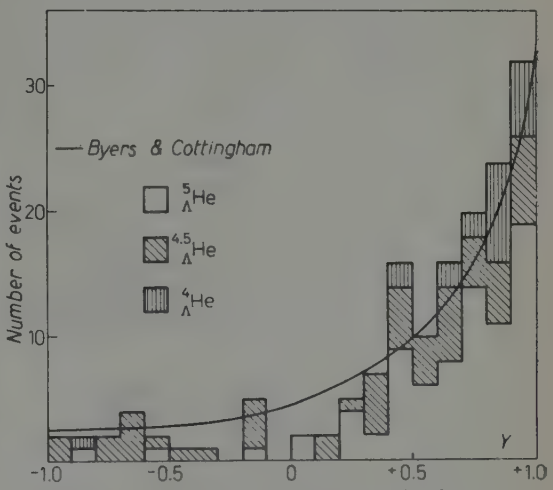

Fig. 4*a*. – Histogram of the distribution of y, for events with $0 \leqslant P_{\pi p} \leqslant 240$ MeV/c.

gram near $x = +1$ is easily understood on purely kinematic grounds with reference to Fig. 1. Such events correspond to configurations in which the proton and the pion are emitted in about opposite directions, *i.e.*, to configurations in which $P_{\pi p}$ is small.

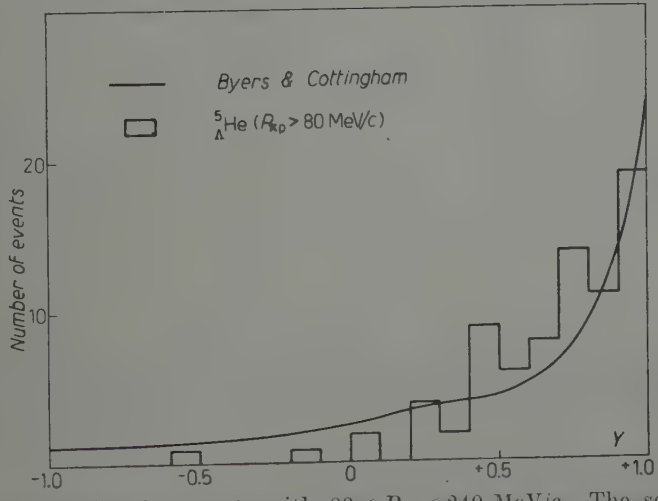

Fig. 4*b*. – y-distribution for events with $80 \leqslant P_{\pi p} \leqslant 240$ MeV/c. The solid curves in Fig. 4*a* and 4*b* respectively correspond to the calculations of Byers and Cottingham [7].

Fig. 4*a* and 4*b* are histograms of the distribution of the cosine y (see Fig. 1 and the introduction for its definition), for all He_Λ events and for unique $^5He_\Lambda$ events ($P_{\pi p} > 80$ MeV/c) respectively. These figures show a marked preference for forward emission of the pion with respect to $P_{\pi p}$; this effect is the same as the one originally pointed out by ZIELINSKI (1).

Finally, Fig. 5 is a histogram of the $P_{\pi p}$-distribution. Here two peaks are seen: a definite one around 125 MeV/c, and a somewhat less conclusive one around 60 MeV/c. This latter possible peak lies in the region of non-uniqueness.

3. – Qualitative interpretation.

It is possible to understand most of the important features of the experimental distribution on the basis of a very simple model, suggested by DALITZ (5). This model involves an extreme final state interaction: $^5He_\Lambda$ is assumed to decay into a pion and a $^5Li^*$, the latter being left in either of two resonant states, located at 4.3 ($p_{\frac{1}{2}}$) and 1.8 MeV ($p_{\frac{3}{2}}$) relative energy, respectively. The sharp peaking of the P_π spectrum near 97 MeV/c (Fig. 2) or equivalently the peaking of E_{rel} in the region of the resonance energies is compatible with this assumption (altough other models may be invoked to explain these distributions) (*).

In the rest system of $^5Li^*$, the $p_{\frac{1}{2}}$ state will yield an isotropic distribution in x. The $p_{\frac{3}{2}}$ state, however, will give an angular distribution of the form $(1+3x^2)$, implying that the proton is preferentially emitted parallel or antiparallel to the pion momentum. The extent to which the experimental distribution of x displays such an anisotropy can be seen from Fig. 3.

The strong forward-backward asymmetry in the y distribution (Fig. 4) can also be interpreted in terms of this model. As seen in Table II, the maxi-

TABLE II. – *Some kinematic quantities for the decay* $^5He_\Lambda \to \pi^- + {}^5Li^*(p + {}^4He + E_{rel})$.

E_{rel} (MeV)	P_π (MeV/c)	P_p^* (a) (MeV/c)	P_p (par.) (b) (MeV/c)	P_p (antip.) (c) (MeV/c)	$P_{\pi p}$ (par.) (MeV/c)	$P_{\pi p}$ (antip.) (MeV/c)
0	102.1	0	—	20.5	—	81.6
1.8 ($p_{\frac{3}{2}}$)	99.2	51.9	32.0	71.9	131.2	27.3
4.3 ($p_{\frac{1}{2}}$)	94.9	80.3	61.2	99.4	156.1	4.5

(a) P_p^* is the proton momentum in the (p-^{4}He) rest frame.
(b) P_p (par.) is the proton momentum in the l.s. when the proton is emitted parallel to the π.
(c) P_p (antip.) is the proton momentum in the l.s. when the proton is emitted antiparallel to the π.

(5) R. H. DALITZ: private communication.

(*) It has been shown by BROWN *et al.* (6) that the parameter E_{rel} (or P_π) is rather insensitive to the presence of final state interaction.

mum proton momentum [P_p (antip.)] for the $p_{\frac{3}{2}}$ resonance is 72 MeV/c, which is less than the pion momentum of 99 MeV/c. Consequently their vector sum ($\boldsymbol{P}_{\pi p}$) will never point antiparallel to the pion momentum, and is in fact confined to a cone about $\boldsymbol{P}_\pi$ with a half-angle $\leqslant \mathrm{tg}^{-1} P_p^*/P_{\pi p}$, as shown in Fig. 1. The corresponding limit on y can be taken from the kinematic relation between x and y, calculated for various E_{rel} ([6]), and reproduced in Fig. 6. At $E_{rel} = 2$ MeV, $0.7 < y < 1$. For $E_{rel} > 4$ MeV, such as may arise from the broad $p_{\frac{1}{2}}$ resonance, no such cone exists, but the y distribution will still be somewhat peaked in the forward direction.

The probability distribution of $P_{\pi p}$ can be written as:

$$\mathrm{d}n/\mathrm{d}P_{\pi p} = (\mathrm{d}n/\mathrm{d}x)\,\mathrm{d}x/\mathrm{d}P_{\pi p}\,,$$

$\mathrm{d}x/\mathrm{d}P_{\pi p}$ is proportional to $P_{\pi p}$, while $\mathrm{d}n/\mathrm{d}x$, for the $p_{\frac{3}{2}}$ resonant state, is of the form $1+3x^2$. This distribution shows a sharp peak at about 130 MeV/c

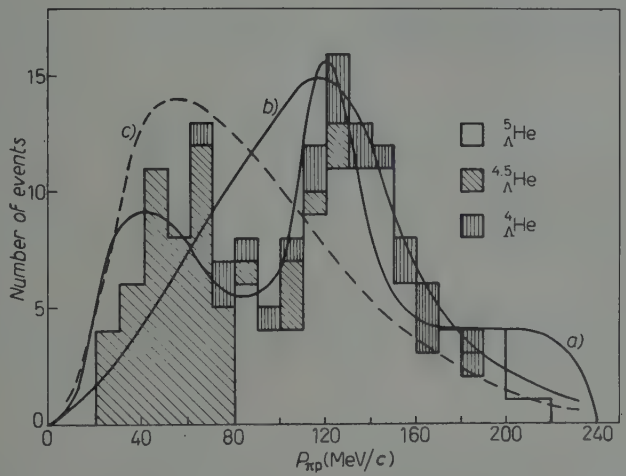

Fig. 5. – Histogram of the distribution of $P_{\pi p}$. Most of the events with $P_{\pi p} \lesssim 80$ MeV/c are non-uniquely identified, having recoil ranges $\lesssim 3$ μm. Curve *a*) represents the $P_{\pi p}$ distribution calculated by Byers and Cottingham ([7]). Curve *b*) (final state interaction) and curve *c*) (no final state interaction) correspond to the calculations of Brown *et al.* ([6]).

and a broad relative maximum at about 50 MeV/c, in fair agreement with the data of Fig. 5. These maxima correspond to cases in which the proton is emitted forward or backward in the ^{5}Li* rest frame.

([6]) L. M. Brown, M. Peshkin and G. Snow: private communication.

4. – Comparison with theoretical calculations and discussion.

The simple model discussed above could not be expected to account for more than some of the qualitative features of the experimental results. A more detailed calculation in the non-relativistic approximation was performed by BYERS and COTTINGHAM (7). In their calculation the initial Λ-^{4}He system was described by a wave function appropriate to a square well potential of suitable range giving the observed binding energy B_Λ. They used a final-state wave function for p-^{4}He so chosen as to yield the correct phase shifts for p-^{4}He scattering, in the c.m. energy range of interest ($(0 \div 10)$ MeV). The resonant $p_{\frac{3}{2}}$ interaction at 1.8 MeV p-^{4}He relative energy (half width 0.8 MeV) was found to have a strong effect on the final-state configurations.

For comparison with the empirical y-distribution, the decay probability of BYERS and COTTINGHAM was integrated over $P_{\pi p}$ both for all $P_{\pi p}$ and also for $P_{\pi p} > 80$ MeV/c, yielding the curves in Fig. 4*a* and 4*b* respectively. In both cases these theoretical curves are compatible with experiment, although to be meaningful, the comparison with all $P_{\pi p}$ calls for a detailed knowledge of the $^4\mathrm{He}_\Lambda$ contamination as well as the y-distribution for $^4\mathrm{He}_\Lambda$.

Curve (*a*) in Fig. 5 represents the Byers-Cottingham distribution for $P_{\pi p}$; it exhibits two characteristic peaks. This curve is in fair agreement with the experimental data. By using relativistic kinematics, the peak near 120 MeV/c would be displaced upwards by about 3.6 MeV/c, thereby improving the agreement.

It is worthwhile to mention that the Byers and Cottingham calculations have been carried out using a value 0 for the ratio of the amplitudes of p- to s-wave emission in the free Λ-decay. Although the results are not very sensitive to the assumed ratio, they find that for $|p/s| = 1$, the peak in the $P_{\pi p}$ distribution at about 120 MeV/c is reduced by 14%; the corresponding reduction at $P_{\pi p} = 200$ MeV/c is 36%. A better agreement with the experimental distribution seems to result from the use of a $|p/s|$ ratio different from zero.

The hump around 60 MeV/c is composed entirely of non-unique $^{4,5}\mathrm{He}_\Lambda$ events; a knowledge of the $^4\mathrm{He}_\Lambda$ contamination would hence once more be essential before valid conclusions could be drawn from our data.

An alternative theoretical approach has been taken by BROWN *et al.* (6). These authors considered the effect of a strong final-state interaction in π-p-recoil decay modes. A detailed mechanism for the final state interaction was

---

(7) N. BYERS and W. N. COTTINGHAM: private communication. To appear in *Nucl. Phys.*

not considered in the model. There exists a unique kinematic relationship between x and y as a function of E_{rel}. This was illustrated in Fig. 6. BROWN *et al.* pointed out that an isotropic y-distribution always corresponds to a sharp forward peaking of the x-distribution; the final-state interaction will smear out the latter. These authors now assume that, to a first approximation, the only effect of the final-state interaction and Pauli principle is to produce an isotropic x distribution. The predicted $P_{\pi D}$ distributions of BROWN *et al.* are reproduced in Fig. 5: (*b*) with final state interaction, (*c*) without final state interaction. Both distributions exhibit only a single broad peak, (*c*) being clearly incompatible with experiment while (*b*) excludes the observed lower peak which, however, is of uncertain character. On the other hand, the experimental x-distribution in the specific case of $^5He_\Lambda$ (Fig. 3) is not isotropic, in contrast with the basic assumption of BROWN *et al.* which leads to curve (*b*) of Fig. 5.

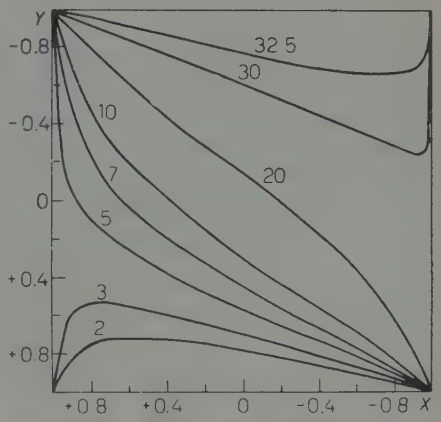

Fig. 6. – Kinematical relationship between x and y, with E_{rel} (MeV) as a parameter.

In conclusion, the data provide good evidence for strong final-state interactions, although no safe deductions concerning their detailed nature may as yet be drawn. On the whole, the very plausible model of Byers and Cottingham, seems to account for the main features of the experimental results.

* * *

It is a pleasure to thank Professor V. L. TELEGDI for his continuous help, co-operation and criticism in the various stages of the present investigation. We are greatly indebted to Professor R. H. DALITZ for many illuminating discussions and suggestions.

We are grateful to Professors L. M. BROWN and J. H. ROBERTS for their valuable advice and criticism during the course of the work.

We acknowledge the many helpful communications from Dr. N. BYERS, Dr. W. N. COTTINGHAM, Professor L. M. BROWN, Professor M. PESHKIN and Professor G. SNOW concerning their theoretical calculations.

Finally we wish to extend our appreciation to Dr. E. J. LOFGREN and the Bevatron staff for providing us with the K^--exposure.

RIASSUNTO

Si interpretano le distribuzioni di alcune quantità cinematiche, definite nel decadimento $^5He_\Lambda \to \pi^- + p + {}^4He$, come dovute ad una forte interazione negli stati finali. In particolare si discutono i risultati sperimentali in relazione a due semplici modelli teorici, uno dei quali si basa sulla specifica interazione nucleare p-^{4}He. I dati sperimentali, sebbene in forma non conclusiva, favoriscono l'ipotesi che le configurazioni negli stati finali siano determinate in modo dominante dalla risonanza $p_{\frac{3}{2}}$ del sistema p-^{4}He.

IL NUOVO CIMENTO Vol. XIII, N. 6 16 Settembre 1959

Coherence Properties of Partially Polarized Electromagnetic Radiation (*).

E. Wolf (**)

Department of Theoretical Physics - University of Manchester

(ricevuto il 4 Giugno 1959)

Summary. — This paper is concerned with the analysis of partial polarization from the standpoint of coherence theory. After observing that the usual analytic definition of the Stokes parameters of a quasi-monochromatic wave are not unique, a simple experiment is analysed, which brings out clearly the observable parameters of a quasi-monochromatic light wave. The analysis leads to a unique coherency matrix and to a unique set of Stokes parameters, the latter being associated with the representation of the coherency matrix in terms of Pauli's spin matrices. In this analysis the concept of Gabor's analytic signal proves to be basic. The degree of coherence between the electric vibrations in any two mutually orthogonal directions of propagation of the wave depends in general on the choice of the two orthogonal directions. It is shown that its maximum value is equal to the degree of polarization of the wave. It is also shown that the degree of polarization may be determined in a new way from relatively simple experiments which involve a compensator and a polarizer, and that this determination is analogous to the determination of the degree of coherence from Young's interference experiment.

1. – Introduction.

Although it is generally known that there is an intimate connection between partial polarization and partial coherence (see, for example, Wiener [1], p. 187), a systematic analysis of the properties of partially polarized radiation from

(*) The research described in this paper has been partially sponsored by the Air Force Cambridge Research Center of the Air Research and Development Command, United States Air Force, through its European Office, under Contract No. AF 61(052)-169.

(**) Now at the Institute of Optics, University of Rochester, Rochester, N.Y.

(1) N. Wiener: *Acta Math.*, **55**, § 9 (1930).

the standpoint of coherence theory does not appear to have been made so far. There are several reasons why it seems desirable to carry out such an analysis. The numerous investigations made in recent years in connection with partially coherent light (ZERNIKE [2]), HOPKINS [3]), WOLF [4a,b,c]), BLANC-LAPIERRE and DUMONTET [5])) have clearly shown that there is still a great deal to be learnt about the statistical properties of high frequency electromagnetic radiation. Moreover, as we shall briefly indicate, the usual treatments of partial polarization are not entirely satisfactory.

The most systematic treatments of partial polarization utilize the concept of Stokes parameters (introduced by G. G. STOKES in 1852 [6])) which are usually defined as follows: Consider a plane, quasi-monochromatic electromagnetic wave and let the components of the electric vector in two mutually perpendicular directions at right angles to the direction of propagation of the wave be represented in the form

$$\left\{\begin{aligned} E_x(t) &= A_1(t)[\cos \Phi_1(t) - \bar{\omega}t], \\ E_y(t) &= A_2(t)[\cos \Phi_2(t) - \bar{\omega}t], \end{aligned}\right. \tag{1.1}$$

where $\bar{\omega}$ denotes the mean frequency and t the time. The Stokes parameters are the four quantities

$$\left\{\begin{aligned} s_0 &= \langle A_1^2\rangle + \langle A_2^2\rangle, \\ s_1 &= \langle A_1^2\rangle - \langle A_2^2\rangle, \\ s_2 &= 2\langle A_1 A_2 \cos(\Phi_1 - \Phi_2)\rangle, \\ s_3 &= 2\langle A_1 A_2 \sin(\Phi_1 - \Phi_2)\rangle, \end{aligned}\right. \tag{1.2}$$

where the sharp brackets denote time average. Although to-day there exists an extensive literature in which the Stokes parameters play a central role (see, for example CHANDRASEKHAR [7]), it does not appear to have been noticed that the above relations do not define the parameters uniquely. For in (1.1) only $E_x(t)$ and $E_y(t)$ can be regarded as uniquely associated with the wave, whereas the A's and Φ's may evidently be chosen in many ways, leading to different sets of Stokes parameters. Only a careful analysis of experiment may be expected to lead to a unique set. Such an analysis is carried out in

---

([2]) F. ZERNIKE: *Physica*, **5**, 785 (1938).

([3]) H. H. HOPKINS: *Proc. Roy. Soc.*, A **208**, 263 (1951).

([4]) E. WOLF: (*a*) *Proc. Roy. Soc.*, A **225**, 96 (1954); (*b*) *Nuovo Cimento*, **12**, 884 (1954); (*c*) *Proc. Roy. Soc.*, A **230**, 96 (1955).

([5]) A. BLANC-LAPIERRE and P. DUMONTET: *Revue d'Optique*, **34**, 1 (1955).

([6]) G. G. STOKES: *Trans. Camb. Phil. Soc.*, **9**, 399 (1852); also his *Mathematical and Physical Papers*, vol. **3** (Cambridge, 1901), p. 233.

([7]) S. CHANDRASEKHAR: *Radiative Transfer* (Oxford, 1950), § 15.

Section 2 of this paper and shows that the unique set obtained is intimately related to the appropriate « degree-of coherence » of the electric vibrations in the two orthogonal directions.

Another unsatisfactory feature of the usual treatments of partial polarization has been clearly pointed out in an interesting recent paper by PANCHARANTHAM ([8], expecially p. 339-340): A partially polarized beam is usually described in terms of incoherent superposition of polarized and unpolarized beams and the interference phenomena arising from the superposition of these beams are analysed by using the concept of coherence and incoherence alone. However, the decomposition may be carried out in many different ways and it is by no means evident that the different decompositions will always lead to identical results. In any case this approach masks completely the *invariant characteristics* of the different representations. These unsatisfactory features can only be expected to be removed by the introduction of intermediate states (partial coherence).

In the present paper the basic properties of a quasi-monochromatic partially polarized electromagnetic wave are discussed from the standpoint of coherency theory and the invariant characteristics of such a wave are clearly brought out. The basic tool used for this purpose is the coherency matrix introduced in a previous paper (WOLF ([4b])), specialized to the problem in question; however, unlike in the previous paper, the coherency matrix is introduced here from the analysis of a simple experiment.

2. – The coherency matrix of a plane, quasi-monochromatic electromagnetic wave.

Consider a plane, quasi-monochromatic wave and let $E_x^{(r)}(t)$ and $E_y^{(r)}(t)$ represent (*) the components of the electric vector $\boldsymbol{E}^{(r)}$ at a typical point in the wave field in two mutually orthogonal directions at right angles to the directions of propagation of the wave. We assume that $\boldsymbol{E}^{(r)}$ may be represented as a Fourier integral and write

$$(2.1)\qquad \begin{cases} E_x^{(r)}(t) = \int_0^\infty a_1(\omega)\cos[\varphi_1(\omega) - \omega t]\,\mathrm{d}\omega\,, \\ E_y^{(r)}(t) = \int_0^\infty a_2(\omega)\cos[\varphi_2(\omega) - \omega t]\,\mathrm{d}\omega\,. \end{cases}$$

([8]) S. PANCHARATNAM: *Proc. Ind. Acad. Sci.*, A **44**, 398 (1956),

(*) The superscript « r » is introduced because the (real) electric wave function will shortly be regarded as the real part of a suitably chosen complex wave function.

Since the wave is assumed to be quasi-monochromatic, the spectral amplitudes $a_1(\omega)$ and $a_2(\omega)$ will be appreciable only in a narrow range

$$\bar{\omega} - \tfrac{1}{2}\Delta\omega \leqslant \omega \leqslant \bar{\omega} + \tfrac{1}{2}\Delta\omega \,, \tag{2.2}$$

where $\Delta\omega$ is small compared with the mean frequency $\bar{\omega}$.

Suppose that the wave is passed through a device (compensator) which introduces retardations in $E_x^{(r)}$ and $E_y^{(r)}$. Let $\varepsilon_1(\omega)$ and $\varepsilon_2(\omega)$ be the phase delays in the Fourier components of frequency ω of $E_x^{(r)}$ and $E_y^{(r)}$ respectively. The electric wave emerging from the compensator has the components

$$\begin{cases} \mathscr{E}_x^{(r)}(t) = \int_0^\infty a_1(\omega) \cos[\varphi_1(\omega) - \varepsilon_1(\omega) - \omega t] \, \mathrm{d}\omega \,, \\ \mathscr{E}_y^{(r)}(t) = \int_0^\infty a_2(\omega) \cos[\varphi_2(\omega) - \varepsilon_2(\omega) - \omega t] \, \mathrm{d}\omega \,, \end{cases} \tag{2.3}$$

it being assumed that reflection and absorption losses are negligible. If we use the identity $\cos[A - \varepsilon] = \cos A \cos\varepsilon + \sin A \sin\varepsilon$ in (2.3) and assume that for any two frequencies ω' and ω'' in the range (2.2)

$$|\varepsilon_1(\omega') - \varepsilon_1(\omega'')| \ll 2\pi \,, \qquad |\varepsilon_2(\omega') - \varepsilon_2(\omega'')| \ll 2\pi \,, \tag{2.4}$$

(2.3) may be re-written as

$$\begin{cases} \mathscr{E}_x^{(r)} = E_x^{(r)}(t) \cos\bar{\varepsilon}_1 + E_x^{(i)}(t) \sin\bar{\varepsilon}_1 \,, \\ \mathscr{E}_y^{(r)} = E_y^{(r)}(t) \cos\bar{\varepsilon}_2 + E_y^{(i)}(t) \sin\bar{\varepsilon}_2 \,, \end{cases} \tag{2.5}$$

where $\bar{\varepsilon}_1 = \varepsilon_1(\bar{\omega})$, $\bar{\varepsilon}_2 = \varepsilon_2(\bar{\omega})$ and $E_x^{(i)}$ and $E_y^{(i)}$ are the Fourier integrals *conjugate* to $E_x^{(r)}$ and $E_y^{(r)}$ respectively, *i.e.*

$$\begin{cases} E_x^{(i)} = \int_0^\infty a_1(\omega) \sin[\varphi_1(\omega) - \omega t] \, \mathrm{d}\omega \,, \\ E_y^{(i)} = \int_0^\infty a_2(\omega) \sin[\varphi_2(\omega) - \omega t] \, \mathrm{d}\omega \,. \end{cases} \tag{2.6}$$

As is well known (cf. TITCHMARSH (9)), any two conjugate functions are related

(9) E. C. TITCHMARSH: *Introduction to the Theory of Fourier Integrals* (Oxford, 1948), 2nd ed., chap. v.

by Hilbert's reciprocity relations, *i.e.* by relations of the form

$$E_x^{(i)}(t) = \frac{P}{\pi}\int_{-\infty}^{\infty}\frac{E_x^{(r)}(t')}{t'-t}\,dt', \qquad E_x^{(r)}(t) = -\frac{P}{\pi}\int_{-\infty}^{\infty}\frac{E_x^{(i)}(t')}{t'-t}\,dt', \tag{2.7}$$

P denoting the Cauchy principal value at $t'=t$.

Suppose now that the wave emerging from the compensator is sent through a polarizer, which only transmits the component which makes an angle θ with the x-direction. This component is given by

$$\mathscr{E}^{(r)}(t;\,\theta,\,\varepsilon_1,\,\varepsilon_2) = \mathscr{E}_x^{(r)}(t)\cos\theta + \mathscr{E}_y^{(r)}(t)\sin\theta\,, \tag{2.8}$$

so that the intensity of the light emerging from the polarizer is

$$\begin{aligned} I(\theta_1,\varepsilon_1,\varepsilon_2) &= 2\langle\mathscr{E}^{(r)2}(t,\theta,\varepsilon_1,\varepsilon_2)\rangle \\ &= 2\langle\mathscr{E}_x^{(r)2}\rangle\cos^2\theta + 2\langle\mathscr{E}_y^{(r)2}\rangle\sin^2\theta + 4\langle\mathscr{E}_x^{(r)}\mathscr{E}_y^{(r)}\rangle\cos\theta\sin\theta\,, \end{aligned} \tag{2.9}$$

where sharp brackets denote time average. Here the wave field was assumed to be stationary (*), so that the intensity I is independent of the time instant at which the average is taken and the factor 2 on the right of the first equation of (2.9) was introduced to simplify later calculations. Next we substitute from (2.5) into (2.9) and use the following relations which may be readily proved from the properties of Hilbert transforms (**):

$$\begin{cases} \langle E_x^{(r)2}\rangle = \langle E_x^{(i)2}\rangle\,, \qquad \langle E_y^{(r)2}\rangle = \langle E_y^{(i)2}\rangle\,, \\ \langle E_x^{(r)}E_y^{(r)}\rangle = \langle E_x^{(i)}E_y^{(i)}\rangle\,, \\ \langle E_x^{(r)}E_y^{(i)}\rangle = -\langle E_x^{(i)}E_y^{(r)}\rangle\,, \\ \langle E_x^{(r)}E_x^{(i)}\rangle = \langle E_y^{(i)}E_y^{(r)}\rangle = 0\,. \end{cases} \tag{2.10}$$

(*) Stationarity in the strict sense of the theory of random functions would imply that the field vectors are not square integrable and hence we would not be justified in using Fourier integral analysis. This difficulty may be avoided in the usual way by assuming that the field exists only for a finite time interval $-T<t<T$ and proceeding to the limit $T\to\infty$ at the end of the calculations. The final results are the same whether or not this refinement is made.

(**) The formulae (2.10) are valid quite generally. When the field is quasi-monochromatic as here assumed, they may be proved in a very simple way by the following

Further, if we set

$$\delta = \bar{\varepsilon}_1 - \bar{\varepsilon}_2 , \tag{2.11}$$

and write $I(\theta, \delta)$ in place of $I(\theta, \bar{\varepsilon}_1, \bar{\varepsilon}_2)$ [since $\bar{\varepsilon}_1$ and $\bar{\varepsilon}_2$ enter the expression for the intensity only through their difference] we obtain the following expression for the time averaged intensity:

$$I(\theta, \delta) = 2\langle E_x^{(r)2}\rangle \cos^2\theta + 2\langle E_y^{(r)2}\rangle \sin^2\theta + \tag{2.12}$$

$$+ 4\cos\theta \sin\theta \{\cos\delta \langle E_x^{(r)} E_y^{(r)}\rangle - \sin\delta \langle E_x^{(r)} E_y^{(i)}\rangle\} .$$

The formulae (2.12) may be expressed in a more convenient form, by using in place of the real wave functions the associated analytic signals of GABOR ([11]),

argument due to BRACEWELL [([10]), p. 102]. We set

$$E_x(t) = E_x^{(r)}(t) + iE_x^{(i)}(t) = A_1(t) \exp[-i\bar{\omega}t] ,$$

$$E_y(t) = E_y^{(r)}(t) + iE_y^{(i)}(t) = A_2(t) \exp[-i\bar{\omega}t] .$$

Then, if the field is quasi-monochromatic, the (generally complex) quantities A_1 and A_2 will vary slowly with t in comparison with the periodic term, and we have, for example,

$$\langle E_x^{(r)2}\rangle = \left\langle \left(\frac{A_1 \exp[-i\omega t] + A_1^* \exp[i\omega t]}{2} \right)^2 \right\rangle =$$

$$= \frac{1}{4}\langle A_1^2 \exp[-2i\bar{\omega}t]\rangle + \frac{1}{2}\langle A_1 A_1^*\rangle + \frac{1}{4}\langle A_1^{*2} \exp[2i\bar{\omega}t]\rangle .$$

The first and the last term on the right vanish because of the rapidly varying terms $\exp[-2i\bar{\omega}t]$ and $\exp[2i\bar{\omega}t]$, so that

$$\langle E_x^{(r)2}\rangle = \tfrac{1}{2}\langle A_1 A_1^*\rangle .$$

Similarly

$$\langle E_x^{(i)2}\rangle = \left\langle \left(\frac{A_1 \exp[-i\bar{\omega}t] - A_1^* \exp[i\bar{\omega}t]}{2i} \right)^2 \right\rangle = \frac{1}{2}\langle A_1 A_1^*\rangle .$$

Comparison of the last two formulae gives the first relation in (2.10); the other relations may be proved in a similar way.

([10]) R. N. BRACEWELL: *Proc. I.R.E.*, **46**, 97 (1958).

([11]) D. GABOR: *Journ. Inst. Elect. Engrs.*, **93**, part III, 429 (1946).

i.e. by using in place of $E_x^{(r)}$ and $E_y^{(r)}$, the functions (*)

$$(2.13)\qquad \begin{cases} E_x(t) = E_x^{(r)}(t) + i\,E_x^{(i)}(t) = \int_0^\infty a_1(\omega)\exp\left[i[\varphi_1(\omega) - \bar{\omega}t]\right]\mathrm{d}\omega\,, \\ E_y(t) = E_y^{(r)}(t) + i\,E_y^{(i)}(t) = \int_0^\infty a_2(\omega)\exp\left[i[\varphi_2(\omega) - \omega t]\right]\mathrm{d}\omega\,. \end{cases}$$

Using (2.10) we have the relations

$$(2.14a)\qquad \langle E_x E_x^*\rangle = 2\langle E_x^{(r)2}\rangle = 2\langle E_x^{(i)2}\rangle\,,$$

$$(2.14b)\qquad \langle E_x E_y^*\rangle = 2\langle E_x^{(r)} E_y^{(r)}\rangle - 2i\langle E_x^{(i)} E_y^{(i)}\rangle\,,$$

etc. With the help of (2.14) the formula (2.12) becomes

$$(2.15)\qquad I(\theta,\delta) = J_{xx}\cos^2\theta + J_{yy}\sin^2\theta + J_{xy}\cos\theta\sin\theta\exp[-i\delta] + J_{yx}\sin\theta\cos\theta\exp[i\delta]\,,$$

where the J's are the elements of the *coherency matrix*

$$(2.16)\qquad \mathbf{J} = \begin{bmatrix} J_{xx} & J_{xy} \\ J_{yx} & J_{yy} \end{bmatrix} = \begin{bmatrix} \langle E_x E_x^*\rangle & \langle E_x E_y^*\rangle \\ \langle E_y E_x^*\rangle & \langle E_y E_y^*\rangle \end{bmatrix}.$$

The formula (2.15) expresses in a compact form the intensity of the wave after transmission through the compensator (which introduces a phase delay δ) and the polarizer (oriented so as to transmit the component which makes an angle θ with the x-axis) in terms of the coherency matrix $\mathbf{J}$ which characterizes the incident wave.

Since $J_{yx} = J_{xy}^*$ the coherency matrix is *Hermitian*. Its trace represents the intensity of the incident wave,

$$(2.17)\qquad \mathrm{Tr}\,\mathbf{J} = J_{xx} + J_{yy} = \langle E_x E_x^*\rangle + \langle E_y E_y^*\rangle = 2\langle E_x^{(r)2}\rangle + 2\langle E_y^{(r)2}\rangle\,,$$

and its non-diagonal elements express the correlation between the x and y-components of the complex vector $\boldsymbol{E}$. Further it follows from Schwarz' inequality

(*) An analytic signal is a complex function characterized by the property that its Fourier integral contains no spectral components of positive (or negative) frequencies. This fact alone implies that the real and imaginary parts of the signal are conjugate functions and hence Hilbert transforms of each other.

for integrals that $|J_{xy}| \leqslant \sqrt{J_{xx}}\sqrt{J_{yy}}$, $|J_{yx}| \leqslant \sqrt{J_{yy}}\sqrt{J_{xx}}$; hence, since $J_{yx} = J_{xy}$,

$$|\mathbf{J}| = J_{xx}J_{yy} - J_{xy}J_{yx} \geqslant 0\,, \tag{2.18}$$

i.e. the discriminant of the coherency matrix is non-negative.

Let $A_1(t)$, $A_2(t)$ be the amplitudes and $\Psi_1(t)$ and $\Psi_2(t)$ the phases of $E_x(t)$ and $E_y(t)$ respectively, *i.e.*

$$E_x(t) = A_1(t)\exp[i\,\Psi_1(t)]\,, \qquad E_y(t) = A_2(t)\exp[i\,\Psi_2(t)]\,. \tag{2.19}$$

Then, from (2.13),

$$\begin{cases} E_x^{(r)}(t) = A_1(t)\cos[\Psi_1(t)]\,, & E_x^{(i)}(t) = A_1(t)\sin[\Psi_1(t)]\,, \\ E_y^{(r)}(t) = A_2(t)\cos[\Psi_2(t)]\,, & E_y^{(i)}(t) = A_2(t)\sin[\Psi_2(t)]\,, \end{cases} \tag{2.20}$$

and, if we introduce quantities $\Phi_1(t)$ and $\Phi_2(t)$ by the relations

$$\Psi_1(t) = \Phi_1(t) - \bar{\omega}t\,, \qquad \Psi_2(t) = \Phi_2(t) - \bar{\omega}t\,, \tag{2.21}$$

where $\bar{\omega}$ is the mean frequency, the components $E_x^{(r)}$, $E_y^{(r)}$ of the (real) electric vector are represented by expressions of the form (1.1), but the representation is now *unique*. In terms of the A's and Ψ's the elements of the coherency matrix are

$$\begin{cases} J_{xx} = \langle A_1^2\rangle\,, \\ J_{yy} = \langle A_2^2\rangle\,, \\ J_{xy} = \langle A_1 A_2 \exp[i(\Psi_1 - \Psi_2)]\rangle\,, \\ J_{yx} = \langle A_1 A_2 \exp[-i(\Psi_1 - \Psi_2)\rangle\,. \end{cases} \tag{2.22}$$

We may now introduce a set of Stokes parameters by the relations

$$\begin{cases} s_0 = \langle A_1^2\rangle + \langle A_2^2\rangle &= J_{xx} + J_{yy}\,, \\ s_1 = \langle A_1^2\rangle - \langle A_2^2\rangle &= J_{xx} - J_{yy}\,, \\ s_2 = 2\langle A_1 A_2 \cos(\Psi_1 - \Psi_2)\rangle &= J_{xy} + J_{yx}\,, \\ s_3 = 2\langle A_1 A_2 \sin(\Psi_1 - \Psi_2)\rangle &= i(J_{yx} - J_{xy})\,. \end{cases} \tag{2.23}$$

We see that this set of Stokes parameters is unique and that uniqueness has been achieved with the help of analytic signals, the introduction of which was suggested by the appearance of conjugate functions in the analysis of our experiment.

The relation between the Stokes parameters and the coherency matrix may also be expressed in the form

$$\mathbf{J} = \tfrac{1}{2}\sum_{i=0}^{3} s_i \boldsymbol{\sigma}_i , \tag{2.24}$$

where $\boldsymbol{\sigma}_0$ is the unit matrix

$$\boldsymbol{\sigma}_0 = \begin{bmatrix} 1 & 0 \\ 0 & 1 \end{bmatrix},$$

and $\boldsymbol{\sigma}_1$, $\boldsymbol{\sigma}_2$, $\boldsymbol{\sigma}_3$, are the Pauli spin matrices

$$\boldsymbol{\sigma}_1 = \begin{bmatrix} 1 & 0 \\ 0 & -1 \end{bmatrix}, \quad \boldsymbol{\sigma}_2 = \begin{bmatrix} 0 & 1 \\ 1 & 0 \end{bmatrix}, \quad \boldsymbol{\sigma}_3 = \begin{bmatrix} 0 & i \\ -i & 0 \end{bmatrix}. \tag{2.26}$$

The connection between a coherency matrix, Stokes parameters and Pauli's spin matrices has been noted previously (FANO [12]); however, as already mentioned, the non-uniqueness of the usual analytic definition of the Stokes parameters appears to have escaped attention.

Finally we mention that the coherency matrix (2.16) was introduced in an earlier paper (WOLF [4b]) from more formal considerations. Our present analysis shows that this matrix appears in a natural way from the analysis of a simple experiment.

3. – Some consequences of the basic intensity formula.

To see the physical significance of the intensity formula (2.15) we re-write it in a somewhat different form. We set

$$\frac{J_{xy}}{\sqrt{J_{xx}}\sqrt{J_{yy}}} = \mu_{xy} = |\mu_{xy}| \exp[i\beta_{xy}] . \tag{3.1}$$

---

[12] U. FANO: *Phys. Rev.*, **93**, 121 (1954).

It follows from (2.18) that

$$|\mu_{xy}| \leqslant 1 .$$

By analogy with the theory of partially coherent scalar fields we may call μ_{xy} *the complex degree of coherence* of the electric vibrations in the x and y directions. It absolute value $|\mu_{xy}|$ is a measure of the degree of correlation of the vibrations and its phase represents their « effective phase difference ».

If we substitute from (3.1) into the intensity formula (2.15) and use the relation $J_{yx} = J_{xy}^*$ we obtain the following expression for the intensity:

$$I(\theta, \delta) = J_{xx} \cos^2 \theta + J_{yy} \sin^2 \theta + 2\sqrt{J_{xx}}\sqrt{J_{yy}} \cos\theta \sin\theta |\mu_{xy}| \cos(\beta_{xy} - \delta) . \tag{3.3}$$

This expression is formally identical with the basic interference law of partially coherent fields [WOLF ([4a]), p. 102, THOMPSON and WOLF ([13]), p. 896]. It shows that the intensity $I(\theta, \delta)$ may be regarded as arising from the interference of two beams of intensities:

$$I^{(1)} = J_{xx} \cos^2 \theta , \qquad I^{(2)} = J_{yy} \sin^2 \theta , \tag{3.4}$$

and with complex degree of coherence μ_{xy}, after a phase difference δ has been introduced between them.

Returning to (2.15) we see that the elements of the coherency matrix of a quasi-monochromatic plane wave may be determined from very simple experiments. It is only necessary to measure the intensity for several different values of θ (orientation of polarizer) and δ (delay introduced by a compensator), and solve the corresponding relations obtained from (2.15). Let $\{\theta, \delta\}$, denote the measurement corresponding to a particular pair θ, δ. A convenient set of measurements is the following:

$$\{0°, 0\}, \quad \{45°, 0\}, \quad \{90°, 0\}, \quad \{135°, 0\}, \quad \left\{45°, \frac{\pi}{2}\right\}, \quad \left\{135°, \frac{\pi}{2}\right\} . \tag{3.5}$$

It follows from (2.15) that, in terms of the intensities determined from these six measurements, the elements of the coherency matrix are given by

$$\begin{cases} J_{xx} = I(0°, 0) , \\ J_{yy} = I(90°, 0) , \\ J_{xy} = \frac{1}{2}\{I(45°, 0) - I(135°, 0)\} + \frac{1}{2} i \left\{I\left(45°, \frac{\pi}{2}\right) - I\left(135°, \frac{\pi}{2}\right)\right\} , \\ J_{yx} = \frac{1}{2}\{I(45°, 0) - I(135°, 0)\} - \frac{1}{2} i \left\{I\left(45°, \frac{\pi}{2}\right) - I\left(135°, \frac{\pi}{2}\right)\right\} . \end{cases} \tag{3.6}$$

([13]) B. J. THOMPSON and E. WOLF: *Journ. Opt. Soc. Amer.*, **47**, 895 (1957).

Thus we see that the elements of the coherency matrix represent *measurable* physical quantities.

In the theory of partially coherent scalar fields, the concept of Michelson's visibility (*) of fringes plays a central role (cf. ZERNIKE (2)). We will now derive an expression for a quantity defined in a similar way and we shall see later that this quantity has a simple physical meaning.

It follows from (2.15) by a straightforward calculation, that the maxima and minima of the intensity (with respect to both θ and δ) are

$$(3.7)\qquad \begin{cases} I_{\max} = \frac{1}{2}(J_{xx}+J_{yy})\left[1+\sqrt{1-\frac{4|\mathbf{J}|}{(J_{xx}+J_{yy})^2}}\right], \\ I_{\min} = \frac{1}{2}(J_{xx}+J_{yy})\left[1-\sqrt{1-\frac{4|\mathbf{J}|}{(J_{xx}+J_{yy})^2}}\right]. \end{cases}$$

Hence

$$(3.8)\qquad \frac{I_{\max}-I_{\min}}{I_{\max}+I_{\min}} = \sqrt{1-\frac{4|\mathbf{J}|}{(J_{xx}+J_{yy})^2}}.$$

Now if the x and y axes are rotated about the direction of propagation of the wave, the coherency matrix will change. There are, however, two invariants for such rotations, namely the discriminant $|\mathbf{J}|$ and the trace $\mathrm{Tr}\mathbf{J} = J_{xx}+J_{yy}$ of the matrix. Since on the right hand side of (3.8) the elements of $\mathbf{J}$ enter only in these combinations, it follows that the expression is invariant with respect to rotations of the axes and hence may be expected to have a physical significance. We shall see shortly (eq. (5.14) below) that it represents the degree of polarization of the wave.

4. – Coherency matrices of natural and of monochromatic radiation.

Light which is most frequently encountered in nature has the property that the intensity of its components in any direction perpendicular to the direction of propagation is the same; and, moreover, the intensity is not af-

---

(*) The visibility $\mathscr{V}$ of fringes at a point P in the fringe pattern is defined by the formula

$$\mathscr{V} = \frac{I_{\max}-I_{\min}}{I_{\max}+I_{\min}},$$

where $I_{\max}$ and $I_{\min}$ are the maximum and minimum intensities in the immediate neighbourhood of P.

fected by any previous retardation of one of the rectangular components relative to the other, into which the light may have been resolved. In other words

$$I(\theta, \delta) = \text{constant} \tag{4.1}$$

for all values of θ and δ. Such light is called *natural light*; and we may define « natural » electromagnetic radiation of any other spectral range in a strictly similar way.

It is evident from (3.3) that $I(\theta, \delta)$ is independent of δ and θ, if and only if

$$|\mu_{xy}| = 0\,, \quad \text{and} \quad J_{xx} = J_{yy}\,. \tag{4.2}$$

The first condition implies that the electric vibrations in the x and y directions are mutually incoherent. According to (3.1) and the relation $J_{yx} = J_{yx}^*$, (4.2) may also be written as

$$J_{xy} = J_{yx} = 0\,, \qquad J_{xx} = J_{yy}\,, \tag{4.3}$$

and it follows that *the coherency matrix of natural radiation* of intensity $J_{xx} + J_{yy} = I$ is

$$\frac{1}{2} I \begin{bmatrix} 1 & 0 \\ 0 & 1 \end{bmatrix}. \tag{4.4}$$

Next let us consider the coherency matrix of monochromatic radiation. In this case the amplitudes A_1 and A_2 and the phases Ψ_1 and Ψ_2 in (2.22) are independent of time and the coherency matrix has the form

$$\begin{bmatrix} A_1^2 & A_1 A_2 \exp[i(\Psi_1 - \Psi_2)] \\ A_1 A_2 \exp[-i(\Psi_1 - \Psi_2)] & A_2^2 \end{bmatrix}. \tag{4.5}$$

We see that in this case

$$|\mathbf{J}| = J_{xx} J_{yy} - J_{xy} J_{yx} = 0\,, \tag{4.6}$$

i.e. the discriminant of the coherency matrix is zero. The complex degree of coherence now is

$$\mu_{xy} = \frac{J_{xy}}{\sqrt{J_{xx}}\sqrt{J_{yy}}} = \exp[(\Psi_1 - \Psi_2)\,, \tag{4.7}$$

i.e. its absolute value is unity (complete coherence) and its phase is equal to the difference between the phases of the two components.

5. – The degree of polarization.

Before deriving an expression for the degree of polarization in terms of the coherency matrix we shall establish a simple theorem relating to the coherency matrix of a wave resulting from the superposition of a number of mutually independent waves.

Consider N mutually independent quasi-monochromatic waves propagated in the same direction (z-say) and let $E_x^{(n)}$, $E_y^{(n)}$ $(n = 1, 2, ..., N)$ be the analytic signals associated with the components of the electric vibrations of the n-th wave in the directions of the x and y-axes. The components of the resulting wave then are

$$E_x = \sum_{n=1}^{N} E_x^{(n)}, \qquad E_y = \sum_{n=1}^{N} E_y^{(n)}, \tag{5.1}$$

so that the elements of the coherency matrix are

$$\begin{cases} J_{kl} = \langle E_k E_l^* \rangle = \sum_{n=1}^{N} \sum_{m=1}^{N} \langle E_k^{(n)} E_l^{(m)*} \rangle , \\ \quad = \sum_{n=1}^{N} \langle E_k^{(n)} E_l^{(n)*} \rangle + \sum_{n \neq m} \langle E_k^{(n)} E_l^{(m)*} \rangle . \end{cases} \tag{5.2}$$

Since the waves are assumed to be independent, each term under the last summation sign is zero, and it follows that

$$J_{kl} = \sum_{n=1}^{N} J_{kl}^{(n)} , \tag{5.3}$$

where $J_{kl}^{(n)} = \langle E_k^{(n)} E^{(n)*} \rangle$ are the elements of the coherency matrix of the n-th wave. The formula (5.3) shows that the coherency matrix of a wave resulting from the superposition of a number of independent waves is the sum of the coherency matrices of the individual waves.

To find an expression for the degree of polarization of a wave, we first represent the wave as a superposition of a wave of natural radiation and a wave of monochromatic radiation, independent of the former. Let $\boldsymbol{J}$ be the coherency matrix of the given wave and let $\boldsymbol{J}^{(1)}$ and $\boldsymbol{J}^{(2)}$ be the coherency matrices of the two independent waves into which we decompose it. Then according to (4.4) and (4.6) $\boldsymbol{J}^{(1)}$ and $\boldsymbol{J}^{(2)}$ must be of the form

$$\boldsymbol{J}^{(1)} = \begin{bmatrix} A & 0 \\ 0 & A \end{bmatrix}, \qquad \boldsymbol{J}^{(2)} = \begin{bmatrix} B & D \\ D^* & C \end{bmatrix}, \tag{5.4}$$

where $A \geqslant 0$, $B \geqslant 0$, $C \geqslant 0$ and

$$BC - DD^* = 0 . \tag{5.5}$$

In order to show that such a decomposition is possible we must determine quantities A, B, C, D, subject to the above conditions, such that the given coherency matrix $\mathbf{J} = [J_{ik}]$ is equal to the sum of two matrices of the form (5.4),

$$\mathbf{J} = \mathbf{J}^{(1)} + \mathbf{J}^{(2)} . \tag{5.6}$$

The relation (5.6) implies that

$$\begin{cases} J_{xx} = A + B , & J_{xy} = D , \\ J_{yx} = D^* , & J_{yy} = A + C . \end{cases} \tag{5.7}$$

On substituting for B, C, D and D^* from (5.7) into (5.5) we find that (*)

$$A = \tfrac{1}{2}(J_{xx} + J_{yy}) \pm \tfrac{1}{2}\sqrt{(J_{xx} + J_{yy})^2 - 4|\mathbf{J}|} . \tag{5.8}$$

Since $J_{yx} = J_{xy}^*$ the product $J_{xy}J_{yx}^*$ is non-negative, and it follows from (2.18) that

$$|\mathbf{J}| \leqslant J_{xx}J_{yy} \leqslant \tfrac{1}{4}(J_{xx} + J_{yy})^2 , \tag{5.9}$$

so that both the roots (5.8) are non-negative. Consider first the solution with the negative sign in front of the square root. We then have from (5.7),

$$\begin{cases} A = \tfrac{1}{2}(J_{xx} + J_{yy}) - \tfrac{1}{2}\sqrt{(J_{xx} + J_{yy})^2 - 4|\mathbf{J}|} , \\ B = \tfrac{1}{2}(J_{xx} - J_{yy}) + \tfrac{1}{2}\sqrt{(J_{xx} + J_{yy})^2 - 4|\mathbf{J}|} , \\ C = \tfrac{1}{2}(J_{yy} - J_{xx}) + \tfrac{1}{2}\sqrt{(J_{xx} + J_{yy})^2 - 4|\mathbf{J}|} , \\ D = J_{xy} , \\ D^* = J_{yx} . \end{cases} \tag{5.10}$$

Now

$$\sqrt{(J_{xx} + J_{yy})^2 - 4|\mathbf{J}|} = \sqrt{(J_{xx} - J_{yy})^2 + 4J_{xy}J_{yx}} \geqslant |J_{xx} - J_{yy}| . \tag{5.11}$$

Hence B and C are also non-negative as required. The other root given by (5.8) (with the positive sign in front of the square root) leads to negative values

(*) A is seen to be a characteristic root (eigenvalue) of the coherency matrix $\mathbf{J}$.

of B and C and must therefore be rejected. We have thus obtained a unique decomposition of the required kind.

The total intensity of the wave is

$$I_{\text{tot}} = \operatorname{Tr} \mathbf{J} = J_{xx} + J_{yy} \; ; \tag{5.12}$$

and the intensity of the monochromatic (and hence *polarized*) part is

$$I_{\text{pol}} = \operatorname{Tr} \mathbf{J}^{(2)} = B + C = \sqrt{(J_{xx} + J_{yy})^2 - 4\,|\mathbf{J}|}\,. \tag{5.13}$$

Hence the *degree of polarization* P of the original wave is

$$P = \frac{I_{\text{pol}}}{I_{\text{tot}}} = \sqrt{1 - \frac{4\,|\mathbf{J}|}{(J_{xx} + J_{yy})^2}}\,. \tag{5.14}$$

Since this expression involves only the two rotational invariants of the coherency matrix $\mathbf{J}$, the degree of polarization is independent of the particular choice of the x and y axes, as might have been expected.

Comparison of (5.14) with (3.8) shows that the quantity $(I_{\max} - I_{\min})/(I_{\max} + I_{\min})$ is precisely the degree of polarization P of the wave.

Unlike the degree of polarization, the degree of coherence depends on the choice of the x and y directions. We shall not investigate in detail the changes in the degree of coherence as the x, y axes are rotated; we shall only consider an extreme case, which is of special physical interest.

If in the expression (5.14) for the degree of polarization P we write out in full the discriminant $\mathbf{J}$, and use the expression (3.1) for the degree of coherence μ_{xy} we find that the following relation holds between P and $|\mu_{xy}|$:

$$1 - P^2 = \frac{J_{xx}\,J_{yy}}{[\frac{1}{2}(J_{xx} + J_{yy})]^2}\,[1 - |\mu_{xy}|^2]\,. \tag{5.15}$$

Since the geometric mean of any two positive numbers cannot exceed their arithmetic mean it follows that $1 - P^2 \leqslant 1 - |\mu_{xy}|^2$, *i.e.*

$$P \geqslant |\mu_{xy}|\,. \tag{5.16}$$

The equality sign in (5.16) will hold if an only if $J_{xx} = J_{yy}$, *i.e.* if the (time averaged) intensities in the two orthogonal directions are equal. We shall now show that a pair of directions always exists for which this is the case.

Suppose that we take a new pair of orthogonal directions x', y' perpendicular to the direction of propagation of the wave and let φ be the angle

between x and x'. The components $E_{x'}$, $E_{y'}$, of the electric vector (in the complex representations (2.13)) in the new directions are

$$\begin{cases} E_{x'} = \quad E_x \cos\varphi + E_y \sin\varphi\,, \\ E_{y'} = -E_x \sin\varphi + E_y \cos\varphi\,. \end{cases} \tag{5.17}$$

Hence the elements of the transformed coherency matrix $\mathbf{J}' = [J_{k'l'}] = [\langle E_{k'} E_{l'}^* \rangle]$ are

$$\begin{cases} J_{x'x'} = J_{xx}c^2 + J_{yy}s^2 + (J_{xy} + J_{yx})cs\,, \\ J_{y'y'} = J_{xx}s^2 + J_{yy}c^2 - (J_{xy} + J_{yx})cs\,, \\ J_{x'y'} = (J_{yy} - J_{xx})cs + J_{xy}c^2 - J_{yx}s^2\,, \\ J_{y'x'} = (J_{yy} - J_{xx})cs + J_{yx}c^2 - J_{xy}s^2\,, \end{cases} \tag{5.18}$$

where

$$c = \cos\varphi\,, \qquad s = \sin\varphi\,. \tag{5.19}$$

The intensities in the x' and y' directions will be equal (*i.e.* $J_{x'x'} = J_{y'y'}$) if

$$J_{xx}c^2 + J_{yy}s^2 + (J_{xy} + J_{yx})cs = J_{xx}s^2 + J_{yy}c^2 - (J_{xy} + J_{yx})cs\,.$$

Solving this equation for φ we obtain

$$\operatorname{tg} 2\varphi = \frac{J_{yy} - J_{xx}}{J_{xy} + J_{yx}}\,. \tag{5.20}$$

Since $J_{yx} = J_{xy}^*$ and J_{xx} and J_{yy} are real, this equation always has a real root. Thus *there always exists a pair of directions for which the two intensities are equal. For this pair of directions the degree of coherence $|\mu_{xy}|$ of the electric vibrations has its maximum value and this value is equal to the degree of polarization of the wave.*

This special pair of directions has a simple geometrical significance. If, as in (5.6) we represent the wave as incoherent mixture of a wave of natural radiation and a wave of monochromatic (and therefore completely polarized) radiation, the angle χ which the major axes of the vibrational ellipse of the polarized portion makes with the x-direction is given by (see CHANDRASEKHAR [7], p. 33, eq. (180))

$$\operatorname{tg} 2\chi = \frac{s_2}{s_1} = \frac{J_{xy} + J_{yx}}{J_{xx} - J_{yy}}\,. \tag{5.21}$$

It follows from (5.20) and (5.21) that $(\mathrm{tg}\,2\chi)\cdot(\mathrm{tg}\,2\varphi) = -1$ so that $\chi - \varphi = 45°$ or 135°. This implies that *the directions for which* $P = |\mu_{xy}|$ *are the bisectors of the principal directions* (*directions of the major and minor axes*) *of the vibrational ellipse of the polarized portion of the wave.*

It is evident from the foregoing discussion that the introduction of coherence concepts into the theory of partial polarization leads to a clearer understanding of the behaviour of partially polarized radiation and suggests new ways for the measurement of its degree of polarization.

RIASSUNTO (*)

In questo articolo si fa l'analisi della polarizzazione parziale dal punto di vista della teoria della coerenza. Dopo aver rilevato che la usuale definizione analitica dei parametri di Stokes per un'onda quasi monocromatica non è univoca, si prende in esame un semplice esperimento il quale introduce, in maniera chiara, i parametri osservabili per un'onda luminosa quasi monocromatica. L'analisi conduce ad un'unica matrice di coerenza e ad un unico gruppo di parametri di Stokes; quest'ultimo è associato alla rappresentazione della matrice di coerenza in funzione delle matrici di spin di Pauli. Tale analisi mostra la fondamentale importanza del concetto di segnale analitico di Gabor. Il grado di coerenza fra le vibrazioni elettriche in due direzioni qualunque, reciprocamente ortogonali, di propagazione dell'onda dipende, in generale, dalla scelta delle due direzioni ortogonali. Si dimostra che il valore massimo di esso uguaglia il grado di polarizzazione dell'onda. Si dimostra altresì che il grado di polarizzazione può essere dedotto, seguendo una via nuova, da esperimenti relativamente semplici che richiedono l'uso di un compensatore e di un polarizzatore, e che tale determinazione è analoga a quella del grado di coerenza ricavata dall'esperimento di interferenza di Young.

(*) *Traduzione a cura della Redazione.*

IL NUOVO CIMENTO Vol. XIII, N. 6 16 Settembre 1959

Polarization of Conversion Electrons Following Beta Decay.

R. L. Becker and M. E. Rose

Oak Ridge National Laboratory - Oak Ridge, Tenn.

(ricevuto il 13 Giugno 1959)

Summary. — Because of the breakdown of the symmetry principles in weak interactions, β-decay provides a means of producing polarized nuclei. In allowed transitions only first rank polarization, and in forbidden transitions higher odd rank orientation, is produced. This orientation is manifested in the polarization of subsequent radiations. The present work contains an essentially complete discussion of the polarization of internal conversion electrons from the K-shell. In allowed transitions there is an appreciable longitudinal and also transverse polarization. The latter is in the plane of the momentum vectors of the β-particle and conversion electron. In general these polarizations also appear in forbidden transitions where contributions from higher odd rank orientation are present. In addition, the forbidden transitions are characterized by a component of polarization perpendicular to the β-conversion electron plane. This component, which arises from the even rank orientations (for example, alignment), is a « classical » effect of the coincidence observation. Unfortunately, this transverse polarization is very small (a few percent at most) under practical conditions. Expressions for the polarization components are given in terms of extensively tabulated angular correlation coefficients and « particle » parameters for the three types of polarization. Numerical results for the longitudinal and transverse in-the-plane polarization parameters are included for mixed as well as for pure multipole transitions. Particular decay schemes involving allowed and first forbidden unique β transitions are considered in detail and numerical values for these polarizations are given.

1. – Introduction.

During the past two years a variety of polarization experiments involving nuclear β-decay have been carried out by numerous investigators. These experiments originally served the important purpose of establishing the breakdown of conservation of parity (P) and the failure of invariance under charge conju-

gation (C) in weak interactions. As techniques developed and improved these measurements came to be used in a more quantitative way to establish (at least approximately) the validity of the two-component neutrino theory [1]. All of the kinds of measurements already carried out, as well as that considered here, provide values of a quantity of the form $2\,\mathrm{Re}\,r/(1+|r|^2)$ where r is a ratio of the so-called parity non-conserving to parity conserving coupling constants. The observations indicate that $r \simeq 1$. Unfortunately near $r=1$, which is the value given by the two-component theory, the measured parameter is rather insensitive to r. The experimental errors have been such that the conclusion as to the validity of the two-component theory is not as firmly established as one would like.

Of the various possible polarization experiments testing the failure of P and C only two kinds have so far given fairly accurate information concerning the ratio r of odd to even coupling constants. These are the measurement of the longitudinal polarization (*) of β particles and of the circular polarization of an electromagnetic radiation in coincidence with the β-decay. The uncertainties associated with the first kind of measurement are in no small measure associated with the loss of intensity entailed in the conversion of longitudinal to transverse polarization in the method of polarization analysis by Mott scattering, which has given the most accurate results reported to date [2]. Other methods of analysis of longitudinal electron polarization involve equally severe intrinsic difficulties. In the second kind of experiment the difficulty arises from the small asymmetries associated with the low degree of electron polarization in magnetized iron.

In view of these difficulties it is evidently of interest to discuss alternative experiments. S. Treiman [3], and Frauenfelder, Jackson, and Wyld [4] have stressed the fact that all the particles in the final state of the β-decay process are oriented, in particular the recoiling nucleus, the orientations of which depend on the β-decay coupling constants. The β-particle itself, for example, possesses a longitudinal polarization, as mentioned above. The orientation of the recoiling nucleus is perhaps more interesting since it is in general

---

[1] T. D. Lee and C. N. Yang: *Phys. Rev.*, **105**, 1671 (1957); A. Salam: *Nuovo Cimento*, **5**, 299 (1957); L. Landau: *Nuclear Physics*, **3**, 127 (1957).

[2] *E.g.* B. H. Ketelle, A. R. Brosi, A. Galonsky and H. B. Willard: *Bull. Am. Phys. Soc.*, **4**, 76 (1959) and unpublished material.

[3] S. Treiman: *Phys. Rev.*, **110**, 448 (1958).

[4] H. Frauenfelder, J. D. Jackson and H. W. Wyld jr.: *Phys. Rev.*, **110**, 451 (1958).

(*) In forbidden transitions a transverse β-polarization in β-γ coincidences also can occur. The main interest in the transverse component is the possibility of detecting a possible breakdown of invariance under time reversal (T). See for example, P. C. Sims and R. M. Steffen: *Conference on Weak Interactions*, Gatlinburg, Tenn., USA (October 1958), *Bull. Am. Phys. Soc.*, **4**, 78 (1959).

more complex (an axially symmetric state of angular momentum J being described by up to $2J+1$ parameters) and since it may be analyzed by a variety of experiments. Measurement of the state of orientation of any ensuing radiation would serve as an analyzer of the orientation of a daughter nucleus in an excited state (4). The β-circularly polarized γ correlation already mentioned is an example. The particular alternative method to be discussed here is the measurement of the polarization of conversion electrons. The advantages are that i) it is unnecessary to use magnetized iron, and ii) the polarization of the conversion electrons is already partially transverse (*), thus eliminating the need for rotation of longitudinal into transverse polarization with consequent loss of intensity. It should also be emphasized, however, that along with these advantages there is the circumstance that the conversion electron must be observed in coincidence with the β-particle (**).

Conversion polarization measurements may also be used in another role, namely, to obtain information of importance for nuclear structure theories. As an example we mention the determination of the multipole mixing ratio in those cases in which the electromagnetic transition is fed only by a β-transition, so that one cannot perform the easier measurement of a γ-γ directional correlation. An instance of this situation is presented in Section 3.

The suggestion of measuring the conversion polarization was first made by FRAUENFELDER, JACKSON, and WYLD (1) who recognized that there would be a longitudinal polarization in analogy with the γ circular polarization, and verified it in the free electron approximation (5). The existence of a transverse polarization in the plane of the two measured directions was pointed out by the present authors (6) who gave the expressions for the polarization of pure multipole K shell internal conversion following allowed β transitions. Assuming a point nucleus a fully relativistic calculation was made, without introducing approximations regarding the Coulomb field. The necessary internal conversion matrix elements had been previously calculated (7) and a comprehensive tabulation of internal conversion coefficients obtained from these matrix elements has been recently published (8). The case of conversion pola-

(*) In comparison with γ-rays the possibility of transverse conversion polarization is a consequence of the non-vanishing rest mass of the electron. The electron polarization approaches that of γ-rays as the transition energy approaches infinity.

(**) Of course, the β-circularly polarized γ experiment also involves coincidence measurements. The relative merit of measuring γ's or conversion electrons largely depends on the relative efficiencies of polarization analysis for photons and electrons together with the magnitude of the internal conversion coefficient.

(5) S. M. DANCOFF and P. MORRISON: *Phys. Rev.*, **55**, 122 (1939).

(6) M. E. ROSE and R. L. BECKER: *Phys. Rev. Letters*, **1**, 116 (1958).

(7) M. E. ROSE *et al.*: *Phys. Rev.*, **83**, 79 (1951).

(8) M. E. ROSE: *Internal Conversion Coefficients* (Amsterdam, 1958).

rization following allowed transitions has also been investigated by BERESTECKIJ and RUDIK [9] and by GEŠKENBEIN [10]. The former use the free electron approximation while the latter, who included the Coulomb field, obtained results in agreement (*) with those of reference [6]. The effect of the Coulomb field is quite pronounced as may be seen by comparing the curves for different Z given in the present paper. Also important is the use of a covariant definition of the polarization operator. In reference [6] the polarization was obtained by calculating the expectation value of the relativistic spin operator as represented in Dirac spinor space [11]. In references [9] and [10] the expectation value of the representation of the relativistic spin operator in the two dimensional space of spin eigenfunctions [11] was calculated; this involves the use of the density matrix formalism. The two approaches are, of course equivalent.

The number of examples of the case discussed above (allowed β transitions followed by pure multipole conversion) which appear suitable for precision determinations of β-decay parameters is rather limited. In an effort to enlarge the list of sources the authors have extended the analysis [12] to mixed multipoles and to first forbidden β-decay. Extensive numerical results have been obtained for K conversion (**); these are included in the present article. One new feature emerges when one considers the forbidden transitions, namely, a third component of polarization. Whereas for allowed transitions the orientation of the daughter nucleus is completely described by tensors of rank 0 and 1, first forbidden transitions may provide non-vanishing tensor moments with ranks up to 3. As reported earlier [6,12,9], the odd rank orientation can give rise only to components of conversion polarization lying in the plane of the two measured directions. However, the even rank orientations give rise to a polarization which is perpendicular to the plane. This third component of polarization is expected to be small since it must vanish in the free electron (no binding) approximation. This can be seen in the following way: When the Coulomb field is neglected the polarization component in question transforms like

$$\boldsymbol{s}\cdot(\boldsymbol{p}\times\boldsymbol{p}_1)(\boldsymbol{p}\cdot\boldsymbol{p}_1)\,. \tag{1}$$

(*) Equations (18) and (31) of reference [9] correspond to equations (6) (9) of reference [6]. Considerable differences in notation are involved.

(**) Some of the numerical results were circulated privately at the Gatlinburg Conference on Weak Interactions, Oct. 1958.

[9] V. B. BERESTECKIJ and A. P. RUDIK: *Nuovo Cimento*, **10**, 375 (1958).

[10] B. V. GEŠKENBEIN: *Nuovo Cimento*, **10**, 365 (1958).

[11] Cf. C. BOUCHIAT and L. MICHEL: *Nuclear Physics*, 5. 416 (1958) or H. A. TOLHOEK: *Revs. Mod. Phys.*, **28**, 277 (1956).

[12] R. L. BECKER and M. E. ROSE: *Bull. Am. Phys. Soc.*, **4**, 79 (1958); *Program of the Conference on Weak Interactions*, Gatlinburg, Tenn., USA, Oct. 1958, pp. 20-22.

2757

Here $\boldsymbol{s}$ is a vector in the direction of the electron spin, $\boldsymbol{p}$ is the momentum of the electron, and $\boldsymbol{p}_1$ is the momentum of the β-particle. The expression (1) changes sign under C and T and consequently the electron polarization perpendicular to $\boldsymbol{p}$ and $\boldsymbol{p}_1$ vanishes in the $Z = 0$ limit. It follows that this polarization component, to exist at all, must be a « Coulomb correction ». It is also seen that this out-of-the-plane polarization is a « classical » effect (such as the appearance of linearly polarized gammas following forbidden β-decay) and does not depend on the breakdown of any of the three symmetry laws.

The present paper contains an essentially complete discussion of the polarization of internally converted K shell electrons. Details of the derivations of previously reported results are given. The formalism has been worked out for nuclear orientations of arbitrary tensor rank. Of course, at the present time practical interest is limited primarily to the first three tensor ranks, as the higher tensor ranks enter only into β transitions which are second forbidden or of higher order. Numerical results for polarization parameters (which are independent of the β transition) are given. Specific transitions are treated numerically in which results for the polarization components are presented. Both allowed and unique first forbidden cases are considered. The latter limitation is made in the interest of avoiding ambiguities arising from the presence of more than one (essentially unknown) nuclear matrix element.

2. – General theory.

2·1. *Preliminaries.* – As with other angular correlation problems it is possible to discuss separately the two parts of the cascade. The first transition, the emission of the β-particle, merely serves to provide an oriented initial state for the second transition, the internal conversion process. If either the direction of the β-particle or the direction of the recoiling nucleus is measured, the state of orientation of the daughter nucleus is axially symmetric about the measured direction. If such a state is characterized by an angular momentum J, it is describable in terms $2J+1$ statistical tensors ([13]). If the axis of quantization is chosen along the measured direction, the density matrix of the daughter state of the β transition is diagonal and each of its $2J+1$ diagonal elements can be interpreted as the population p_M of a pure state with magnetic quantum number M. The dynamics of the β process thus provide a set of $2J+1$ numbers p_M, which depend on the nature of the β-coupling

([13]) U. FANO: Report No. 1214, National Bureau of Standards, USA (1951) (unpublished); M. E. ROSE: *Phys. Rev.*, **108**, 362 (1957); L. C. BIEDENHARN: *Ann. of Phys.*, **4**, 104 (1958).

(*e.g.* if P and C were not violated then p_M would be an even function of M) and on the degree of forbiddenness as well as other parameters (β-energy, etc.). The populations p_M may be expressed in various ways, for example

$$p_M = \sum_{\nu=0}^{2J} a_\nu M^\nu \tag{2a}$$

$$= \sum_{\nu=0}^{2J} \alpha_\nu C(J\nu J;\, M0)\,, \tag{2b}$$

where $C(J\nu J;\, M0)$ is a Clebsch-Gordan coefficient. The α_ν are proportional to the statistical tensors. If one lets R^0_ν denote the statistical tensor of rank ν and projection 0, then

$$\alpha_\nu = [(2\nu+1)/(2J+1)]^{\frac{1}{2}} R^0_\nu\,. \tag{2c}$$

ALDER, STECH, and WINTER ([14]) in their treatment of the β-circularly polarized γ correlation have employed a still differently normalized set of parameters, effectively

$$\beta_\nu = (2\nu+1)^{-\frac{1}{2}}\alpha_\nu = (2J+1)^{-\frac{1}{2}} R^0_\nu \sim b_\nu F_\nu\,. \tag{2d}$$

The parameters α_ν will be specified explicitly in Section 2·5 for the transitions considered in this paper.

The polarization « vector » of the conversion electrons is in our formulation given by

$$\boldsymbol{P} = \frac{\langle (\psi_\infty, \boldsymbol{P}_{op}\psi_\infty)\rangle}{\langle (\psi_\infty, \psi_\infty)\rangle}\,. \tag{3}$$

Here $\boldsymbol{P}_{op}$ is the relativistic polarization operator acting in spinor space, ψ_∞ is the asymptotic form of a solution of the Dirac equation, in the spherically symmetric Coulomb field of a point nucleus, which has the form of an outgoing wave (proportional to $\exp[ipr]/r$). The round brackets denote scalar products with respect to spinor indices only. The angular brackets refer to an average over the ensemble of initial magnetic substates with the weight factors p_M for the nuclear substates, to a sum over final magnetic substates and to sums over the electronic magnetic substates as well. As has been explained elsewhere ([15]) the probability density $(\psi_\infty, \psi_\infty)$ can be expressed in terms of matrix

([14]) K. ALDER, B. STECH and A. WINTER: *Phys. Rev.*, **107**, 728 (1957).

([15]) M. E. ROSE, L. C. BIEDENHARN and G. B. ARFKEN: *Phys. Rev.*, **85**, 5 (1952). This shall be denoted RBA henceforth.

elements of the perturbation $\mathscr{H}_1$ responsible for the conversion process between the initial bound state and a final state which has the asymptotic form of a Coulomb modified plane wave plus an incoming spherical wave. The same holds true for the « spin probability » density $(\psi_\infty, \boldsymbol{P}_{op}\psi_\infty)$.

It is very important to take into account the binding of the electron by the Coulomb field. While the formalism applies for an arbitrary central field, the numerical results presented below refer to an unscreened point nucleus. For K shell conversion we have verified that the effect of screening is negligible. It is also to be expected that the corrections introduced by considering the finite size of the nucleus are less important than for the internal conversion coefficient, since in the polarization calculation only ratios of radial matrix elements are involved.

The nuclear states involved in the β-conversion cascade are labelled by the angular momentum and magnetic quantum numbers. The cascade is then described by

$$(J_1, M_1) \xrightarrow{\beta} (J, M) \xrightarrow{\text{c.e.}} (J_2, M_2) .$$

The notation used for the electronic Dirac central field problem shall follow those of RBA for which, with $m = \hbar = c = 1$, the Dirac Hamiltonian with eigenvalue E, is

$$H_0 = -(\boldsymbol{\alpha}\cdot\boldsymbol{p} + \beta - V) ,$$

the mean velocity is

$$v = -(\psi, \boldsymbol{\alpha}\psi)$$

and the lower two components of the 4-spinors are « large » in the non-relativistic limit. Moreover, the γ matrices are

$$\gamma_4 = -\beta = \begin{pmatrix} -I & 0 \\ 0 & I \end{pmatrix}, \quad \boldsymbol{\gamma} = -i\boldsymbol{\alpha}\gamma_4 , \qquad \gamma_5 = \gamma_1\gamma_2\gamma_3\gamma_4$$

and the spin operator is

$$\boldsymbol{\sigma} = \boldsymbol{\alpha}\gamma_5 = \gamma_5\boldsymbol{\alpha} .$$

The angular momentum eigenstates involved are completely labelled by the magnetic quantum number μ and the eigenvalue $\varkappa$ of $\beta(\boldsymbol{\sigma}\cdot\boldsymbol{L}+1)$

(4a) $$\varkappa = k \operatorname{sgn}\varkappa = \pm 1, \ \pm 2, \ \ldots ; \qquad k = |\varkappa|$$

which is related to the total electronic angular momentum

(4b) $$j = k - \tfrac{1}{2}$$

and the parity $(-)^l$ where

(4c) $$l = l_\varkappa = k\,, \qquad \varkappa \geqslant 1\,,$$
$$= k-1\,, \qquad \varkappa \leqslant -1\,.$$

We shall also employ the notation

(4d) $$\bar{l} = l_{-\varkappa} = k-1\,, \qquad \varkappa \geqslant 1\,,$$
$$= k\,, \qquad \varkappa \leqslant -1\,.$$

An arbitrary electron state of definite energy, regular at the origin, may be expanded in terms of the standing wave eigenfunctions corresponding to definite values of $\varkappa$ and μ which shall be denoted by

(5a) $$\Phi^\mu_\varkappa(\boldsymbol{r}) = \begin{pmatrix} -if_\varkappa(r) & \chi^\mu_{-\varkappa}(\hat{\boldsymbol{r}}) \\ g_\varkappa(r) & \chi^\mu_\varkappa(\hat{\boldsymbol{r}}) \end{pmatrix},$$

where the two-component (Pauli) spin-angular eigenfunctions $\chi^\mu_\varkappa$ are defined by

(5b) $$\chi^\mu_\varkappa(\hat{\boldsymbol{r}}) = \sum_\sigma C(l\tfrac{1}{2}j;\ \mu-\sigma,\ \sigma)\chi^\sigma_{\frac{1}{2}} Y^{\mu-\sigma}_l(\hat{\boldsymbol{r}})\,.$$

Here the $\chi^\sigma_{\frac{1}{2}}$ are intrinsic spin eigenfunctions ($\sigma = \pm\tfrac{1}{2}$) and $\hat{\boldsymbol{r}}$ is the unit vector in the direction $\boldsymbol{r}$. In (5b) the first factor is a vector addition coefficient (C-coefficient). In terms of these eigenfunctions the asymptotic outgoing wave function ψ_∞, representing the final state (as calculated in lowest order of perturbation theory), for the internal conversion of an electron originally in the initial state $\Phi^{\mu_i}_{\varkappa_i}$ and accompanying the nuclear transition $(JM) \to (J_2M_2)$, has been given by eq. (21) of RBA. Dropping irrelevant constant factors and with some other simplifications this becomes

(6) $$\psi_\infty(\mu_i;\boldsymbol{r}) \sim \frac{\exp[ipr]}{r} \sum_{\varkappa\mu} (\exp[-i\delta_\varkappa]\,\Phi^\mu_\varkappa \Psi(J_2M_2)\,|\,\mathscr{H}_1\,|\,\Phi^{\mu_i}_{\varkappa_i}\Psi(JM)) \cdot$$
$$\cdot \begin{pmatrix} (E+1)^{-\frac{1}{2}} & \chi^\mu_{-\varkappa} \\ (E-1)^{-\frac{1}{2}} & \chi^\mu_\varkappa \end{pmatrix},$$

where Ψ represents a nuclear state. The $\delta_\varkappa = \delta_\varkappa(Z)$ are the total phases for the central field in which the electron moves. For the Coulomb field of a point nucleus they are given (*) by

$$(7a) \qquad \delta_\varkappa(Z) = \eta_{l\varkappa}(Z) - \frac{\pi}{2}\gamma_k(Z) - \arg\Gamma(\gamma_k(Z) + i\alpha ZE/p) + (\alpha ZE/p)\ln 2pr\,.$$

Here

$$(7b) \qquad \gamma_k(Z) = (k^2 - \alpha^2 Z^2)^{\frac{1}{2}} > 0$$

and

$$(7c) \qquad \exp[2i\eta_\varkappa(Z)] = -\frac{\varkappa - i\alpha Z/p}{\gamma_k(Z) + i\alpha ZE/p}\,; \qquad p = (E^2-1)^{\frac{1}{2}}\,.$$

The radial functions $f_\varkappa(r)$ and $g_\varkappa(r)$ depend on the phase shift $\delta_\varkappa$. Even though $\eta_{l\varkappa}$ and, hence, $\delta_\varkappa$ is ambiguous to the extent of a multiple of π the phase of $\exp[-i\delta_\varkappa]\Phi^\mu_\varkappa$ is unambiguous.

The matrix element in eq. (6) involves integration over both electronic and nuclear co-ordinates. By specializing to the case of a point nucleus the operator $\mathscr{H}_1$ factors into the product of an operator in nuclear space and one in electronic space ([15]). The matrix element therefore factors also. Making use of the Wigner-Eckart theorem applied to the multipole expansion of $\mathscr{H}_1$, the result, obtained in RBA, may be written

$$(8a) \qquad (\exp[-i\delta_\varkappa]\Phi^\mu_\varkappa|\mathscr{H}_1|\Phi^{\mu_i}_{\varkappa_i}) =$$
$$= \sum_{\pi,L} C(JLJ_2;\ M,\ M_2 - M)\,C(Lj_ij;\ \mu-\mu_i,\ \mu_i)\delta_{\mu+M_2,\,\mu_i+M}\,\mathscr{N}(\pi L)\,\mathscr{E}_k(\pi L)\,.$$

Here L is the multipole order and $\pi = M$ or E specifies whether it is of magnetic or electric character. The $\mathscr{N}(\pi L)$ are the reduced nuclear matrix elements. They have the significance that the ratio of *photon* intensities of the $(\pi' L')$ and (πL) multipoles is just $|\mathscr{N}(\pi' L')/\mathscr{N}(\pi L)|^2$. (**). For given L the character π of the radiation is uniquely related to the parity change in the nuclear transition $J \to J_2$. This is of utmost importance for the conversion process since the dynamics of this process is strongly parity dependent.

The $\mathscr{E}_k(\pi L)$ are reduced electronic matrix elements. These are related to

(*) The r dependent logarithmic term is independent of $\varkappa$ and therefore does not enter into physical results where only $\delta_\varkappa - \delta_{\varkappa'}$ occurs.

(**) With time reversal invariance for strong interactions, the $\mathscr{N}(\pi L)$ may be taken to be real. There should be no confusion of the use of $\pi = M$ with the use of M as a magnetic number, for π will be used only together with L, as EL or ML.

the $Q(\varkappa L\pi)$ of RBA by

$$\mathscr{E}_k(\pi L) = \frac{\exp[i\delta_\varkappa]Q(\varkappa L\pi)}{[L(L+1)]^{\frac{1}{2}}} . \tag{8b}$$

In terms of the basic radial matrix elements R_i $(i=1,2,3,4)$ and R_i' $(i=3,4)$ defined in eqs. (13) and (17) of reference [7] we have, except for an irrelevant common factor $i(4\pi)^{-\frac{1}{2}}$,

$$Q(\varkappa LM;\varkappa_i) = (\varkappa+\varkappa_i)[R_3'+R_4']_{\varkappa LM\varkappa_i} \tag{8c}$$

and

$$Q(\varkappa LE;\varkappa_i) = [L(R_1+R_2-R_3+R_4)-(\varkappa-\varkappa_i)(R_3+R_4)]_{\varkappa LE\varkappa_i} \tag{8d}$$

The factors $\varkappa\pm\varkappa_i$ are sometimes seen in the less compact form

$$\varkappa\pm\varkappa_i = [l(l+1)-j(j+1)-\tfrac{1}{4}]\pm[l_i(l_i+1)-j_i(j_i+1)-\tfrac{1}{4}] .$$

The numerical work presented in this paper is limited to the K shell for which $\varkappa_i=-1$ and for which the above matrix elements have been calculated. Although $\mathscr{E}_k(\pi L)$ depends on the sign of $\varkappa$ the subscript is written as k because the sign of $\varkappa$ is given once π, L, and k are specified. This is evident from the selection rules for internal conversion of an $s_{\frac{1}{2}}$ electron, see Table I.

TABLE I. – *Final state quantum numbers for internal conversion of an $s_{\frac{1}{2}}$ electron. L is the multipole order.*

	$\varkappa$	j	l
ML	$L+1$	$L+\frac{1}{2}$	$L+1$
	$-L$	$L-\frac{1}{2}$	$L-1$
EL	L	$L-\frac{1}{2}$	L
	$-L-1$	$L+\frac{1}{2}$	L

Of course for $j_i=\frac{1}{2}$ there are only two final states for a given multipole (πL). Note that for given L the electric and magnetic multipoles have $\varkappa$ values which merely differ in sign, since these fields have opposite parity. For a mixed transition (ML, EL') it is necessary that $L+L'$ be odd. It is also important to realize that all the final states available to the conversion electron have the same parity. That is, if l and l' are assigned to two final states then $l\pm l'$ is even. This is true for mixtures as well as for pure multipoles. As will be

seen it is this fact which rules out transverse polarization out of the plane of the two measured directions for odd tensor ranks ν.

It is convenient to calculate separately the expectation values occurring in the numerator and denominator of eq. (3), except for common factors which we drop immediately. The remaining factor in the denominator, which is proportional to the β — c. e. angular correlation ([15,16]), may be written, using eqs. (2b), (6), and (8a), as (*)

$$(9a) \qquad (\psi_\infty, \psi_\infty) \sim I(\theta) = \sum_\nu \alpha_\nu \sum_{\pi\pi' LL'}{}' (2 - \delta_{\pi\pi'}\delta_{LL'}) \mathcal{N}(\pi L)\mathcal{N}(\pi' L') I_\nu(\theta; \pi L \pi' L') .$$

The prime on the summation sign in (9a) means $L' \geqslant L$. Also

$$(9b) \qquad I_\nu(\theta; \pi L \pi' L') = \frac{2E}{p} \operatorname{Re} \sum_{\varkappa\varkappa'} \mathscr{E}_\varkappa(\pi L)\, \mathscr{E}^*_{\varkappa'}(\pi' L') \sum_{M\mu\mu_i} C(J\nu J;\, M0) \cdot$$
$$\cdot C(JLJ_2;\, M, \mu_i - \mu)\, C(JL'J_2;\, M, \mu_i - \mu)\, C(Lj_i j;\, \mu - \mu_i, \mu_i) \cdot$$
$$\cdot C(L' j_i j';\, \mu - \mu_i, \mu_i) (\chi^\mu_{\varkappa'}(\hat{\boldsymbol{r}}), \chi^\mu_\varkappa(\hat{\boldsymbol{r}})) .$$

Here θ is the angle between $\boldsymbol{p}_1$ and $\boldsymbol{p}$, where $\boldsymbol{p}_1 = p_1 \hat{\boldsymbol{e}}_z$ is the momentum of the β-particle (or recoiling nucleus, whichever is measured) and $\boldsymbol{p}$ is the momentum of the conversion electron. This angle is contained in ([17])

$$(9c) \qquad (\chi^\mu_{\varkappa'}(\hat{\boldsymbol{r}}), \chi^\mu_\varkappa(\hat{\boldsymbol{r}})) = \left[\frac{(2l+1)(2l'+1)(2j+1)(2j'+1)}{4\pi}\right]^{\frac{1}{2}} (-)^{\mu+\frac{1}{2}} \cdot$$
$$\cdot \sum_\lambda (2\lambda+1)^{-\frac{1}{2}} C(l' l \lambda\, 00)\, C(j' j \lambda;\, -\mu, \mu) W(l' j' l j;\, \tfrac{1}{2}\lambda) Y^0_\lambda(\hat{\boldsymbol{r}}) ,$$

since the polar axis has been chosen along $\boldsymbol{p}_1$ and since asymptotically $\boldsymbol{p}$ is along $\boldsymbol{r}$. From the fact that $l + l'$ is even (this is true for internal conversion from any shell) the coefficient $C(l' l \lambda;\, 00)$ vanishes unless λ is even. Equation (9c) is obtained by using eq. (5b), the spherical harmonics coupling rule and a Racah recoupling.

Although the angular correlation with the isotropic term normalized to unity, $W(\theta)$, is given in the literature ([15,16]), the evaluation of $I(\theta)$ is sketched

([16]) L. C. BIEDENHARN and M. E. ROSE: *Revs. Mod. Phys.*, **25**, 729 (1953).

([17]) This equation has been derived in detail on p. 158 of M. E. ROSE: *Elementary Theory of Angular Momentum* (New York, 1957). RBA eq. (26) contains another form of this equation.

(*) It is assumed with no loss of generality that a representation is chosen in which the nuclear matrix elements are real. This is always possible (cf. reference ([16])) since electromagnetic interactions are invariant under time reversal.

in Appendix A since for the calculation of the ploarization from eq. (3) it is necessary to obtain the absolute magnitude of the isotropic term. As only even ranks ν contribute to the angular correlation and only pure multipole terms contribute to the isotropic part, eq. (9*a*) may be rewritten in the form

$$I(\theta) = [\alpha_0 \sum_{\pi L} |\mathcal{N}(\pi L)|^2 I_0(\pi L)]\, W(\theta)\,, \tag{9d}$$

with

$$W(\theta) = 1 + \sum_{\substack{\nu \text{ even} \\ >0}} \frac{\alpha_\nu}{\alpha_0} \frac{\sum_{\pi L \pi' L'} \mathcal{N}(\pi L)\, \mathcal{N}^*(\pi' L')\, I_\nu(\theta; \pi L \pi' L')}{\sum_{\pi L} |\mathcal{N}(\pi L)|^2 I_0(\pi L)}\,. \tag{9e}$$

It has become customary to write angular correlations in a form (cf. reference ([16])) which is easily compared with the corresponding correlation in which one of the radiations is replaced by a standard radiation, which is conventionally chosen to be a photon. In the present context this means writing (cf. eq. (2*d*))

$$\frac{I_\nu(\theta; \pi L \pi' L')}{[I_0(\pi L)\, I_0(\pi' L')]^{\frac{1}{2}}} = (2\nu+1)^{-\frac{1}{2}} F_\nu(LL' J_2 J)\, b_\nu(\pi L \pi' L')\, P_\nu(\cos\theta)\,. \tag{9f}$$

Here $F_\nu(LL'J_2J)$ is the « geometrical factor » characteristic of electromagnetic radiation defined ([16,18]) by

$$F_\nu(LL' J_2 J) = (-)^{J_2 - J - 1}[(2L+1)(2L'+1(2J+1)]^{\frac{1}{2}} \cdot C(LL'\nu;\, 1,\, -1)\, W(JJLL';\, \nu J_2)\,, \tag{9g}$$

for which $F_0(LL'J_2J) = \delta_{LL'}$ and $b_\nu(\pi L \pi' L')$ is a « particle parameter » for the conversion electron. For the photon $b_\nu = 1$. Thus the conversion electron parameters $b_\nu(\pi L \pi' L')$ indicate directly how the conversion electron angular correlation differs from the corresponding photon correlation. It is shown in Appendix A that

$$I_0(\pi L) = \frac{E}{\pi_\mu} \frac{2J_2+1}{2L+1} D_0(\pi L)\,, \tag{9h}$$

with

$$D_0(\pi L) = L\,|\mathscr{E}_L(\pi L)|^2 + (L+1)\,|\mathscr{E}_{L+1}(\pi L)|^2\,. \tag{9i}$$

([18]) M. Ferentz and N. Rosenzweig: Argonne National Laboratory (USA) Report 5324, « Table of F Coefficients ».

2·2. *Evaluation of* $\langle(\boldsymbol{P}_{op})\rangle$. – We have been using the notation of RBA for the Dirac central field problem. In this representation the relativistic polarization operator ([11]) acting in the space of spinor components is

$$\boldsymbol{P}_{op} = (\boldsymbol{\sigma}\cdot\hat{\boldsymbol{p}})\hat{\boldsymbol{p}} - \beta(\boldsymbol{\sigma}\cdot\hat{\boldsymbol{t}}_i)\,\hat{\boldsymbol{t}}_i - \beta(\boldsymbol{\sigma}\cdot\hat{\boldsymbol{t}}_0)\hat{\boldsymbol{t}}_0\,, \tag{10a}$$

where β and $\boldsymbol{\sigma}$ are the familiar Dirac operators and $\hat{\boldsymbol{p}}$, $\hat{\boldsymbol{t}}_i$, and $\hat{\boldsymbol{t}}_0$ form an orthogonal basis of unit vectors. A positive longitudinal polarization is defined as being in the direction of

$$\hat{\boldsymbol{p}} = \cos\theta\,\hat{\boldsymbol{e}}_z + \sin\theta(\cos\varphi\,\hat{\boldsymbol{e}}_x + \sin\varphi\,\hat{\boldsymbol{e}}_y) \tag{10b}$$

A positive transverse polarization in the plane of $\hat{\boldsymbol{p}}_1 = \hat{\boldsymbol{e}}_z$ and $\hat{\boldsymbol{p}}$ is in the direction of

$$\hat{\boldsymbol{t}}_i = \hat{\boldsymbol{p}}\times(\hat{\boldsymbol{p}}_1\times\hat{\boldsymbol{p}})/\sin\theta = (\hat{\boldsymbol{p}}_1 - \cos\theta\,\hat{\boldsymbol{p}})/\sin\theta\,. \tag{10c}$$

A positive transverse polarization out of the plane of $\hat{\boldsymbol{p}}_1$ and $\hat{\boldsymbol{p}}$ is in the direction of

$$\hat{\boldsymbol{t}}_0 = (\hat{\boldsymbol{p}}_1\times\hat{\boldsymbol{p}})/\sin\theta = \cos\varphi\,\hat{\boldsymbol{e}}_y - \sin\varphi\,\hat{\boldsymbol{e}}_x\,. \tag{10d}$$

The numerator of eq. (3), except for factors in common with the denominator, is

$$\langle(\psi_\infty, \boldsymbol{P}_{op}\psi_\infty)\rangle \sim V(\theta) = \sum_\nu \alpha_\nu \sum_{\pi L\pi' L'}{}' (2-\delta_{\pi\pi'}\delta_{LL'})\mathcal{N}(\pi L)\mathcal{N}^*(\pi' L')V_\nu(\theta;\pi L\pi L'), \tag{11a}$$

where

$$V_\nu(\theta;\pi L\pi' L') = \mathrm{Re}\sum_{\varkappa\varkappa'} \mathscr{E}_k(\pi L)\,\mathscr{E}^*_{k'}(\pi' L') \sum_{M,\mu,\mu_i} C(J\nu J;\, M0)\cdot \tag{11b}$$

$$\cdot C(JLJ_2;\, M, \mu_i - \mu)\, C(JL'J_2;\, M, \mu_i - \mu)\, C(Lj\,j;\, \mu-\mu_i, \mu_i)\, C(L'j_i j';\, \mu-\mu_i, \mu_i)\cdot$$

$$\cdot\left[\frac{E-1}{p}\,(\chi^\mu_{-\varkappa'}, \boldsymbol{\sigma}\cdot\overleftrightarrow{\boldsymbol{D}}\chi^\mu_{-\varkappa}) + \frac{E+1}{p}\,(\chi^\mu_{\varkappa'}, \boldsymbol{\sigma}\cdot\overleftrightarrow{\boldsymbol{I}}\chi^\mu_{\varkappa})\right],$$

with the dyadics $\overleftrightarrow{\boldsymbol{D}}$ and $\overleftrightarrow{\boldsymbol{I}}$ defined as

$$\overleftrightarrow{\boldsymbol{D}} = \hat{\boldsymbol{p}}\,\hat{\boldsymbol{p}} - (\hat{\boldsymbol{t}}_i\,\hat{\boldsymbol{t}}_i + \hat{\boldsymbol{t}}_0\hat{\boldsymbol{t}}_0)\,, \qquad \overleftrightarrow{\boldsymbol{I}} = \hat{\boldsymbol{p}}\,\boldsymbol{p} + \hat{\boldsymbol{t}}_i\hat{\boldsymbol{t}}_i + \hat{\boldsymbol{t}}_0\hat{\boldsymbol{t}}_0\,. \tag{12}$$

In eq. (11*b*) $\boldsymbol{\sigma}$ is, of course, the Pauli two-by-two spin matrix vector.

In order to evaluate the spinor scalar products which occur in the square bracket of (11*b*) it is convenient to introduce the spherical basis. For any

vector $\boldsymbol{v}$, the spherical components are

$$(13a) \qquad v_{\pm 1} = \mp \frac{1}{\sqrt{2}}(v_x \pm i v_y) = \hat{\boldsymbol{\xi}}_{\pm 1}\cdot\boldsymbol{v}, \qquad v_0 = v_z = \hat{\boldsymbol{\xi}}_0\cdot\boldsymbol{v},$$

where the corresponding complex unit vectors are

$$(13b) \qquad \hat{\boldsymbol{\xi}}_{\pm 1} = \mp \frac{1}{\sqrt{2}}(\hat{\boldsymbol{e}}_x \pm i\hat{\boldsymbol{e}}_y), \qquad \boldsymbol{\xi}_0 = \hat{\boldsymbol{e}}_z,$$

so that $\hat{\boldsymbol{\xi}}_n\cdot\hat{\boldsymbol{\xi}}^*_{n'} = \delta_{nn'}$ and $\hat{\boldsymbol{\xi}}^*_n = (-)^n\hat{\boldsymbol{\xi}}_{-n}$. Then

$$(13c) \qquad \boldsymbol{v} = \sum_{n=-1}^{1}(-)^n v_n \hat{\boldsymbol{\xi}}_{-n}.$$

Using the fact that $\frac{1}{2}\sigma_n$ are angular momentum operators for spin $\frac{1}{2}$ one obtains (*)

$$(14) \qquad (\chi^{\mu}_{\kappa'}, \sigma_n\chi^{\mu}_{\kappa}) = \left[\frac{3(2l+1)(2l'+1)}{2\pi}\right]^{\frac{1}{2}}\sum_{\lambda} C(l'l\lambda;\,00)\; Y^n_{\lambda}(\hat{\boldsymbol{r}})\cdot$$

$$\cdot\sum_{s}(-)^{l'-s-j'}(2s+1)W(\lambda l' j\tfrac{1}{2};\,ls)W(1\tfrac{1}{2}j'l';\,\tfrac{1}{2}s)\,C(1sj';\,n,\,\mu-n)\;C(\lambda sj;\,n,\,\mu-n).$$

As in $I(\theta)$ λ is even, as the first C-coefficient in (14) shows.

Upon substituting eqs. (13c) and (14) in eq. (11b) the sums over the magnetic quantum number M, μ_i, and μ and the sum over the auxiliary angular momentum parameter s may be carried out by Racah algebra (see Appendix B). One obtains

$$(15a) \qquad \boldsymbol{V}_{\nu}(\theta;\,\pi L\pi' L') = (-)^{J-J_2+L+L'}[3(2J+1)/2\pi(2\nu+1)]^{\frac{1}{2}}(2J_2+1)\cdot$$

$$\cdot W(JJLL';\,\nu J_2)\,\mathrm{Re}\sum_{\kappa\kappa'}\mathscr{E}_k(\pi L)\,\mathscr{E}^*_{k'}(\pi' L')(2j+1)(2j'+1)W(jLj'L';\,\tfrac{1}{2}\nu)\cdot$$

$$\cdot\left[\frac{E-1}{p}\boldsymbol{G}_{\nu}(\theta;\,-\kappa,\,-\kappa';\,\pi L\pi' L')\cdot\overleftrightarrow{\boldsymbol{D}} + \frac{E+1}{p}\boldsymbol{G}_{\nu}(\theta;\,\kappa\kappa';\,\pi L\pi' L')\right],$$

where

$$(15b) \qquad \boldsymbol{G}_{\nu}(\theta;\,\kappa\kappa'\pi L\pi' L') = \sum_{\lambda}(-)^{j+\frac{1}{2}+l-\nu}[(2l+1)(2l'+1)]^{\frac{1}{2}}C(ll'\lambda;\,00)\cdot$$

$$\cdot X(\nu jj';\,\lambda ll';\,1\tfrac{1}{2}\tfrac{1}{2})\boldsymbol{T}^0_{\nu\lambda}(\hat{\boldsymbol{r}}),$$

(*) This follows easily from eq. (5b) by using the relation

$$(\chi^{\sigma'}_{\frac{1}{2}},\,\tfrac{1}{2}\sigma_n\chi^{\sigma}_{\frac{1}{2}}) = \delta_{\sigma',n+\sigma}(-)^n[\tfrac{1}{2}(\tfrac{1}{2}+1)]^{\frac{1}{2}}C(\tfrac{1}{2}\,1\,\tfrac{1}{2};\,n+\sigma,\,-n)$$

see eq. (5.13) of reference [16], and performing two Racah recouplings.

involving an X-coefficient (*) and a « vector spherical harmonic » with the phase as defined by ROSE (19),

$$\boldsymbol{T}^0_{\nu\lambda}(\hat{\boldsymbol{r}}) = \sum_n C(1\lambda\nu; -n, n)\hat{\boldsymbol{\xi}}_{-n} Y^n_\lambda(\hat{\boldsymbol{r}}) . \tag{16}$$

These are spin angular functions for spin one and are evaluated in Appendix B. The sum over λ in (15b) is limited to the values $\lambda = \nu \pm 1, \nu$. Since λ is even the λ values are $\lambda = \nu \pm 1$ for ν odd, and $\lambda = \nu$ for ν even. For odd ν, $\boldsymbol{T}^0_{\nu,\nu\pm1}$ lies in the plane of the two measured directions, and for ν even $\boldsymbol{T}^0_{\nu\nu}$ is perpendicular to this plane.

The further evaluation of $\boldsymbol{V}_\nu$ is carried out in Appendix B, with the result

$$\boldsymbol{V}_{\nu\hat{q}}(\theta; \pi L\pi' L') \equiv \hat{\boldsymbol{q}}\cdot\boldsymbol{V}_\nu(\theta; \pi L\pi' L') = (-)^{L+L'+1}\frac{E}{\pi p}\frac{(2J_2+1)}{(2L+1)(2L'+1)}\cdot \tag{15c}$$

$$\cdot\left[\frac{L(L+1)\,L'(L'+1)}{2\nu+1}\right]^{\frac{1}{2}} F_\nu(LL'J_2J)\, M_{\nu\hat{q}}(\pi L\pi' L')\, P^q_\nu(\cos\theta) ,$$

where

$$\begin{cases} \hat{\boldsymbol{q}} = \hat{\boldsymbol{p}},\ \hat{\boldsymbol{t}}_i, \text{ or } \hat{\boldsymbol{t}}_3 \\ q = 0, \quad \text{for } \hat{\boldsymbol{q}} = \hat{\boldsymbol{p}} \\ \quad = 1, \quad \text{for } \hat{\boldsymbol{q}} = \hat{\boldsymbol{t}}_i \text{ or } \hat{\boldsymbol{t}}_0 \end{cases} \tag{15d}$$

and the $M_{\nu\hat{q}}(\pi L\pi' L')$ are given in Table III of Appendix B.

2·3. *Formal results for the polarization.* – As for the directional correlation one may introduce conversion parameters b_ν for the polarization components. In analogy with eq. (9f) one writes

$$\frac{V_{\nu\hat{q}}(\theta; \pi L\pi' L')}{[I_0(\pi L)\, I_0(\pi' L')]^{\frac{1}{2}}} = (2\nu+1)^{-\frac{1}{2}} F_\nu(LL'J_2J)\, b_{\nu\hat{q}}(\pi L\pi' L')\, P^q_\nu(\cos\theta) . \tag{17}$$

Using eq. (9h) for $I_0(\pi L)$ and eq. (15c) for $V_{\nu\hat{q}}(\theta; \pi L\pi' L')$ it follows that

$$b_{\nu\hat{q}}(\pi L\pi' L') = (-)^{L+L'+1}\left[\frac{L(L+1)\,L'(L'+1)}{(2L+1)(2L'+1)}\right]^{\frac{1}{2}}\frac{M_{\nu\hat{q}}(\pi L\pi' L')}{[D_0(\pi L)\, D_0(\pi' L')]^{\frac{1}{2}}} , \tag{17a}$$

(*) Cf. for example, reference (17), sec. 35.

(19) M. E. ROSE: *Multipole Fields* (New York, 1955), eq. (2.43), or eq. (5.57) of reference (17).

which has the same form as the expression, eq. (A.11), for the directional correlation parameters, namely

$$(17b)\qquad b_\nu(\pi L\pi' L') = (-)^{L+L'}\left[\frac{L(L+1)\,L'(L'+1)}{(2L+1)\,(2L'+1)}\right]^{\frac{1}{2}} \frac{M_\nu(\pi L\pi' L')}{[D_0(\pi L)\,D_0(\pi' L')]^{\frac{1}{2}}}\,.$$

From Appendices A and B it may be seen that the linear combinations of electronic matrix elements appearing in $M_{\nu\hat{p}}$ and in M_ν are the same and also that $M_{\nu\hat{t}_i}$ and $M_{\nu\hat{t}_0}$ involve the real and imaginary parts of the same combinations of matrix elements. Thus, the four sets of conversion electron parameters may be expressed in terms of the following four ratios of matrix elements:

$$(18a)\qquad r_1(\pi L\pi' L') = [D_0(\pi L)D_0(\pi' L')]^{-\frac{1}{2}}\,\mathrm{Re}\,[\mathscr{E}_L(\pi L) - \mathscr{E}_{L+1}(\pi L)]\cdot \cdot[\mathscr{E}^*_{L'}(\pi' L') - \mathscr{E}^*_{L'+1}(\pi' L')]\,,$$

$$(18b)\qquad r_2(\pi L\pi' L') = [D_0(\pi L)D_0(\pi' L')]^{-\frac{1}{2}}\,\mathrm{Re}\,[(L+L'+1)(L+L')\cdot \cdot\mathscr{E}_L(\pi L)\,\mathscr{E}^*_{L'}(\pi' L') + (L+L'+2)(L+L'+1)\,\mathscr{E}_{L+1}(\pi L)\,\mathscr{E}^*_{L'+1}(\pi' L') - - (L-L'-1)(L-L')\,\mathscr{E}_L(\pi L)\,\mathscr{E}^*_{L'+1}(\pi' L') - - (L-L'+1)(L-L')\,\mathscr{E}_{L+1}(\pi L)\,\mathscr{E}^*_{L'}(\pi' L')]\,,$$

$$(18c)\qquad r_3(\pi L\pi' L') = [D_0(\pi L)D_0(\pi' L')]^{-\frac{1}{2}}[-(L-L')\,\mathscr{E}_L(\pi L)\,\mathscr{E}^*_{L'}(\pi' L') + + (L-L')\,\mathscr{E}_{L+1}(\pi L)\,\mathscr{E}^*_{L'+1}(\pi' L') + (L+L'+1)\,\mathscr{E}_L(\pi L)\,\mathscr{E}^*_{L'+1}(\pi' L') - - (L+L'+1)\,\mathscr{E}_{L+1}(\pi L)\,\mathscr{E}^*_{L'}(\pi' L')]\,,$$

$$(18d)\qquad r_4(\pi L\pi' L') = [D_0(\pi L)D_0(\pi' L')]^{-\frac{1}{2}}[-(L+L')\,\mathscr{E}_L(\pi L)\,\mathscr{E}^*_{L'}(\pi' L') + + (L+L'+2)\,\mathscr{E}_{L+1}(\pi L)\,\mathscr{E}^*_{L'+1}(\pi' L') + (L-L'-1)\,\mathscr{E}_L(\pi L)\,\mathscr{E}^*_{L'+1}(\pi' L') - - (L-L'+1)\,\mathscr{E}_{L+1}(\pi L)\,\mathscr{E}^*_{L'}(\pi' L')]\,,$$

where $D_0(\pi L)$ is defined in Eq. (9*i*).

Setting

$$(19)\qquad \bar{\pi} = \begin{cases} E, & \text{for } \pi = M \\ M, & \text{for } \pi = E \end{cases}, \qquad \sigma(\pi) = \begin{cases} 0, & \pi = M \\ 1, & \pi = E \end{cases}$$

$$a = L(L+1) + L'(L'+1)\,, \qquad d = \nu(\nu+1)\,,$$

$$c = \left[\frac{L(L+1)\,L'(L'+1)}{(2L+1)(2L'+1)}\right]^{\frac{1}{2}}, \qquad \left.\begin{matrix} e_\nu \\ o_\nu \end{matrix}\right\} = \frac{1}{2}[1 \pm (-)^\nu]$$

the resulting expressions for the conversion parameters are:

Directional correlation:

$$(19a) \qquad \pi' = \pi: \qquad b_\nu(\pi L \pi' L') = \frac{ce_\nu}{a - d}[r_2(\pi L \pi' L') - d r_1(\pi L \pi L')] ,$$

$$(19b) \qquad \pi' \neq \pi: \qquad b_\nu(\pi L \bar{\pi} L') = ce_\nu r_1(\pi L \bar{\pi} L')$$

Longitudinal polarization:

$$(19c) \qquad \pi' = \pi: \qquad b_{\nu\hat{p}}(\pi L \pi L') = - co_\nu r_1(\pi L \pi L') ,$$

$$(19d) \qquad \pi' \neq \pi: \qquad b_{\nu\hat{p}}(\pi L \bar{\pi} L') = - \frac{co_\nu}{a - d}[r_2(\pi L \bar{\pi} L') - d r_1(\pi L \bar{\pi} L')] .$$

Transverse polarization in the plane of $\hat{p}_1$ and $\hat{p}$:

$$(19e) \qquad \pi' = \pi: \qquad b_{\nu\hat{t}_i}(\pi L \pi L') = (-)^{\sigma(\pi)} \frac{co_\nu}{d} \operatorname{Re} r_4(\pi L \pi L') ,$$

$$(19f) \qquad \pi' \neq \pi: \qquad b_{\nu\hat{t}_i}(\pi L \bar{\pi} L') =$$

$$= (-)^{\sigma(\pi)} \frac{co_\nu}{d(a - d)}[(L - L')(L + L' + 1) \operatorname{Re} r_4(\pi L \bar{\pi} L') - d \operatorname{Re} r_3(\pi L \bar{\pi} L')] .$$

Transverse polarization out of the plane of $\hat{p}_1$ *and* $\hat{p}$:

$$(19g) \qquad \pi' = \pi: \qquad b_{\nu\hat{t}_0}(\pi L \pi L') =$$

$$= (-)^{\sigma(\pi)} \frac{ce_\nu}{d(a - d)}[(L - L')(L + L' + 1) \operatorname{Im} r_4(\pi L \pi L') - d \operatorname{Im} r_3(\pi L \pi L')] ,$$

$$(19h) \qquad \pi' \neq \pi: \qquad b_{\nu\hat{t}_0}(\pi L \bar{\pi} L') = (-)^{\sigma(\pi)} \frac{ce_\nu}{d} \operatorname{Im} r_4(\pi L \bar{\pi} L') .$$

It is interesting to note that for pure multipoles there exists a relation between the longitudinal polarization parameter and the lowest order directional correlation parameter, namely

$$(20) \qquad b_{\nu\hat{p}}(\pi L \pi L) = [L(L+1)/3 - 1] b_2(\pi L \pi L) - L(L+1)/3 .$$

This result is obtained from the fact that

$$r_2(\pi L \pi L) = 2(2L + 1) .$$

The result (20) implies that with a knowledge of the properties of the β-transition a measurement of either the directional correlation or the longitudinal polarization allows a prediction of the other.

The conversion parameters in eqs. (19*b*) and (19*c*) are independent of ν where they do not vanish. In other cases the ν dependence is given by the following equations (*):

$$(20a)\qquad b_\nu(\pi L\pi L') = \frac{a-6}{a-d}\, b_2(\pi L\pi L') + \frac{d-6}{a-d}\, b_{1\hat{\nu}}(\pi L\pi L')\,,$$

$$(20b)\qquad b_{\nu\hat{\nu}}(\pi L\pi L') = \frac{-\delta_\nu}{2(a-d)}\,[a(2-d)\,b_2(\pi L\pi L') - d(a-2)\,b_{1\hat{\nu}}(\pi L\pi L')]\,.$$

The directional correlation parameter $b_2(\pi L\bar{\pi}L')$ has been tabulated in reference ([16]), Table IV.

$$(20c)\qquad b_{\nu\hat{t}_i}(\pi L\pi L') = (2/d)\,b_{1\hat{t}_i}(\pi L\pi L')\,,$$

$$(20d)\qquad b_{\nu\hat{t}_i}(\pi L\bar{\pi}L') = \frac{10+d}{6d}\, b_{1\hat{t}_i}(\pi L\bar{\pi}L') - \frac{5}{6d}\,\frac{(2-d)(a-12)}{a-d}\, b_{3\hat{t}_i}(\pi L\pi L')\,,$$

$$(20e)\qquad b_{\nu\hat{t}_0}(\pi L\pi L') = \frac{60-3d}{7d}\,\frac{a-6}{a-d}\, b_{2\hat{t}_0}(\pi L\pi L') - \frac{10}{7d}\,\frac{(6-d)(a-20)}{a-d}\, b_{4\hat{t}_0}(\pi L\pi L')\,,$$

$$(20f)\qquad b_{\nu\hat{t}_0}(\pi L\bar{\pi}L') = (6/d)\,b_{2\hat{t}_0}(\pi L\bar{\pi}L')\,.$$

For an arbitrary multipole mixture eqs. (9*d*), (9*f*), (11*a*) and (17) imply

$$(21)\qquad \boldsymbol{P}(\theta) = \sum_{\hat{q}} \hat{\boldsymbol{q}}\, P_{\hat{q}}(\theta)\,,$$

$$(21a)\qquad P_{\hat{q}}(\theta) = \Big\{\sum_\nu (2\nu+1)^{-\frac{1}{2}}(\alpha_\nu/\alpha_0) \sum_{\pi L\pi' L'}{}' (2-\delta_{\pi\pi'}\delta_{LL'})\,\mathcal{N}(\pi L)\mathcal{N}(\pi' L')\cdot$$
$$\cdot[I_0(\pi L)I_0(\pi' L')]^{\frac{1}{2}}\, F_\nu(LL'J_2J)\, b_{\nu\hat{q}}(\pi L\pi' L')\, P_\nu^q(\cos\theta)\Big\}\cdot$$
$$\cdot\Big\{[\sum_{\pi L} |\mathcal{N}(\pi L)|^2 I_0(\pi L)]\, W(\theta)\Big\}^{-1}\,,$$

where the directional correlation is

$$(21b)\qquad W(\theta) = 1 + [\sum_{\pi L} |\mathcal{N}(\pi L)|^2 I_0(\pi L)]^{-1} \sum_{\nu>0} e_\nu (2\nu+1)^{-\frac{1}{2}}(\alpha_\nu/\alpha_0)\cdot$$
$$\cdot \sum_{\pi L\pi' L'}{}' (2-\delta_{\pi\pi'}\delta_{LL'})\,\mathcal{N}(\pi L)\mathcal{N}(\pi' L')[I_0(\pi L)I_0(\pi' L')]^{\frac{1}{2}} F_\nu(LL'J_2J)\cdot$$
$$\cdot b_\nu(\pi L\pi' L')\, P_\nu(\cos\theta)\,.$$

The symbols $\hat{\boldsymbol{q}}$ and q were defined in eq. (15*d*).

(*) From (20*a*), the already established relation, reference ([15]),

$$b_\nu(\pi L\pi L) = 1 + \frac{\nu(\nu+1)}{6}\,\frac{L(L+1)-3}{2L(L+1)-\nu(\nu+1)}\,[b_2(\pi L\pi L)-1]$$

follows at once.

Gamma ray multipole mixture parameters may be defined by

$$\delta(\pi L;\,\pi' L') = \mathcal{N}(\pi' L')/\mathcal{N}(\pi L) = \pm[I_\gamma(\pi' L')/I_\gamma(\pi L)]^{\frac{1}{2}}, \tag{22}$$

where $I_\gamma(\pi L)$ is the intensity of pure πL-pole γ-emission. The corresponding conversion multipole mixture parameters are

$$\bar{\delta}(\pi L;\,\pi' L') = \left[\frac{b_0(\pi' L')}{b_0(\pi L)}\right]^{\frac{1}{2}} \delta(\pi L;\,\pi' L') = \left[\frac{c(\pi' L')}{c(\pi L)}\right]^{\frac{1}{2}} \delta(\pi L;\,\pi' L')\,, \tag{22a}$$

where $c(\pi L)$ is the conversion coefficient. Note that the (real) phases of $\bar{\delta}$ and δ are the same. Adopting a certain multipole, $\pi_0 L_0$, as a standard the polarization for a multipole mixture including $\pi_0 L_0$ may be written generally

$$P_{\hat{q}}(\theta) = \Big\{\sum_\nu (2\nu+1)^{-\frac{1}{2}}(\alpha_\nu/\alpha_0) \sum_{\pi L \pi' L'}{}' (2 - \delta_{\pi\pi'}\delta_{LL'})\, \bar{\delta}(\pi_0 L_0;\,\pi L)\cdot \tag{23a}$$

$$\cdot\, \bar{\delta}(\pi_0 L_0;\,\pi' L')\, F_\nu(LL' J_2 J) b_{\nu\hat{q}}(\pi L \pi' L') P_\nu^q(\cos\theta)\Big\}\Big\{\Big[\sum_{\pi L} \bar{\delta}^2(\pi_0 L_0;\,\pi L)\Big] W(\theta)\Big\}^{-1},$$

with

$$W(\theta) = 1 + \Big[\sum_{\pi L} \bar{\delta}^2(\pi_0 L_0;\,\pi L)\Big]^{-1} \sum_{\nu>0} e_\nu (2\nu+1)^{-\frac{1}{2}}(\alpha_\nu/\alpha_0) \sum_{\pi L \pi' L'}{}' (2 - \delta_{\pi\pi'}\delta_{LL'})\cdot \tag{23b}$$

$$\cdot\, \bar{\delta}(\pi_0 L_0;\,\pi L)\, \bar{\delta}(\pi_0 L_0;\,\pi' L')\, F_\nu(LL' J_2 J) b_\nu(\pi L \pi' L')\, P_\nu(\cos\theta)\,.$$

In practice the only multipole mixture usually considered is $\pi L \bar{\pi} L + 1$, for example, $M1$-$E2$ or $E1$-$M2$ mixtures. In this case (23a) becomes

$$P_{\hat{q}}(\theta) = \tag{24}$$

$$= \frac{P_{\hat{q}}(\theta;\,\pi L) + 2\,\bar{\delta}(\pi L;\,\bar{\pi} L + 1)\, \bar{P}_{\hat{q}}(\theta;\,\pi L,\,\bar{\pi} L + 1) + \bar{\delta}^2(\pi L \bar{\pi} L + 1)\, P_{\hat{q}}(\theta;\,\bar{\pi} L + 1)}{[1 + \bar{\delta}^2(\pi L;\,\bar{\pi} L + 1)] W(\theta)},$$

with

$$P_{\hat{q}}(\theta;\,\pi L) = \sum_\nu (2\nu+1)^{-\frac{1}{2}}(\alpha_\nu/\alpha_0)\, F_\nu(LL J_2 J) b_{\nu\hat{q}}(\pi L) P_\nu^q(\cos\theta)\,, \tag{24a}$$

$$\bar{P}_{\hat{q}}(\theta;\,\pi L \bar{\pi} L + 1) = \sum_\nu (2\nu+1)^{-\frac{1}{2}}(\alpha_\nu/\alpha_0)\, F_\nu(LL' J_2 J) b_{\nu\hat{q}}(\pi L \bar{\pi} L + 1) P_\nu^q(\cos\theta), \tag{24b}$$

and

$$W(\theta) = 1 + [1 + \bar{\delta}^2(\pi L;\,\bar{\pi} L + 1)]^{-1} \sum_\nu e_\nu (2\nu+1)^{-\frac{1}{2}} \frac{\alpha_\nu}{\alpha_0} [F_\nu(LL J_2 J)\, b_\nu(\pi L) + \tag{24c}$$

$$+ 2\bar{\delta}(\pi L;\,\bar{\pi} L + 1)\, F_\nu(LL + 1 J_2 J)\, b_\nu(\pi L \bar{\pi} L + 1) +$$

$$+ \bar{\delta}^2(\pi L;\,\pi L + 1)\, F_\nu(L + 1,\, L + 1,\, J_2 J)\, b_\nu(\bar{\pi} L + 1)]\, P_\nu(\cos\theta)\,.$$

2·4. *Limiting cases.* – In this Section we consider limiting cases which serve partially as a check on the results and partially as an aid in the interpretation of them. It is not intended that the limiting values be used as an accurate representation of experimental data. However these values can be useful in extrapolating the numerical results.

2·4.1. The high energy limit (Casimir limit). – When $E \to \infty$ the electronic matrix elements approach the limiting values

$$\mathscr{E}_k(\pi L) \xrightarrow[E\to\infty]{} \text{const.} \frac{(-i)^{L+1}}{[L(L+1)]^{\frac{1}{2}}} \begin{cases} \varkappa - 1\,, & \text{for } \pi = M \\ -i(\varkappa+1)\,, & \text{for } \pi = E. \end{cases} \tag{25}$$

Let $\varkappa_\pi(k)$ be the value of $\varkappa$ for a multipole of character π when k is given. Since

$$\varkappa_E(k) = -\varkappa_M(k) \tag{25a}$$

one may write, using σ defined in eq. (19),

$$\mathscr{E}_k(\pi L) \xrightarrow[E\to\infty]{} \text{const.} \frac{(-i)^{L+1-\sigma}}{[L(L+1)]^{\frac{1}{2}}} [\varkappa_M(k) - 1]\,. \tag{25b}$$

Then

$$b_\nu\ (\pi L \pi' L') \to (-)^{[L'-L+\sigma(\pi)-\sigma(\pi')]/2}\,, \tag{26a}$$

$$b_{\nu\hat{p}}(\pi L \pi' L') \to (-)^{[2+L'-L+\sigma(\pi)-\sigma(\pi')]/2}\,, \tag{26b}$$

$$b_{\nu\hat{t}_1}(\pi L \pi' L') \to 0\,, \tag{26c}$$

$$b_{\nu\hat{t}_0}(\pi L \pi' L') \to 0\,. \tag{26d}$$

Thus, all the transverse polarization vanishes at high energies and the absolute magnitude of the β- (longitudinally polarized) conversion electron correlation approaches that of the β-γ c.p. correlation ([14]). This close relation between correlations with γ rays as compared with high energy conversion electrons also holds, cf. eq. (26*a*), when no polarization is measured ([16]). In contrast, the transverse polarization out of the plane bears no such simple relation to the linear γ polarization although they arise from the same type (*i.e.* even ranks) of nuclear orientation.

2·4.2. Free electron or low Z approximation. ([5,9]) – In this limiting case the electron in the continuum is treated as a free particle and the binding in the initial state is neglected. This means that the small component, $f_{\varkappa_i}$, for the bound state is set equal to zero and the continuum functions are spherical Bessel functions. Then in eq. (8*c*) $R_4' = 0$ and in (8*d*) $R_1 = R_4 = 0$.

For magnetic multipoles

$$\mathscr{E}_k(ML) = (2L+1-k)(-)^k Z_L\,, \tag{27}$$

where

$$Z_L = 2(\alpha Z p)^{\frac{3}{2}}[\pi(E+1)\,L(L+1)]^{-\frac{1}{2}}\, i^L \int_0^\infty j_L(pr)\, h_L(Kr) r^2\,\mathrm{d}r\,, \tag{27a}$$

and $K = E - \gamma_1 \simeq E - 1$ is the transition energy. For electric multipoles

$$\mathscr{E}_{L+1}(EL) = 2(\alpha Z)^{\frac{3}{2}}[Lp(E+1)/\pi(L+1)]^{\frac{1}{2}}(-i)^{L+1}\int_0^\infty j_L(pr)\, h_L(Kr) r^2\,\mathrm{d}r\,, \tag{27b}$$

and

$$\frac{\mathscr{E}_L(EL)}{\mathscr{E}_{L+1}(EL)} = 1 - \frac{2L+1}{L}\,\frac{E-1}{E+1}\,. \tag{27c}$$

It is easily seen from the k dependence exhibited in Eq. (27) that $r_3(MLML') = r_4(MLML') = 0$. Therefore all transverse polarizations for magnetic transitions vanish in this limit, in agreement with reference [9].

Moreover the integral which appears in eqs. (27*a*) and (27*b*) is pure imaginary. This follows from the fact that its real part is

$$\int_0^\infty j_L(pr)\, j_L(Kr) r^2\,\mathrm{d}r = \frac{\pi}{2p^2}\,\delta(p-K)\,,$$

and this vanishes since $(K \neq p)$; here $K+1 = (1+p^2)^{\frac{1}{2}}$. From this result it may be verified that $r_3(\pi L \pi' L')$ and $r_4(\pi L \pi' L')$ are real. Consequently the transverse polarization out of the plane vanishes for all types of transitions in this limit.

In contrast the limiting transverse polarization in the plane does not vanish for $EL - EL'$ or $ML - EL'$ transitions. Also the longitudinal polarizations for all cases have non-vanishing limiting values.

2·4.3. Non-relativistic limit. – Only electric multipoles will be considered. The non-relativistic limit is formally expressed by the conditions $p \ll 1$, $\alpha Z \ll 1$ (but $\alpha Z/p$ arbitrary). These imply that the small components vanish both for initial and for final states and that

$$\mathscr{E}_k(EL) = [L/(L+1)]^{\frac{1}{2}} \exp[i\delta_\varkappa] R_2\,.$$

It will be noted that in $\mathscr{E}_k(EL)$ the final state wave function enters as $\exp[i\delta_\varkappa]g_\varkappa$.

For a particular multipole, EL, the two final states with $\varkappa = L$ and $\varkappa = -L-1$ have the same value of l, namely $l = L$. Making the appropriate approximations in the radial functions of the continuum states ([20]) and using contiguous relations for the confluent hypergeometric functions one finds

$$\exp[i\delta_L]g_L = \exp[i\delta_{-L-1}]g_{-L-1}, \tag{28}$$

and consequently

$$\mathscr{E}_L(EL) = \mathscr{E}_{L+1}(EL), \tag{28a}$$

that is, the matrix elements depend only on L and not on $\varkappa$. From eqs. (18) one immediately obtains

$$r_1 = r_3 = r_4 = 0 \qquad \text{for} \quad EL\text{-}EL'. \tag{28b}$$

From eqs. (19) one concludes that all components of the polarization vanish for electric transitions in the non-relativistic limit. This result is not entirely trivial since the electron is here treated as a Pauli particle and not as a spinless particle.

2·5. *Parameters of nuclear orientation following* β*-decay.* – As discussed in Section 2·1 the diagonal density matrix of the daughter nucleus following β-decay is being described in terms of tensor parameters α_ν. Just as for the conversion link, it is convenient ([16]) to write the tensor parameters for the β-decay link as products of an F-function and a « particle parameter ». For a β-transition involving multipole orders L_1 and L_1' one may write

$$\alpha_\nu(L_1L_1') = (2\nu+1)^{\frac{1}{2}} F_\nu(L_1L_1'J_1J)b_\nu(L_1L_1'). \tag{29}$$

One may measure in coincidence with the conversion electron either the β-particle or the recoiling nucleus. Particle parameters for these cases will be discussed separately.

2·5.1. Coincidences with the β-particle. – β-particle parameters with the normalization of eq. (29) have been given by ALDER, STECH and

([20]) M. E. ROSE: *Phys. Rev.*, **51**, 484 (1937).

WINTER ([14]) for the S, T, and P interactions (*). A more extensive list of β-particle parameters with different normalization has been worked out by MORITA and MORITA ([21]). The latter parameters are given to higher order approximation in the Coulomb field than are those of reference ([14]). In terms of the Moritas' parameters, which we shall denote $b^{\nu}_{L_1L_1'}$, one would have (in the present notation)

$$\alpha_\nu(L_1L_1') = \tfrac{1}{4}(-)^{J_1-J}(2\nu+1)^{\frac{1}{2}}(2J+1)^{\frac{1}{2}}W(JJL_1L_1';\,\nu J_1)b^{\nu}_{L_1L_1'}. \tag{30}$$

The connection between the two sets of parameters is

$$b^{\nu}_{L_1L_1'} = -4\,(2L_1+1)(2L_1'+1)]^{\frac{1}{2}}C(L_1L_1'\nu;\,1,\,-1)b_\nu(L_1L_1'). \tag{30a}$$

For allowed transitions involving $\beta^{\pm}$-particles of speed v one has ([22])

$$\frac{\alpha_1}{\alpha_0} = [J(J+1)]^{\frac{1}{2}}\frac{v}{c}\xi^{-1}\Big\{\mp(\beta_{AA}-\beta_{TT})\lambda_{J_1J}|M_{GT}|^2 + \\ + \delta_{J_1J}\,2\,\mathrm{Re}\,[(\beta_{ST}-\beta_{VA})\,M_FM_{GT}^*/[J_1(J_1+1)]^{\frac{1}{2}}]\Big\}, \tag{31}$$

with

$$\beta_{XY} = C_XC_Y'^* + C_X'C_Y^*, \qquad (X, Y = S, T, P, A, V), \tag{31a}$$

$$\lambda_{J_1J} = (-)^{J_1-J}[6(2J+1)/J(J+1)]\,W(JJ11;\,1J_1) \\ = [J(J+1) - J_1(J_1+1) + 2]/2J(J+1),$$

$$= \begin{cases} (J_1+1)^{-1}, & J = J_1+1 \\ J_1(J_1+1)^{-1}, & J = J_1 \\ -J_1^{-1}, & J = J_1-1 \end{cases} \tag{31b}$$

and

$$\xi = (\alpha_{SS}+\alpha_{VV})|M_F|^2 + (\alpha_{TT}+\alpha_{AA})|M_{GT}|^2 \tag{31c}$$

with

$$\alpha_{XY} = C_XC_Y^* + C_X'C_Y'^*. \tag{31d}$$

(*) Note that in reference ([14]) L and L' pertain to the β transition and λ and λ' refer to the γ transition. Also the tensor rank is k instead of ν.

([21]) M. MORITA and R. S. MORITA: *Phys. Rev.*, **107**, 1316 (1957) (allowed transitions), **109**, 2048 (1958) (first forbidden transitions). The tensor rank is denoted by n, L and L' refer to the β transition, and L_1 and L_1' refer to the γ-transition.

([22]) See, for example, the article by C. S. WU in the *Proceedings of the Rehovoth Conference on Nuclear Structure*, ed. by H. LIPKIN (Amsterdam, 1957).

For first forbidden transitions the rather complete results of MORITA and MORITA ([21]) may be used. In the case of the first forbidden unique transitions ($L_1 = L_1' = 2$; $\Delta J = 2$, yes), assuming pure axial vector for the Gamow-Teller part of the coupling we have independently obtained the following results, in agreement with MORITA and MORITA when one neglects their Coulomb corrections (which are small for unique transitions):

$$\frac{\alpha_1(A)}{\alpha_0(A)} = \frac{1}{4}\frac{\beta_{AA}}{\alpha_{AA}}\frac{J(J+1) - J_1(J_1+1) + 6}{[J(J+1)]^{\frac{1}{2}}} B_1(W)\,, \tag{32a}$$

$$\frac{\alpha_2(A)}{\alpha_0(A)} = -\frac{1}{4}\frac{A'(A'+1) - 8J(J+1)}{[J(J+1)(2J-1)(2J+3)]^{\frac{1}{2}}} B_2(W)\,, \tag{32b}$$

with $A' = J_1(J_1+1) - J(J+1) - 6$;

$$\frac{\alpha_3(A)}{\alpha_0(A)} = \frac{3}{5}\frac{\beta_{AA}}{\alpha_{AA}}\left\{\left[\frac{(2J-1)(J-1)J}{(J+1)(J+2)(2J+3)}\right]^{\frac{1}{2}}\delta_{J_1,J+2} - \left[\frac{(J+1)(J+2)(2J+3)}{(2J-1)(J-1)J}\right]^{\frac{1}{2}}\delta_{J_1,J-2}\right\} B_3(W)\,. \tag{32c}$$

Here α and β have been defined above and

$$\begin{cases} B_1(W) = \dfrac{p_1}{W}\dfrac{\frac{3}{5}p_1^2 + q^2}{p_1^2 + q^2}\,, \\ B_2(W) = p_1^2/p_1^2 + q^2)\,, \\ B_3(W) = \dfrac{p_1}{W}\dfrac{p_1^2}{p_1^2 + q^2}\,, \end{cases} \tag{32d}$$

where p_1 and q are the momenta of the β-particle and neutrino, respectively, and W is the total energy (including the rest energy) of the β.

2·5.2. Coincidences with the recoiling nucleus. – Of course, in the case of β-decay it is much more difficult to measure the direction of the recoiling nucleus than it is to measure the direction of the β-particle. However, in the case of electron capture it is of interest to consider the recoil measurement. Expressions for the orientation of the recoil nucleus following allowed K-capture have been given by TREIMAN ([3]) and by FRAUENFELDER, JACKSON, and WYLD ([4]). These authors have also given the orientation of the recoil nucleus following allowed β-decay and have pointed out how, in general, one may obtain the recoil orientation by a reinterpretation of the expression for the distribution of the direction of recoils from initially oriented nuclei.

The recoil orientation parameter, which we denote by $(\alpha_1/\alpha_0)_r$, for allowed K capture in the approximation $\alpha Z \ll 1$ is [3]

$$\left(\frac{\alpha_1}{\alpha_0}\right)_r = [J(J+1)]^{\frac{1}{2}}\left(\frac{a_1}{a_0}\right)_r = -[J(J+1)]^{\frac{1}{2}}\frac{B_-}{(1+b)J}, \tag{33}$$

where

$$\xi B_-/J = (\beta_{TT}+\beta_{AA}+2\,\mathrm{Re}\,\beta_{TA})\lambda_{J_1J}|M_{GT}|^2 - \\ -\delta_{J_1J}[J(J+1)]^{-\frac{1}{2}}2\,\mathrm{Re}\,[(\beta_{SA}+\beta_{VT}+\beta_{VA}+\beta_{ST})M_F M_{GT}^*], \tag{33a}$$

$$\xi b = 2\,\mathrm{Re}\,[\alpha_{TA}|M_{GT}|^2+\alpha_{SV}|M_F|^2], \tag{33b}$$

with λ_{J_1J} and ξ as given in eqs. (31*b*) and (31*c*).

Assuming the maximum parity non-conservation in β-decay implies (in the conventional notation [22])

$$C_V' = C_V, \quad C_A' = C_A, \quad C_S' = -C_S, \quad C_T' = -C_T \qquad \text{(and hence } b=0\text{)}$$

which is predicted by the two component neutrino theory. In this case [4]

$$\left(\frac{\alpha_1}{\alpha_0}\right)_r = -[J(J+1)]^{\frac{1}{2}}\xi^{-1}\,2\,\mathrm{Re}\{(|C_A|^2-|C_T|^2)\lambda_{J_1J}|M_{GT}|^2 + \\ +\delta_{J_1J}[J(J+1)]^{-\frac{1}{2}}2(C_S C_T^* - C_V C_A^*)M_F M_{GT}^*\}. \tag{34}$$

It is pointed out in reference [1] that because $|C_T|^2$ and $|C_A|^2$ enter in Eq. (34) with opposite signs the measurement of the recoil polarization is a test of whether the GT interaction is predominantly A or T. It is not, unfortunately, a sensitive way of detecting the presence of a small admixture of T along with the predominating A.

3. – Numerical results.

As indicated above the numerical results are based on values of conversion matrix elements for the unscreened K-electron in the field of a point nucleus [7]. The results presented below are conveniently divided into two groups.

In the first we give the particle parameters $b_{\nu\hat{q}}$ for longitudinal and in-the-plane transverse polarization. These depend on the properties of the conversion transition and are independent of the detailed description of the β-transition. These particle parameters for the polarization may therefore be used for any β-transition, allowed or forbidden. For each decay scheme particle parameters for the β-transition can be worked out and this has been done

here (see Section 2·5) for allowed and unique first forbidden transitions. Other cases appear elsewhere in the literature ([21]). The polarization is then obtained by inserting the particle parameters into eqs. (24)–(24*c*). In Figs. 1-8 the particle parameters have been given as a function of K, the transition energy in mc^2 units, and for various values of Z. Only dipole and quadrupole transitions are calculated for reasons discussed below. In Figs. 9-12 the particle parameters for the interference terms between electric and magnetic multipoles are given. Again, only dipole-quadrupole mixtures are considered since other mixtures are rare. For forbidden transitions we need $b_{3\hat{p}}$ and $b_{3\hat{t}_i}$. For pure multipoles these are obtained from $b_{1\hat{p}}$ and $b_{1\hat{t}_i}$. The same is true for $b_{3\hat{p}}$ for mixed multipoles. For $b_{3\hat{t}_i}$ the results are shown in Figs. 13 and 14.

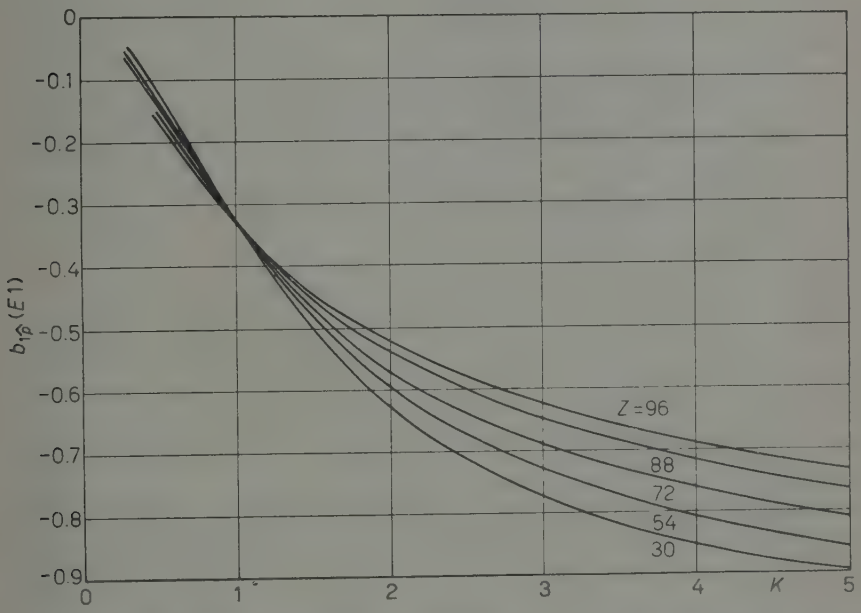

Fig. 1. – The longitudinal polarization parameter $b_{1\hat{p}}$ for conversion electrons emitted in pure $E1$ transitions as a function of transition energy K (in mc^2 units). Each curve is labelled with the value of Z.

In the second group of curves we have selected particular decay schemes and have given the actual polarization to be expected in various cases. In selecting the specific examples presented below we have kept in mind a number of practical considerations:

a) The lifetime of the intermediate state must be short, preferably not longer than 10^{-9} s. This is to avoid attenuation of the correlation by depolar-

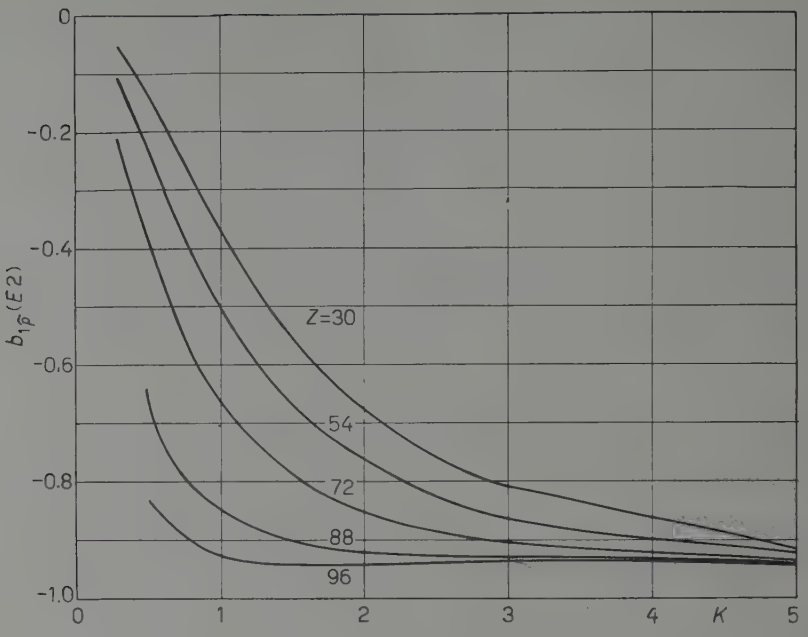

Fig. 2. – The same as Fig. 1 but for $E2$ transitions.

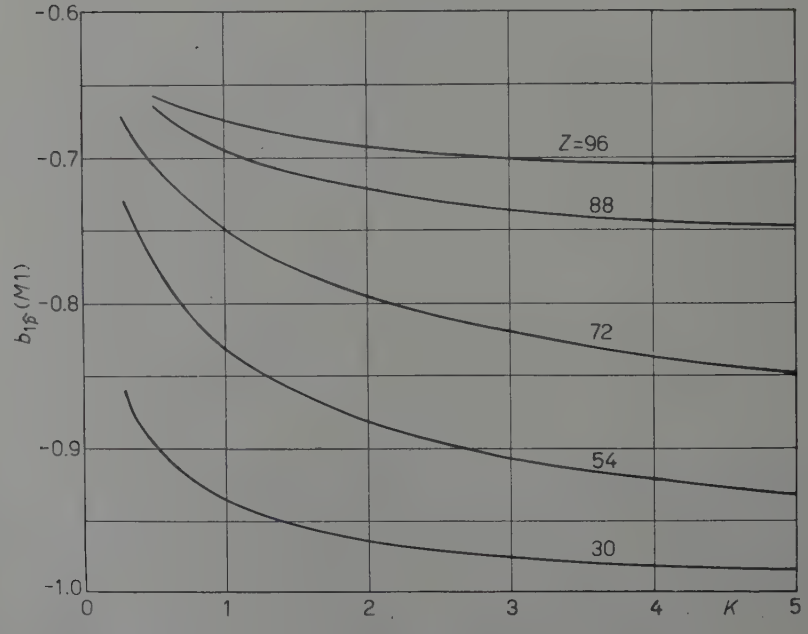

Fig. 3. – The same as Fig. 1 but for $M1$ transitions.

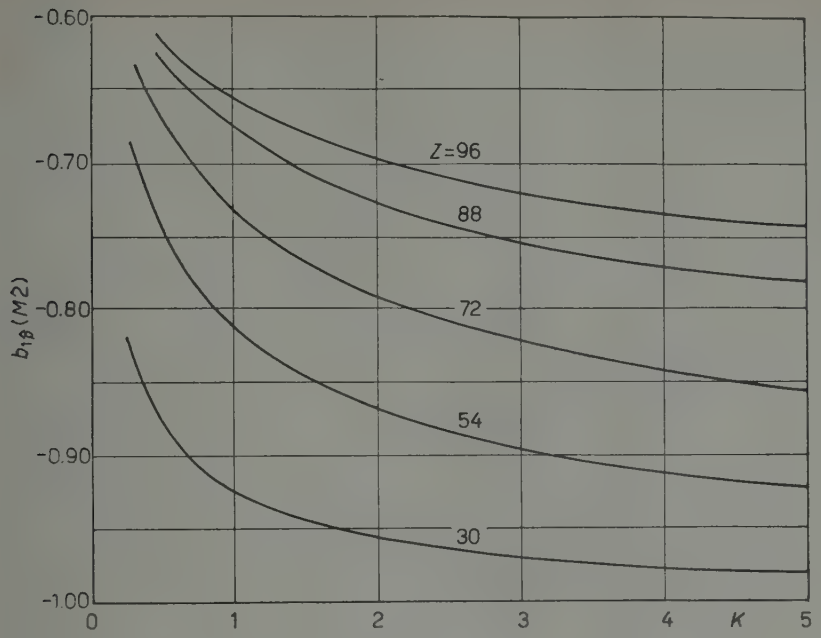

Fig. 4. – The same as Fig. 1 but for $M2$ transitions.

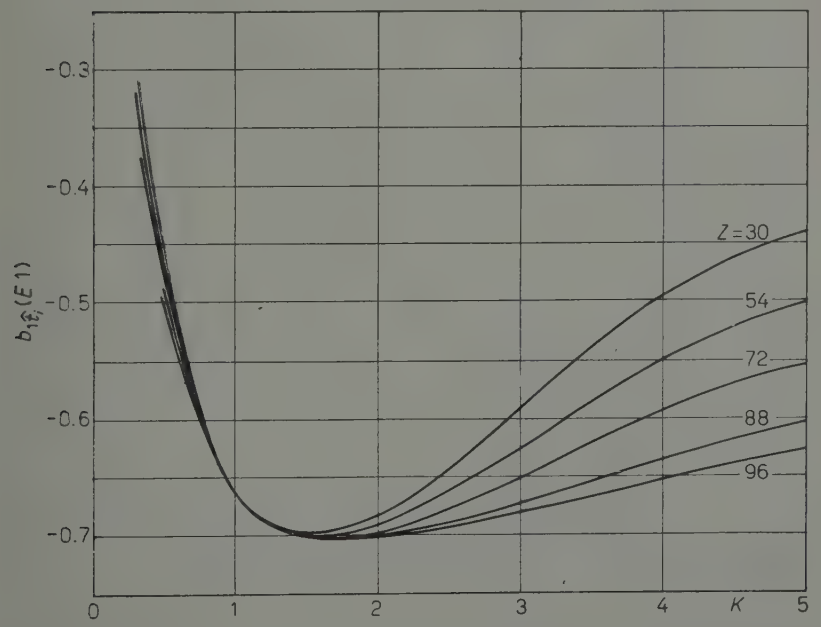

Fig. 5. – The polarization parameter $b_{1\hat{t}_i}$ for in-the-plane transverse polarization for conversion electrons emitted in pure $E1$ transitions as a function of the transition energy K (in mc^2 units). Each curve is labelled with the value of Z.

ization due to spin-coupling. It is for this reason that we have not presented results for octupole and higher transitions.

b) The conversion coefficient should not be too small, preferably 10^{-3} at least.

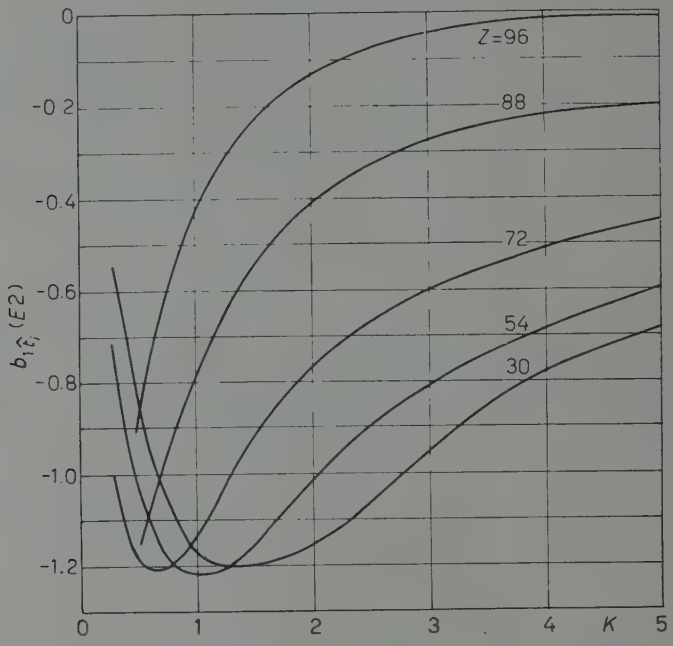

Fig. 6. – The same as Fig. 5 but for $E2$ transitions.

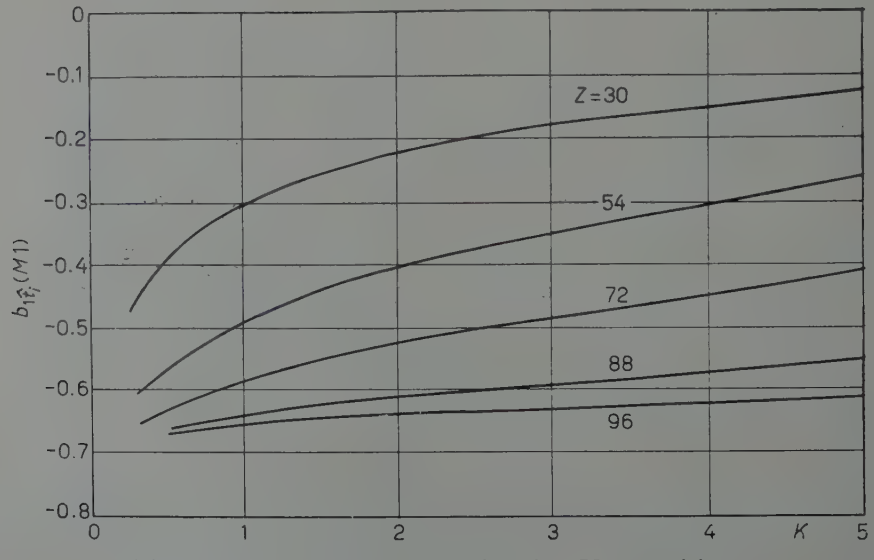

Fig. 7. – The same as Fig. 5 but for $M1$ transitions.

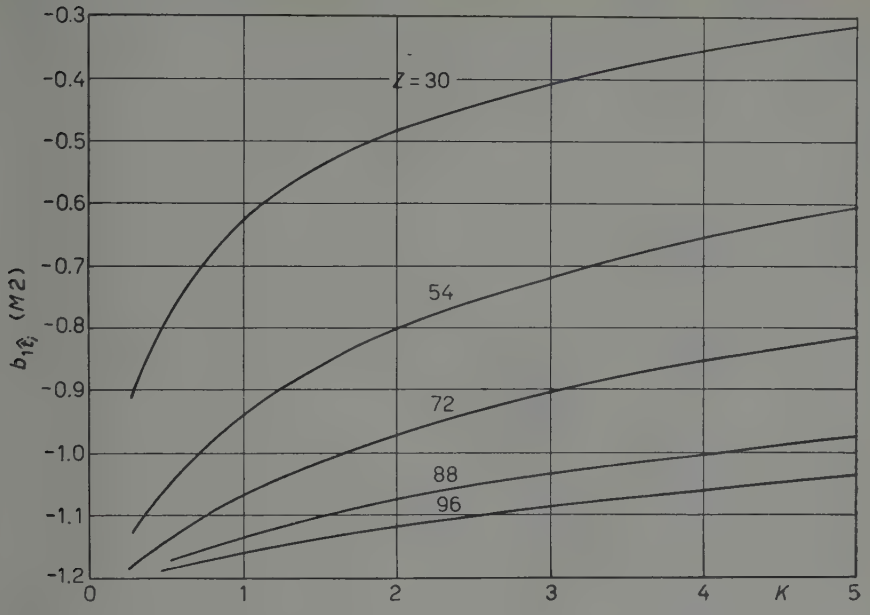

Fig. 8. – The same as Fig. 5 but for $M2$ transitions.

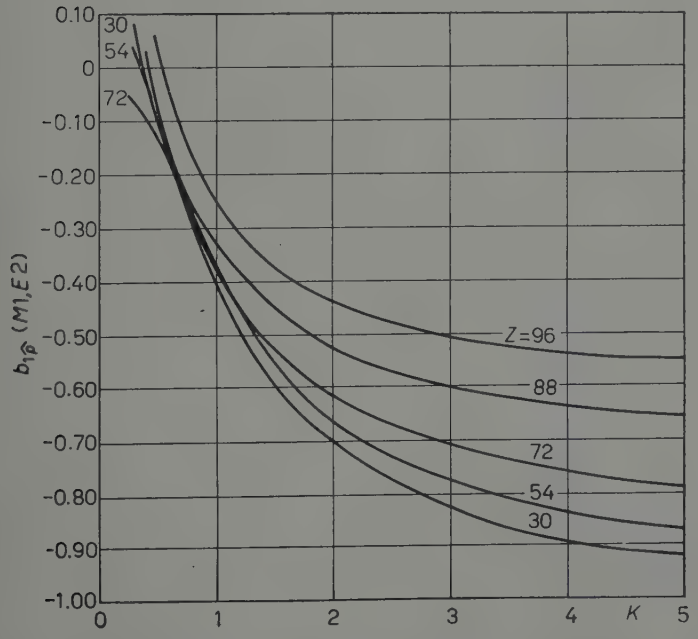

Fig. 9. – The polarization parameter $b_{1\hat{p}}$ for longitudinal polarization in mixed $M1$-$E2$ transitions as a function of K, the transition energy in mc^2 units. This parameter is used in the interference term, see eqs. (24).

c) Condition *b*) is best fulfilled for low energy conversion electrons but this clearly leads to difficulties unless very thin sources can be used and, in that case, the intensity of observed particles may become prohibitively small. We have not considered transitions wherein the conversion energy is less than 50 keV.

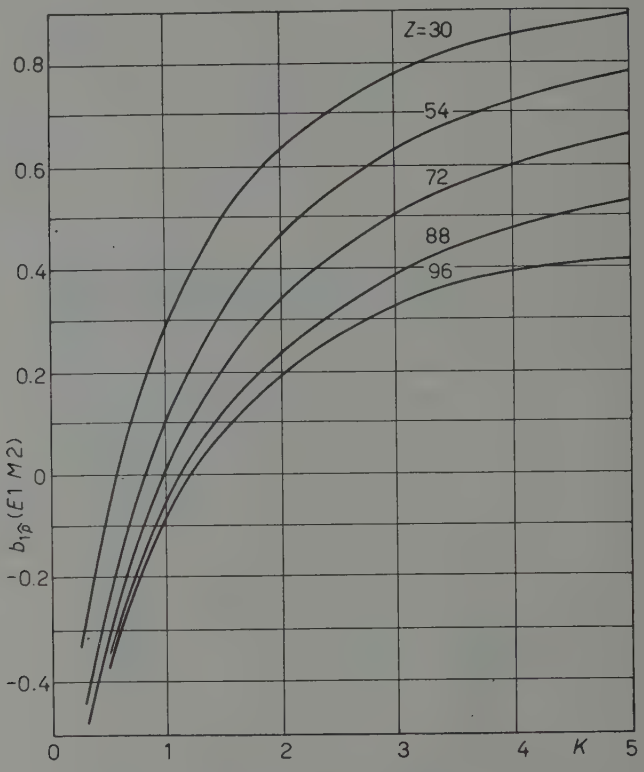

Fig. 10. – The same as Fig. 9 but for $E1$-$M2$ mixed transitions.

d) The branching ratio to the excited state of the converting nucleus should not be negligibly small. In the case of (unique) forbidden transitions it has not been possible to find, among the known decay schemes, a β-c.e. branch which satisfies the above conditions, and some compromise with these requirements is necessary. In that case we have felt it preferable to consider transitions with a low branching ratio (^{144}Pr) rather than one with a favorable branching ratio but very small conversion electron energy (*e.g.* ^{166}Ho).

e) For the complete analysis of possible experimental results it is certainly desirable that the nuclear spins of all levels involved be known.

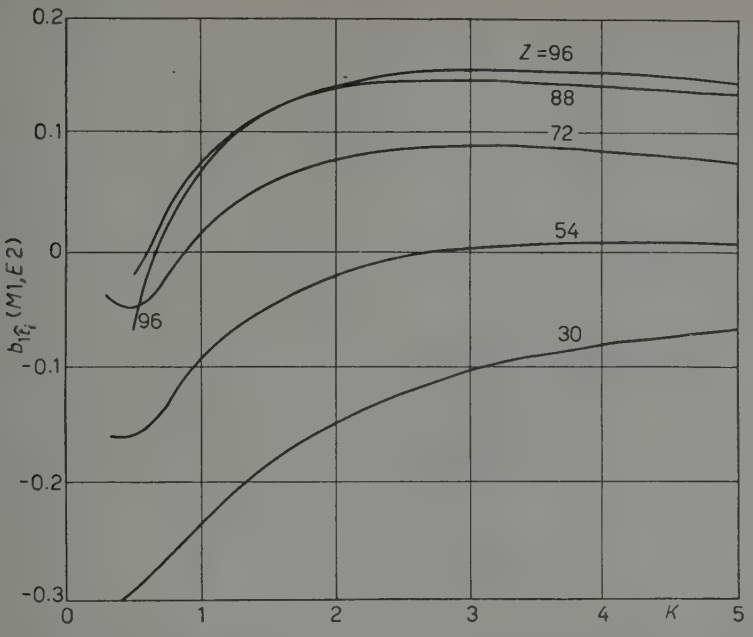

Fig. 11. – The polarization parameter $b_{1\hat{t}_i}$ for transverse in-the-plane polarization in mixed $M1$-$E2$ transitions as a function of K, the transition energy in mc^2 units cf. eqs. (24).

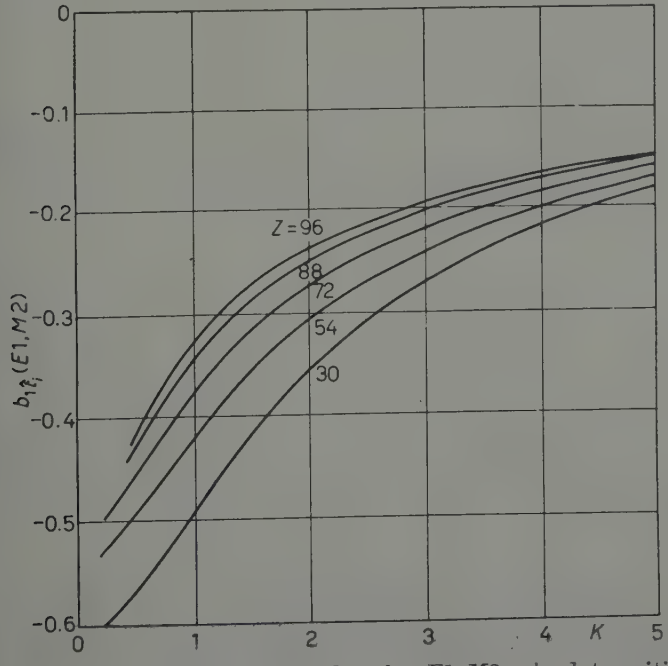

Fig. 12. – The same as Fig. 11 but for $E1$-$M2$ mixed transitions.

f) It is also desirable that the degree of forbiddenness of the β-transition be reasonably well-established.

g) The β half life must be conveniently long.

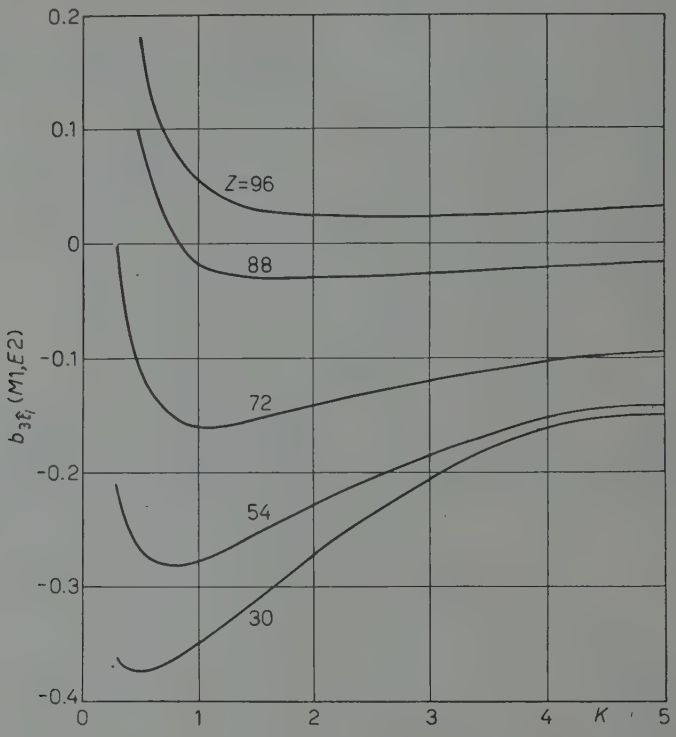

Fig. 13. – The polarization parameter $b_{3\hat{t}_i}$ for transverse in-the-plane polarization in mixed $M1$-$E2$ transitions as a function of K.

Among the allowed transitions ^{131}I (8.1 days) seems to meet all of the above requirements. There are two interesting transitions in the ^{131}Xe daughter following an 87.2 percent β branch ([23]). The lifetime of the converting state is about $2 \cdot 10^{-11}$ s and the transition energies are 364 keV to ground and 284 keV to the first excited state (*). The former transition, which is more suitable on intensity considerations, is an $M1$-$E2$ mixture but the mixture parameter δ or $\bar{\delta}$ is not known accurately. In Fig. 15 we have plotted the

([23]) All decay scheme data are quoted from the compilation of STROMINGER, HOLLANDER and SEABORG: *University of California Radiation Laboratory Report* UCRL-1928.

(*) Calculated polarizations for the 284 keV transition have been given in our previous communication, reference ([6]).

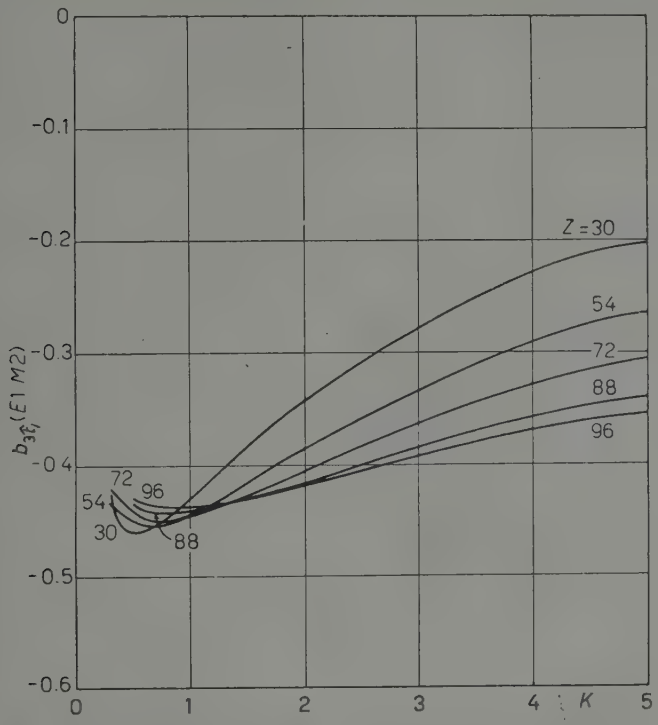

Fig. 14. – The same as Fig. 13 but for $E1$-$M2$ transitions.

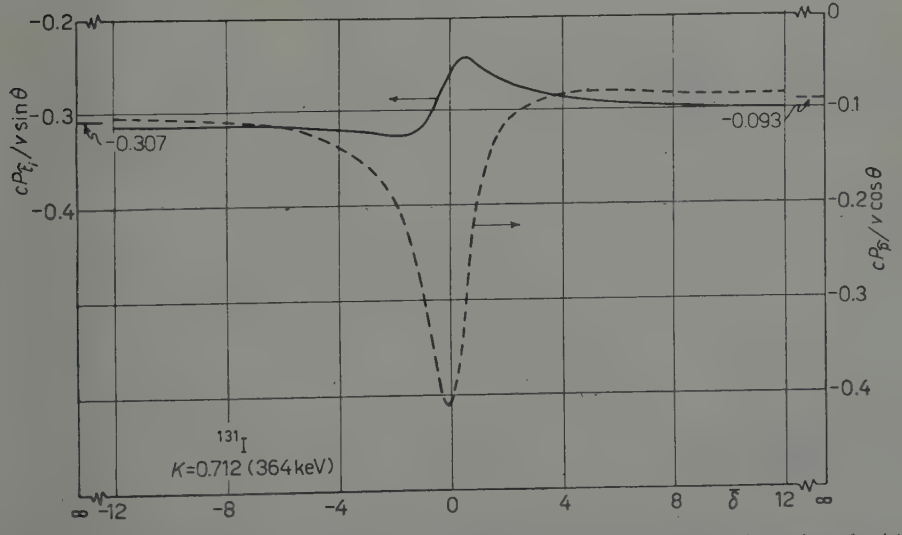

Fig. 15. – The maximum longitudinal and transverse polarizations (in units of v/c) of the conversion electrons in the 364 keV transition in ^{131}I versus $\bar{\delta}$. The ratio of $E2$ to $M1$ intensities of conversion electrons is $\bar{\delta}^2$. The short horizontal strokes represent the polarization in the limits $\bar{\delta} \to \pm\infty$.

2787

calculated polarizations, longitudinal and in-the-plane transverse, for the 364 keV transition as a function of $\bar{\delta}$. It is seen that these polarizations are quite appreciable. In the absence of information on $\bar{\delta}$ a polarization measurement could fix the value of this parameter. For an almost pure $M1$ transition this method of determining $\bar{\delta}$ would be expecially sensitive.

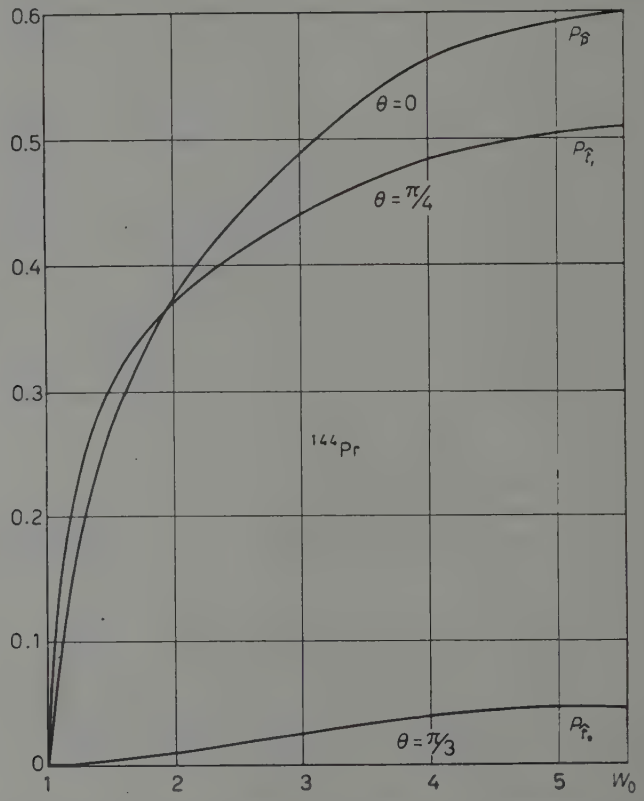

Fig. 16. – Longitudinal and two types of transverse polarization for the conversion electrons following the unique first forbidden ^{144}Pr β-decay. The abscissa is the β-energy (including rest energy) and the angle between β and conversion electron labels each curve.

The 47 day ^{203}Hg transition is also interesting but it is almost certainly first-forbidden non-unique. Values of the polarization parameters can be obtained from the $M1$-$E2$ curves given here. The actual polarization depends on the values of the first forbidden matrix elements.

Among the unique first forbidden transitions leading to an excited state the 0^- to 2^+ transition in 24 m ^{144}Pr (in equilibrium with 285 day ^{144}Ce) has been considered. While the branching ratio to the 694 keV state is small the coincidence observation eliminates all but accidental coincidences with the main ground state group of β-particles. In Fig. 16 the results for all three

polarizations are shown. The results for the polarization are plotted as a function of β-particle energy W at angles θ for which the maximum effects would be observed. While the longitudinal and in-the-plane transverse polarizations are quite large, the out-of-plane polarization is so small as to make this measurement of doubtful interest.

The out-of-plane polarization has also been calculated for the transition to the 1.853 MeV state of 104 day ^{88}Y. However, it is only about 1 percent at maximum. As mentioned, the transition in 27 hour ^{166}Ho to the first excited state 2^+ is also first forbidden unique and has a branching ratio of about 0.37. However, the $E2$ transition following β-decay is only 80 keV. The out-of-plane polarization would be larger for the heavy nuclei but there is no clear cut evidence for a forbidden unique transition leading to an excited state among these emitters. There are a few transitions leading to K-conversion but these have not been treated numerically because of the scarcity of data on nuclear spins and radiative half-lives.

* * *

We wish to acknowledge the computational help of Mr. C. P. Bhalla, Mr. P. Haigh and Mr. H. Owens.

Appendix A

Evaluation of $I_\nu(\theta)$. The quantity $I_\nu(\theta; \pi L \pi' L')$ is defined in Eq. (9*b*). If we insert Eq. (9*c*) the following sum over magnetic quantum numbers occurs:

$$S(LL'\lambda\nu) = \sum_{M\mu\mu_i} C(J\nu J;\, M0)\, C(JLJ_2;\, M,\, \mu_i - \mu)\, C(JL'J_2;\, M,\, \mu_i - \mu) \cdot C(Lj_i j;\, \mu - \mu_i,\, \mu_i)\, C(L'j_i j';\, \mu - \mu_i,\, \mu_i)\, C(\lambda j' j;\, 0\mu)\,. \tag{A.1}$$

This is readily done by standard methods, giving

$$S(LL'\lambda\nu) = \delta_{\lambda\nu}(-)^{J-J_2+L+L'+j_i-j-\nu}(2\nu+1)^{-1}(2J_2+1)(2j+1) \cdot [(2J+1)(2j'+1)]^{\frac{1}{2}}\, W(JJLL';\, \nu J_2)\, W(jLj'L';\, j_i\nu)\,. \tag{A.2}$$

As λ is restricted to even values, $I_\nu(\theta; \pi L \pi' L')$ vanishes except for even ν. Using $Y^0_\nu(\hat{\mathbf{r}}) = [(2\nu+1)/4\pi]^{\frac{1}{2}}\, P_\nu(\cos\theta)$ and $j_i = \frac{1}{2}$, one obtains

$$I_\nu(\theta; \pi L \pi' L') = (-)^{J-J_2+L+L'}(E/\pi p)(2J_2+1)(2J+1)^{\frac{1}{2}}\, W(JJLL';\, \nu J_2) \cdot P_\nu(\cos\theta)\, \mathrm{Re} \sum_{\varkappa\varkappa'} H_\nu(\varkappa, \varkappa';\, \pi L \pi' L')\, \mathscr{E}_\varkappa(\pi L)\, \mathscr{E}^*_{\varkappa'}(\pi' L')\,. \tag{A.3}$$

Here $H_\nu(\varkappa, \varkappa'; \pi L \pi' L')$ is a «geometrical» function which will be needed for odd ν in later applications (Appendix B) as well as for even ν in the present application. To unify the two cases we introduce

$$\text{(A.4)} \qquad \tilde{\varkappa} = \begin{cases} \varkappa, & \nu \text{ even} \\ -\varkappa, & \nu \text{ odd} \end{cases}, \qquad \tilde{l} = l_{\tilde{\varkappa}} = \begin{cases} l, & \nu \text{ even} \\ \bar{l}, & \nu \text{ odd} \end{cases}.$$

Then

$$\text{(A-4}a\text{)} \quad H_\nu(\tilde{\varkappa}, \varkappa'; \pi L \pi' L') = (-)^{l'} (2j+1)(2j'+1)(2l'+1)^{\frac{1}{2}} C(\nu l' \tilde{l}; 00) \cdot W(jLj'L'; \tfrac{1}{2}\nu)\, W(j\tilde{l}j'l'; \tfrac{1}{2}\nu)\,.$$

Symmetry properties of the H function. It will be useful at this point to develop some symmetry properties of the H function. These are obtained from the relation, valid for any ν,

$$\text{(A.5)} \qquad [(2\tilde{l}+1)(2l'+1)]^{\frac{1}{2}} C(\tilde{l} l' \nu; 00)\, W(j\tilde{l}j'l'; \tfrac{1}{2}\nu) = C(jj'\nu; \tfrac{1}{2}, -\tfrac{1}{2})\,.$$

In (A.5) it is necessary that $\tilde{l} + l' + \nu$ be even. This relation may be derived as follows: starting with the Racah recoupling relation

$$C(\tilde{l}\tfrac{1}{2}j; 0\mu)\, C(l'\tfrac{1}{2}j'; 0\mu) = (-)^{j+j'+\tilde{l}+l'+\mu+\frac{1}{2}} \cdot [(2j+1)(2j'+1)]^{\frac{1}{2}} \sum_f C(\tilde{l} l' f; 00)\, C(jj'f; \mu, -\mu)\, W(j\tilde{l}j'l'; \tfrac{1}{2}f)\,,$$

we multiply both sides by $(-)^{\mu+\frac{1}{2}} C(jj'\nu; \mu, -\mu)$ and sum over μ. The left hand side becomes

$$2(-)^{\tilde{l}+l'+j+j'} \left[\frac{(j+\frac{1}{2})(j'+\frac{1}{2})}{(2\tilde{l}+1)(2l'+1)}\right]^{\frac{1}{2}} C(jj'\nu; \tfrac{1}{2}, -\tfrac{1}{2})\,.$$

Equating this to the right hand side gives (A.5). From (A.4a) and (A.5)

$$\text{(A.6)} \qquad H_\nu(\tilde{\varkappa}, \varkappa'; \pi L \pi' L') = (2\nu+1)^{-\frac{1}{2}} (2j+1)(2j'+1)\, C(jj'\nu; \tfrac{1}{2}, -\tfrac{1}{2}) W(jLj'L'; \tfrac{1}{2}\nu)\,.$$

Therefore, for any $\pi L \pi' L'$,

$$\text{(A.7)} \qquad H_\nu(\tilde{\varkappa}, \varkappa') = H_\nu(-\tilde{\varkappa}, -\varkappa') = H_\nu(\varkappa', \tilde{\varkappa}) = H_\nu(-\varkappa', -\tilde{\varkappa})\,.$$

These symmetry properties imply that H_ν has the same value for an ML-ML' transition as for an EL-EL' transition, and has the same value for an EL-ML' transition as for an ML-EL' transition.

Evaluation of the H function. It is convenient to express $I_\nu(\theta; \pi L \pi' L')$ in terms of the well known F-coefficient ([16,15]), see eq. (9g), which contains $C(LL'\nu; 1, -1)$. Referring to Table I it is seen that l and l' can be expressed

in terms of L, $L\pm1$ and L', $L'\pm1$. Taking $\pi'=E$ only $l'=L'$ is needed. The case $\pi'=M$ follows from the symmetry relations of H_ν. We use the well known relation [16]

$$C(\tilde{l}L'\nu;\,00)=\frac{-2[L(L+1)\,L'\,(L'+1)]^{\frac{1}{2}}}{\beta_\nu(\tilde{l}LL')}\,C(LL'\nu;\,1,\,-1)\,, \tag{A.8}$$

with

$$\beta_\nu(\tilde{l}LL')=\begin{cases} L(L+1)+L'(L'+1)-\nu(\nu+1), & \tilde{l}=L \\ -[(\nu+L+L'+1)(L+L'-\nu)(L-L'+\nu)(\nu-L+L'+1)]^{\frac{1}{2}}, & \tilde{l}=L-1, \\ [(\nu+L+L'+2)(\nu+L-L'+1)(L+L'-\nu+1)(\nu-L+L')]^{\frac{1}{2}}, & \tilde{l}=L+1). \end{cases} \tag{A.8a}$$

Substituting eq. (A.8) in eq. (A.4a), we have

$$H_\nu(\tilde{\varkappa}\varkappa';\,\pi L\pi'L')=-2\left[\frac{L(L+1)\,L'(L'+1)}{(2L+1)(2L'+1)(2\nu+1)}\right]^{\frac{1}{2}}C(LL'\nu;\,1,\,-1)\cdot \cdot U_\nu(\tilde{\varkappa}\varkappa';\,\pi L\pi'\,L')\,. \tag{A.8b}$$

where

$$U_\nu(\tilde{\varkappa}\varkappa';\,\pi L\pi'L')=[(2L+1)(2\tilde{l}+1)]^{\frac{1}{2}}\,(2L'+1)(2j+1)(2j'+1)\cdot \cdot\beta_\nu^{-1}(\tilde{l}LL')\,W(jLj'L';\,\tfrac{1}{2}\nu)\,W(jlj'l';\,\tfrac{1}{2}\nu)\,. \tag{A.8c}$$

Upon evaluation of the Racah coefficients we find the simple expressions for U_ν given in Table II.

TABLE II. – *Values of* $U_\nu(\varkappa\varkappa';\,\pi L\pi'L')$.

$L+L'-\nu$	k	k'	$\tilde{l}$	$U_\nu(\tilde{\varkappa}\varkappa';\,\pi L\pi'L')$
Even	L	L'	L	$(L+L'+\nu+1)(L+L'-\nu)/[L(L+1)+L'(L'+1)-\nu(\nu+1)]$
	$L+1$	$L'+1$	L	$(L+L'+\nu+2)(L+L'-\nu+1)/[L(L+1)+L'(L'+1)-\nu(\nu+1)]$
	L	$L'+1$	L	$(\nu-L+L'+1)(\nu+L-L')/[L(L+1)+L'(L'+1)-\nu(\nu+1)]$
	$L+1$	L'	L	$(\nu+L-L'+1)(\nu-L+L')/[L(L+1)+L'(L'+1)-\nu(\nu+1)]$
Odd	L	L'	$L-1$	-1
	L	$L'+1$	$L-1$	$+1$
	$L+1$	L'	$L+1$	$+1$
	$L+1$	$L'+1$	$L+1$	-1

If use is made of eqs. (9g), (A.8b) and Table II, Eq. (A.3) becomes

$$I_\nu(\theta;\,\pi L\pi'L')=(-)^{L+L'}\,(E/\pi p)(2J_2+1)\,F_\nu(LL'J_2J)\cdot \cdot\frac{[L(L+1)\,L'(L'+1)]^{\frac{1}{2}}}{(2L+1)(2L'+1)}\,\frac{1}{(2\nu+1)^{\frac{1}{2}}}\,M_\nu(\pi L\pi'L')\,P_\nu(\cos\theta)\,, \tag{A.9}$$

where the linear combinations of electronic matrix elements needed are: for $\pi' = \pi$

$$M_\nu(\pi L \pi L') = [L(L+1) + L'(L'+1) - \nu(\nu+1)]^{-1} \cdot \tag{A.9a}$$
$$\cdot \mathrm{Re}\,\{(L+L'+\nu+1)(L+L'-\nu)\,\mathscr{E}_L(\pi L)\,\mathscr{E}^*_{L'}(\pi L') +$$
$$+ (L+L'+\nu+2)(L+L'-\nu+1)\,\mathscr{E}_{L+1}(\pi L)\,\mathscr{E}^*_{L'+1}(\pi L') +$$
$$+ (\nu-L+L'+1)(\nu+L-L')\,\mathscr{E}_L(\pi L)\,\mathscr{E}^*_{L'+1}(\pi L') +$$
$$+ (\nu+L-L'+1)(\nu-L+L')\,\mathscr{E}_{L+1}(\pi L)\,\mathscr{E}^*_{L'}(\pi L')\}$$

and for $\pi' = \bar{\pi} \neq \pi$

$$M_\nu(\pi L \bar{\pi} L') = \mathrm{Re}\,\{-\mathscr{E}_L(\pi L)\,\mathscr{E}^*_{L'}(\bar{\pi} L') - \mathscr{E}_{L+1}(\pi L)\,\mathscr{E}^*_{L+1}(\bar{\pi} L') + \tag{A.9b}$$
$$+ \mathscr{E}_L(\pi L)\,\mathscr{E}^*_{L'+1}(\bar{\pi} L') + \mathscr{E}_{L+1}(\pi L)\,\mathscr{E}^*_{L'}(\pi L')\}\,.$$

For $\nu = 0$, $F_0(LL'J_2J) = \delta_{LL'}$. Thus,

$$I_0(\pi L) = \frac{E}{\pi p}\,\frac{2J_2+1}{2L+1}\,D_0(\pi L) \tag{A.10}$$

with

$$D_0(\pi L) = L\,|\mathscr{E}_L(\pi L)|^2 + (L+1)\,|\mathscr{E}_{L+1}(\pi L)|^2\,. \tag{A.10a}$$

The conversion electron parameters for the directional correlation defined in Eq. (9f) are seen to be

$$b_\nu(\pi L \pi' L') = (-)^{L+L'}\left[\frac{L(L+1)\,L'(L'+1)}{(2L+1)(2L'+1)}\right]^{\frac{1}{2}} \frac{M_\nu(\pi L \pi' L')}{[D_0(\pi L)\,D_0(\pi' L')]^{\frac{1}{2}}}\,. \tag{A.11}$$

Appendix B

Evaluation of $V_\nu(\theta)$. In order to derive Eq. (15a) one first performs the sum over M, μ_i, μ. One finds

$$\sum_{M\mu_i\mu} C(J\nu J;\, M0)\,C(JLJ_2;\, M,\, \mu_i-\mu)\,C(JL'J_2;\, M,\, \mu_i-\mu) \cdot \tag{B.1}$$
$$\cdot C(Lj_ij;\, \mu-\mu_i),\, \mu_i\,C(L'j_ij';\, \mu-\mu_i,\, \mu_i)\,C(1sj';\, n,\, \mu-n) \cdot$$
$$\cdot C(\lambda sj;\, n,\, \mu-n) = (-)^{J-J_2+L+L'+j+\frac{1}{2}-n}[(2J+1)/(2\nu+1)]^{\frac{1}{2}}\,(2J_2+1)(2j'+1)(2j+1) \cdot$$
$$\cdot C(\lambda 1\nu;\, n,\, -n)\,W(JJL'L;\, \nu J_2)\,W(L'j'Lj;\, \tfrac{1}{2}\nu)\,W(\lambda s\nu j';\, j1)\,.$$

The sum over n from eq. (13c) is then simply

$$\sum_n C(\lambda 1\nu;\, n,\, -n)\,\hat{\boldsymbol{\xi}}_{-n}\,Y^n_\lambda(\hat{\boldsymbol{r}}) = (-)^{\lambda+1-\nu}\boldsymbol{T}^0_{\nu\lambda}(\hat{\boldsymbol{r}})\,, \tag{B.2}$$

where the vector spherical harmonic $\boldsymbol{T}^0_{\nu\lambda}(\hat{\boldsymbol{r}})$ is defined in eq. (16). The sum over s from eq. (14) gives

$$\text{(B.3)} \qquad \sum_s (-)^{l'-s-j'}(2s+1)W(\lambda l' j\tfrac{1}{2};\, ls)W(1\tfrac{1}{2}\, j' l';\, \tfrac{1}{2}s)W(\lambda s\nu j';\, j1) = \\ = (-)^{1+\lambda+l}X(\nu j j';\, \lambda l l';\, 1\tfrac{1}{2}\tfrac{1}{2})\,.$$

Here X is the well-known X-coefficient of Fano (*). Equations (15a) and (15b) follow immediately by collecting terms.

Evaluation of the vector spherical harmonics, $\boldsymbol{T}^0_{\nu\lambda}(\boldsymbol{r})$. The spin-angular functions for spin one (vector) particles,

$$\text{(B.4)} \qquad \boldsymbol{T}^M_{\nu\lambda}(\hat{\boldsymbol{r}}) = \sum_n C(1\lambda\nu;\; M-n,\; n)\; Y^n_\lambda(\hat{\boldsymbol{r}})\hat{\boldsymbol{\xi}}_{M-n}\,,$$

simplify for the case $M=0$ to

$$\text{(B.4}a\text{)} \quad \boldsymbol{T}^0_{\nu,\nu\pm1}(\hat{\boldsymbol{r}}) = C(\nu\pm1,\, 1\;\nu;\; 1,\; -1)[\,Y^1_{\nu\pm1}(\hat{\boldsymbol{r}})\hat{\boldsymbol{\xi}}_{-1} + Y^{-1}_{\nu\pm1}(\hat{\boldsymbol{r}})\hat{\boldsymbol{\xi}}_{+1}] + \\ + C(\nu\pm1,\, 1,\; \nu;\; 00)\; Y^0_{\nu\pm1}(\hat{\boldsymbol{r}})\hat{\boldsymbol{\xi}}_0\,,$$

and

$$\text{(B.4}b\text{)} \qquad \boldsymbol{T}^0_{\nu,\nu}(\hat{\boldsymbol{r}}) = -\,C(\nu 1\nu;\; 1,\; -1)(\,Y^1_\nu(\hat{\boldsymbol{r}})\,\hat{\boldsymbol{\xi}}_{-1} - Y^{-1}_\nu(\hat{\boldsymbol{r}})\,\hat{\boldsymbol{\xi}}_1)\,.$$

Writing the spherical harmonics as

$$\text{(B.4}c\text{)} \qquad Y^m_\lambda(\hat{\boldsymbol{r}}) = \mathscr{P}^m_\lambda(\theta)\exp[im\varphi]\,,$$

with

$$\text{(B.4}d\text{)} \qquad \mathscr{P}^{-m}_\lambda(\theta) = (-)^m\,\mathscr{P}^m_\lambda(\theta)\,,$$

one sees that the vectors

$$\exp[i\varphi]\hat{\boldsymbol{\xi}}_{-1} - \exp[-i\varphi]\hat{\boldsymbol{\xi}}_1 = \sqrt{2}\,(\sin\theta\,\hat{\boldsymbol{p}} - \cos\theta\,\hat{\boldsymbol{t}}\,)$$

and

$$\hat{\boldsymbol{\xi}}_0 = \cos\theta\,\hat{\boldsymbol{p}} + \sin\theta\,\hat{\boldsymbol{t}}_i\,,$$

which enter into $\boldsymbol{T}^0_{\nu,\nu\pm1}$, are both real and lie entirely within the plane of $\hat{\boldsymbol{p}}_1$ and $\hat{\boldsymbol{p}}$. But $\boldsymbol{T}^0_{\nu,\nu}$ is proportional to

$$\exp[i\varphi]\hat{\boldsymbol{\xi}}_{-1} + \exp[-i\varphi]\boldsymbol{\xi}_1 = -\,i\sqrt{2}\,\hat{\boldsymbol{t}}_0\,,$$

which is imaginary and perpendicular to this plane. Upon evaluating the C-coefficients in (B.4a) and (B.4b), $\mathscr{P}^1_\lambda(\theta)$ with $\lambda=\nu\pm1,\nu$, and $\mathscr{P}^0_\nu(\theta)$, where

$$\text{(B.4}e\text{)} \qquad \mathscr{P}^m_\lambda(\theta) = (-)^m\left[\frac{2\lambda+1}{2\pi}\,\frac{(\lambda-m)\,!}{(\lambda+m)\,!}\right]^{\frac{1}{2}} P^m_\lambda(\cos\theta)\,,$$

(*) Cf. reference ([17]), p. 191.

and P_λ^m is an associated Legendre function, we obtain

$$\text{(B.4}f\text{)}\quad \begin{cases} \boldsymbol{T}^0_{\nu\nu}(\hat{\boldsymbol{r}}) = -\,i[(2\nu+1)/4\pi\nu(\nu+1)]^{\frac{1}{2}}\,P^1_\nu(\cos\theta)\hat{\boldsymbol{t}}_0\,, \\ \boldsymbol{T}^0_{\nu,\nu+1}(\hat{\boldsymbol{r}}) = -\,[4\pi(\nu+1)]^{-\frac{1}{2}}\{[\sin\theta\,P^1_{\nu+1}(\cos\theta)+(\nu+1)\cos\theta\,P_{\nu+1}(\cos\theta)]\hat{\boldsymbol{p}}+ \\ \qquad\qquad +[-\cos\theta\,P^1_{\nu+1}(\cos\theta)+(\nu+1)\sin\theta\,P_{\nu+1}(\cos\theta)]\hat{\boldsymbol{t}}_i\}, \\ \boldsymbol{T}^0_{\nu,\nu-1}(\hat{\boldsymbol{r}}) = (4\pi\nu)^{-\frac{1}{2}}\{[-\sin\theta\,P^1_{\nu-1}(\cos\theta)+\nu\cos\theta\,P_{\nu-1}(\cos\theta)]\hat{\boldsymbol{p}}+ \\ \qquad\qquad +[\cos\theta\,P^1_{\nu-1}(\cos\theta)+\nu\sin\theta\,P_{\nu-1}(\cos\theta)]\hat{\boldsymbol{t}}_i\}. \end{cases}$$

The recurrence relations obeyed by the associated Legendre functions allow the latter two vector spherical harmonics to be rewritten as

$$\text{(B.4}g\text{)}\qquad \boldsymbol{T}^0_{\nu,\nu+1}(\hat{\boldsymbol{r}}) = -\,[4\pi(\nu+1)]^{-\frac{1}{2}}[(\nu+1)\,P_\nu(\cos\theta)\,\hat{\boldsymbol{p}} - P^1_\nu(\cos\theta)\hat{\boldsymbol{t}}_i]$$

and

$$\text{(B.4}h\text{)}\qquad \boldsymbol{T}^0_{\nu,\nu-1}(\hat{\boldsymbol{r}}) = (4\pi\nu)^{-\frac{1}{2}}[\nu P_\nu(\cos\theta)\,\hat{\boldsymbol{p}} + P^1_\nu(\cos\theta)\hat{\boldsymbol{t}}_i]\,.$$

Evaluation of the degenerate X-coefficient. It has been shown by ROSE and BIEDENHARN [24] that

$$X(\nu jj';\,\nu ll';\,1\tfrac{1}{2}\tfrac{1}{2}) = \frac{(-)^{\nu+l+l'}\,(-)^{j+l+\frac{1}{2}}(\varkappa-\varkappa')}{[6\nu(\nu+1)(2\nu+1)]^{\frac{1}{2}}}\,W(jlj'l';\,\tfrac{1}{2}\nu)\,,$$

$$C(\nu+1,\,l',\,l;\,00)\,X(\nu jj';\,\nu+1,\,ll';\,1\tfrac{1}{2}\tfrac{1}{2}) =$$

$$= \frac{(-)^{j+l+\frac{1}{2}}(\varkappa+\varkappa'+\nu+1)}{[6(\nu+1)(2\nu+1)(2\nu+3)]^{\frac{1}{2}}}\,C(\nu l'\bar{l};\,00)\,W(j\bar{l}j'l';\,\tfrac{1}{2}\nu)\,,$$

and

$$C(\nu-1,\,l'l;\,00)\,X(\nu jj';\,\nu-1,\,ll';\,1\tfrac{1}{2}\tfrac{1}{2}) =$$

$$= \frac{(-)^{j+l+\frac{1}{2}}(\varkappa+\varkappa'-\nu)}{[6\nu(\nu+1)(2\nu-1)]^{\frac{1}{2}}}\,C(\nu l'\,\bar{l};\,00)\,W(j\bar{l}j'l';\,\tfrac{1}{2}\nu)\,.$$

These may be written in a form convenient for use in the evaluation of $\boldsymbol{V}_\nu(\theta)$, namely

$$\text{(B.5)}\qquad [(2l+1)(2l'+1)]^{\frac{1}{2}}\,(-)^l\,C(ll'\lambda;\,00)\,X(\nu jj';\,\lambda ll';\,1\tfrac{1}{2}\tfrac{1}{2}) =$$

$$= \frac{(-)^{j+\frac{1}{2}+l'}}{[6(2\nu+1)]^{\frac{1}{2}}}\,(2l'+1)^{\frac{1}{2}}\,C(\nu l'\tilde{l};\,00)\,W(j\tilde{l}j'l';\,\tfrac{1}{2}\nu)\,\xi(\lambda,\varkappa,\varkappa')\,,$$

where

$$\text{(B.5}a\text{)}\qquad \xi(\lambda,\varkappa,\varkappa') = \begin{cases} (\varkappa-\varkappa')(2\nu+1)^{\frac{1}{2}}\,[\nu(\nu+1)]^{-\frac{1}{2}}\,, & \lambda=\nu, \\ (\varkappa+\varkappa'+\nu+1)/(\nu+1)^{\frac{1}{2}}\,, & \lambda=\nu+1, \\ (\varkappa+\varkappa'-\nu)/\nu^{\frac{1}{2}}\,, & \lambda=\nu-1. \end{cases}$$

[24] M. E. ROSE and L. C. BIEDENHARN: Oak Ridge National Laboratory Report 1779 (1954), unpublished, eqs. (31*a*), (31*b*) and (31*c*).

Substituting eq. (B.5) into eq. (15*b*) gives

$$\text{(B.6)} \qquad \boldsymbol{G}_\nu(\theta;\varkappa\varkappa';\pi L\pi' L') = (-)^{\nu+l'}[(2l'+1)/6(2\nu+1)]^{\frac{1}{2}}\, C(\nu l'\tilde{l};\,00)\cdot \cdot W(j\tilde{l}j'l';\,\tfrac{1}{2}\nu)\sum_{\lambda}\xi(\lambda,\tilde{\varkappa},\varkappa')\,\boldsymbol{T}^0_{\nu\lambda}(\hat{\boldsymbol{r}})\,.$$

The values of $\xi(\lambda,\tilde{\varkappa},\varkappa')$ are available in eq. (B.5*a*), and those of $\boldsymbol{T}^0_{\nu\lambda}(\hat{\boldsymbol{r}})$ in (B.4 *f-h*). With these substitutions, eq. (B.6) becomes, for ν even,

$$\text{(B.6}a\text{)} \qquad \boldsymbol{G}_\nu(\theta;\varkappa\varkappa';\pi L\pi' L') = i\,\frac{(-)^{\nu+1+l'}}{\nu(\nu+1)}\left[\frac{(2\nu+1)(2l'+1)}{24\pi}\right]^{\frac{1}{2}}(\varkappa-\varkappa')\cdot \cdot C(\nu l'l;\,00)\,W(jlj'l';\,\tfrac{1}{2}\nu)\,P^1_\nu(\cos\theta)\,\hat{\boldsymbol{t}}_0\,,$$

and for ν odd

$$\text{(B.6}b\text{)} \qquad \boldsymbol{G}_\nu(\theta;\varkappa\varkappa';\pi L\pi' L') = \frac{(-)^{\nu+l'}}{\nu(\nu+1)}\left[\frac{(2\nu+1)(2l'+1)}{24\pi}\right]^{\frac{1}{2}}\cdot \cdot C(\nu l'\bar{l};\,00)\,W(j\bar{l}j'l';\,\tfrac{1}{2}\nu)\left\{-\nu(\nu+1)\,P_\nu(\cos\theta)\,\hat{\boldsymbol{p}} + (\varkappa+\varkappa')\,P^1_\nu(\cos\theta)\hat{\boldsymbol{t}}\right\}.$$

We transform (B.6*b*) by Eq. (A.5). This demonstrates that the longitudinal component of $\boldsymbol{G}_\nu$ is invariant under the transformation $\varkappa,\ \varkappa'\to-\varkappa,\ -\varkappa'$ whereas the transverse component changes sign. Reference to eq. (12) shows that

$$\text{(B.6}c\text{)} \qquad \boldsymbol{G}_\nu(-\varkappa,-\varkappa')\cdot\overleftrightarrow{\boldsymbol{D}} = \boldsymbol{G}_\nu(\varkappa,\varkappa')\,.$$

Using the symbols $\hat{\boldsymbol{q}}$ and q introduced in eq. (15*d*) and designating the polarization components separately by writing

$$\text{(B.7)} \qquad \boldsymbol{V}_\nu(\theta;\pi L\pi' L') = \sum_{\hat{q}}\hat{\boldsymbol{q}}\,V_{\nu\hat{q}}(\theta;\pi L\pi' L')$$

the components of $\boldsymbol{V}_\nu$ in (15*a*) reduce to

$$\text{(B.7}a\text{)} \qquad V_{\nu\hat{q}}(\theta;\pi L\pi' L') = (-)^{J-J_2+L+L'+1}(E/2\pi p)(2J_2+1)(2\mathrm{J}+1)^{\frac{1}{2}}\cdot \cdot W(JJLL';\nu J_2)\,P^q_\nu(\cos\theta)\,\mathrm{Re}\sum_{\varkappa\varkappa'}H_\nu(\tilde{\varkappa}\varkappa';\pi L\pi' L')\,A_{\nu\hat{q}}(\varkappa\varkappa')\,\mathscr{E}_k(\pi L)\,\mathscr{E}^*_{k'}(\pi' L')\,,$$

involving the same « geometrical » function as was encountered in the evaluation of $I_\nu(\theta)$ in Appendix A. The three components are distinguished only by the angular factor $P^q_\nu(\cos\theta)$ and by

$$\text{(B.7}b\text{)} \qquad A_{\nu\hat{q}}(\varkappa\varkappa') = \begin{cases} -1\,, & \hat{\boldsymbol{q}}=\hat{\boldsymbol{p}},\\ (\varkappa+\varkappa')/\nu(\nu+1)\,, & \hat{\boldsymbol{q}}=\hat{\boldsymbol{t}}_t,\\ i(\varkappa-\varkappa')/\nu(\nu+1)\,, & \hat{\boldsymbol{q}}=\hat{\boldsymbol{t}}_0. \end{cases}$$

TABLE III. – *Values of* $M_{\nu\hat{q}}(\pi L\pi' L')$ (*).

Longitudinal ($\hat{\boldsymbol{q}} = \hat{\boldsymbol{p}}$, $q = 0$, ν odd)

$$\pi' = \pi: \quad \mathrm{Re}\{\mathscr{E}_L(\pi L)\,\mathscr{E}^*_{L'}(\pi' L') + \mathscr{E}_{L+1}(\pi L)\,\mathscr{E}^*_{L'-1}(\pi' L') - \mathscr{E}_L(\pi L)\,\mathscr{E}^*_{L'-1}(\pi' L') - \mathscr{E}_{L-1}(\pi L)\,\mathscr{E}^*_{L'}(\pi' L')\}\,.$$

$$\pi' \neq \pi: \quad -[L(L+1)+L'(L'+1)-\nu(\nu+1)]^{-1}\,\mathrm{Re}\{(L+L'+\nu+1)(L+L'-\nu)\mathscr{E}_L(\pi L)\mathscr{E}^*_{L'}(\pi' L') + (L+L'+\nu+2)(L+L'-\nu+1)\cdot$$
$$\cdot\mathscr{E}_{L-1}(\pi L)\mathscr{E}^*_{L'+1}(\pi' L') + (\nu-L+L'+1)(\nu+L-L')\mathscr{E}_L(\pi L)\mathscr{E}^*_{L'-1}(\pi' L') + (\nu+L-L'+1)(\nu-L+L')\mathscr{E}_{L+1}(\pi L)\mathscr{E}^*_{L'}(\pi' L')\}\,.$$

Transverse in the plane ($\hat{\boldsymbol{q}} = \hat{\boldsymbol{t}}_i$, $q = 1$, ν odd)

$$\pi' = \pi: \quad (-)^\sigma[\nu(\nu+1)]^{-1}\,\mathrm{Re}\{(L+L')\,\mathscr{E}_L(\pi L)\,\mathscr{E}^*_{L'}(\pi L') - (L+L'+2)\,\mathscr{E}_{L+1}(\pi L)\,\mathscr{E}^*_{L'+1}(\pi L') +$$
$$+ (-L+L'+1)\,\mathscr{E}_L(\pi L)\,\mathscr{E}^*_{L'+1}(\pi L') + (L+1-L')\,\mathscr{E}_{L+1}(\pi L)\,\mathscr{E}^*_{L'}(\pi L')\}\,.$$

$$\pi' \neq \pi: \quad (-)^\sigma\{\nu(\nu+1)[L(L+1)+L'(L'+1)-\nu(\nu+1)]\}^{-1}\mathrm{Re}\{(L+L')(L+L'+\nu+1)(L+L'-\nu)\,\mathscr{E}_L(\pi L)\,\mathscr{E}^*_{L'}(\pi' L') +$$
$$+ (L-L')(L+L'+\nu+2)(L+L'-\nu+1)\,\mathscr{E}_{L+1}(\pi L)\,\mathscr{E}^*_{L'+1}(\pi' L') - (L+L'+1)(\nu-L+L'+1)(\nu+L-L')\cdot$$
$$\cdot\mathscr{E}_L(\pi L)\,\mathscr{E}^*_{L'+1}(\pi' L') + (L+1+L')(\nu+L-L'+1)(\nu-L+L')\mathscr{E}_{L+1}(\pi L)\mathscr{E}^*_{L'}(\pi' L')\}\,.$$

Transverse out of the plane ($\hat{\boldsymbol{q}} = \hat{\boldsymbol{t}}_0$, $q = 1$, ν even)

$$\pi' = \pi: \quad (-)^{\sigma+1}\{\nu(\nu+1)[L(L+1)+L'(L'+1)-\nu(\nu+1)]\}^{-1}\,\mathrm{Im}\{(-L+L')(L+L'+\nu+1)(L+L'-\nu)\,\mathscr{E}_L(\pi L)\,\mathscr{E}^*_{L'}(\pi L') +$$
$$+ (L-L')(L+L'+\nu+2)(L+L'-\nu+1)\,\mathscr{E}_{L+1}(\pi L)\,\mathscr{E}^*_{L'+1}(\pi L') - (L+L'+1)(\nu-L+L'+1)(\nu+L-L')\cdot$$
$$\cdot\mathscr{E}_L(\pi L)\,\mathscr{E}^*_{L'+1}(\pi L') + (L+1+L')(\nu+L-L'+1)(\nu-L+L')\,\mathscr{E}_{L+1}(\pi L)\,\mathscr{E}^*_{L'}(\pi L')\}\,.$$

$$\pi' \neq \pi: \quad (-)^{\sigma+1}[\nu(\nu+1)]^{-1}\,\mathrm{Im}\{(L+L')\,\mathscr{E}_L(\pi L)\,\mathscr{E}^*_{L'}(\pi' L') - (L+L'+2)\,\mathscr{E}_{L+1}(\pi L)\,\mathscr{E}_{L'+1}(\pi' L') + (-L+L'+1)\cdot$$
$$\cdot\mathscr{E}_L(\pi L)\,\mathscr{E}^*_{L'+1}(\pi' L') + (L+1-L')'\,\mathscr{E}_{L+1}(\pi L)\,\mathscr{E}^*_{L'}(\pi' L')\}\,.$$

(*) $\sigma = \sigma(\pi) = 0$ for $\pi = M$ and $= 1$ for $\pi = E$.

Making use of the evaluation of H_ν in Appendix A and extracting the F-coefficient, cf. eq. (9g), one has

$$(B.8) \qquad V_{\nu\hat{q}}(\theta; \pi L \pi' L') = (-)^{L+L'+1} \frac{E(2J_2+1)}{\pi p (2L+1)(2L'+1)} \left[\frac{L(L+1)\,L'(L'+1)}{2\nu+1}\right]^{\frac{1}{2}} \cdot \\ \cdot M_{\nu\hat{q}}(\pi L \pi' L')\, P_\nu^q(\cos\theta)\,,$$

where the linear combinations of electronic matrix elements involved are

$$(B.8a) \qquad M_{\nu\hat{q}}(\pi L \pi' L') = \mathrm{Re} \sum_{\varkappa\varkappa'} U_\nu(\tilde{\varkappa}\varkappa'; \pi L \pi' L')\, A_{\nu\hat{q}}(\varkappa\varkappa')\, \mathscr{E}_k(\pi L)\, \mathscr{E}^*_{k'}(\pi' L')\,.$$

Table II in Appendix A gives values for U_ν. Combining this factor with $A_{\nu\hat{q}}(\varkappa, \varkappa')$ one obtains the results for $M_{\nu\hat{q}}$ given in Table III.

RIASSUNTO (*)

A causa dell'insuccesso dei principi di simmetria per le interazioni deboli, il decadimento β fornisce un mezzo per produrre nuclei polarizzati. Nelle transizioni permesse si produce solo una polarizzazione del primo ordine, nelle transizioni proibite una orientazione superiore di ordine dispari. Tale orientazione si manifesta nella polarizzazione delle radiazioni susseguenti. Il presente lavoro fornisce una discussione sostanzialmente completa sulla polarizzazione di elettroni di conversione interna derivanti dallo strato K. Sussiste, per le transizioni permesse, un apprezzabile polarizzazione longitudinale, ed anche trasversale. Quest'ultima giace sul piano degli impulsi vettori delle particelle β e dell'elettrone di conversione. Tali polarizzazioni si manifestano, in generale, anche nelle transizioni proibite nelle quali sono presenti i contributi da parte delle orientazioni superiori di ordine dispari. Oltre a ciò, le transizioni proibite sono caratterizzate da una componente di polarizzazione perpendicolare al piano dell'elettrone β di conversione. Tale componente che trae origine dalle orientazioni di ordine pari (per esempio, l'allineamento) è un effetto « classico » dell'osservazione di coincidenza. Sfortunatamente, questa polarizzazione trasversa è, in condizioni normali, molto debole (al massimo alcune unità per cento). Le espressioni per le componenti di polarizzazione sono date in funzione dei coefficienti della correlazione angolare estesamente tabulati, e dei parametri delle particelle per i tre tipi di polarizzazione. Si danno anche i risultati inerenti ai parametri longitudinali e trasversali di polarizzazione nel piano sia per le transizioni miste che per quelle di multipolo pure. Sono presi in esame, in modo dettagliato, particolari schemi di decadimento riguardanti transizioni permesse e transizioni β uniche proibite in prima approssimazione e si riportano i valori numerici di tali polarizzazioni.

(*) *Traduzione a cura della Redazione.*

IL NUOVO CIMENTO Vol. XIII, N. 6 16 Settembre 1959

Generalized Current Conservation and Low Energy Limit of Photon Interactions (*).

E. Kazes

University of Wisconsin - Madison, Wis.

(ricevuto il 18 Giugno 1959)

Summary. — If the fields that describe a system are renormalizable their interaction with low energy photons in the first two orders in the frequency is shown to be given by the « static » properties of the system. This is shown to essentially follow from current conservation. Compton scattering, bremsstrahlung and photo-pion production are examined. In the latter case, although our result is gauge invariant in the first two orders in the frequency, we are not certain of obtaining all terms of this order. The missing terms probably arise from Feynman diagrams in which the photon is connected to a part containing no charged links to the rest.

Introduction.

It is known [1-3] that the scattering of low frequency photons from spin $\frac{1}{2}$ particles is completely determined by the charge, mass and anomalous magnetic moment in the first two orders of the frequency. More recently Low [4] has shown that the bremsstrahlung of low energy photons in the first two orders can also be related to the scattering amplitude without photon emission. These results will be shown to follow from the fact that in any Feynman diagram containing spin $\frac{1}{2}$ Dirac particles, spin zero bosons and photons, it is possible to follow a charged particle that enters the diagram to some charged par-

(*) Supported y the Wisconsin Alumni Research Foundation.

(1) M. Gell-Mann and M. L. Goldberger: *Phys. Rev.*, **96**, 1433 (1954).

(2) F. E. Low: *Phys. Rev.*, **96**, 1428 (1954).

(3) A. Klein: *Phys. Rev.*, **99**, 998 (1955).

(4) F. E. Low: *Phys. Rev.*, **110**, 974 (1958).

ticle of the same or different type, but of the same charge that leaves it without following any neutral particles. This observation yields a generalization of the ordinary Ward identity and relates any Feynman diagram to one containing one less photon. With the aid of this all electromagnetic low energy theorems are related to the « static » properties of diagrams involving one less photon. The « static » properties in question are not always expressed in term of the charge and the magnetic moment of the system but are in general given by derivatives of the vertex operator, the propagator or scattering matrix of the diagram involving one less photon.

In Section 1, the consequences of the generalized current conservation are established. In Section 2, they are applied to Compton scattering. In Section 3, the bremsstrahlung from any process is examined. In Section 4, photo-pion production is investigated.

1. – Generalized current conservation.

Any Feynman diagram contains propagators $S(p)$ for Dirac particles, $\Delta(q)$ for meson and photon propagators in addition to vertex operators $ie\gamma_\nu$, $e(2q+k)_\nu$ for the interaction of a photon with these in addition to mesons with double photon vertices. We shall limit ourselves to renormalizable field theories which require that the elementary meson-nucleon interaction be independent of momentum. As pointed out later, for the essentially kinematical considerations of this section this may not even be necessary. The part of a diagram involving a single photon-meson vertex will be indicated by

$$\Gamma_\nu(q', q) = \Delta(q')(q'+q)_\nu \Delta(q) .$$

It is readily shown that if a photon of momentum k and polarization μ is attached to a Dirac particle, meson propagator and single photon-meson vertex (for the latter case this must be done in all possible ways) and the resultant diagram is multiplied by k_μ, the following substitution results

$$\text{(1.1)} \qquad \begin{cases} S(p) \to e[S(p) - S(p+k)] , \\ \Delta(q) \to e[\Delta(q) - \Delta(q+k)] , \\ \Gamma_\nu(q', q) \to e[\Gamma_\nu(q', q) - \Gamma_\nu(q'+k, q+k)] . \end{cases}$$

If the elements $S(p)$, $\Delta(q)$, $\Gamma_\nu(q', q)$ are designated by $\mathscr{S}(t)$ the operation described above results in the substitution

$$\mathscr{S}(t) \to e[\mathscr{S}(t) - \mathscr{S}(t+k)] .$$

Considering any part of a Feynman diagram that is connected to the rest by neutral particles it will be shown that if a photon of momentum k and polarization μ is attached in every possible place of this partial diagram and the result multiplied by k_μ the result is zero after adding all possible insertions. Omitting, for the sake of simplicity, the propagators of neutral particles and all integrals we find that the Feynman diagram involved is proportional to

$$\mathcal{S}(t_n)O_n \dots \mathcal{S}(t_2)O_2\,\mathcal{S}(t_1)O_1\,,$$

where only the propagators of charged particles or the single photon-meson vertex is indicated. $O_1, \dots, O_n$ represent any of the possible meson-nucleon and photon-nucleon vertex operators or mesons with double photon vertices. Now inserting a photon on these elements and multiplying by k_μ and using equantion (1.1) yields

$$\begin{aligned}(1.2)\qquad e\{&\mathcal{S}(t_n+k)O_n \dots \mathcal{S}(t_2+k)O_2[\mathcal{S}(t_1)-\mathcal{S}(t_1+k)]O_1+\\ &+\mathcal{S}(t_n+k)O_n \dots \mathcal{S}(t_3+k)O_3[\mathcal{S}(t_2)-\mathcal{S}(t_2+k)]O_2\,\mathcal{S}(t_1)O_1+\\ &+\dots+\\ &+\mathcal{S}(t_n+k)O_n[\mathcal{S}(t_{n-1})-\mathcal{S}(t_{n-1}+k)]O_{n-1}\dots O_2\,\mathcal{S}(t_1)O_1+\\ &+[\mathcal{S}(t_n)-\mathcal{S}(t_n+k)]O_n\,\mathcal{S}(t_{n-1})O_{n-1}\dots O_2\,\mathcal{S}(t_1)O_1\}\,,\end{aligned}$$

where the first line corresponds to inserting a photon between O_1 and O_2, the second line to inserting a photon between O_2 and O_3, etc. It is clear that as a consequence of the definition of $\mathcal{S}$ no insertions at any of the vertices $O_1 \dots O_n$ are needed since none involves a single photon-pion vertex and all interactions are renormalizable. The expression in (1.2) is zero as a consequence of the cancellation of half of each line with the consecutive line and half of the first line with half of the last. In obtaining the last cancellation the integration variable around the closed charge loops must be changed.

Now consider any Feynman diagram with an arbitrary number of external lines closed loops and one open charged line. Compton scattering, photo-pion production and bremsstrahlung are in this class for our purpose. Again suppressing neutral propagators, all closed loops and integrations, such a diagram will be proportional to the product of functions $\mathcal{S}$ of the charged particles on the open charged line, such that

$$(1.3)\qquad M(p', q'; p, q) = \mathcal{S}(t_n)O_n\,\mathcal{S}(t_{n-1}) \dots \mathcal{S}(t_2)O_2\,\mathcal{S}(t_1)\,,$$

p and p' are the initial and final charged particles, q, q' refer to all initial and final neutral particles, and t labels charged particles only. Inserting a photon k_μ wherever possible in the diagram represented by Equation (1.3) and calling

the result $M_\mu(p'+k, q'; p, q, k)$, then using Equation (1.1), and our previous result about closed charged loops in (1.3) it follows that

$$
\begin{aligned}
(1.4) \qquad & k_\mu M_\mu(p'+k, q'; p, q, k) = \\
& = e\{\mathscr{S}(t_n+k)O_n\,\mathscr{S}(t_{n-1}+k)\ldots O_2[\mathscr{S}(t_1)-\mathscr{S}(t_1+k)] + \\
& + \mathscr{S}(t_n+k)O_n\,\mathscr{S}(t_{n-1}+k)\ldots O_3[\mathscr{S}(t_2)-\mathscr{S}(t_2+k)]O_2\,\mathscr{S}(t_1) + \\
& + \ldots + \\
& + [\mathscr{S}(t_n)-\mathscr{S}(t_n+k)]O_n\,\mathscr{S}(t_{n-1})\ldots O_2\,\mathscr{S}(t_1)\} \\
& = e[M(p', q'; p, q) - M(p'+k, q'\ p+k, q)] \,.
\end{aligned}
$$

In M_μ p and $p'+k$ represent the momenta of the initial and final charged particles.

When more than one open charged line is present, equation (1.4) is modified by adding additional terms for each open line while holding all other momenta same as in M.

Having established the generalized current conservation, equation (1.4), for any Feynman diagram it is observed to reduce to the generalized Ward identity ([5]) when M is a propagation function in which case M_μ becomes the vertex operator, *i.e.*,

$$
(1.5) \qquad (p'_\mu - p_\mu)\Lambda_\mu(p', p) = e[S'^{-1}(p') - S'^{-1}(p)] \,.
$$

Furthermore, if the propagators of external lines are removed and an expectation value between initial and final wave functions taken, equation (1.4) yields the usual statement of gauge invariance, *i.e.*

$$
k_\mu \overline{u}(p'+k)\,S^{-1}(p'+k)\,M_\mu(p'+k, q; p, q, k)\,S^{-1}(p)\,u(p) = 0 \,.
$$

It should be noted that if renormalization is performed as described by MATTHEWS and SALAM ([6]) by adding counter terms to the hamiltonian none of the considerations that led to equation (1.4) are changed. Hence we shall use (1.4) with renormalized quantities without introducing a new notation.

([5]) Y. TAKAHASHI: *Nuovo Cimento*, **6**, 370 (1957).
([6]) P. T. MATTHEWS and A. SALAM: *Phys. Rev.*, **94**, 185 (1954).

Since we shall be interested in processes where the external particles are on the mass shell it is convenient to introduce a new quantity $\mathscr{M}_\mu$ defined by

$$(1.6) \qquad M_\mu(p'+k, q'; p, q, k) = S'(p'+k)\mathscr{M}_\mu(p'+k, q'; p, q, k)\, S'(p)\,,$$

where all quantities have been renormalized.

Using Equation (1.6) in (1.4) one obtains

$$(1.7) \qquad k_\mu \mathscr{M}_\mu(p'+k, q'; p, q, k) =$$
$$= e[S'^{-1}(p'+k)\, S'(p')\mathscr{M}(p', q'; p, q) - \mathscr{M}(p'+k, q'; p+k, q) S'(p+k) S'^{-1}(p)]\,.$$

2. – Compton scattering.

Consider the scattering of a photon q_μ from a spin $\frac{1}{2}$ particle of momentum p to a final state q', p'. The quantity of interest, $\mathscr{M}$ in Equation (1.7), will be the vertex operator. Thus the scattering amplitude $\mathscr{M}_{\nu\mu}(p', q'; p, q)$ obeys the relation

$$(2.1) \qquad q_\mu \mathscr{M}_{\nu\mu}(p', q'; p, q) =$$
$$= e[S'^{-1}(p') S'(p'-q) \Lambda_\nu(p'-q, p) - \Lambda_\nu(p', p+q) S'(p+q) S'^{-1}(p)]\,.$$

Following Gell-Mann and Goldberger [1] we split all Feynman diagrams into class A, consisting of those which are separated by a physical nucleon and their crossed diagram, and class B consisting of the rest. Since

$$(2.2) \qquad \mathscr{M}^{\mathrm{A}}_{\mu\nu}(p', q; p, q) = \Lambda_\nu(p', p+q) S'(p+q) \Lambda_\mu(p+q, p) +$$
$$+ \Lambda_\mu(p', p-q') S'(p-q') \Lambda_\nu(p-q', p)\,,$$

using Equations (2.2) and (1.5)

$$q_\mu \mathscr{M}^{\mathrm{A}}_{\nu\mu}(p', q; p, q) = e[\Lambda_\nu(p', p+q) S'(p+q)(S'^{-1}(p+q) - S'^{-1}(p)) +$$
$$+ (S'^{-1}(p') - S'^{-1}(p'-q))(S'(p-q') \Lambda_\nu(p-q', p)]\,.$$

Substituting this in Equation (2.1)

$$(2.3) \qquad q_\nu \mathscr{M}^{\mathrm{B}}_{\nu\mu}(p', q; p, q) = e[\Lambda_\nu(p-q', p) - \Lambda_\nu(p', p+q)]\,.$$

We obtain $\mathcal{M}^{\mathrm{B}}_{\nu\mu}$ to first order in q or q' from equation (2.3) by expanding $\Lambda_\nu\, p-q',\, p)$ and $\Lambda_\nu(p',\, p+q)$ about the point $p'_\mu = p_\mu$ to second order in q, q', and then it readily is seen that

$$\mathcal{M}^{\mathrm{B}}_{\mu\nu} = -e\left[\frac{\partial}{\partial p'_\mu}\Lambda_\nu(p',\, p) + \frac{\partial}{\partial p_\mu}\Lambda_\nu(p',\, p) + \frac{1}{2}\, q_\lambda \frac{\partial^2}{\partial p_\lambda \partial p_\mu}\Lambda_\nu(p',\, p) + \right.$$

$$\left. + \frac{1}{2}\,(q_\lambda - 2q'_\lambda)\frac{\partial^2}{\partial p'_\lambda \partial p'_\mu}\Lambda_\nu(p',\, p) + (q-q')\frac{\partial^2}{\partial p'_\lambda \partial p_\mu}\Lambda_\nu(p',\, p)\right] + e\, S_{\nu\mu}\,,$$

satisfies (2.3) if

$$S_{\nu\mu} q_\mu = 0\,. \tag{2.5}$$

All derivatives are evaluated at $p'_\mu = p_\mu$ after differentiation. Since we require Equation (2.5) to be satisfied for all small q_μ (we have not required $q^2 = 0$ so far) it follows that $S_{\nu\mu}$ must at least be linear in q unless it is identically zero (7). Comparison of

$$q'_\nu \mathcal{M}^{\mathrm{B}}_{\nu\mu} = e[\Lambda_\mu(p',\, p-q') - \Lambda_\mu(p'+q',\, p)]\,, \tag{2.6}$$

with $q'_\nu \mathcal{M}^{\mathrm{B}}_{\nu\mu}$ calculated from equation (2.4) in addition to the linearity of $S_{\nu\mu}$ with respect to q yields:

$$\left(\frac{\partial}{\partial p'_\mu} + \frac{\partial}{\partial p_\mu}\right)\Lambda_\nu(p',\, p) = \left(\frac{\partial}{\partial p'_\nu} + \frac{\partial}{\partial p_\nu}\right)\Lambda_\mu(p',\, p)\,, \tag{2.7}$$

$$\left(\frac{\partial}{\partial p'_\mu} + \frac{\partial}{\partial p_\mu}\right)\left(\frac{\partial}{\partial p'_\lambda}\Lambda_\nu(p',\, p) + \frac{\partial}{\partial p'_\nu}\Lambda_\lambda(p',\, p)\right) =$$

$$= \left(\frac{\partial^2}{\partial p'_\lambda \partial p'_\nu} + \frac{\partial^2}{\partial p_\lambda \partial p_\nu} + \frac{\partial^2}{\partial p'_\nu \partial p_\lambda} + \frac{\partial^2}{\partial p'_\lambda \partial p_\nu}\right)\Lambda_\mu(p',\, p)\,, \tag{2.8}$$

$$S_{\nu\mu} = \frac{1}{2}\, q_\lambda \left(\frac{\partial^2}{\partial p'_\lambda \partial p'_\mu} + \frac{\partial^2}{\partial p_\lambda \partial p_\mu} + 2\frac{\partial^2}{\partial p'_\lambda \partial p_\mu}\right)\Lambda_\nu(p',\, p) -$$

$$- q_\lambda \frac{\partial}{\partial p'_\lambda}\left(\frac{\partial}{\partial p'_\nu} + \frac{\partial}{\partial p_\nu}\right)\Lambda_\mu(p',\, p)\,, \tag{2.9}$$

with all quantities evaluated at $p'_\mu = p_\mu$ after differentiation.

---

(7) It has been assumed that $S_{\nu\mu}$ has a well defined limit as $q_\mu \to 0$ in an arbitrary way.

Substituting equation (2.9) in equation (2.4) yields

$$(2.10)\quad \mathscr{M}^{\mathrm{B}}_{\nu\mu} = -e\left[\left(\frac{\partial}{\partial p'_\mu}+\frac{\partial}{\partial p_\mu}\right)\Lambda_\nu(p',p)+\right.$$
$$\left.+\,q_\lambda\frac{\partial}{\partial p'_\lambda}\left(\frac{\partial}{\partial p'_\nu}+\frac{\partial}{\partial p_\nu}\right)\Lambda(p',p)-q'_\lambda\frac{\partial}{\partial p'_\lambda}\left(\frac{\partial}{\partial p'_\mu}+\frac{\partial}{\partial p_\mu}\right)\Lambda_\nu(p',p)\right].$$

Using the properties of the vertex operator which are established in Appendix A it follows that the term

$$q_\lambda\frac{\partial^2}{\partial p'_\lambda\,\partial p'_\nu}\Lambda_\mu(p',p)-q'_\lambda\frac{\partial^2}{\partial p_\lambda\,\partial p_\mu}\Lambda_\nu(p',p)$$

in equation (2.8) will not contribute to $\mathscr{M}^{\mathrm{B}}_{\nu\mu}$ to first order in the frequency. This result for $\mathscr{M}^{\mathrm{B}}_{\nu\mu}$ is also established by GELL-MANN and GOLDBERGER [1]. Using the results of Appendix A, to the first order in photon frequency

$$(2.11)\quad \Lambda_\mu(p+q,p)=\Lambda_\mu(p,p)+\frac{1}{2}q_\lambda\frac{\partial}{\partial p_\lambda}\Lambda_\mu(p,p)+$$
$$+\,e[\sigma_{\mu\lambda}q_\lambda l^+_{2.2}+2\varepsilon_{\mu ijk}\,p_i\,q_j\gamma_k\gamma_5 l^+_{3,1}],$$

$$(2.12)\quad \Lambda_\nu(p+q-q',p+q)=\Lambda_\nu(p,p)+\frac{1}{2}(2q_\lambda-q'_\lambda)\frac{\partial}{\partial p_\lambda}\Lambda_\nu(p,p)-$$
$$-\,e[\sigma_{\nu\lambda}q'_\lambda l^+_{2,2}+2\varepsilon_{\nu ijk}p_i q'_j\gamma_k\gamma_5 l^+_{3.1}],$$

where $l^+_{2,2}$, $l^+_{3,1}$ are evaluated at $p'_\mu=p_\mu$.

If $\hat{n}$ and $\hat{n}'$ are unit vectors in the direction of the initial and final photon, and $\boldsymbol{p}=0$:

$$\varepsilon'_\nu\mathscr{M}^{\Lambda}_{\nu\mu}\varepsilon_\mu = e^2\left\{-\frac{F}{M}\boldsymbol{\epsilon}'\cdot\boldsymbol{\epsilon}-\frac{iq_0}{2M^2}\boldsymbol{\sigma}\cdot\boldsymbol{\epsilon}'\times\boldsymbol{\epsilon}-\right.$$
$$-\frac{q_0}{2M^2}i\boldsymbol{\sigma}\cdot[(\boldsymbol{\epsilon}'\times n')\times(\boldsymbol{\epsilon}\times n)](F+4M^2il^+_{3,1}+2Mil^+_{2,2})^2+$$
$$+\frac{iq_0}{2M^2}(F+4M^2il^+_{3,1}+2Mil^+_{2,2})(\hat{n}\cdot\boldsymbol{\epsilon}'\boldsymbol{\sigma}\cdot\boldsymbol{\epsilon}\times\hat{n}-$$
$$\left.-\,\hat{n}'\cdot\boldsymbol{\epsilon}\,\boldsymbol{\sigma}\cdot\boldsymbol{\epsilon}'\times\hat{n}'+2\boldsymbol{\sigma}\cdot\boldsymbol{\epsilon}'\times\boldsymbol{\epsilon})-4q_0l^+_{3,1}\boldsymbol{\sigma}\cdot\boldsymbol{\epsilon}'\times\boldsymbol{\epsilon}\right\},$$

$$\varepsilon'_\nu\mathscr{M}^{\mathrm{B}}_{\nu\mu}\varepsilon_\mu = e^2\left\{-\frac{1-F}{M}\boldsymbol{\epsilon}'\cdot\boldsymbol{\epsilon}+4q_0l^+_{3,1}\boldsymbol{\sigma}\cdot\boldsymbol{\epsilon}'\times\boldsymbol{\epsilon}\right\},$$

where the initial and final Pauli spinors have been suppressed, and q_0 is the incident photon energy. Also the anomalous magnetic moment can be shown to be

$$\mu_A = e\left(\frac{F-1}{2M} + 2Mil_{3,1}^{+} + il_{2,2}^{+}\right). \tag{2.13}$$

Eliminating $F+4M^2il_{3,1}^{+}+2Mil_{2,2}^{+}$ from $\varepsilon_\nu'(\mathcal{M}_{\nu\mu}^{\Lambda}+\mathcal{M}_{\nu\mu}^{\mathrm{B}})\varepsilon_\mu$ we obtain the result recorded several ([1-3])times which expresses the Compton scattering amplitude to first order in the frequency in terms of the charge and magnetic moment alone.

3. – Bremsstrahlung.

Consider the scattering of a charged particle from p to p' in an external field or from another neutral particle and the emission of soft photons of momentum k' polarization ν in this process. Reference to any specific process is made merely for clarity, and all following results apply equally well to bremsstrahlung in Compton scattering or any other process.

If $T(p', p)$ refers to the scattering amplitude then the bremsstrahlung amplitude $T_\nu(k', p'; p)$ is related to it by

$$\begin{aligned} k_\nu' T_\nu(k', p'; p) = \\ = e[T(p', p-k')S'(p-k')S'^{-1}(p) - S'^{-1}(p')S'(p'+k')T(p'+k'; p)]. \end{aligned} \tag{3.1}$$

Again the A diagrams are obtained from

$$\begin{aligned} T_\nu^{\mathrm{A}}(k', p'; p) = T(p', p-k')S'(p-k')\Lambda_\nu(p-k', p) + \\ + \Lambda_\nu(p', p'+k')S'(p'+k')T(p'+k', p). \end{aligned} \tag{3.2}$$

Using (3.2) and (1.5) in (3.1)

$$k_\nu' T_\nu^{\mathrm{B}}(k', p'; p) = e[T(p', p-k') - T(p'+k', p)].$$

Since T_ν^{A} is proportional to $1/k_0'$ it will suffice to obtain T_ν^{B} to zero order in the frequency. Thus

$$T_\nu^{\mathrm{B}}(k', p', p) = -e\left(\frac{\partial}{\partial p_\nu'} + \frac{\partial}{\partial p_\nu}\right) T(p', p). \tag{3.3}$$

An arbitrary function satisfying $S_\nu k_\nu' = 0$ is not needed if we assume $T_\nu^{\mathrm{B}}(k', p'; p)$ to be analytic as $k_\mu' \to 0$ since any analytic function of this type must be proportional to k'. Using (2.11) and (2.12) it is readily verified that expres-

sions of the type $S'(p-k')\Lambda_\nu(p-k', p)$ appearing in (2.2) yield terms which are not expressible in terms of the charge and magnetic moment of incident particle. We shall only give the result for the bremsstrahlung from a charged boson, since for a Dirac particle the final expression is too unwieldy. The corresponding case for a Dirac particle treated by Low [4] retains all terms of order $1/k_0'$ but not all constant terms.

The electromagnetic vertex operator for a charged boson is of the form

$$g_\mu(p', p) = (p'+p)_\mu n^+(p^2, p'^2, (p'-p)^2) + (p'-p)_\mu n^-((p^2, p'^2, (p'-p)^2),$$

where as a consequence of charge conjugation invariance n^+ ,n^- are even, odd respectively, under the interchange of p' and p. Hence to the first order in the frequency and using the generalized Ward identity (1.5)

$$g_\mu(p-k', p) = 2p^\mu e[\dot{\Delta}'^{-1}(p^2) - p\cdot k' \ddot{\Delta}'^{-1}(p^2)] - k'_\mu e \dot{\Delta}'^{-1}(p^2), \tag{3.4}$$

$$g_\mu(p', p'+k') = 2p'_\mu e[\dot{\Delta}'^{-1}(p^2) + p'\cdot k' \ddot{\Delta}'^{-1}(p^2)] + e k'_\mu \dot{\Delta}'^{-1}(p^2) \tag{3.5}$$

and

$$\Delta'(p-k') = (-2p\cdot k' \dot{\Delta}'^{-1}(p^2) + 2(p\cdot k')^2 \ddot{\Delta}'^{-1}(p^2))^{-1}, \tag{3.6}$$

$$\Delta'(p'+k') = (2p'\cdot k' \dot{\Delta}'^{-1}(p^2) + 2(p'\cdot k')^2 \ddot{\Delta}'^{-1}(p^2))^{-1}. \tag{3.7}$$

Where

$$\dot{\Delta}'^{-1}(p^2) = \frac{\mathrm{d}}{\mathrm{d}p^2}\Delta'^{-1}(p^2), \qquad \text{etc.}$$

and $\Delta'(p^2)$ is the renormalized boson propagator. Using (3.4)–(3.7) in (3.2)

$$\varepsilon'_\nu T^{\mathrm{A}}_\nu(k', p'; p) = e\left[\frac{p'\cdot\varepsilon'}{p'\cdot k'} T(p'+k', p) - \frac{p\cdot\varepsilon}{p\cdot k'} T(p', p-k')\right].$$

The expression

$$(T^{\mathrm{A}}_\nu + T^{\mathrm{B}}_\nu)\varepsilon'_\nu$$

thus obtained is in agreement with Low [4]. It should be emphasized that the above result does not only apply to bremsstrahlung in scattering, and for the case of bremsstrahlung in Compton scattering from bosons, for example, we merely need reinterpret $T(p', p)$ as the Compton amplitude in the absence of soft photon emission.

4. – Photon-pion emission.

Consider positive pions of momentum q produced from an initial proton of momentum p and let k, p' represent the initial photon and final neutron.

From (1.7) it follows that

$$k_\mu \mathcal{M}_\mu(p', q; p, k) = \tag{4.1}$$
$$= e[\Delta'^{-1}(q)\,\Delta'(q-k)\,\Lambda_5(p', p) - \Lambda_5(p', p+k)\,S(p+k)\,S'^{-1}(p)]\,,$$

Here $\Lambda_5(p', p)$ is the pion-nucleon vertex operator. Again defining the A diagrams correspond to those which are separated by a proton, π^+ and neutron line

$$\mathcal{M}^{\mathrm{A}}_\mu(p', q; p, k) = \Lambda_5(p', p+k)\,S'(p+k)\,\Lambda^{\mathrm{p}}_\mu(p+k, p) + \tag{4.2}$$
$$+ g_\mu(q, q-k)\,\Delta'(q-k)\,\Lambda_5(p', p) + \Lambda^{\mathrm{n}}_\mu(p', p'-k)\,S'(p'-k)\,\Lambda_5(p'-k, p)\,,$$

Λ^{p}_μ and Λ^{n}_μ represent the proton and neutron electromagnetic vertex respectively. As a consequence of the results of the first section

$$k_\mu \Lambda^{\mathrm{n}}_\mu(p', p'-k) = 0\,. \tag{4.3}$$

From (4.3) and (4.1)

$$k_\mu \mathcal{M}^{\mathrm{B}}_\mu(p', q; p, k) = e[\Lambda_5(p', p) - \Lambda_5(p', p+k)]\,. \tag{4.4}$$

As in Compton scattering a solution for $\mathcal{M}^{\mathrm{B}}_\mu$ correct to the first order in the frequency is

$$k_\mu \mathcal{M}^{\mathrm{B}}_\mu(p', q; p, k) = e\left[-\frac{\partial}{\partial p_\mu}\Lambda_5(p', p) + \frac{1}{2}k_\lambda \frac{\partial^2}{\partial p_\lambda \partial p_\mu}\Lambda_5(p', p)\right] + S'_\mu\,, \tag{4.5}$$

where $S'_\mu k_\mu = 0$. Unlike the case for Compton scattering or bremsstrahlung we have no way of determining S'_μ. This quantity may arise from photo-pion production by virtual neutrons or closed charge loops. But the omission of this term still keeps the result gauge invariant up to terms linear in the frequency. Since the pion-nucleon vertex operator is of the form

$$\Lambda_5(p', p) = \gamma_5 f_1(p^2, p'^2, (p-p')^2) + \frac{\gamma_5}{M}(ip\cdot\gamma + M) f_2(p^2, p'^2, (p-p')^2) + \tag{4.6}$$
$$+ (ip'\cdot\gamma + M)\frac{\gamma_5}{M} f_3(p^2, p'^2, (p-p')^2)$$
$$+ (ip'\cdot\gamma + M)\frac{\gamma_5}{M^2}(ip\cdot\gamma + M) f_4(p^2, p'^2, (p-p')^1)\,,$$

choosing $\boldsymbol{p} = 0$

$$\bar{u}(p')\,\varepsilon_\mu \frac{\partial}{\partial p_\mu} \Lambda_5(p', p)\, u(p) = \bar{u}(p') \frac{\gamma_5}{M} i\gamma\cdot\varepsilon f_2(-m^2, -m^2, (q-k)^2) u(p)\,,$$

$$\bar{u}(p')\,\varepsilon_\mu \frac{\partial^2}{\partial p_\mu\, \partial p_\lambda} \Lambda_5(p', p) u(p) = \bar{u}(p') \frac{\gamma_5}{M} i\gamma\cdot\varepsilon f_2' 2p\cdot k n(p)\,,$$

where

$$f_2' = \frac{\mathrm{d}}{\mathrm{d}p^2} f_2(p^2, -m^2, (q-k)^2)\,.$$

Thus

$$\bar{u}(p')\,\varepsilon_\mu \mathscr{M}^{\mathrm{B}}_\mu(p', q; p, k)\, u(p') = \tag{4.7}$$

$$= -\frac{ei}{M}\,\bar{u}\,(p')\gamma_5\gamma\cdot\varepsilon\, u(p)\big\{f_2((-m^2, -m^2, (q-k)^2) + q_0 M f_2'(-m^2, -m^2, (q-k)^2)\big\}\,.$$

Hence a knowledge of the vertex operators and the nucleon propagation function suffices to obtain a gauge invariant photomeson production amplitude to the first two orders in the frequency.

At the threshold of photo-pion production neglecting terms of the order of the pion-mass, using (4.6), (4.7) and (A.2) in (4.2)

$$\varepsilon_\mu \mathscr{M}^{\mathrm{A}}_\mu = -\frac{e}{2M}(f_1 + 2f_2)\boldsymbol{\sigma}\cdot\boldsymbol{\epsilon}\,,$$

$$\varepsilon_\mu \mathscr{M}^{\mathrm{B}}_\mu = \frac{e}{M} f_2 \boldsymbol{\sigma}\cdot\boldsymbol{\epsilon}\,,$$

which yields the Kroll-Ruderman theorem.

5. – Discussion.

It is readily established that the substitution (1.1) is also valid for some non-renormalizable interactions, for example ps-pv. Hence in the lowest order of such non-renormalizable interactions all our results will also be valid. And if to handle these interactions a cut-off that preserves gauge invariance is introduced the validity of our results may be pushed further.

If all vertex operators and propagation functions that enter into a scattering problem are known, the A diagram for Compton scattering would be completely determined. But it is further possible to give an expression for B diagrams that formally satisfy equation (2.3) for all frequencies. Hence a fully gauge invariant expression could be generated in terms of the vertex operator and propagation function. But the deviation from the correct answer arises from diagrams in which one of the photons ends on a closed charged loop or a neutral particle. For example $S_{\nu\mu}$ in Section 2 probably arises like this. It is not always possible to determine these functions without knowing more about the dynamics of the system. At low frequencies these contributions were evaluated for Compton scattering and bremsstrahlung assuming analyticity.

Should it turn out that $\Lambda_\mu(p+k, p)$ does not have a power series development $k_\mu = 0$ or that $S_{\nu\mu}$ of Section 2 is not an analytic function at $k_\mu = 0$ the low energy theorems would probably not be so simple as to express Compton scattering in terms of the charge and magnetic moment alone. And further the conclusions (A.7)–(A.10) need not be valid. Likewise if the arbitrary function S_ν that enters the bremsstrahlung problem should not be analytic we could say nothing about it.

* * *

I would like to thank Prof. R. G. Sachs and Dr. I. Manning for discussions and questions that led to the generalized current conservation, and also Professor M. L. Goldberger for suggesting its application to low energy Compton scattering.

Appendix

Requiring the vertex operator $\Lambda_\mu(p', p)$ totransform as a proper 4-vector under Lorentz transformation and that in charge conjugation it obeys

$$C\Lambda_\mu(p', p)C^{-1} = -\Lambda_\mu^T(-p, -p'),$$

it follows that it must be of the form

$$\begin{aligned}(\text{A.1})\quad \Lambda_\mu(p', p) = e[&P_\mu l^+_{0,1} + Q_\mu l^-_{0,2} + \gamma_\mu l^+_{1,1} + P_\mu P\cdot\gamma\, l^+_{1,2} + P_\mu Q\cdot\gamma l^-_{1,3} + Q_\mu P\gamma\, l^-_{1,4} + \\ &+ Q_\mu Q\cdot\gamma\, l^+_{1,5} + \sigma_{\mu\nu}P_\nu l^-_{2,1} + \sigma_{\mu\nu}Q_\nu l^+_{2,2} + P_\mu Q_\lambda \sigma_{\lambda\nu}P_\nu l^+_{2,3} + \\ &+ Q_\mu Q_\lambda \sigma_{\lambda\nu}P_\nu l^-_{2,4} + \varepsilon_{\mu\cdot\cdot\cdot}P_\tau Q_\sigma \gamma_\iota \gamma_5 l^+_{3,1}],\end{aligned}$$

where

$$P_\mu = p'_\mu + p_\mu\,, \qquad Q_\mu = p'_\mu - p_\mu\,,$$

$$\sigma_{\mu\nu} = \frac{1}{2i}(\gamma_\mu\gamma_\nu - \gamma_\nu\gamma_\mu)$$

and the l^+, l^- are functions of p^2, p'^2, $(p'-p)^2$ only which are even and odd espectively under the interchange of p_μ and p'_μ.

Using the generalized Ward identity, equation (1.5), and a fermion propagation function of the form

$$S'(p+q) = \{i\gamma(p+q)\,G[(p+q)^2] + M\,F[(p+q)^2]\}^{-1}\,, \tag{A.2}$$

with the vertex operator in equation (A.1) we get

$$(p'^2 - p^2)\,l^+_{0,1} + (p'-p)^2 l^-_{0,2} = M(F(p'^2) - F(p^2))\,, \tag{A.3}$$

$$l^+_{1,1} + (p'^2 - p^2) l^-_{1,3} + (p'-p)^2\,l^+_{1,5} = \frac{i}{2}\,(G(p'^2) + G(p^2))\,, \tag{A.4}$$

$$(p'^2 - p) l^+_{1,2} + (p'-p)^2 l^-_{1,4} = \frac{i}{2}\,(G(p'^2) - G(p^2))\,, \tag{A.5}$$

$$l^-_{2,1} + (p'^2 - p^2)\,l^+_{3,3} + (p'-p)^2\,l^-_{2,4} = 0\,. \tag{A.6}$$

In obtaining the vertex operator to the first order in the frequency we make the assumption that the functions G, F, $l^\pm$ admit a power series expansion with respect to their arguments.

The requirement (2.5) with $S_{\mu\nu}$ determined from (2.9) require the following restrictions on the form factors not derivable from the requirements of the generalized Ward identity,

$$\frac{\mathrm{d}}{\mathrm{d}p^2}\,l^-_{2,1}(p'^2, p^2, 0)\Big|_{p'_\mu = p_\mu} = 0\,, \tag{A.7}$$

$$l^+_{2,3}(p^2, p^2, 0) = 0\,, \tag{A.8}$$

$$\frac{\mathrm{d}}{\mathrm{d}p^2}\,l^+_{2,2}(p^2, p^2, 0) = 0\,, \tag{A.9}$$

$$\frac{\mathrm{d}}{\mathrm{d}p^2}\,l^+_{3,1}(p^2, p^2, 0) = 0\,. \tag{A.10}$$

(A.7) and (A.8) eliminate the functions F_1, F_3 appearing in equation (3.8) of GELL-MANN and GOLDBERGER [1]. But we see no reason for suppressing $l^+_{3,1}$, in (A.1).

Furthermore if time reversal invariance is imposed

$$\Lambda_\mu^+(p', p) = \pm \gamma_4 \Lambda_\mu(p, p')\gamma_4 ,$$

where the upper sign is used for $\mu = 1, 2, 3$ and the lower sign for $\mu = 4$. This requires that $l_{0,1}^+$, $l_{0,2}^-$ be real and that the rest be pure imaginary.

RIASSUNTO (*)

Si dimostra che, se i campi che descrivono un sistema sono rinormalizzabili, le interazioni di essi con fotoni di debole energia nei primi due ordini della frequenza, sono date dalle proprietà « statiche » del sistema. Si dimostra che ciò deriva essenzialmente dalla conservazione della corrente. Sono presi in esame lo scattering Compton, la bremsstrahlung e la produzione di foto-pioni. In quest'ultimo caso, sebbene il nostro risultato sia gauge invariante nei primi due ordini della frequenza, non siamo certi di ottenere tutti i termini di tale ordine. I termini mancanti risultano, con ogni probabilità, dai diagrammi di Feynmann, nei quali il fotone è connesso con una parte che non contiene alcun legame carico col resto.

(*) *Traduzione a cura della Redazione.*

IL NUOVO CIMENTO Vol. XIII, N. 6 16 Settembre 1959

The Electron Decay Mode of the Pion.

J. Ashkin (*), T. Fazzini, G. Fidecaro, A. W. Merrison
H. Paul (**) and A. V. Tollestrup (***)

CERN - Genève

(ricevuto il 14 Luglio 1959)

Summary. – This paper presents evidence for the existence of the electron decay mode of the pion. The branching-ratio we have found for this mode, compared with the normal muon decay, is $(1.22 \pm 0.30) \cdot 10^{-4}$. This is in good agreement with the $V—A$ theory of weak interactions.

1. – Introduction.

The electron decay mode of the pion has been the subject of much theoretical and experimental investigation. Some years ago Ruderman and Finkelstein (1) pointed out that, although it was difficult to predict the absolute decay rate of the pion, exact calculations could be made of the branching-ratio $(\pi \to e + \nu)/(\pi \to \mu + \nu)$. Their model for the decay of the pion was that already used by Sakata (2) of the pion decaying into a virtual nucleon-antinucleon pair and the subsequent annihilation of the pair through a weak four-fermion interaction. They showed that for the usual five relativistic interactions, the electron decay mode was forbidden if the weak interaction is scalar, vector, or tensor. In the case of the pseudo-scalar interaction they showed that the branching-ratio was given by the factor $[(m_\pi^2 - m_e^2)/(m_\pi^2 - m_\mu^2)]^2$; that is, the electron decay mode is 5.48 times more probable than the muon decay

(*) Ford Foundation Fellow, on leave from Carnegie Institute of Technology, Pittsburgh.

(**) Ford Foundation Fellow, on leave from Institut für Radiumforschung, Vienna.

(***) National Science Foundation Fellow, on leave from California Institute of Technology, Pasadena.

(1) M. A. Ruderman and R. J. Finkelstein: *Phys. Rev.*, **76**, 1458 (1949).

(2) S. Sakata: *Phys. Rev.*, **58**, 576 (1940).

mode. For the case of the axial vector interaction, however, this factor must be multiplied by the ratio of the squares of the masses of the electron and muon. This reduces the branching-ratio to $1.28 \cdot 10^{-4}$. These arguments were later reinforced by TREIMAN and WYLD (3). It must be emphasized that they do not depend on the strong interaction part of the decay process, but only on the assumption that the electron and muon are coupled symmetrically to nucleons.

If one hopes to understand the weak interactions in terms of some « universal » interaction, then clearly the evidence concerning the electron decay of the pion has to be related to all other evidence about weak interactions. The evidence about the nature of the nuclear β decay was however, somewhat confused until the beginning of 1958. There was considerable support for a universal Fermi interaction of a vector and axial vector character, and this had been emphasized particularly by SUDARSHAN and MARSHAK (4), FEYNMAN and GELL-MANN (5), and SAKURAI (6). There were three major pieces of experimental evidence against this, however. The ^{6}He electron-neutrino angular correlation determined by RUSTAD and RUBY (7) had given a clear result that this Gamow-Teller transition went largely through a tensor interaction, and this was supported by the work of SHERR and MILLER on ^{22}Ne (8). There was also the non-existence of the leptonic decay modes of the hyperons. The third piece of evidence concerned the non-appearance of the β decay of the pion.

Until early 1958, three attempts had been made to detect the electron decay mode. The first was by FRIEDMAN and RAINWATER (9) using photographic emulsions. Their result was not completely conclusive as they detected « one or zero π-e event compared to 1 419 π-μ events ». This was followed by the work of LOKANATHAN and STEINBERGER (10), using an electron range telescope to detect the electron, which gave a result for the branching-ratio of $(-0.3 \pm 0.9) \cdot 10^{-4}$. Lastly, there was the experiment of ANDERSON and LATTES (11), using a Siegbahn-type magnetic spectrometer, which gave the result $(-0.4 \pm 9.0) \cdot 10^{-6}$. It is clear that these results completely preclude a pseudoscalar interaction, and suggest very strongly that the interaction cannot be axial vector either.

However, at the end of 1957, WU and SCHWARZSCHILD (12) examined

(3) S. B. TREIMAN and H. W. WYLD Jr.: *Phys. Rev.*, **101**, 1552 (1956).
(4) E. C. G. SUDARSHAN and R. E. MARSHAK: *Phys. Rev.*, **109**, 1860 (1958).
(5) R. P. FEYNMAN and M. GELL-MANN: *Phys. Rev.*, **109**, 193 (1958).
(6) J. J. SAKURAI: *Nuovo Cimento*, **7**, 649 (1958).
(7) B. M. RUSTAD and S. L. RUBY: *Phys. Rev.*, **97**, 991 (1955).
(8) R. SHERR and R. H. MILLER: *Phys. Rev.*, **93**, 1076 (1954).
(9) H. L. FRIEDMAN and J. RAINWATER: *Phys. Rev.*, **84**, 684 (1951).
(10) S. LOKANATHAN and J. STEINBERGER: *Suppl. Nuovo Cimento*, **2**, 151 (1955).
(11) H. L. ANDERSON and C. M. G. LATTES: *Nuovo Cimento*, **6**, 1356 (1957).
(12) C. S. WU and A. SCHWARZSCHILD: *Columbia University Report* CU - 173 (1958).

critically the Rustad and Ruby experiment and came to the conclusion that it had been in error. A later experiment by HERRMANNSFELDT *et al.* ([13]) has demonstrated that the ^{6}He β decay goes through an axial vector interaction. Recently, there has also been evidence for the leptonic decays of hyperons, though not in the ratio given by the vector interaction ([14]). The present paper describes evidence which we have found for the electron decay of the pion; our preliminary results have already been published ([15]).

The detection of the electron decay mode of the pion is difficult because of the large background of electrons arising from muons produced in the normal π-μ decay. However, the μ-electrons can be distinguished in three ways. Firstly, they have a continuous spectrum with a maximum kinetic energy of 52.3 MeV, compared with the line spectrum of electrons from π-e decay of 69.3 MeV. Secondly, the π-e electrons should show a simple exponential decay with the mean life identical with that of the π-μ decay, while the π-μ-e electron time distribution would correspond to a two-stage radio-active decay, with a fast rise (approx. π-μ mean life) and a slow fall (approx. μ-e mean life). Lastly, three charged particles can be seen in the π-μ-e chain, while only two are shown in the π-e decay.

Essentially, our experimental method consisted in bringing a beam of positive pions to rest in a scintillation counter. The decay electron was detected in a range telescope which had sufficient absorber in it tho reject most of the electrons from μ decay. Whenever the range telescope was triggered by a sufficiently energetic electron we examined with a fast oscilloscope the pion pulse in the stopping counter and the pulse following it. In this way we were able to recognize the π-e and the π-μ-e chains of decay. The method has the great advantage of recording the time information in these processes so that it was easy to reject random events, and in addition we were able to show that the process we identified as the π-e decay mode had an exponential decay and had the same mean life as the π-μ mode.

In this paper we present more experimental information and a more detailed description of the experiment. By making a Monte Carlo calculation to estimate the efficiency of the electron telescope, we have been able to show that the value of the branching-ratio $(\pi \to e + \nu)/(\pi \to \mu + \nu)$ is in good agreement with an axial vector form for the weak interaction.

([13]) W. B. HERRMANSFELDT ,R. L. BURMAN, P. STAHELIN, J. S. ALLEN and T. H. BRAID: *Phys. Rev. Letters*, **1**, 61 (1958).

([14]) F. S. CRAWFORD jr., M. CRESTI, M. L. GOOD, G. R. KALBFLEISCH, M. L. STEVENSON, H. K. TICHO: *Phys. Rev. Letters*, **1**, 377 (1958); P. NORDIN, J. OREAR, L. REED, A. H. ROSENFELD, F. T. SOLMITZ, H. D. TAFT and R. D. TRIPP: *Phys. Rev. Letters*, **1**, 380 (1958).

([15]) T. FAZZINI, G. FIDECARO, A. W. MERRISON, H. PAUL and A. V. TOLLESTRUP: *Phys. Rev. Letters*, **1**, 247 (1958).

Since the publication of our preliminary results ([15]), other laboratories have observed the π-e decay both in a bubble chamber ([16]) and in magnetic spectrometers ([17,18]).

2. – Apparatus.

2·1. *Meson beam.* – As no description has yet been published of the method of extraction of the internally-produced meson beams of the CERN 600 MeV Synchro-cyclotron, we will give here some details of the experimental arrangement.

The arrangement is shown in Fig. 1. The poles of the cyclotron magnet have a radius of 250 cm, and the meson target is mounted with its inner edge on a radius of 226 cm. This is just inside the $n=0.2$ point. Mesons from the target spiral out through the fringe field of the cyclotron and the target is adjusted in azimuth until those rays which are parallel in the horizontal direction fall on the entrance to the first meson bending magnet. There will be one azimuth corresponding to a particular energy for which this will be true. This magnet, which is a double-focusing magnet of the type analysed by Cross ([19]), is set so that there is no focusing in the horizontal direction, so that a beam parallel in the horizontal direction emerges from the magnet. On the other hand, in the vertical direction the rays emerging from the cyclotron field appear to be diverging, and these the magnet also puts into a parallel beam. The meson beam then passes through a hole in the heavy-concrete shielding-wall, $5\frac{1}{2}$ m thick, and is then incident upon a second bending magnet, identical with the first, whose principal function is then to form a small image.

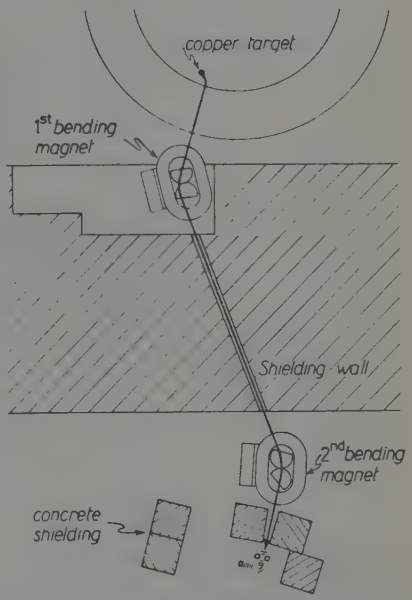

Fig. 1. – Layout of the pion beam.

([16]) G. Impeduglia, R. Plano, A. Prodell, N. Samios, M. Schwartz and J. Steinberger: *Phys. Rev. Letters*, **1**, 249 (1958).

([17]) H. L. Anderson, T. Fujii, R. H. Miller and L. Tau: *Phys. Rev. Letters*, **2**, 53 (1959).

([18]) For other results see the *Proceedings of the Gatlinburg Conference on Weak Interactions* (to be published in *Rev. Mod. Phys.*).

([19]) W. G. Cross: *Rev. Sci. Instr.*, **22**, 717 (1951).

The meson path, up to the entrance of the second magnet, is *in vacuo*. After this the mesons pass through a thin-walled bag filled with hydrogen. This reduces the multiple Coulomb scattering of the beam to negligible proportions. The mesons are then brought to a focus in an image which is 4 cm high and about 10 cm wide. The height is determined by the height of the cyclotron target and the magnification in the magnet system, and the width by the dispersion in the magnets. The image contains a momentum band of about 5%.

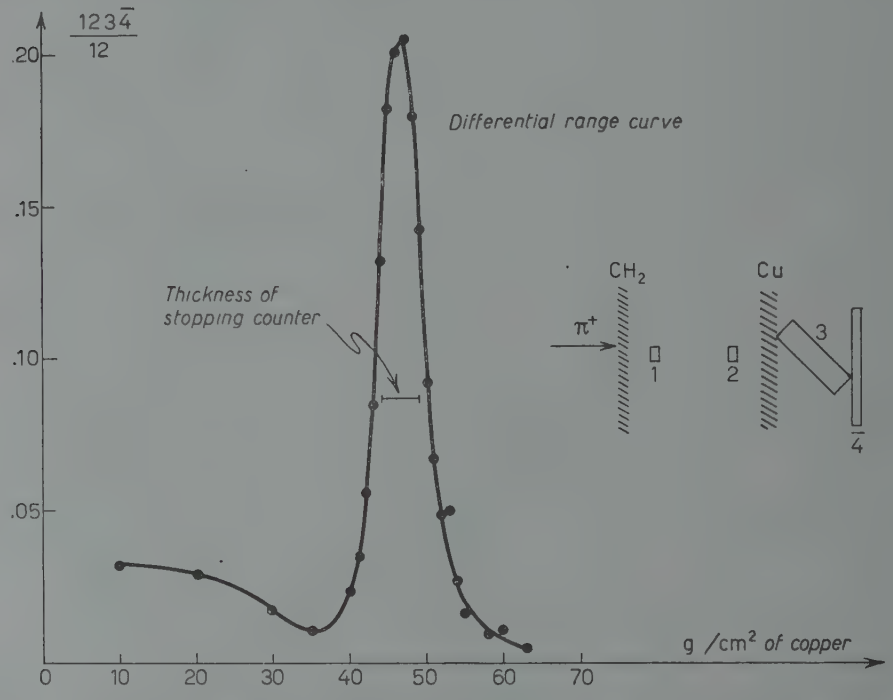

Fig. 2. A typical differential range curve for the 127 MeV π^+ beam obtained with the pion telescope.

With this system it is possible to extract mesons from the cyclotron of energies varying between a lower limit of 127 MeV and an upper limit in excess of 300 MeV. The upper limit is determined largely by the smallness of the production cross-section for high energies, and the lower limit by a mechanical obstruction in the cyclotron. This obstruction has been removed since this experiment was completed.

The present experiment was made with stopped positive pions which we obtained by slowing down the 127 MeV π^+ beam. For most of the experimental runs the rate of stopping mesons was about 600/s. Fig. 2 shows a typical range curve.

2·2. *Experimental arrangement.* – The layout of the experiment is shown diagrammatically in Fig. 3. The 127 MeV pions were first filtered by 2 cm polythene to remove protons of the same momentum. They then passed through

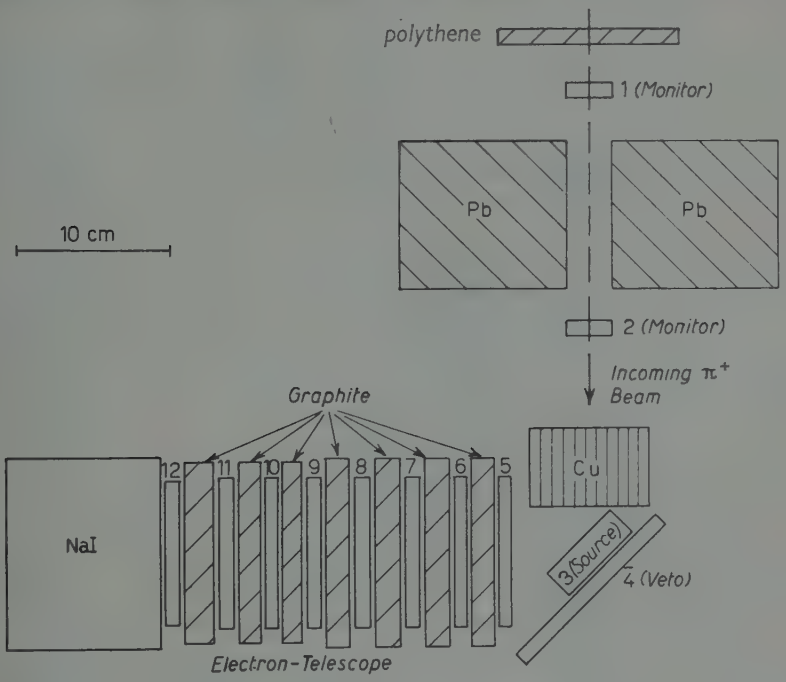

Fig. 3. – The experimental arrangement.

the monitor counters 1 and 2, which were 5 cm high, 3 cm wide, and 1 cm thick, mounted on either side of a thick lead collimator. The hole in the collimator was the same size as these counters. The pions were then slowed down in a block of copper and about 30% came to rest in counter 3, the so-called source counter. Counter 3 was 5 cm high, 6 cm wide and 2 cm thick. It was inclined at an angle of about 45° to the beam, in this way presenting an effective thickness of about 3 cm to the beam. To identify particles stopping in counter 3, 123 were in fast (9 ns) coincidence, with counter 4 in anticoincidence.

Energetic particles coming from 3 were then examined in the range telescope made up of counters 5-12, with various amounts of absorber between them, which were in separate fast coincidence (9 ns). Counters 5-11 were 10 cm×10 cm×1 cm. Counter 12 was again 1 cm thick but was circular with a diameter of 9.5 cm. Behind this telescope we placed a large cylindrical NaI(Tl) counter, of 5 inches diameter and 4 inches thick.

The reason for using so many counters in the range telescope was to reduce the probability that an electron should convert into a γ-ray which later re-

converts into an electron. In this way an electron would appear to have a greater range than it actually possesses.

The two fast telescopes, $1\,2\,3\,\bar{4}$ and 5-12, were connected by a slow coincidence gate in such a way that if a 5-12 pulse occurred in the time interval 60 ns before to 160 ns after the $1\,2\,3\,\bar{4}$ pulse, then photographs were taken of the pulses from counter 3 and counter 12, suitably delayed, and from the NaI counter. The pulses from 3 and 12 were recorded on a fast oscilloscope. The slow NaI pulses were recorded on a slow oscilloscope which also displayed pulses from counter 2 and from the output of the $1\,2\,3\,\bar{4}$ coincidence circuit. We recorded a pair of photographs, slow and fast, about once every two hours.

2·3. *Electronics.* – A simplified block diagram is shown in Fig. 4. The counters each had a positive and a negative output available. The pulses which operated the coincidence circuits were shaped at the counters by means of 125 ohm clipping cables 4 ns long. The clipping lines were not short-circuited but terminated with a 47 ohm resistance which eliminated entirely the overshoot.

Special emphasis was put on the stopping counter, counter 3. Saturation effects in this counter are very dangerous as they make the counter insensitive for some time after a large pulse. In the case of the fairly large pulses from the stopping pions, if saturation occurs, a number of π-e and π-μ decays are missed. After adopting the circuit shown in Fig. 5 where the voltage in the last stages was very much increased in comparison with the other counters, it was possible to see even electrons and muons buried in the pion pulse, *i.e.* at a minimum distance from the pion pulse of 5 or 6 ns, while an ordinary counter was insensitive for 18 or 20 ns after a pion pulse. The pulses for the fast oscilloscope were taken at the anode of counters 3 and 12 and shaped at the counter with a 1 ns delay cable. The overshoot was completely eliminated with a 19 ohm terminating resistance.

The whole electronic equipment was located in a counting room which was separated from the counters by a cable length of about 120 m. All the cables were RG 63/U, 125 ohm impedance, except for the pair of cables which transmitted the pulses to the fast oscilloscope, which were special 70 ohm low attenuation cables type HM/7/Al made by Telcon. The total delay time of the pulses in the low attenuation cable was more than one microsecond. In spite of this, the rise time was rather well preserved as can be seen from Fig. 7 (see Section 3). Without this special cable it would have been impossible to make the necessary delays.

The coincidence circuits have already been described ([20]). Each coincidence circuit was followed by two Hewlett-Packard distributed amplifiers (an

([20]) T. FAZZINI and G. FIDECARO: to be published.

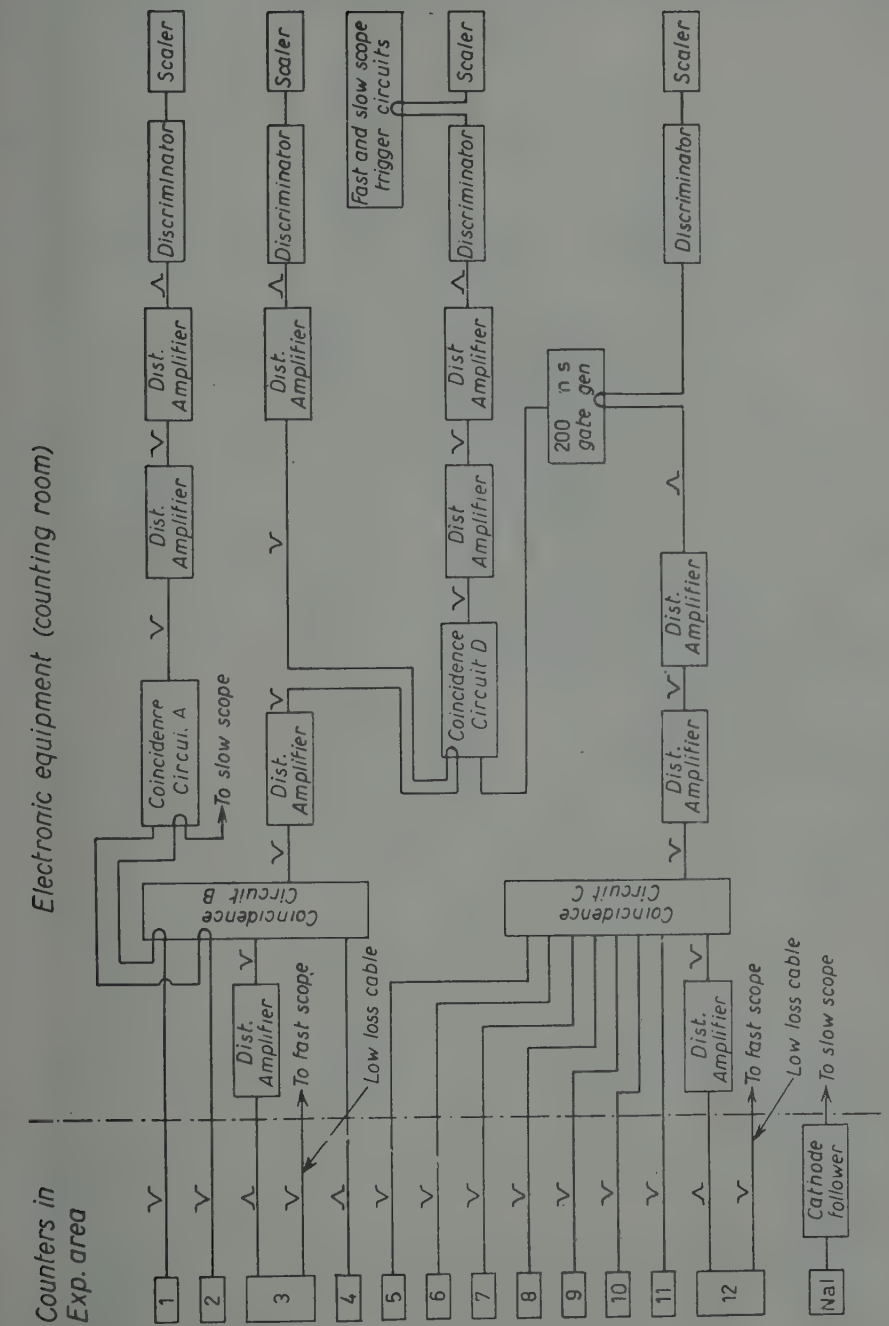

Fig. 4. – A simplified block diagram of the electronics.

inverting and a non-inverting type) followed in turn by a fast discriminator described by FARLEY ([21]). Fig. 6 shows a typical delay curve for the electron telescope.

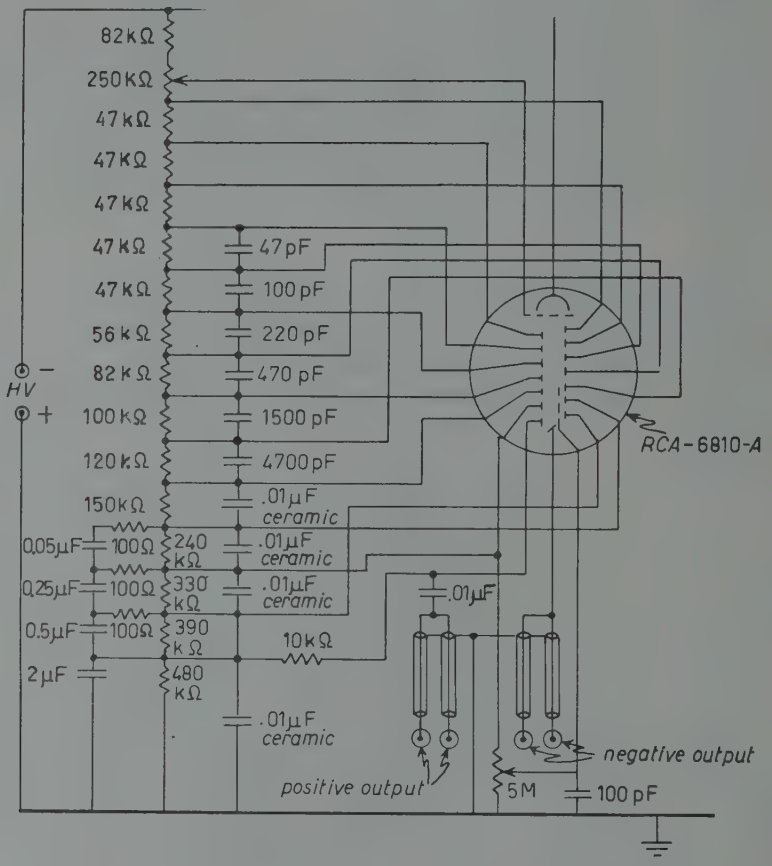

Fig. 5. – The resistance chain of the stopping counter.

The 12 coincidences which were used as a monitor were recorded by coincidence circuit A, and the $123\bar{4}$ coincidences by circuit B (Fig. 4). The 8 counters of the electron telescope gave a coincidence in circuit C. The pulses from C triggered a pulse generator which passed a 220 ns pulse on to the last coincidence circuit D, to make a coincidence between the pion telescope $1\,2\,3\,\bar{4}$ and the electron telescope. The output of D triggered both the fast and slow oscilloscopes. With this arrangement the pion pulse occurred always at the same point of the time bases of both oscilloscopes. The fast oscilloscope was a travelling wave oscilloscope with a bandwith of 2 000 MHz (3 db point)

([21]) F. J. M. FARLEY: *Rev. Sci. Instr.*, **29**, 595 (1958).

made by EDGERTON, GERMESHAUSEN and GREER. The deflection in cm per volt was about the same as for the 517 A Tektronix oscilloscope, but since the travelling wave scope has a spot size smaller than 5/100 mm, the effective sensitivity in terms of «trace width» was (5÷10) times better. The delays were adjusted in such a way that not only could delayed coincidences be seen (π-e, π-μ-e) with a maximum delay of 160 ns, but also those coincidences where the e pulse arrived before the pion pulse. This was essential for the analysis of random events. Pulses from counters 3 and 12 appeared with opposite polarity on the fast oscilloscope because they were sent independently to the two systems of deflecting plates (Fig. 7). The time calibration was obtained by displaying a 100 MHz sine wave every 15 minutes.

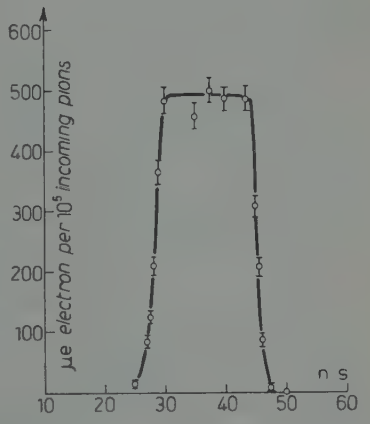

Fig. 6. – A typical delay curve for the electron telescope.

The slow oscilloscope was a Tektronix 545. Three pulses which could be clearly distinguished were displayed on it, the NaI pulse, and the pulses 1 2 3 $\bar{4}$ and 2. The three pulses appeared at about 4 microseconds from the beginning of the trace. It was possible in this way to explore the incoming pion beam up to 4 μs before the interesting pion had arrived.

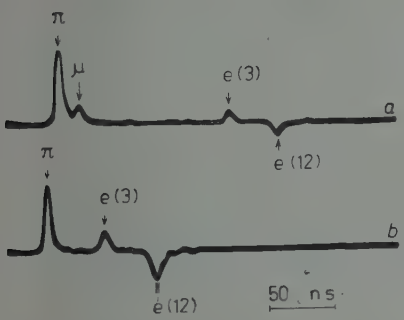

Fig. 7. – Photographs of typical π-μ-e and π-e events.

Plateau and delay curves were measured for each counter at the beginning of the experiment, and checked afterward from time to time. The resolving power of the coincidence circuit was about 9 ns. Fig. 6 shows a typical delay curve.

The fast oscilloscope pictures were recorded on Eastman Kodak Linagraph film, which was run continuously. This was done using the optical arrangement supplied with the fast oscilloscope but the mechanical movement was that from a Dumont camera.

3. – Experimental results.

Altogether, we have recorded 243 photographs on the fast oscilloscope in about 200 hours of running. These could be classified into four categories.

i) π-μ-e *events*, where the stopping pion, the muon and the subsequent electron are clearly visible. Fig. 7 *a*) shows a typical event of this class. *e*(3) is the electron pulse in counter 3 and *e*(12) the electron pulse in counter 12, which—determined by a delay cable—must always occur a fixed time after *e*(3). The muon pulse was, of course, of constant height.

ii) « π-e » *events*. These events look identical with class i) except that no μ-pulse is visible. This class will clearly contain also those π-μ-e events where the μ-pulse is obscured by the π-pulse (which we call false « π-e » events), and this effect is discussed later. Fig. 7 *b*) shows a typical event of this class. We have accepted as π-e events only those where the π and e pulses are separated by at least 8.3 ns.

iii) *Prompt events*, where a prompt coincidence has occurred between the two telescopes. This class will include events, for example, where a charge exchange π^0 has been produced in 3, one of the γ-rays has been converted and the subsequent electron has triggered 5-12. It will include also π-e events where the electron appears very close to the pion.

iv) *Random events*. These are the events with a clearly improper time distribution. The only dangerous random event is, of course, one which resembles a π-e and to estimate the number of these we searched for randoms which looked like time inverted π-e events (e-π). We found no such events.

We ran the experiment with several different thicknesses of absorber in the telescope and the distribution of events in the four categories is shown in Table I.

TABLE I.

	Total thickness of telescope				Total
	30.16 g/cm²	31.18 g/cm²	32.31 g/cm²	34.25 g/cm²	
π-μ-e	8	8	5	1	22
π-e (including false « π-e » events)	9	17	28	19	73
False « π-e »	2.5	2.5	1.5	0.3	6.8
Prompt	6	8	39	29	82
Random	18	16	22	10	66
Stopped pions $\cdot 10^6$	27.3	67.6	210.8	154.1	459.8

Even with the thickest telescope some π-μ-e events are recorded and, of course, it is critical in the experiment to decide how many π-μ-e events will resemble the π-e events because of insufficient time resolution between the

pion and muon pulses. We determined this number in the following way. We removed all the absorber from the telescope and recorded the pulses from counters 3 and 12 in the usual way. As the energy discrimination against π-μ-e events is now small, virtually all the events we recorded were due to π-μ-e decays. We then scanned these photographs to see how many false « π-e » events we saw. The ratio of these events to π-μ-e events was 0.31. Then the number of false π-e events included in the π-e category in an actual experimental run is simply 0.31 times the number of π-μ-e events observed in that run. This number is included also in Table I.

The information given by the pulses $123\bar{4}$ and 2 displayed on the slow oscilloscope was used at an early stage of the experiment to reinforce the preliminary evidence for the existence of the π-e decay which came from an analysis of the fast oscilloscope traces. But after the energy discrimination of the electron telescope was improved (by increasing the number of counters from 5 to 8) we no longer found it necessary to make use of this information in the analysis.

The π-μ-e events were accompanied by a very small NaI pulse or no pulse at all. On the other hand, we have verified that the π-e events were accompanied by pulses of all sizes up to a maximum pulse height which depended on the telescope thickness. We did not use this information in a quantitative way because of the small number of pulses recorded.

4. – Analysis of the experimental results.

We shall shows in this Section, using the criteria outlined in Section 1 and implicit in the design of the experiment, that the above results are good evidence for the existence of the electron decay mode of the pion and that those events we have labelled π-e are, in fact, electron decays. We have already used the fact that only two charged particles are involved in this reaction in the classification of the events. We can now examine the range of the electrons from the π-e decays and their time distribution.

Range curves for the π-e events and the false π-e events, calculated from the observed π-μ-e decays, are shown in Fig. 8.

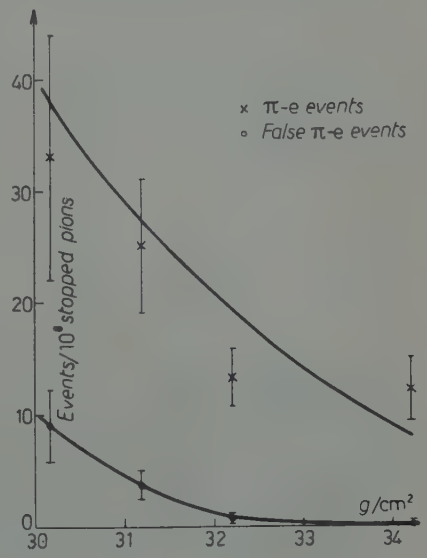

Fig. 8. – Experimental range curves for the π-e events and the background of false π-e events.

It is clear from these curves that the contamination of the π-e events by false π-e events is very small, and is reduced rapidly as the thickness of the absorber is increased. It runs from 30% for the thinnest absorber to 2% for the thickest absorber. It is clear also that the electrons from the π-e events have considerably greater range than the electrons from the μ-e decay. The upper curve in the figure is the range curve which would be expected from 69 MeV electrons, assuming the branching-ratio to be $1.28 \cdot 10^{-4}$ and calculating the detection efficiency of the electron telescope as described in detail in Section 5. Included in it is a correction for the fact that our π-e events have a small contamination of false π-e decays.

An integral decay curve for the π-e events is shown in Fig. 9. The curve shown is that expected from an exponential decay with a mean life of 22 ns, with an appropriate correction for a constant background. The mean life we computed from our 73 events was (22 ± 3) ns, which agrees very well with the mean life for π-μ decay of (25.6 ± 0.5) ns given by K. M. CROWE [22].

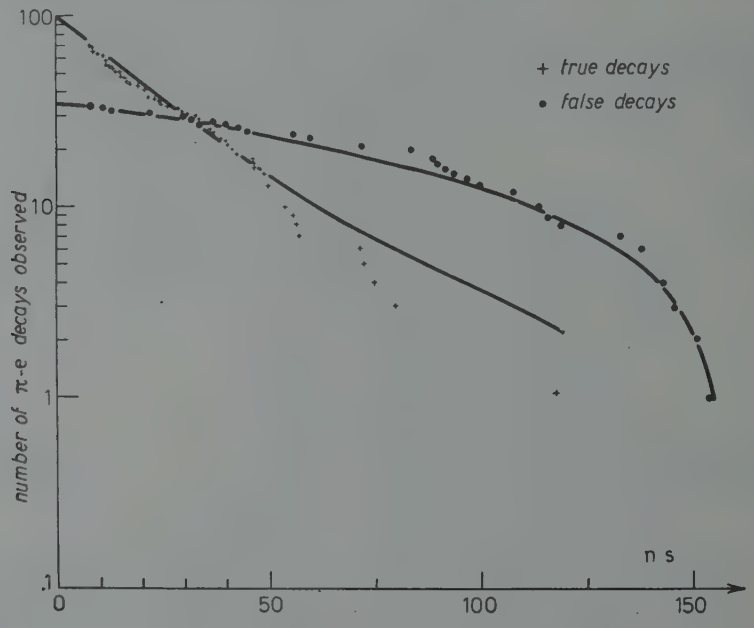

Fig. 9. – Integral decay curves for π-e events and false π-e events.

Shown also in Fig. 9 is an integral decay curve for the false «π-e» events from π-μ-e decay obtained from runs with the absorber removed. Because the μ-e half-life is long compared with the 160 ns interval during which we

[22] K. M. CROWE: *Nuovo Cimento*, **5**, 541 (1957).

recorded our events, the time distribution of the μ-e decays should appear practically linear (on a linear scale). Indeed they follow closely the curve drawn (Fig. 9) which is the translation of the linear curve into a logarithmic plot.

We have also determined from our runs with no absorber the time distribution of π-μ events, and this again shows an exponential decay which agrees with the measured pion mean life (Fig. 10).

These two curves, the π-μ and false « π-e » distributions are important checks on the apparatus because they show, first, that the apparatus can measure successfully exponential time distributions of short mean life and, secondly, that it does not invent such time distributions from decays with a long mean life like, for example, the muon decay.

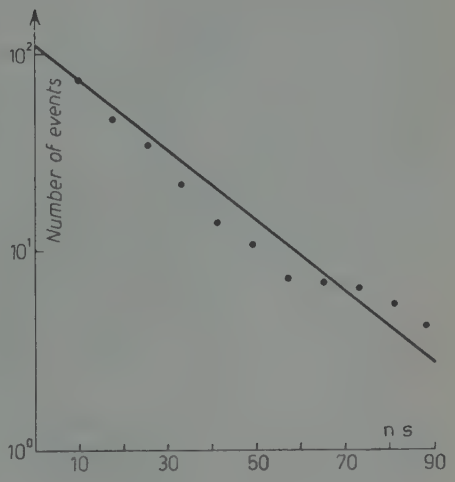

Fig. 10. – Integral decay curve for π-μ events, corrected for the gate lenght. The straight line is for 25.6 ns.

In summary, then, the 73 π-e events have the following characteristics:

a) only two charged particles are present in these events, and the spurious contribution with large absorber from μ decay is very small;

b) the decay electron has a range which is longer than the μ decay electrons and is consistent with an energy of 69 MeV;

c) the events show an exponential time distribution which has a mean life identical with that for π-μ decay measured in the same apparatus.

The above results seem to be conclusive evidence for the existence of the electron decay mode of the pion.

5. – The detection efficiency of the electron telescope.

The most important conclusion of the experiment is that the electron decay of the pion exists. But it is important also to determine the branching-ratio between this mode of decay and the normal decay into a muon. The limiting factor is in determining the detection efficiency of the electron telescope. We have done this by means of Monte Carlo calculations on a high-speed digital computer and in this section we shall describe these calculations.

5·1. *Monte Carlo calculation.* – The positron telescope contains a large number of closely spaced counters in coincidence. With this construction it is sufficient to follow the history of the incident positron alone, neglecting the small increase in detection efficiency arising from the possibility that a high energy γ-ray radiated by the positron will convert to a pair before reaching the next counter or the one after. The radiated γ-rays thus enter into the discussion only to the extent that they represent an energy loss of the positron. The Monte Carlo calculation therefore consists in tracing the passage of a large number of individual positrons through the telescope taking into account the systematic energy loss by ionization and the random processes involved in the multiple Coulomb scattering and bremsstrahlung.

The rate of energy loss by ionization for positrons has been computed from the expression given by ROSSI [23] and corrected according to Sternheimer's [24] calculation of the density effect. Over the energy range of interest the $\mathrm{d}E/\mathrm{d}x$ for positrons is about three per cent less than that for electrons. Neglect of the density effect would result in $\mathrm{d}E/\mathrm{d}x$ being too large by between 10 and 25% depending on the positron energy. Statistical fluctuations in the ionization loss have not been included.

The multiple scattering has been treated in the small angle approximation, considering separately the projections in two perpendicular planes xz and yz, z being the axis of the telescope. The probability distribution for increments $\Delta\Theta_x$ and $\Delta\Theta_y$ in the projected angles Θ_x and Θ_y, after traversing a thin layer of thickness t radiation lengths, are taken as Gaussians with root mean square angles [25]

$$\sqrt{\overline{(\Delta\Theta_x)^2}} = \sqrt{\overline{(\Delta\Theta_y)^2}} = \frac{2.12}{\sqrt{2}} \cdot \frac{\sqrt{t}}{E},$$

where E is the positron energy in MeV. Choice of $\Delta\Theta_x$ and $\Delta\Theta_y$ for a particular positron of a certain energy going through one layer is made by selecting at random from 100 intervals of angle arranged according to the Gaussian law to have equal probability.

For the bremsstrahlung we have calculated the differential cross-sections according to the formulas given by BETHE and HEITLER [26] which include the influence of screening for different energies E_0 of the radiating positron. The radiation lengths of carbon and hydrogen have been taken as 42.5 and 58 g/cm^2 respectively, as quoted by BETHE and ASHKIN [27]. These are values

---

[23] B. ROSSI: *High-Energy Particles* (New Jersey, 1952), p. 27.
[24] R. STERNHEIMER: *Phys. Rev.*, **88**, 851 (1952); **103**, 511 (1956).
[25] B. ROSSI: *High-Energy Particles* (New Jersey, 1952), p. 68.
[26] H. A. BETHE and W. HEITLER: *Proc. Roy. Soc.*, A **146**, 83 (1934).
[27] H. A. BETHE and J. ASHKIN: Part II, Vol. I of *Experimental Nuclear Physics*, E. SEGRÈ, Ed. (New York, 1953), p. 266.

based on the Born approximation, and take account of the bremsstrahlung in the field of the atomic electrons as well as the nucleus according to the calculations of WHEELER and LAMB [28]. The thickness of a characteristic layer in the telescope has been taken so that there is approximately a 10% total probability for radiating a γ-ray with fractional energy $v = h\nu/E_0$ greater than $v_{min} = 0.001$. Using the bremsstrahlung distribution we have divided the range of fractional energy v into 1000 intervals of equal probability obtaining in this way approximately 100 intervals for $v > v_{min}$ with the remaining 900 intervals corresponding to γ-rays whose energy we consider to be zero.

While traversing the telescope positrons may also undergo annihilation in flight against electrons. Instead of incorporating this process in the Monte Carlo calculation, the final efficiency has been corrected by multiplying with the average probability that a positron escapes annihilation (approximately 80%). For positrons which have been slowed down by ionization from an initial energy E_0 to a final energy E_f, the accumulated probability of annihilation W is

$$W = \int_{E_f}^{E_0} \frac{ZN\sigma_a(E)\mathrm{d}E}{(\mathrm{d}E/\mathrm{d}x)},$$

where $\sigma_a(E)$ is the annihilation cross-section [29] for the collision of a positron of energy E against an electron at rest, ZN is the number of electrons per cm^3 of the stopping material, and $\mathrm{d}E/\mathrm{d}x$ is the rate of energy loss by ionization. In Fig. 11 the annihilation probability W is given as a function of final positron energy for slowing down in carbon from 70 MeV initial energy. To obtain the reduction in detection efficiency shown in Table III we have averaged the probability of survival, $1 - W$, over the energy spectrum found by the Monte Carlo method for positrons reaching the last counter of the telescope. We have also added

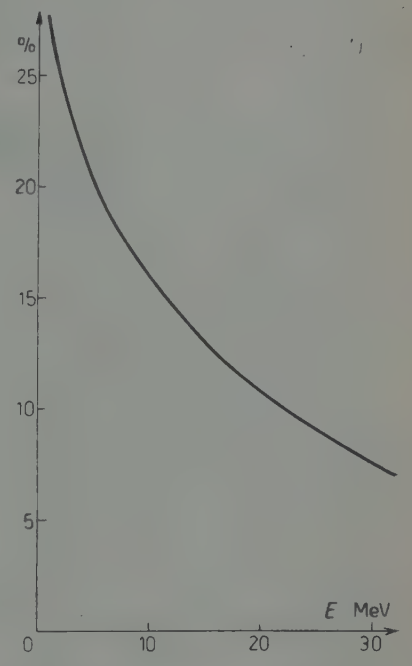

Fig. 11. – Integrated probability of annihilation of a positron in carbon from 70 MeV to E.

[28] J. A. WHEELER and W. E. LAMB: *Phys. Rev.*, **55**, 858 (1939).

[29] P. A. M. DIRAC: *Proc. Camb. Phil. Soc.*, **26**, 361 (1930); see also W. HEITLER: *Quantum Theory of Radiation*, 3rd Edition (Oxford, 1954), p. 270 and 385.

a small positive increment to $1 - W$ coming from the fact that part of the energy is lost by the positron in the form of radiation instead of ionization.

For the geometrical history of the positrons we assume that they are created at the centre of the stopping counter with an isotropic angular distribution. The direction (Θ, φ) of an individual positron is selected at random by choosing from 100 equal intervals of $\cos \Theta$ and of φ according to two random numbers.

The polar angle Θ has been restricted to a forward cone of fixed aperture (solid angle $\Delta\Omega = 0.05 \cdot 4\pi$) taken several times larger than the aperture sub tended by the last counter of the telescope so that it is very unlikely for a positron emitted outside this cone to be detected. To correct for the fact that the actual positrons originate from different points and hence suffer a different energy loss in the stopping counter we suppose that they are created with a continuous energy spectrum instead of a line spectrum. This spectrum is computed for positrons created uniformly in the stopping counter, moving all parallel to the z direction, and losing energy only by ionization. Selection of the energy of the positron is made with a third random number. A fourth random number is needed to decide how much energy the positron will lose by radiation inside the stopping counter.

After these four random numbers have been chosen, one has a certain positron of known energy and direction (Θ, φ) falling on the first counter of the telescope at a point (x, y, z). Next the positron is followed inside the telescope through successive layers, 62 for the thickest telescope, 58, 56 and 54 for the others. Fortunately, to a very good approximation, it has been possible to make the division in terms of layers all having the same thickness in radiation lengths, no matter whether it is a layer of counter or of carbon absorber. Within each layer the multiple scattering, bremsstrahlung, and ionization loss are taken into account as discussed previously.

Positrons which go through the last counter of the telescope are recorded by the computer in four different registers, according to the initial value of Θ. From the results we can verify that the maximum initial angle was chosen large enough. Positrons which fail to reach the last counter have been rejected for one of three possible reasons;

a) the positron has escaped laterally from the telescope;

b) the projected angle Θ_x or Θ_y has exceeded an upper limit chosen as 90°;

c) the kinetic energy has fallen below a limit chosen as 0.5 MeV.

The conditions *b*) and *c*) are closely related since large angle scatterings become more probable as the kinetic energy becomes very small. These conditions have been introduced to avoid unnecessary complications and are in no way critical for the result, judging from computations in which the angular limits have been drastically changed and from the calculated energy spectrum of the positrons going through the last counter.

Almost all of the calculations have been made with the CERN Mercury Computer. The initial programme was written (by Mr. D. S. LAKE) in the basic code for Mercury, and all the final calculations were made with this. We rewrote this programme in Autocode, and this increased considerably our insight into the physical content of the final computation. In the case of one of the telescopes an independent calculation was made with the Finac Computer in Rome, using a different procedure for generating the sequence of pseudo-random numbers needed for the multiple scattering and radiation.

In the CERN calculations the random numbers are obtained from the recurrence relation [30]

$$\xi_{n+1} = K\xi_n \text{ (modulo } 2^{29}), \tag{3}$$

where

$$K = 43^5, \qquad \xi_0 = 1.$$

The resulting ξ_n form a sequence of pseudo-random integers below 2^{29}. The sequence eventually repeats, but only after a cycle of length $2^{29-2} = 2^{27}$, or approximately 10^8. Division of the ξ_n by 2^{29} produces a sequence of numbers in the open interval $(0, 1)$ which should have a practically uniform distribution. Subsequently multiplying by 100 or 1000 and taking the integer part of the product gives two or three digit random numbers as needed.

The Rome calculation used a sequence generated in a similar fashion but with 5^{15} for K (having 35 binary digits) and the product $K\xi_n$ taken modulo 2^{39}. The cycle length in this case is $2^{39-2} = 2^{37}$ or approximately $1.4 \cdot 10^{11}$. Two and three digit random numbers were obtained from the ξ_n in a somewhat different way than for the CERN sequence, using the leading 7 or 10 binary digits of ξ_n to form the integers directly, taking care to reject integers exceeding 99 or 999 respectively.

5·2. *Numerical estimates.* – It is convenient to define the efficiency of the telescope as

$$\varepsilon = \frac{\Delta\Omega}{4\pi} p = 0.05\, p, \tag{4}$$

where $\Delta\Omega (= 0.05 \times 4\pi)$ is the solid angle of the forward cone to which the positrons have been restricted and p is the probability that a positron emitted by the source into this cone will ultimately be detected. In practice, p is taken from the Monte Carlo calculation as the number of positrons reaching the last counter of the telescope divided by the total number of positrons started.

---

[30] *Symposium on the Monte-Carlo Methods*, H. A. MEYER ed. (New York, 1956), p. 17.

The results are shown in Table II where ε is given, along with its statistical error, for each of the four telescopes. For comparison we have also given the purely geometrical efficiency ε_g which is the solid angle subtended at the source by the last counter divided by 4π. The ratio of ε to ε_g is therefore a measure of the reduction in detection probability due to the intervening telescope. The trend of $\varepsilon/\varepsilon_g$ as a function of telescope thickness is shown in Fig. 12.

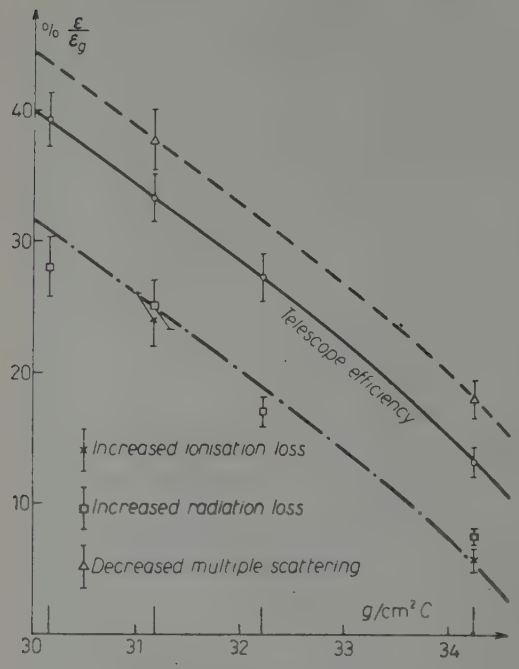

Fig. 12. – Telescope efficiencies as a function of total thickness.

In the case of the thickest telescope where the ratio $\varepsilon/\varepsilon_g$ is only 13% we can expect that the efficiency will be especially sensitive to small changes in the parameters used in the calculations. To have a measure of this sensitivity for all the telescopes we have therefore repeated the calculations for three separate changes in parameters: *a*) the ionization loss $-\mathrm{d}E/\mathrm{d}x$ has been uniformly increased by 5%; *b*) the radiation probabilities have been increased by 20%; *c*) the root mean square angles for multiple scattering have been reduced by 20%. The results are also shown in Fig. 12.

TABLE II.

Telescope thickness g/cm² Carbon	Geometrical efficiency ε_g	Efficiency ε	$\varepsilon/\varepsilon_g$ per cent
30.2	$9.65 \cdot 10^{-3}$	$(3.80 \pm 0.20) \cdot 10^{-3}$	39.4 ± 2.1
31.2	$9.30 \cdot 10^{-3}$	$(3.11 \pm 0.19) \cdot 10^{-3}$	33.4 ± 2.0
32.2	$8.90 \cdot 10^{-3}$	$(2.43 \pm 0.16) \cdot 10^{-3}$	27.3 ± 1.8
34.3	$8.25 \cdot 10^{-3}$	$(1.09 \pm 0.09) \cdot 10^{-3}$	13.2 ± 1.1

The efficiency is evidently very strongly dependent on the ionization loss. This is not surprising in view of the fact that the total energy lost by ionization in the thickest telescope is 62 MeV (for a positron traversing a straight path

from the centre of the source counter to the end of the last counter), thus leaving a margin of only 7 MeV residual energy. The principal uncertainty in our knowledge of dE/dx is associated with the density effect, for which we have used the recent most accurate calculations of STERNHEIMER. A change in dE/dx of 2% corresponds to a 17% change in the branching-ratio.

Assuming that the absolute bremsstrahlung cross-sections are known to an accuracy of 2 or 3% in the case of carbon, as seems probable, the curves of Fig. 12 show that the corresponding inaccuracy in efficiency is not large. More important is the effect of altering the multiple scattering, where the 20% reduction ([31]) of the root mean square angle given in Eq. (1) is in the direction required by the more accurate Molière theory ([32]). The efficiency is thereby increased but the statistical accuracy is not sufficient to give a good quantitative estimate of the change. Assuming the dashed curve in Fig. 12 to be correct, the branching-ratio would be correspondingly reduced by 20%.

In general we feel that the over-all uncertainty in the efficiency calculation is adequately represented by enlarging the error in the final branching ratio from the purely statistical value of 12% to a total of 25%. It is doubtful whether further refinements of the Monte Carlo calculations will yield results which are essentially more reliable.

6. – The branching ratio for the electron decay mode.

We now use the results of the previous section to determine the branching ratio of the electron decay mode. Table III summarizes the experimental results and the corrections which have to be applied. Column 6 gives the number of true π-e decays and the associated statistical error obtained by subtracting the false π-e of Col. 4 from the total number listed in Col. 3. Since we have counted as π-e only those decays in which the e appears more than 8.3 ns after the π, we can observe only the fraction $\exp[-8.3/25.6]$, or 0.723 of the actual number of π-e events which take place. Col. 7 therefore gives as the number of « events », the number of true π-e divided by 0.723, and this divided by the number of stopped pions is listed in Col. 8. In Col. 9 we give the efficiency of detection of the positrons as found from the Monte Carlo calculation, and in Col. 10 the probability that the positrons escape annihilation in their passage through the telescope. The product of these is the net detection efficiency given in Col. 11. The branching-ratio R, and its

---

([31]) W. H. BARKAS and A. H. ROSENFELD: *University of California Rad. Lab. Report* UCRL - 8030 (1958).

([32]) G. MOLIÈRE: *Zeits. f. Naturf.*, **2***a*, 133 (1947); **3***a*, 78 (1948).

1	2	3	4	5	6
Telescope thickness g/cm²	Stopped pions pions $\cdot 10^6$	π-e	π-μ-e	False π-e	True π-e
30.16	27.28	9	8	2.5	6.5 ± 3
31.18	67.61	17	8	2.5	14.5 ± 4
32.21	210.80	28	5	1.5	26.5 ± 5
34.25	154.11	19	1	0.3	18.7 ± 4

statistical error, in Col. 12 is finally obtained from the quotient of the number of events per stopped pion (Col. 8) and the net efficiency (Col. 11).

It seems most reasonable to take an average of the four values of R weighted according to the number of true π-e decays of Col. 6. The result is:

$$R = (1.22 \pm 0.30) \cdot 10^{-4} .$$

Only one-half of the error stated is statistical, the other half takes into account the uncertainties in the telescope efficiency.

In comparing a measurement with the theoretical prediction for the branching ratio, it has been pointed out that there is an appreciable radiative correction allowing for photon emission (internal bremsstrahlung) accompanying the π-e decay. According to the calculations of BERMAN [33] and KINOSHITA [34], the branching ratio for π-e decay with the electron having an energy greater than $E_{max} - \Delta E$ is

$$R(\Delta E) = \left\{1.100 + 0.027 \log\left(\frac{2\Delta E}{m_e}\right)\right\} \cdot 10^{-4},$$

where m_e is the electron mass in energy units.

This gives a surprisingly large reduction from $1.28 \cdot 10^{-4}$, the value neglecting radiative effects. Thus for $\Delta E = 5$ MeV, R is reduced to $1.18 \cdot 10^{-4}$ and for $\Delta E = 10$ MeV R is $1.20 \cdot 10^{-4}$. To apply the correction in our case it is necessary to know the detection efficiency of the electron telescope as a function of initial electron energy. An estimate based on the computed energy

---

([33]) S. M. BERMAN: *Phys. Rev. Letters*, **1**, 468 (1958).
([34]) T. KINOSHITA: *Phys. Rev. Letters*, **2**, 477 (1959).

7	8	9	10	11	12
nts= ie π-e 723	Events / Stopped π $\cdot 10^{-6}$	Efficiency ε $\cdot 10^{-3}$	Annihilation correction	Net efficiency $\cdot 10^{-3}$	Branching ratio R $\cdot 10^{-4}$
9.0	0.330 ± 0.162	3.80	0.853	3.24	1.02 ± 0.50
0.1	0.297 ± 0.087	3.11	0.847	2.63	1.13 ± 0.33
6.7	0.174 ± 0.035	2.43	0.839	2.04	0.85 ± 0.17
5.9	0.168 ± 0.040	1.09	0.819	0.89	1.89 ± 0.45

spectrum of electrons reaching the end of the telescope shows that the *effective* branching-ratio with which our experimental number is to be compared is given by:

$$R_{\text{eff}} = 1.18 \cdot 10^{-4} .$$

7. – Conclusion.

It can be seen from the preceding section that not only does the electron decay mode of the pion exist, but also that the branching-ratio, compared with the normal muon decay, is in good agreement with the hypothesis that the decay goes through an axial vector interaction. There is, of course, great interest in making as accurate a determination of this branching-ratio as possible, particularly because of the large radiative corrections involved. In the present experiment, however, the major source of uncertainty is in the determination of the efficiency of the electron telescope and we feel we have taken this to its reliable limit.

* * *

We should like to thank Prof. G. BERNARDINI for many discussions and his continuous encouragement. Most of the apparatus was built by our technicians Mr. M. FELL and Mr. M. RENEVEY with great skill and care, and Mr. F. BLYTHE was responsible for all the drawing work involved. We should like to thank Mr. O. FREDRIKKSON and the cyclotron crew for their efficient and helpful running of the machine. Dr. I. HALPERN helped considerably in the running of the experiment. The original programme for the Monte Carlo calculations on the CERN Mercury computer was written by Mr. D. S. LAKE and for this and for his help in initiating us in the use of Autocode we are very

much indebted to him. We are grateful also to the staff of the Istituto Nazionale per le Applicazioni del Calcolo in Rome who performed the calculations on the Rome Finac computer.

RIASSUNTO

Si descrive un esperimento in cui viene provata l'esistenza del decadimento elettronico del pione. Il rapporto $\pi e/\pi\mu$ è stato trovato uguale a $(1.22 \pm 0.30)\cdot 10^{-4}$ in buon accordo con la teoria $V-A$ delle interazioni deboli.

LETTERE ALLA REDAZIONE

(La responsabilità scientifica degli scritti inseriti in questa rubrica è completamente lasciata dalla Direzione del periodico ai singoli autori)

Photodisintegration of Deuterons in the Presence of the Pion-theoretical Potential.

J. IWADARE (*), M. MATSUMOTO (**), S. OTSUKI (***), R. TAMAGAKI (***) and W. WATARI (***)

(*) *Research Institute for Fundamental Physics, Kyoto University - Kyoto*
(**) *Department of Physics, Siga University - Siga*
(***) *Department of Physics, Nagoya University - Nagoya*
(***) *Department of Physics, Kyoto Universtiy - Kyoto*
(***) *Department of Physics, Osaka City University - Osaka*

(ricevuto il 22 Aprile 1959)

The pion theory of nuclear forces has been extensively investigated and verified by the analyses of the deuteron problem and the nucleon-nucleon scattering up to 150 MeV [1,2]. The photodisintegration of deuterons will add a crucial test to the potential. In the course of the works referred above, the d(γ, p)n reaction at 22.4 MeV was examined by some of the present authors [3].

The angular distribution of the protons is expressed in the form

$$\frac{\mathrm{d}\sigma}{\mathrm{d}\Omega} = a + b \sin^2\theta(1 + 2\beta\cos\theta) .$$

The $\sin^2\theta$ term is mainly due to the $E1$ transition, the β term due to the interference of $E1$-$E2$ transitions. If there were no tensor forces at all, a would be entirely due to the $M1$ transition, and would be very small ($a/b \lesssim 0.03$). Experimental data give $a/b \sim 0.1$ and $p \sim 0.1$ ($E_\gamma \sim 20$ MeV).

It was pointed out that the large D state probability of the deuteron ($\sim 7\%$) and the strongly positive tensor force in the 30 state are essential in reproducing the rather large value of a [3]. Since the ${}^3D_1 \to {}^3F_2$ $E1$ transition was ignored at that time, it was still necessary to invoke an extraordinary large $M1$ transition to get a large a ($a/b \sim 0.1$). Now that the importance of ${}^3F_2$ final state is well recognized, one can test the validity of the pion potential using the d(γ, p)n reaction data at higher energies [4].

In the present report we shall show the preliminary results of the analyses with the pion-theoretical potential. The calculations were made for the $M1+E1$ tran-

(1) J. IWADARE, S. OTSUKI, R. TAMAGAKI, and W. WATARI: *Suppl. Prog. Theor. Phys.*, N. 3 (1956), Part II.

(2) *Prog. Theor. Phys.*, to be published.

(3) J. IWADARE, S. OTSUKI, M. SANO, S. TAKAGI and W. WATARI: *Prog. Theor. Phys.*, **16**, 658 (1956); see also S. H. HSIEH: *Prog. Theor. Phys.*, **21**, 185 (1959).

(4) N. AUSTERN: *Phys. Rev.*, **108**, 973 (1957).

sition, using the deuteron wave function determined by the pion-theoretical potential ([1]) and the asymptotic form of the final wave functions. The coefficients a and b, and the angular dependence of the polarization of protons $P(\theta)$ are shown in Figs. 1 and 2. For the sake of comparison, a, and b calculated by DE SWART and MARSHAK ([5]) and a, b and $P(\theta)$ by DE SWART, CZYŻ and SAWICKI ([6]), on the basis of the $L \cdot S$ potential introduced by SIGNELL and MARSHAK, are shown in the same figures.

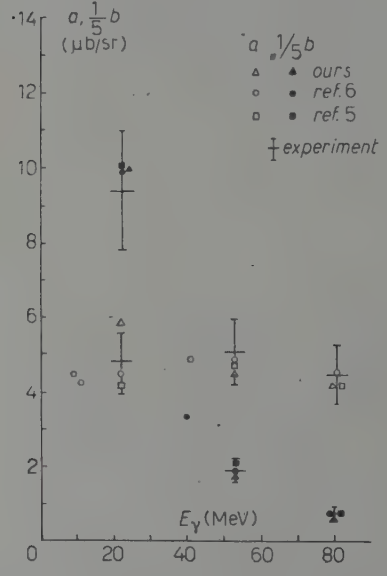

Fig. 1. – Angular distribution of the protons in the d(γ, p)n reaction. Cross section is expressed in the form: $d\sigma/d\Omega = a + b \sin^2\theta(1 + 2\beta \cos\theta)$.

The agreement of the calculated angular distribution with the experimental one is reasonable. This agreement is again due to the large D-state part of the deuteron determined by the sign and the magnitude of the observed Q-moment, and the strongly positive tensor potential in the ${}^3O$ state. The distortion of the final ${}^3P_J$ waves, the ${}^3D_1 \to {}^3P_J$ transitions, and the ${}^3D_1 \to {}^3F_2$ transition all contribute constructively to a. Unfortunately there is no experimental result for $P(\theta)$ available at present.

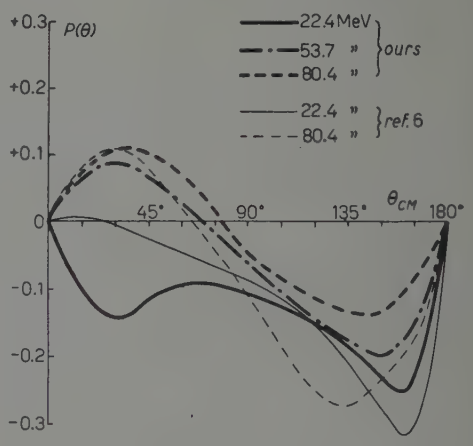

Fig. 2. – Polarization of the emitted protons in the d(γ, p)n reaction. The polarization is measured in the direction of the vector

$$n = \frac{k_\gamma \times k_p}{|k_\gamma \times k_p|}$$

The difference between our results from the pion potential and those from the Signell-Marshak potential is not appreciable. It would not be easy to distinguish two theories, even if the polarization data became available. Similar situations exist also for the nucleon-nucleon scattering at high energies.

It is our opinion that it would not be possible to find out any justification for the attempts to modify the pion-theoretical potential in the outer region, which theoretically has sound bases.

More accurate calculations are now in progress, and the results will be submitted to the *Progress of Theoretical Physics* (Japan) in near future.

([5]) J. J. DE SWART and R. E. MARSHAK: *Phys. Rev.*, **111**, 272 (1958).

([6]) J. J. DE SWART, W. CZYŻ and J. SAWICKI: *Phys. Rev. Letters*, **2**, 51 (1959).

IL NUOVO CIMENTO Vol. XIII, N. 6 16 Settembre 1959

Application of Fixed Angle Dispersion Relations to Proton-Proton Scattering.

W. Alles and A. Tomasini

Istituto di Fisica dell'Università - Bologna
Istituto Nazionale di Fisica Nucleare - Sezione di Bologna

(ricevuto il 15 Maggio 1959)

Fixed angle dispersion relations for nucleon-nucleon scattering have been recently written down by Cini, Fubini and Stanghellini (1). A two fold application of these relations to proton-proton scattering is possible, *i.e.*: to determine the pion-nucleon coupling constant f^2 if enough data on the phase shifts are available or to start from the knowledge of the coupling constant to try to discriminate among different phase shift sets. The present paper is limited to the study of the proton-proton singlet state, where the quasi-knowledge of the $^1S_0$ phase shift at energies up to 40 MeV (2,3) permits a quasi-determination of the coupling constant f^2.

The dispersion relation for the singlet scattering amplitude $T_{ss}(\omega, \cos\vartheta)$ is, according to CFS (1):

$$\text{(1)} \qquad \operatorname{Re} T_{ss}(\omega, \cos\vartheta) = \frac{\frac{1}{2}Mf^2}{2(1+\cos\vartheta)\omega+1} + \frac{\frac{1}{2}Mf^2}{2(1-\cos\vartheta)\omega+1} + \\ + \frac{1}{\pi}\int_0^{\infty} \frac{\operatorname{Im} T_{ss}(\omega', \cos\vartheta)}{\omega'-\omega}\,\mathrm{d}\omega' + \frac{1}{\pi}\int_{-\infty}^{-\omega_{\min}} \frac{\Omega_{ss}(\omega', c)}{\omega'-\omega}\,\mathrm{d}\omega',$$

with $\omega = q^2$, $q = p/\mu c$, p being the proton momentum in the CM system and μ and M the pion and proton masses respectively. The last term on the right hand side having no poles from $-\omega_{\min} = -2/(1+|\cos\vartheta|)$ to $+\infty$.

The singlet scattering amplitude being:

$$T_{ss}(\omega, \cos\vartheta) = \frac{1}{q}\sum_{l \text{ even}} (2l+1)\exp[i\delta_l]\sin\delta_l P_l(\cos\vartheta),$$

(1) M. Cini, S. Fubini and A. Stanghellini: to be published in the *Phys. Rev.* Further literature on nucleon-nucleon dispersion relations will be found in this paper.
(2) B. Cork: *Phys. Rev.*, **80**, 323 (1950).
(3) M. H. MacGregor: UCRL-5348.

we have chosen $\cos\vartheta = 1/\sqrt{3}$ in order to eliminate the contribution of the ${}^1D_2$ wave. Thus, neglecting ${}^1G_4$ wave effects, $T_{ss}(\omega, 1/\sqrt{3})$ reduces to

$$T_{ss}(\omega, 1/\sqrt{3}) = \frac{\exp[i\delta_0]\sin\delta_0}{q}.$$

From (1) one immediately obtains that

$$(2) \qquad F(\omega) = \left\{ \operatorname{Re} T_{ss}(\omega, 1/\sqrt{3}) - \frac{1}{\pi}\int_{\text{II}}^{\infty} \frac{\operatorname{Im} T_{ss}(\omega', 1/\sqrt{3})}{\omega' - \omega}\, \mathrm{d}\omega' \right\} \cdot$$

$$\cdot [2(1 + 1/\sqrt{3})\omega + 1][2(1 - 1/\sqrt{3})\omega + 1],$$

is analytic from $-\omega_{\min}$ to $+\infty$ and

$$F(-0.317) = 0.732(\tfrac{1}{2}Mf^2), \qquad F(-1.182) = -2.73(\tfrac{1}{2}Mf^2).$$

The value of $F(\omega)$ at the nearest to the physical region pole is small compared to the value of $F(\omega)$ for $\omega \geqslant 0$, while the value of $F(\omega)$ is fairly large at the second pole but to far from the physical region to allow a meaningful extrapolation. We have therefore considered the function

$$(3) \qquad f(\omega) = \left\{ \operatorname{Re} T_{ss}(\omega, 1/\sqrt{3}) - \frac{1}{\pi}\int_{\text{II}}^{\infty} \frac{\operatorname{Im} T_{ss}(\omega', 1/\sqrt{3})}{\omega' - \omega}\, \mathrm{d}\omega' - \right.$$

$$\left. - \frac{\frac{1}{2}Mf^2}{2(1 - 1/\sqrt{3})\omega + 1} \right\} \left[2\left(1 + \frac{1}{\sqrt{3}}\right)\omega + 1 \right],$$

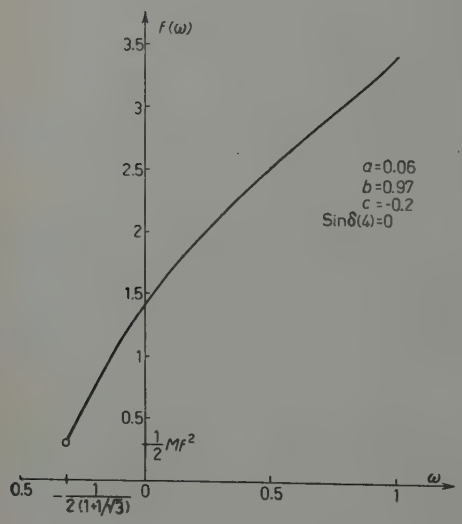

Fig. 1. – A typical $f(\omega)$ curve (see text).

which has only one pole at $\omega = -1/[2(1 + 1/\sqrt{3})] = -0.317$ and $f(-0.317) = \frac{1}{2}Mf^2$, taking care by successive iterations that the f^2 used in subtracting the contribution of the second pole is equal to the f^2 found by extrapolation of $f(\omega)$.

For the ${}^1S_0$ phase shift we have assumed the following energy dependence:

$$(4) \qquad q\operatorname{cotg}\delta_0 = a + b\omega + c\omega^2, \qquad 0 \leqslant \omega \leqslant 1,$$

$$(5) \qquad \sin\delta_0 = A + B\omega + C\omega^2, \qquad 1 \leqslant \omega \leqslant 4,$$

the choice of the form of $\sin\delta_0$ above $\omega = 1$ being determined by ease of calculation of the integral in (3). The coefficients in (5) have been taken so as to render continuous δ_0 and its de-

rivative at $\omega=1$ and leaving as a parameter sin δ_0 (4). The integrals have been carried out up to $\omega'=4$ and $f(\omega)$ has thus been calculated for $0\leqslant\omega\leqslant 1$ and fitted with a third degree polynomial in ω. The fit being always very good and its maximum deviation from $f(\omega)$ inferior to 2.5 ‰. A typical $f(\omega)$ curve is shown in Fig. 1.

The low energy p-p scattering fitted only with $^1S_0$ wave (2) indicates $a=0.06$, $b=0.97$ and $c=-0.2$ determining $f^2=0.082$ in good agreement with other determinations of the pion-nucleon coupling constant. Nevertheless, MACGREGOR (3) has shown that if P and D waves are introduced in the analysis of low energy proton-proton scattering the $^1S_0$ phase shift remains fairly undetermined. We have therefore variated a, b, c and sin δ_0 (4) to study the dependence on these parameters of the f^2 determined by this method.

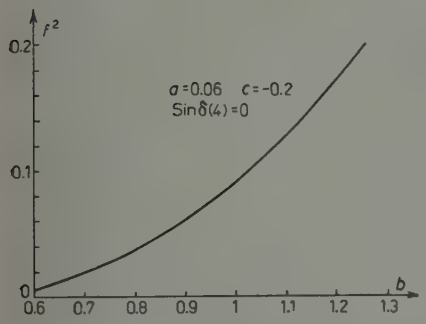

Fig. 2. – Coupling constant determined by this method as a function of b, with $q\,\mathrm{cotg}\,\delta_0=a+b\omega+c\omega^2$.

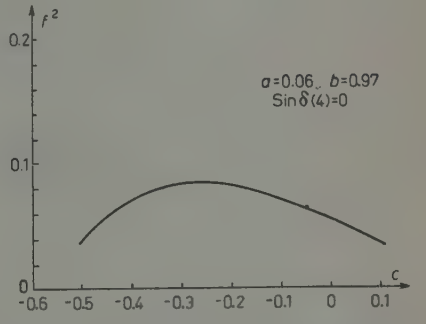

Fig. 3. – Coupling constant determined by this method as a function of c, with $q\,\mathrm{cotg}\,\delta_0=a+b\omega+c\omega^2$.

Figs. 2 and 3 summarize the resulting f^2 for different choices of the parameters b and c. Fig. 2 shows that f^2 is strongly dependent on b (half of the effective range), increasing monotonically with increasing b. Fig. 3 shows that f^2 has a stationary value around $c=-0.25$, decreasing once c deviates from this point. The dependence on the other parameters a and sin δ_0 (4) (the reciprocal scattering length and the $^1S_0$ phase shift at 160 MeV) is weaker. Variating a from 0.04 to 0.08, f^2 variates by 20% and variating sin δ (4) from -0.6 to $+0.6$, f^2 variates by 10%.

* * *

We are most grateful to Profs. CINI, FUBINI and STANGHELLINI who have suggested this subject to us, and to Prof. PUPPI without whose advice and constant encouragement this work would not have been possible. The assistance of the STAFF of the IBM-650 computer of the University of Bologna has been invaluable to us.

IL NUOVO CIMENTO Vol. XIII, N. 6 16 Settembre 1959

On the Surface Effect in Nuclear Photoreactions.

V. De Sabbata

Istituto di Fisica dell'Università - Ferrara
Istituto Nazionale di Fisica Nucleare - Sezione di Bologna

A. Tomasini

Istituto di Fisica dell'Università - Bologna
Istituto Nazionale di Fisica Nucleare - Sezione di Bologna

(ricevuto il 6 Giugno 1959)

Recent experiments on nuclear photoeffect chiefly concerning the angular distributions and the energetic spectra, show that the direct interaction between the incident γ and a single nuclear particle play an important role.

Particularly the angular distributions of protons are asymmetric in respect to 90 showing often a forward peak, generally accepted as a dipole-quadrupole interference.

In this note we study the interaction of γ-rays with the nucleons at the nuclear surface. As a preliminarly stage of this study we have used a model like that of Austern, Butler and Mc Manus [1], which in this case is perhaps very crude: namely we have assumed that the final wavefunction of the nucleon can be described by a plane wave; so far we have neglected the distortion of the plane wave due to the nuclear potential. We have assumed that the eigenfunctions of a shell-model in a square-well describe the initial states.

The integrals which appear in the expression of the probability transition are extended from the nuclear radius $R = r_0 A^{\frac{1}{3}}\, 10^{-13}$ cm up to infinity.

The main contribution will be given by more weakly bound nucleons *i.e.* by those states for which the wavefunction shows a tail extending more out of the nucleus.

The computations are made for various nuclei and for different values of the incident γ energy. We have chosen two different values of r_0 namely $r_0 = 1.2$ and $r_0 = 1.4$.

The cross-section is given by

$$\sigma = \frac{8\pi^3 \nu}{c} |H|^2 \varrho \,, \tag{1}$$

[1] N. Austern, S. T. Butler and H. Mc Manus: *Phys. Rev.*, **92**, 350 (1953).

where

$$H = \boldsymbol{e} \times \int u_f^* \sum_s e_s \boldsymbol{r}_s \exp[i\boldsymbol{k}\cdot\boldsymbol{r}_s]\, u_i \, \mathrm{d}\tau \,, \qquad |\boldsymbol{k}| = \frac{1}{\lambda} = \frac{2\pi\nu}{c} \,, \tag{2}$$

is the matrix element of the component, in the $\boldsymbol{e}$ direction, of the electric moment of the sistem, and:

ν the frequency of the incident γ-ray;
ϱ is the density of final states for unitary interval of energy;
$\boldsymbol{e}$ is the polarization unit vector;
u_f^* and u_i the final and initial wave functions respectively;
$\boldsymbol{r}_s$ the position of the e_s charge.

If the γ-ray is circularly polarized and the dipole approximation is assumed, then:

$$H = e' \int u_f^* (x + iy) u_i \, \mathrm{d}\tau \,, \tag{3}$$

where e' is the effective charge ($= -eZ/A$ and eN/A for the neutrons and protons respectively).

The angular distribution is:

$$\sum_{nl} N_l \alpha_{nl} \Big\{ l(l+1)(D_{l+1} + D_{l-1})^2 + \\ + [\tfrac{1}{2}(l+1)(l+2)\,|D_{l+1}|^2 + \tfrac{1}{2} l(l-1)\,|D_{l-1}|^2 - 3 D_{l+1} D_{l-1} l(l+1)] \sin^2\vartheta \Big\} \,, \tag{4}$$

where N_l are the normalization coefficients and $\sum_{nl}$ stands for summation over the nuclear levels, D_{l+1} and D_{l-1} are the radial parts of the integrals (3):

$$D_{l+1} = \int_R^\infty j_{l+1}(\alpha_{nl} r) h_l(\beta_{nl} r) r^3 \, \mathrm{d}r \,,$$

$$D_{l-1} = \int_R^\infty j_{l-1}(\alpha_{nl} r)\, h_l(\beta_{nl} r) r^3 \, \mathrm{d}r \,,$$

with:

$$\alpha_{nl} = \left[\frac{2M}{\hbar^2}(h\nu - \varepsilon_{nl})\right]^{\frac{1}{2}}; \qquad \beta_{nl} = \left[\frac{2M}{\hbar^2}\varepsilon_{nl}\right]^{\frac{1}{2}} \,,$$

where ε_{nl} is connected with the energetic levels of the nucleus as given by FEENBERG [2], ϑ in (4) is the angle between the direction of the bombarding photons and of the emerging particle.

One can remark the presence of an interference term between the $l \to l-1$ and $l \to l-1$ transitions. This term obviously disappears when integration over ϑ is carried in order to evaluate the total cross-section.

---

[2] E. FEENBERG: *Shell Theory of the Nucleus* (Princeton, 1955), p. 19.

This interference term causing a variation of the angular distribution with the incident energy of the γ-ray, the ratio b/a of the $a+b\sin^2\vartheta$ formula can be also negative.

We have also considered the general case without expanding (2) in terms of multipoles. In this case, in the center of mass system (2), becomes for neutrons

$$H = -\frac{eZ}{A}\int \exp\left[-i\boldsymbol{k}_1\cdot\boldsymbol{r}\right](x+iy)u_i\,\mathrm{d}\tau\,, \tag{5}$$

where

$$\boldsymbol{k}_1 = \boldsymbol{\alpha}_{nl} + \frac{1}{A}\,\boldsymbol{k} \sim \boldsymbol{\alpha}_{nl}\,,$$

and for neutrons the dipole approximation is a good one. In the case of protons (2) gives

$$H = -\frac{Z-1}{A}\,e\int \exp\left[-i\boldsymbol{k}_1\cdot\boldsymbol{r}\right](x+iy)u_i\,\mathrm{d}\tau + \frac{A-1}{A}\,e\int \exp\left[-i\boldsymbol{k}_2\cdot\boldsymbol{r}\right](x+iy)u_i\,\mathrm{d}\tau\,, \tag{6}$$

where

$$\boldsymbol{k}_2 = \boldsymbol{\alpha}_{nl} - \frac{A-1}{A}\,\boldsymbol{k} \sim \boldsymbol{\alpha}_{nl} - \boldsymbol{k}\,, \qquad \text{(not negligible)}\,.$$

The second term in (6) gives a valuable contribution and causes an asymmetric angular distribution in respect to 90°.

Preliminary results for the photoneutrons of ^{16}O are given in Tables I and II. The calculations are carried out for two different values of r_0.

TABLE I. – *Cross-section for* ^{16}O.

E \ r_0	$\sigma\cdot 10^{26}$					
	1.4			1.2		
	$1p$	$1s$	$1p+1s$	$1p$	$1s$	$1p+1s$
17.6	1.26	—	1.26	0.93	—	0.93
20	1.12	1.30	2.42	0.85	—	0.85
22	0.91	1.73	2.64	0.83	—	0.83
24	0.91	1.79	2.70	0.75	—	0.75
26	0.74	0.89	1.63	0.71	0.42	1.16
28				0.69	1.00	1.69
30				0.52	1.16	1.68
32				0.49	1.18	1.67
34				0.28	1.07	1.35

The value $r_0=1.2$ seems to give a better result. One can note that for this r_0, the angular distribution for $E=17.6$ MeV has a negative value of b/a and this seems to be in agreement with the experimental results of SPICER [3].

[3] B. M. SPICER: *Phys. Rev.*, **99**, 33 (1955).

The results of Spicer are for photoprotons with an incident energy of the γ-ray between 13.5 and 18.7 MeV; in the dipole approximation the results for photoprotons are the same as for photoneutrons). One can also note that for $r_0=1.2$ the contribution of the inner level of ^{16}O namely the $1s$ begins to have importance at an energy above 26 MeV giving a maximum near $(28\div30)$ MeV.

TABLE II. – *Angular distributions for* ^{16}O.

E \ r_0	$a+b\sin^2\vartheta$			
	1.2		1.4	
	a	b	a	b
	$1p$	$1p+1s$	$1p$	$1p+1s$
17.6	1.881	$-0.352=$	0.589	$0.88=$
20	1.101	$0.725=$	0.146	$1.34+2.70$
22	0.725	$1.091=$	0.084	$1.14+3.59$
24	0.426	$1.360=$	0.019	$0.99+3.73$
26	0.263	$1.561+1.605$	0.007	$0.80+1.87$

This is a general result of this model and one can try to explain the experimentally observed second maximun above the giant resonance with the contribution of inner levels which obviously appear at higher incident energies.

Similar results we have for a nucleus with $A=40$ (and $N=Z$) Tables III and IV show in the case of $r_0=1.2$ the presence of a second maximum and an angular distribution with a negative b/a ratio at lower energies.

TABLE III. – *Cross-section for* $A=40$.

E \ r_0	$\sigma\cdot10^{26}$									
	1.2					1.4				
	$2s$	$1d$	$1p$	$1s$	$\sum$	$2s$	$1d$	$1p$	$1s$	$\sum$
17.6	0.095	2.97	—	—	3.06	0.041	2.37	4.22	—	6.63
20	0.00025	3.42	—	—	3.42	0.163	2.03	3.53	—	5.72
22	0.140	3.02	3.52	—	6.68	0.109	1.69	3.77	0.104	5.67
24	0.290	2.90	2.34	—	5.53	0.102	1.39	4.07	1.501	7.06
26	0.437	2.75	1.88	—	5.07	0.086	1.15	3.39	2.105	6.74
28	0.587	2.42	2.14	—	5.15					
30	0.692	2.06	2.35	0.0722	5.17					
32	0.680	1.86	2.48	0.730	5.75					
34	0.622	1.55	2.47	1.24	5.88					
36	0.605	1.42	1.75	1.23	5.01					

TABLE IV. – *Angular distributions for* $A=40$.

$a + b \sin^2 \vartheta$				
E \ r_0	1.2		1.4	
	a	b	a	b
17.6	8.45	— 4.19	23.6	— 9.58
20	6.13	— 1.58	13.2	3.58
22	33.4	— 2.68	5.43	16.3
24	26.9	— 3.10	2.01	27.4
26	17.7	0.82	0.62	27.6
28	11.9	5.13		
30	6.26	9.19		
32	3.27	15.4		
34	1.48	19.4		
36	0.27	17.3		

The assistance of the IBM-650 Staff of Bologna University has been very useful for us and in particular we thank Dr. S. GIAMBUZZI who has set up the program for the computer.

IL NUOVO CIMENTO Vol. XIII, N. 6 16 Settembre 1959

Application of Fixed Angle Dispersion Relations to Nucleon-Nucleon Scattering in the Triplet State.

W. Alles and A. Tomasini

Istituto di Fisica dell'Università - Bologna
Istituto Nazionale di Fisica Nucleare - Sezione di Bologna

(ricevuto il 10 Giugno 1959)

The dispersion relations for nucleon-nucleon scattering written down by Cini, Fubini and Stanghellini (1), which were previously applied to the scattering in the singlet state (2), have now been applied to the scattering in the triplet state.

Triplet phase shifts for $l \geqslant 1$ are practically unknown (3) except at 310 MeV (4), and we have limited our work to the study of the ${}^3S_1$ phase shift.

The T_{11} and T_{00} scattering amplitudes are given by (5)

$$(1) \qquad \begin{cases} T_{11} = \dfrac{1}{2q} \sum_{l=0}^{\infty} \{(l+2)a_l^{l+1} + (2l+1)a_l^l + (l-1)a_l^{l-1}\} P_l(c) \,, \\ T_{00} = \dfrac{2}{2q} \sum_{l=0}^{\infty} \{(l+1)b_l^{l+1} + lb_l^{l-1}\} P_l(c) \,, \end{cases}$$

with $q = p/\mu c$, $c = \cos\theta$; for the other notations see reference (5). We have used the combination:

$$(2) \qquad \Theta = \tfrac{1}{6}\{2[T_{11}(c) + T_{11}(-c)] + T_{00}(c) + T_{00}(-c)\} \,,$$

where only even phase shifts are present; choosing $c = 1/\sqrt{3}$ and neglecting all phase shifts with $l \geqslant 4$, (2) becomes:

$$(3) \qquad \Theta = \frac{1}{q}(\alpha^1 \cos^2 \varepsilon_1 + \beta^1 \sin^2 \varepsilon_1) \,.$$

(1) M. Cini, S. Fubini and A. Stanghellini: to be published on *Phys. Rev.*
(2) W. Alles and A. Tomasini: *Nuovo Cimento*, (1959), referred to as I (to be published).
(3) For triplet P phase shifts see MacGregor: UCRL-5348.
(4) H. P. Stapp, T. J. Ypsilantis and N. Metropolis: *Phys. Rev.*, **105**, 307 (1957).
(5) P. Cziffra, M. H. MacGregor, M. J. Moravcsik and H. P. Stapp: UCRL-8510; M. L. Goldberger, Y. Nambu and R. Oehme: *Ann. Phys.*, **2**, 226 (1957).

At low energy the $^3D_1$ phase shift and mixing parameter ε_1 are both small; $\beta^1 \sin^2 \varepsilon_1$ can be neglected and $\cos^2 \varepsilon_1 \simeq 1$ in (3).

The dispersion relation for Θ is, according to C.F.S. [1]:

$$(4) \qquad \mathrm{Re}\,\Theta = \frac{\frac{1}{2}Mf^2}{1+2\omega(1-1/\sqrt{3})} + \frac{\frac{1}{2}Mf^2}{1+2\omega(1+1/\sqrt{3})} - \frac{\bar{A}}{\omega+\omega_D} + \\ + \frac{1}{\pi}\int_0^\infty \frac{\mathrm{Im}\,\theta}{\omega'-\omega}\,\mathrm{d}\omega' + \frac{1}{\pi}\int_{-\infty}^{-\omega_{\min}} \frac{\bar{\Omega}}{\omega'-\omega}\,\mathrm{d}\omega',$$

with

$$\bar{A} = \frac{1}{3}(2A_{11}+A_{00}) = \frac{2K(1-\varrho^2)}{(1+\varrho^2)(1-kr_e)}, \qquad \omega = q^2:$$

$\bar{A}$ depends on ϱ^2 and not on ϱ: if we put $\varrho^2=0$ we make an error of a few percent. Equation (4) can be used in several ways; the best way would be to use the function:

$$(5) \quad F(\omega) = \left[\mathrm{Re}\,\Theta - \frac{1}{\pi}\int_0^\infty \frac{\mathrm{Im}\,\Theta}{\omega'-\omega}\,\mathrm{d}\omega' + \frac{\bar{A}}{\omega+\omega_D} - \frac{\frac{1}{2}Mf^2}{1+2\omega(1-1/\sqrt{3})}\right](1+2\omega(1+1/\sqrt{3}),$$

which at $\omega = -1/2(1+1/\sqrt{3})$ should be equal to $\frac{1}{2}Mf^2$, since the values of $F(\omega)$ for $\omega \geqslant 0$ are not much greater than the residue of the pole.

However $\bar{A}/(\omega+\omega_D)$ is positive while

$$\mathrm{Re}\,\Theta - \frac{1}{\pi}\int_0^\infty \frac{\mathrm{Im}\,\Theta}{\omega'-\omega}\,\mathrm{d}\omega' - \frac{\frac{1}{2}Mf^2}{1+2\omega(1-1/\sqrt{3})},$$

is negative and of the same order of magnitude; thus a small error in the evaluation of $\bar{A}$ would give a large error in f^2.

We have therefore considered the function:

$$(6) \quad f(\omega) = \left[\mathrm{Re}\,\Theta - \frac{1}{\pi}\int_0^\infty \frac{\mathrm{Im}\,\Theta}{\omega'-\omega}\,\mathrm{d}\omega' - \frac{\frac{1}{2}Mf^2}{1+2\omega(1-1/\sqrt{3})}\right](\omega+\omega_D)\left(1+2\omega\left(1+\frac{1}{\sqrt{3}}\right)\right),$$

which at $\omega = -\omega_D$ is equal to $\bar{A}(1-3.154\omega_D)$ and at $\omega = -1/3.154$ to $\frac{1}{2}f^2M(\omega_D - 1/3.154)$. As in I, f^2 has been evaluated with an iteration method.

At low energy the $^3S_1$ phase shift is given by:

$$(7) \qquad q\,\mathrm{cotg}\,\delta = -\frac{1}{a} + \frac{1}{2}r_0q^2 - Pr_0^3q^4,$$

with $a=3.80$; if $P=0$, r_0 is equal to $r(0,-\omega_D)=1.214$ evaluated with the binding energy of the deuteron, while for $P \neq 0$

$$r_0 = r(0,-\omega_D)(1-2Pr^2\omega_D):$$

we have assumed the dependence (7) up to $\omega=1$.

For $\omega \geqslant 1$ we have assumed, as in I:

$$\sin\delta = A + B\omega + C\omega^2 , \tag{8}$$

the coefficients in (8) having been chosen so as to render continuous δ and its derivative at $\omega=1$, and leaving $\sin\delta\,(4)$ as a free parameter. The integration has been carried out up to $\omega=4$, and $f(\omega)$ has been calculated up to $\omega=1$, and fitted with a third degree polynomial in ω. A typical fit of $f(\omega)$ is shown in Fig. 1; the absolute deviation from $f(\omega)$ is always less than 0.003.

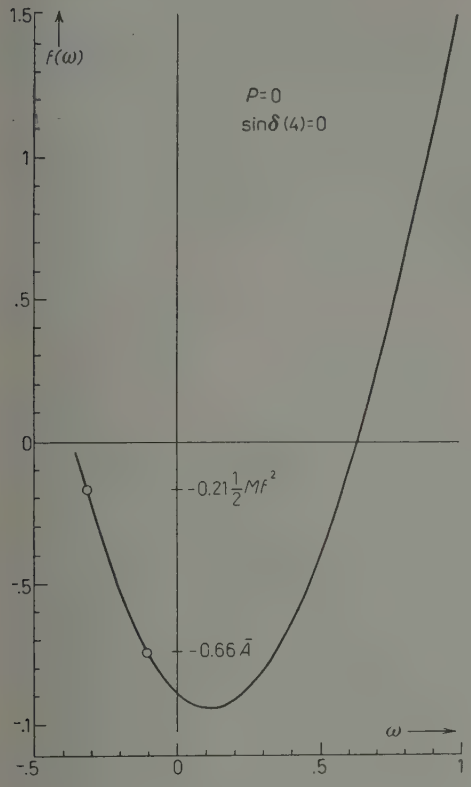

Fig. 1.

The values obtained for A are always good irrespective of the values

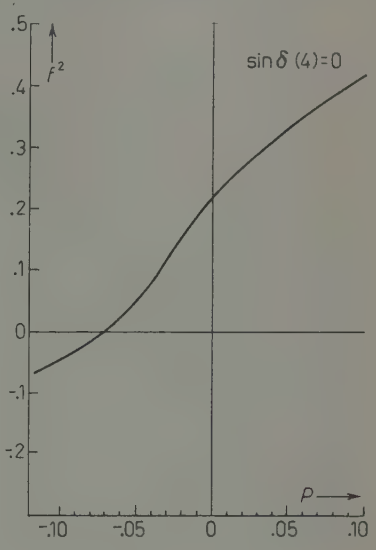

Fig. 2.

of $\sin\delta\,(4)$ and P; the dependence of f^2 on $\sin\delta\,(4)$ is also weak; Fig. 2 summarizes the resulting f^2 for different choices of P.

These results seem to indicate $P \simeq -0.04$; however the residue of the pole is small compared to the values of $f(\omega)$ for $\omega \geqslant 0$, and some doubts remain on the validity of this conclusion, although the fit of $f(\omega)$ is good.

The result $P < 0$, is in agreement with those of the Signell and Marshak model (6).

The numerical calculations have been performed with the University of Bologna IBM-650 electronic computer.

* * *

We wish to thank Profs. Cini, Fubini and Stanghellini, who also have suggested this subject to us, and Profs. Puppi and Minguzzi for useful discussions and advices.

(6) P. S. Signell and R. E. Marshak: *Phys. Rev.*, **109**, 1229 (1958).

IL NUOVO CIMENTO Vol. XIII, N. 6 16 Settembre 1959

Wightman Functions and Jacobi Identity.

P. Gulmanelli and E. Montaldi

Istituto di Scienze Fisiche dell'Università - Milano
Istituto Nazionale di Fisica Nucleare - Sezione di Milano

(ricevuto il 12 Giugno 1959)

In the frame of the present axiomatic scheme of quantum field theory the integral representations of vacuum expectation values of products of Heisenberg operators have gained an increasing importance [1].

Dyson [2] has recently proposed an integral representation for the double commutators of three scalar fields $A(x_1)$, $B(x_2)$, $C(x_3)$, which takes explicitly into account the consequences of microscopic causality, stated as usual by the requirement that two field operators commute at space-like distances. Such a representation however fails to exhibit the basic symmetry property embodied in the Jacobi identity.

In view of the interest for future applications it seems worth-while to call attention on a possible way of overcoming this difficulty.

Our considerations rest essentially on a result by V. N. Gribov [3], which can be expressed as follows:

$$(1) \qquad \langle \varphi(x_1)\varphi(x_2)\varphi(x_3)\rangle_0 = \int_0^\infty \mathrm{d}\alpha \int_0^\infty \mathrm{d}\beta \int_0^\infty \mathrm{d}\gamma f(\alpha, \beta, \gamma)\, \Delta^{(+)}(y_{12}; \gamma)\, \Delta^{(+)}(y_{13}; \beta)\, \Delta^{(+)}(y_{23}; \alpha)\,,$$

where $y_{rs} = x_r - x_s$, and φ is a scalar field operator.

Furthermore as a consequence of causality requirements $f(\alpha, \beta, \gamma)$ is a totally symmetric function. In eq. (1) the fields are taken equal, but as we shall see later the extension to the case of different fields can be done in a straightforward way.

---

(1) H. Lehmann: *Nuovo Cimento*, **11**, 342 (1954); A. S. Wightman: *Phys. Rev.*, **101**, 860 (1956); R. Jost and H. Lehmann: *Nuovo Cimento*, **5**, 1598 (1957); G. Källén and A. S. Wightman: *Dan. Mat.-Fys. Skr.*, **1**, no. 6 (1958); G. Källén and H. Wilhelmsson: preprint (1958).

(2) F. J. Dyson: *Phys. Rev.*, **111**, 1717 (1958) (hereafter referred to as I).

(3) V. N. Gribov: *Journ. Exp. Theor., Phys.* **34** (7), 903 (1958).

From eq. (1) it follows immediately that

$$(2)\qquad \langle[\varphi(x_1),[\varphi(x_2),\varphi(x_3)]]\rangle_0 =$$

$$=\iiint \mathrm{d}\alpha\,\mathrm{d}\beta\,\mathrm{d}\gamma f(\alpha,\beta,\gamma)\,\Delta(y_{23};\alpha)\{\Delta^{(+)}(y_{12};\gamma)\,\Delta^{(+)}(y_{13};\beta)-\Delta^{(+)}(y_{21};\gamma)\,\Delta^{(+)}(y_{31};\beta)\}\,.$$

The connection with Dyson formulae can easily be established. If one goes over to the momentum representation of the Δ functions, by means of a simple change of integration variables, one obtains

$$(3)\qquad \Delta^{(+)}(y_{12};\gamma)\,\Delta^{(+)}(y_{13};\beta)\,\Delta(y_{23};\alpha) =$$

$$=\int \mathrm{d}^4h'\,\mathrm{d}^4h''\exp\left[ih'\cdot(x_1-x_2)+ih''\cdot(x_2-x_3)\right]W_1(h',h'')\,,$$

where

$$(4)\qquad W_1(h',h'') =$$

$$=\frac{i}{(2\pi)^9}\int \mathrm{d}^4h\,\theta(h_0)\,\theta(h'_0-h_0)\,\varepsilon(h''_0-h'_0+h_0)\,\delta(h^2+\gamma^2)\,\delta\big((h'-h)^2+\beta^2\big)\,\delta\big((h''-h'-h)^2+\alpha^2\big),$$

and similarly

$$(3')\qquad \Delta^{(+)}(y_{21};\gamma)\,\Delta^{(+)}(y_{31};\beta)\,\Delta(y_{23};\alpha) =$$

$$=\int \mathrm{d}^4h'\,\mathrm{d}^4h''\exp\left[ih'\cdot(x_1-x_2)+ih''\cdot(x_2-x_3)\right]W_2(h',h'')\,,$$

$$(4')\qquad W_2(h',h'') =$$

$$=\frac{i}{(2\pi)^9}\int \mathrm{d}^4h\,\theta(-h_0)\,\theta(h_0-h'_0)\,\varepsilon(h''_0-h'_0+h_0)\,\delta(h^2+\gamma^2)\,\delta\big((h'-h)^2+\beta^2\big)\,\delta\big((h''-h'+h)^2-\alpha^2\big).$$

By inspection of the structure of the integrals (4) and (4') one sees that:

$$(5)\qquad W_1-W_2=0 \qquad \text{if} \qquad h'^2>0\,, \qquad \text{or both} \qquad h''^2>0\,,\quad (h'-h'')^2>0\,.$$

This holds true, then, also for the integral

$$\iiint \mathrm{d}\alpha\,\mathrm{d}\beta\,\mathrm{d}\gamma f(\alpha,\beta,\gamma)\,(W_1-W_2)\,,$$

which in our notation corresponds to the function $F(p,q)$ defined by (I.3), (I.5). (Remark that the metric we employ is different from Dyson's).

Now if one permutes cyclically the points x_1, x_2, x_3 in eq. (2) and then adds up, one sees that, by virtue of the symmetry properties of f, the Jacobi identity is satisfied.

When considering three different fields $A(x_1)$, $B(x_2)$, $C(x_3)$, the argument applies with trivial changes. It suffices to label the function $f(\alpha, \beta, \gamma)$ by three indices, whose order corresponds to that of the fields in the double commutator. As a consequence of the causality condition one obtains now

$$f_{ABC}(\alpha, \beta, \gamma) = f_{BAC}(\beta, \alpha, \gamma) = f_{ACB}(\alpha, \gamma, \beta) . \tag{6}$$

instead of the total symmetry of f.

* * *

It is a pleasure for us to thank Prof. P. CALDIROLA and Prof. A. LOINGER for their kind interest and comments.

IL NUOVO CIMENTO Vol. XIII, N. 6 16 Settembre 1959

On Surface Direct Photoneutrons (*).

A. Agodi, E. Eberle and L. Sertorio

Istituto di Fisica dell'Università - Catania
Centro Siciliano di Fisica Nucleare - Catania

(ricevuto il 23 Giugno 1959)

The experimental results (1) on the energy spectra of photoneutrons from ^{40}Ca and ^{103}Rh targets, irradiated with bremsstrahlung photons of 30 MeV max. energy, have shown features unexpected on the basis of Wilkinson's theory (2).

In fact the ^{40}Ca spectrum shows an unusually high yield of photoneutrons around 3.5 MeV, in qualitative agreement with (I), but also an excess of photoneutrons with energy above, say, 7 MeV.

The ^{103}Rh spectrum, while in qualitative agreement with (I) at low energy and around 8.5 MeV, shows an excess of photoneutrons between 4 to 7 MeV.

We have investigated the possibility of understanding the mentioned experimental results only in terms of $E1$ single particle transitions by taking into account off resonance effects neglected in Wilkinson's theory.

Now, explaining the 3.5 MeV peak in the energy spectrum of the photoneutrons from ^{40}Ca according to (I), it turns out that the high energy yield ought to be due essentially to direct processes at photon energies far from the giant resonance. At such photon energies the $E1$ direct photoeffect is expected (3) to give a contribution to the yield of the same order of magnitude as that predicted by Wilkinson's theory at energies in the neighbourhood of the giant resonance.

We have pointed out that, if the interaction between the emitted nucleon and the residual nucleus is described by a complex potential well (3,4), at nucleon energies of the order of 10 MeV the imaginary part of the well becomes three to four times deeper than at 3 MeV (5). This has the effect of drastically reducing the amplitude of the final single particle wave function inside the nucleus. This, in turn, implies that at energies

(*) A first report on this work has been given at the 1948 Meeting of the Società Italiana di Fisica (Palermo, Nov. 1958).

(1) A. Agodi, S. Cavallaro, G. Cortini, V. Emma, C. Milone, R. Rinzivillo, A. Rubbino and F. Ferrero: *Proc. of the* 1958 *Paris Conf. on Nucl. Phys.*

(2) D. H. Wilkinson: *Physica*, **22**, 1039 (1956); A. Agodi: *Nuovo Cimento*, **8**, 515 (1958), to be further referred to as (I).

(3) G. E. Brown and J. S. Levinger: *Proc. Phys. Soc.*, **71**, 733 (1958).

(4) C. Bloch: *Nuclear Physics*, **4**, 503 (1957).

(5) A. Melkanoff *et al.*: *Phys. Rev.*, **101**, 507 (1957); A. M. Lane and C. F. Wandel: *Phys. Rev.*, **98**, 1524 (1955); M. Cini and S. Fubini: *Nuovo Cimento*, **2**, 75 (1955).

somewhat higher than that of the giant resonance, the direct photoeffect can be studied in good approximation with methods similar to those well known in the theory of surface type direct reactions ([6]).

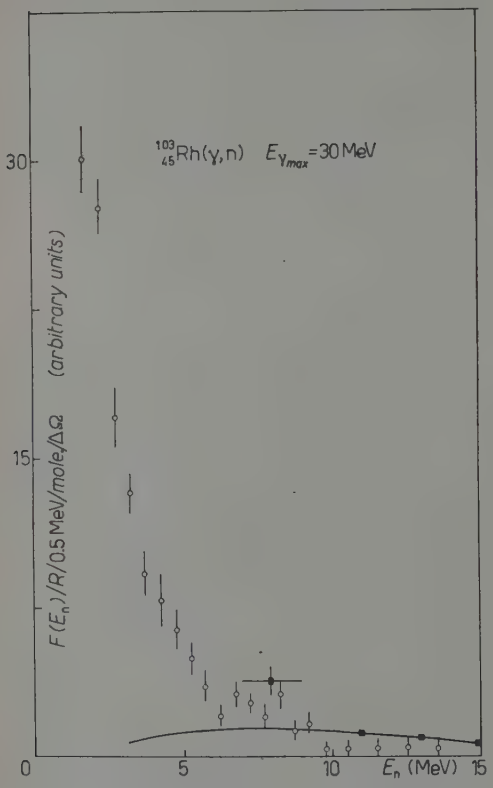

Fig. 1. – ^{40}Ca photoneutron energy spectrum at 90°.
- experimental points
- theoretical points, surface contribution
- theoretical points, according to (I).

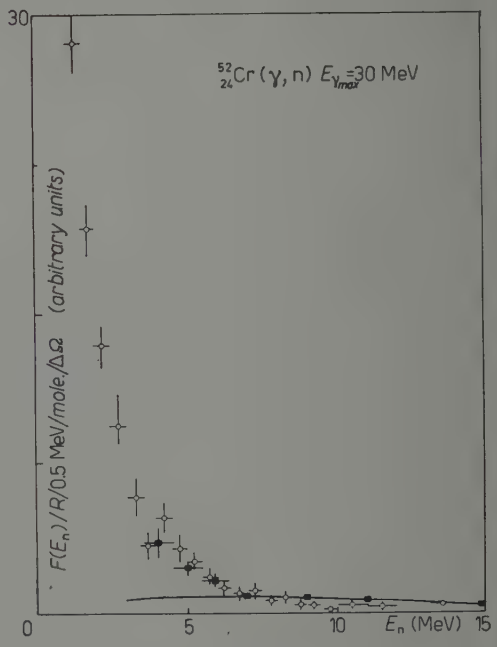

Fig. 2. – ^{52}Cr photoneutron energy spectrum, at 90°.
- experimental points
- theoretical points, surface contribution
- theoretical points, according to (I).

A preliminary calculation of such surface effects in the energy spectra of the photoneutrons from ^{40}Ca, ^{52}Cr and ^{103}Rh has been performed by assuming *j-j* coupling for the initial shell model nuclear state and considering transitions from the last filled neutron shell only. In the mentioned nuclei the last filled neutron shell is also that of highest orbital angular momentum, which, according to Wilkinson's theory, gives the most important contribution to photon absorption in the neighbourhood of the giant resonance.

The probability amplitude for the (γ, n) surface reaction to first order in the electric charge has been expressed in terms of single particle reduced matrix elements of the *E*1 interaction hamiltonian ([7]).

With the aim of obtaining a first

([6]) N. AUSTERN, S. T. BUTLER and H. MCMANUS: *Phys. Rev.*, **92**, 350 (1953); I. HOROWITZ: *Physica*, **22**, 969 (1956); S. T. BUTLER: *Phys. Rev.*, **106**, 272 (1957).

([7]) A. M. LANE and L. A. RADICATI: *Proc. Phys. Soc.*, A **67**, 167 (1954).

approximation, we have evaluated these reduced matrix elements by taking as final wave function a plane wave with amplitude different from zero only outside the target nucleus, and as initial wave function that of a bound state in a rectangular (real) well, with binding energy equal to the threshold energy of the (γ, n) reaction.

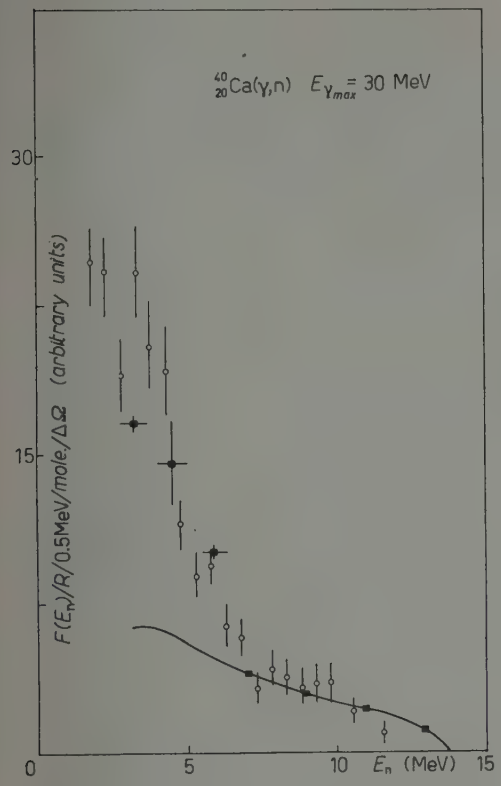

Fig. 3. – ^{103}Rh photoneutron energy spectrum, at 90°.
○ experimental points
■ theoretical points, surface contribution
-■- theoretical points, according to (I).

We have calculated in this way the energy spectra of the surface direct photoneutrons emitted in the plane orthogonal to the direction of the incoming photon beam, assumed with a bremsstrahlung spectrum of 30 MeV max. energy. The results obtained for ^{30}Ca, ^{52}Cr and ^{103}Rh targets are the curves shown in the Fig. 1, 2, 3 respectively.

The energy spectra of the direct photoneutrons due to absorption of photons with energy in the neighbourhood of the giant resonance have been calculated according to (I), and the results are shown in the same figures.

It seems that the theoretical points fit reasonably well those giving the experimental results.

A more detailed account of the calculations and a discussion of the involved approximations will be given elsewhere.

* * *

We thank heartily Prof. M. Cini and Prof. G. Cortini for many interesting discussions.

IL NUOVO CIMENTO Vol. XIII, N. 6 16 Settembre 1959

Renormalization of a Parity Non-Conserving Theory.

C. H. Albright, R. Haag and S. B. Treiman
Palmer Physical Laboratory, Princeton University - Princeton, N. J.

(ricevuto il 26 Giugno 1959)

In a recent paper (1), K. Sekine has extended the work of d'Espagnat and Prentki (2) on the construction of a parity non-conserving theory by explicitly working out the equations which determine the renormalization constants of the theory. However, an application of lowest order perturbation theory leads him to conclude that these equations do not admit a consistent solution — unless the theory is in fact made parity conserving. We do not agree with this conclusion and shall outline our reasons in the present note. The treatment given here is very concise and is meant to be read in connection with Sekine's original work. Put briefly, we believe that Sekine's discussion is correct in its general approach and, in fact, in most particulars. The error, we believe, lies in a technical oversight which occurs in his discussion of the lowest order perturbation approximation.

Sekine considers a relativistic field theory involving two fermion fields, ψ and χ, and a boson field φ. They interact with scalar and pseudoscalar couplings, so that the theory is parity violating. But CP invariance holds. The unrenormalized fields are taken to satisfy the canonical equal-time commutation relations. This entails certain restrictions on the weight functions which characterize the spectral representation of the propagators of the theory; these restrictions in effect define the renormalization constants of the theory. The analysis generalizes corresponding discussions given by Källén (3) and Lehmann (4) for parity-conserving theories. For our present purposes the situation is most clearly brought out in terms of the unrenormalized propagators. The renormalized quantities, owing to their implicit character, tend to obscure matters if one is not careful.

Following Sekine, we consider the matrix elements respectively, of $\psi(x)$ and $\psi^{(0)}(x)$ between the physical vacuum $|0\rangle$ and a physical one-particle state $|1\rangle$. Here $\psi(x)$ is the unrenormalized field; $\psi^{(0)}$, the corresponding « in » field. The latter satisfies the usual free field equations of motion and canonical commutation relations. From general invariance considerations, the matrix elements are related by

$$\langle 0|\psi(x)|1\rangle = (N + N'\gamma_5)\langle 0|\psi^{(0)}(x)|1\rangle\,, \tag{1}$$

(1) K. Sekine: *Nuovo Cimento*, **11**, 87 (1959).
(2) B. d'Espagnat and J. Prentki: *Nuovo Cimento*, **6**, 2989 (1957).
(3) G. Källén: *Helv. Phys. Acta*, **25**, 417 (1952); *Physica*, **19**, 850 (1953).
(4) H. Lehmann: *Nuovo Cimento*, **11**, 342 (1954).

where N and N' are the two renormalization constants associated with a parity non-conserving theory. The equal-time commutation relations are taken to be

$$\{\psi(x), \overline{\psi}(x')\}_{x_0=x_0'} = \gamma_4 \delta(\boldsymbol{x} - \boldsymbol{x}') \,. \tag{2}$$

In the immediately following steps we depart slightly from Sekine's paper. Let us consider the unrenormalized propagator $S^{(+)\prime}(x-x')$. Because of the CP invariance of the theory this quantity has the structure

$$S^{(+)\prime}(x-x') = i\langle 0 \,|\, \psi(x)\, \overline{\psi}(x') \,|\, 0\rangle = \tag{3}$$

$$= -\frac{i}{(2\pi)^3} \int \mathrm{d}^4 k\, \theta(k_0) \exp\left[ik\cdot(x-x')\right] \left\{ i\gamma\cdot k R_1(-k^2) + R_2(-k^2) + i\gamma_5 \gamma\cdot k R_3(-k^2)\right\} .$$

This, together with the equal-time condition of eq. (2), leads to the following conditions on the spectral functions:

$$\int_0^\infty \mathrm{d}\varkappa^2 R_1(\varkappa^2) = 1 \,, \qquad \int_0^\infty \mathrm{d}\varkappa^2 R_3(\varkappa^2) = 0 \,. \tag{4}$$

In the standard way we can now expand $\langle 0 \,|\, \psi(x)\, \overline{\psi}(x') \,|\, 0\rangle$ in a sum of contributions from a complete set of physical states, singling out in particular, via eq. (1), the contribution from the one particle state. In this way we find

$$\begin{cases} R_1(\varkappa^2) = & (N^2 + N'^2)\delta(\varkappa^2 - m^2) + \sigma_1(\varkappa^2) \,, \\ R_2(\varkappa^2) = & -m(N^2 - N'^2)\delta(\varkappa^2 - m^2) + \sigma_2(\varkappa^2) \,, \\ R_3(\varkappa^2) = & \quad 2NN'\delta(\varkappa^2 - m^2) + \sigma_3(\varkappa^2) \,; \end{cases} \tag{5}$$

the σ_i represent the contributions from states other than the one-fermion state and vanish for $\varkappa^2 \leqslant (m+\mu)^2$, where m and μ are the fermion and boson masses respectively. So far these results are all implicitly contained in Sekine's paper, but he chooses to emphasize corresponding matters for the renormalized fields.

Consider now what happens when a perturbation expansion is made. In zeroeth order, where the couplings are completely ignored, we of course find

$$\begin{aligned} R_1^{(0)} = & \quad \delta(\varkappa^2 - m^2) \,, \\ R_2^{(0)} = & -m\,\delta(\varkappa^2 - m^2) \,, \\ R_3^{(0)} = & \quad 0 \,. \end{aligned}$$

These results correspond to the zeroeth order values $N=1$, $N'=0$ for the renormalization constants.

In the next order, following Sekine, we write

$$\left(\gamma_\mu \frac{\partial}{\partial x_\mu} + m\right)\left(\gamma_\mu^x \frac{\partial}{\partial x_\mu'} - m\right)\langle 0 \,|\, \psi(x)\, \overline{\psi}(x') \,|\, 0\rangle \equiv -\langle 0 \,|\, f(x)\overline{f}(x') \,|\, 0\rangle \approx \tag{6}$$

$$\approx -g^2 \langle 0 \,|\, (\alpha + \beta\gamma_5)\chi^{(0)}(x)\, \overline{\chi}^{(0)}(x')(\alpha - \beta\gamma_5) \,|\, 0\rangle \langle 0 \,|\, \varphi^{(0)*}(x)\varphi^{(0)}(x') \,|\, 0\rangle \,,$$

where αg and βg are respectively the scalar and pseudoscalar coupling constants. Comparison of (6) with (3) yields as a possible solution for R_3

$$(7) \qquad ''R_3(\varkappa^2)'' = -\frac{2\alpha\beta J(\varkappa^2)}{\varkappa^2(\varkappa^2 - m^2)},$$

where $J(\varkappa^2)$ is proportional to g^2 and is defined in Sekine's paper. This solution (or rather, its analog for the renormalized propagator) is the one which he in fact adopts. It is inconsistent with eq. (4) and represents the contradiction which Sekine claims.

But to any solution of (6) one can always add a solution of the homogeneous equation obtained by setting the right-hand side equal to zero. In effect, this means one can add to (7) any multiple of $\delta(\varkappa^2 - m^2)$. From (5) we see that the correct solution must be taken to be

$$(8) \qquad \dot{R}_3(\varkappa^2) = 2NN'\delta(\varkappa^2 - m^2) - \frac{2\alpha\beta J(\varkappa^2)}{\varkappa^2(\varkappa^2 - m^2)}.$$

Together with a corresponding expression for $R_1(\varkappa^2)$ this determines, via eqs. (4), the renormalization constants N and N' to order g^2. There is no contradiction.

IL NUOVO CIMENTO Vol. XIII, N. 5 16 Settembre 1959

Considerations on the Cross Section for Pion Production in Proton-Proton Collisions.

E. Ferrari

Istituto di Fisica dell'Università - Roma
Istituto Nazionale di Fisica Nucleare - Sezione di Roma

(ricevuto il 10 Luglio 1959)

This note deals with the application of the Chew and Low [1] extrapolation method to the processes

(1) $$p+p \to n+p+\pi^+$$

(2) $$p+p \to p+p+\pi^0 .$$

We will denote by p_1, k_1 and p_2, k_2, q_2 the 4-momenta of the incoming protons and outgoing nucleons and pion respectively. We put also [2]

(3) $$\Delta^2 = (k_2 - k_1)^2 \qquad u^2 = -(p_2 + q_2)^2 .$$

The Chew-Low result states that the differential cross section for processes (1) and (2) with respect to the variables Δ^2 and u^2, for $\Delta^2 \simeq -\mu^2$ (outside the physical region) approaches

(4) $$\frac{\mathrm{d}^2\sigma}{\mathrm{d}\Delta^2 \mathrm{d}u^2} \xrightarrow{\Delta^2 \to -\mu^2} \frac{f^2}{2\pi} \frac{\Delta^2}{\mu^2} \frac{\varkappa u}{q_L^2} \frac{\sigma_s(\varkappa)}{(\Delta^2+\mu^2)^2} .$$

Here f^2 is the renormalized π^0-proton coupling constant, $\varkappa$ is the magnitude of the momentum of the pion and the nucleon in elastic π-p scattering (in the c.m.s.) at total energy u [3], q_L is the momentum of the incident proton in the laboratory

---

(1) G. F. Chew and F. E. Low: *Unstable particles as targets in scattering experiments* (to be published in *Phys. Rev.*).

(2) In (1) it is indicated how the quantities Δ^2 and u^2 can be related to quantities measurable in the lab. syst. In the following M = nucleon mass, μ = pion mass.

(3) $$\varkappa = \frac{1}{2u}\left[u^4 - 2u^2(M^2+\mu^2) + (M^2-\mu^2)^2\right]^{\frac{1}{2}} .$$

system and $\sigma_s(\varkappa)$ is the cross section for the elastic scattering

$$(4') \qquad \pi_0+\mathrm{p}\to\begin{cases}\pi^++\mathrm{n}\\ \pi^0+\mathrm{p}\end{cases},$$

in the case of processes (1) and (2) respectively.

It can be shown that the right-hand side of (4) is exactly obtained (also in the physical region, where $\Delta^2>0$) if we consider the contribution of the graph shown in Fig. 1 to processes (1) or (2). This graph is the only one which produces a 2nd order pole in the cross section for $\Delta^2=-\mu^2$, and near this point it should therefore give the dominant contribution.

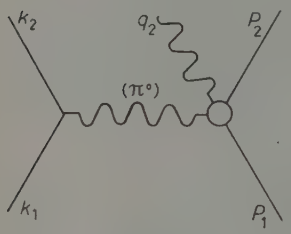

Fig. 1.

For fixed u, one can check Eq. (4) by determining the cross section $\mathrm{d}^2\sigma/\mathrm{d}\Delta^2\,\mathrm{d}u^2$ experimentally and then multiplying it by [4]

$$2\pi q_{\mathrm{L}}^2\,\frac{(\Delta^2+\mu^2)^2}{\varkappa u}\,.$$

The result, considered as a function of Δ^2, should extrapolate for $\Delta^2\to-\mu^2$ to the product $-f^2\sigma_s(\varkappa)$ which is well known, especially for $\varkappa$ in the neighbourhood of the resonance value. We wish to point out that so far the extrapolation method has been tentatively applied to cases in which the residue of the extrapolation is not known, with the hope of obtaining information about it. In our case, since the residue is known with satisfactory accuracy, an experimental verification of (4) is suggested as a test of the applicability of the method, and could give an indication of the best way to extrapolate (see note [4]). It is apparent that, should the extrapolation procedure prove to be difficult in this case, its application to cases in which the residue is not known would be probably unsuccessful.

The energy T of the incident proton in the lab. syst. should be chosen so that u may assume all the values for which the cross section σ_s is well known, in particular near the resonance value ($u=1.314M$). Since u varies from $M+\mu$ to $W-M$ [5], the most favourable values for W are the ones larger than $\sim 2.3M$, which corresponds to $T\geqslant 630$ MeV.

In order to keep u constant the experimentalist must make a selection from his experimental data. It is not justified to try to improve statistics by putting together all data referring to a given Δ^2 and to expect the function of Δ^2 obtained in this way to extrapolate to some « average » cross section for elastic scattering, integrated over u^2 from the minimum to the maximum value. If we consider (cfr. Fig. 2*a* for $T=600$ and 900 MeV) the phase space diagram for the process in the Δ^2-u^2 plane we see that, for fixed Δ^2, u varies only up to a maximum value

---

[4] This manner of extrapolating, which gives a negative residue, is the way suggested by Chew and Low. One could, however, tentatively multiply both sides of (4) by an arbitrary function of Δ^2 alone, containing no poles for $\Delta^2>-\mu^2$: a convenient choice might make the extrapolation easier.

[5] W is defined (as in [1]) through

$$W^2=-(p_1+k_1)^2=4M^2(1+T/2M)\,.$$

It is a constant parameter for fixed T.

dependent on Δ^2 itself; but integration of (4) up to this Δ^2-dependent limit of u^2 is of no use for the extrapolation procedure, since this limit is not real for $-4M^2 < \Delta^2 < 0$. An integration over u between $M+\mu$ and a fixed value of u,

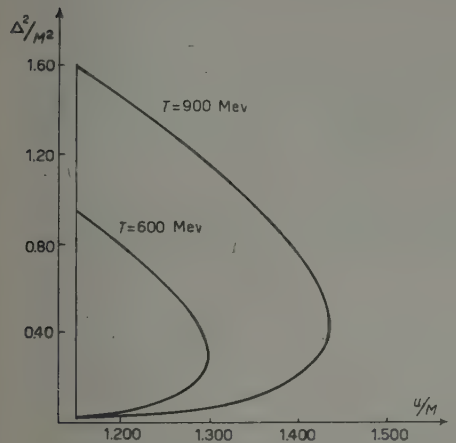

Fig. 2*a*. – Phase-space diagram in the $\Delta^2 - u^2$ plane.

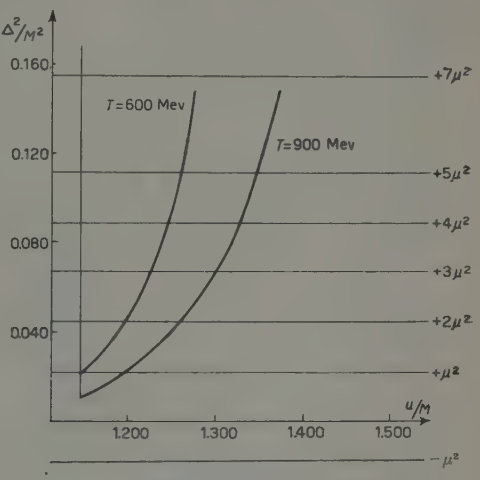

Fig. 2*b*. – Dependence on u of the lower limit of Δ^2. The right hand scale gives Δ^2 in units of μ^2.

denoted by u^*, can be reasonably performed only referring to a rectangular region of the $\Delta^2 - \mu^2$ plane entirely contained in the phase space diagram of Fig. 2*a*. Since the lower limit of Δ^2 varies rather slowly for u close to the minimum value, such a region can be chosen as to include all the experimental points which are of much more interest for the extrapolation. We have calculated the result to expect for such a procedure. For fixed Δ^2 we have

$$\lim_{\Delta^2 \to -\mu^2} 2\pi q_L^2 (\Delta^2 + \mu^2)^2 \int_{(M+\mu)^2}^{u^{*2}} \frac{\mathrm{d}^2\sigma}{\mathrm{d}\Delta^2 \mathrm{d}u^2}\, \mathrm{d}u^2 = -f^2 \int_{(M+\mu)^2}^{u^{*2}} \varkappa u\, \sigma_s(\varkappa)\, \mathrm{d}u^2 . \tag{5}$$

The integral on the right-hand side of (5) can be computed using some simplifications (6). The result is (for process (1))

$$\int_{(M+\mu)^2}^{u^{*2}} \varkappa u\, \sigma_s(\varkappa)\, \mathrm{d}u^2 \simeq \left[\frac{(u+M)^5}{u^3}\right]_{\text{Average}} \left\{ \cosh^{-1} G - \right.$$

$$- \sum_{i=1}^{2} \left(A_i \log \frac{[\alpha_i G - 1 + \gamma_i (G^2-1)^{\frac{1}{2}}]^2 + [\beta_i G + \delta_i (G^2-1)^{\frac{1}{2}}]^2}{(\alpha_i - G)^2 + \beta_i^2} + \right.$$

$$\left. \left. + 2B_i \operatorname{tg}^{-1} \frac{-\beta_i (G^2-1) + (\alpha_i \delta_i - \beta_i \gamma_i - \delta_i G)(G^2-1)^{\frac{1}{2}}}{-\alpha_i (G^2+1) + (\alpha_i^2 + \beta_i^2 + 1) G + (\alpha_i \gamma_i + \beta_i \delta_i - \gamma_i G)(G^2-1)^{\frac{1}{2}}} \right) \right\} . \tag{6}$$

(6) In this integration only the resonant phase-shift α_{33} has been kept in σ_s, for which we have used the Anderson formula. Of course this result is less accurate for $u^* \gg 1.5\ M$, because in this region α_{33} is no longer predominant.

where $G = (u^* - M)/\mu$, and

$$A_1 = -0{,}439 \quad B_1 = -0.0977 \quad \alpha_1 = -1.951 \quad \beta_1 = +7.431 \quad \gamma_1 = +1.935 \quad \delta_1 = -7.493$$

$$A_2 = +0.0575 \quad B_2 = +0.0516 \quad \alpha_2 = +1.951 \quad \beta_2 = +0.378 \quad \gamma_2 = +1.689 \quad \delta_2 = +0.436.$$

The value of the function tg^{-1} must be comprised between 0 and $\pi/2$ in the case $i = 1$, between $-\pi$ and 0 in the case $i = 2$. The average value occurring in the formula can be easily calculated; it can be substituted with good approximation by the function calculated at the point $u = (u^* + M)/2$:

$$\left|\frac{(u+M)^5}{u^3}\right|_{\text{Average}} \simeq \frac{1}{4}\frac{(u^*+3M)^5}{(u^*+M)^3}.$$

The term $\cosh^{-1} G$ is dominant for $G \gg 1$; for values of G of the order unity, however, the contribution of the sum cannot be neglected.

In order to conclude this argument we point out that process (2), though having a smaller cross section than process (1), gives twice as much information for each experimental event. If one considers, together with the graph of Fig. 1, the one with p_2 and k_2 exchanged, each of the final protons can be considered as a «spectator particle» (in the Chew-Low sense). One then obtains two relations identical to (4), the one as a function of u^2 and Δ^2 and the other as a function of l^2 and s^2, where

$$(6') \qquad l^2 = -(k_2 + q_2)^2, \qquad s^2 = (p_2 - k_1)^2,$$

which span exactly the same phase space region as u^2 and Δ^2. These two relations, for fixed $u^2(l^2)$ and $\Delta^2(s^2) < \mu^2$ extrapolate to the same residue. One can therefore consider both cases together and experimentally make all the measurements of interest for both the final protons, collecting the results in the same diagram (7).

We shall now briefly outline a second argument, from which we shall show how it is possible, by starting from the above considerations, to draw some theoretical conclusions about the behaviour of the cross section (also in the physical region, far from the extrapolation value). It seems likely that due to the presence of the resonant vertex in the graph of Fig. 1 as well as in the other 3 graphs, which are obtained from it by exchanging the momenta of initial and final nucleons, these graphs with the exchange of one pion only should give the dominant contribution, whereas graphs with the exchange of more particles may be neglected. This of course will only be true if u is not too far from the resonance value. Calling $\langle T \rangle$ the total matrix element obtained from the graphs of this type, the most general expression for the cross section is the following

$$(7) \quad \mathrm{d}^4\sigma = \frac{2\pi}{q_{1.}M}\,|\langle T\rangle|^2 \delta(p_1 + k_1 - p_2 - k_2 - q_2) \cdot$$
$$\cdot \delta(k_2^2 + M^2)\,\delta(p_2^2 + M^2)\,\delta(q_2^2 + \mu^2)\,\mathrm{d}^4k_2\,\mathrm{d}^4p_2\,\mathrm{d}^4q_2\,.$$

(7) This does not apply to process (1) (apart from obvious experimental difficulties) since, by the exchange of p_2 and k_2, f^2 and σ_2 (and therefore the value of the residue) are altered.

From this formula all the expressions of interest can be deduced with convenient integrations (*e.g.* to get $d^2\sigma/d\Delta^2 du^2$ one has to integrate over d^4p_2, d^4q_2: cfr. [1]). Further integration over u^2 gives the energy spectrum of the final proton). The region where this calculation should be more reliable is for T between 600 and 1100 MeV, where the interval of variation of u includes the peak of the 33-resonance without extending too far beyond. Calculations are rather complicated, and are being carried out. Final state interactions between nucleons can be neglected at these energies, or considered in $\langle T \rangle$ as a small correction.

* * *

We thank Prof. M. CINI for his suggestions and his constant advice, Dr. G. JONA-LASINIO and Dr. H. MUNCZEK for help in calculations, and Dr. F. SELLERI for valuable discussion.

IL NUOVO CIMENTO Vol. XIII, N. 6 16 Settembre 1959

On the Gürsey Baryon Equation.

V. Amar and M. Pauri

Istituto di Scienze Fisiche dell'Università - Milano
Istituto Nazionale di Fisica Nucleare - Sezione di Milano

(ricevuto il 28 Luglio 1959)

Two years ago, Gürsey [1] derived an eight-component spinor equation which displays, quite expressively, some relations between charge independence, baryon conservation, and the Pauli [2] transformation.

Gürsey interpreted the two spinors composing the eight-component spinor, as describing proton and neutron and studied the free case and the interaction with π-mesons.

However, it is possible to introduce also in Gürsey's scheme an external electromagnetic interaction.

Two independent types of electromagnetic interactions related to a different interpretation of the eight-component spinor, have been studied in a recent paper by Dallaporta and Toyoda [3]. Their procedure is connected with the concepts of « boson » and « spinor conjugation » already introduced by Budini, Dallaporta and Fonda [4] but this development requires putting aside the connection between the ordinary isotopic space and the symmetries of the Gürsey equation.

More exactly, this requirement is partly related to the different choice made by the above mentioned authors as regards the Gürsey transformation (4), and, in particular, to the fact that a pair of charged baryons (with equal or opposite sign of the charge) is obtained with each of the two types of interactions; in such a way that the Pauli transformation is no longer related to isotopic rotations.

It is easy to show that an electromagnetic interaction can be inserted in the Gürsey equation without losing the nucleon interpretation and the symmetries which naturally deal with it; furthermore, if one remains within the limits of the doublet-approximation [5], it is possible to describe all the baryons making use of Gürsey's formalism.

---

(1) F. Gürsey: *Nuovo Cimento*, **7**, 411 (1958).
(2) W. Pauli: *Nuovo Cimento*, **6**, 204 (1957).
(3) N. Dallaporta and T. Toyoda: *Nuovo Cimento*, **12**, 593 (1959).
(4) P. Budini, N. Dallaporta and L. Fonda: *Nuovo Cimento*, **9**, 316 (1958).
(5) M. Gell-Mann: *Phys. Rev.*, **106**, 1296 (1957); A. Pais: *Phys. Rev.*, **110**, 574 (1958).

An external electromagnetic interaction must be such as to maintain the equation reducible and to make it invariant, not with respect to the Pauli full group, but — so far as the isotopic spin is concerned — only with respect to the transformations corresponding to rotations around the third axis.

We shall write the Gürsey equation in the form:

$$\{\Gamma^\mu \partial_\mu - im\Gamma_5\}\Omega = 0\,, \tag{1}$$

where

$$\Omega = \begin{pmatrix}\zeta\\ \chi\end{pmatrix}, \qquad \Gamma^\mu = \begin{pmatrix}0 & \gamma^\mu\\ \gamma^\mu & 0\end{pmatrix}, \qquad \Gamma_5 = \begin{pmatrix}-\gamma_5 & 0\\ 0 & \gamma_5\end{pmatrix},$$

and the representation of the Dirac matrices is assumed to be as follows

$$\gamma_0 = \begin{pmatrix}0 & I\\ I & 0\end{pmatrix}, \qquad \gamma^k = \begin{pmatrix}0 & -\sigma^k\\ \sigma^k & 0\end{pmatrix}, \qquad \gamma_5 = \begin{pmatrix}I & 0\\ 0 & -I\end{pmatrix}.$$

We, then, may write the following, as equation with the electromagnetic coupling:

$$\left\{\Gamma^\mu\left[\partial_\mu - \frac{ieA_\mu}{2}(1+\Gamma_5)\right] - im\Gamma_5\right\}\Omega = 0\,, \tag{2}$$

which is obviously reducible, due to the commutability of Γ^μ and Γ_5.

Equation (2), explicitly written, is:

$$\begin{cases} \gamma^\mu\partial_\mu\zeta - \dfrac{ieA_\mu}{2}(1+\gamma_5)\gamma^\mu\zeta = +im\gamma_5\chi\,, \\ \gamma^\mu\partial_\mu\chi - \dfrac{ieA_\mu}{2}(1-\gamma_5)\gamma^\mu\chi = -im\gamma_5\zeta\,, \end{cases} \tag{3}$$

and, after reduction through the following transformation [3]:

$$\begin{pmatrix}\psi\\ \tilde{\psi}\end{pmatrix} = T\begin{pmatrix}\zeta\\ \chi\end{pmatrix} = \begin{pmatrix}\beta & \alpha\\ \alpha & -\beta\end{pmatrix}\begin{pmatrix}\zeta\\ \chi\end{pmatrix}; \qquad \left(\alpha = \frac{1+\gamma_5}{2}\,,\ \beta = \frac{1-\gamma_5}{2}\right), \tag{4}$$

where ψ and $\tilde{\psi}$ mean respectively ψ_p and $-i\psi_n^c$ (Gürsey choice), it appears in the natural form:

$$\begin{cases} [\gamma^\mu(\partial_\mu - ieA_\mu) - im]\psi_p = 0\,, \\ [\gamma^\mu\partial_\mu - im]\psi_n = 0\,. \end{cases} \tag{5}$$

In terms of « wave matrices » (*) equation (3) becomes

$$(6)\qquad \begin{cases} D\bar{Z}^{+} - \dfrac{ieA_\mu}{2}\hat{\sigma}_\mu \bar{Z}^{+}(1+\sigma_3) = \quad imX \\ D\bar{X}^{+} - \dfrac{ieA_\mu}{2}\hat{\sigma}_\mu \bar{X}^{+}(\sigma_3 - 1) = -imZ\,, \end{cases}$$

where:

$$D = \partial_0 - \boldsymbol{\sigma}\cdot\boldsymbol{\nabla}\,, \qquad \hat{\sigma}_\mu = (I, -\boldsymbol{\sigma})\,,$$

and the correspondence $\zeta \to Z$, $\chi \to X$ between four-spinors and « wave matrices » is assumed.

With the form (6) of the equation all the required invariances may be easily verified.

a) The invariance under

$$(7)\qquad \begin{cases} Z \to Z' = ZU = Z\exp[i\lambda]\,, \\ X \to X' = \bar{X}^{+}U = X\exp[-i\lambda]\,, \end{cases}$$

(Touschek transformation [6] on χ and ζ) is connected with the baryon number gauge transformation.

b) The Pauli transformation in terms of 2×2 matrices has a representation:

$$(8)\qquad \begin{cases} Z \to Z' = ZR \;\; = Z\exp[i\boldsymbol{\sigma}\cdot\boldsymbol{l}]\,, \\ X \to X' = X\bar{R}^{+} = X\exp[i\boldsymbol{\sigma}\cdot\boldsymbol{l}]\,. \end{cases}$$

As required, equation (6) is not invariant under the group (8), but it is still invariant under

$$(9)\qquad \begin{cases} Z \to Z' = ZR \;\; = Z\exp[i\sigma_3 l_3]\,, \\ X \to X' = X\bar{R}^{+} = X\exp[i\sigma_3 l_3]\,, \end{cases}$$

i.e. under rotations around the third isotopic axis.

(*) We assume with Gürsey the following correspondence between four-spinors and « wave matrices »

$$\psi = \begin{pmatrix} \psi_1 \\ \psi_2 \\ \psi_3 \\ \psi_4 \end{pmatrix} \to \Psi = \begin{pmatrix} \psi_1 & -\psi_4^{*} \\ \psi_2 & \psi_3^{*} \end{pmatrix},$$

and we define:

$$\bar{\Psi} = \Psi^{-1}\,\mathrm{Det}\,(\Psi)\,.$$

(6) B. F. Touschek: *Nuovo Cimento*, **5**, 1281 (1957).

c) In particular (6) is invariant under the transformation

$$(10) \qquad \begin{cases} Z \to Z' = Z\hat{S} \;\; = Z \exp\left[\dfrac{i}{2}(1+\sigma_3)\alpha\right], \\ X \to X' = X\bar{S}^{+} = X \exp\left[-\dfrac{i}{2}(1-\sigma_3)\alpha\right]. \end{cases}$$

which is a combination of (7) and (9) (see Nishijima transformation [7]) and is connected with charge conservation.

Finally, we point out that from (6), solving with respect to Z and X, one obtains a pair of second order, two-component relativistic wave equations connected with two possible choices (even or odd components) which correspond, in the baryon case, to the similar possibilities for the iterated Dirac equation as studied by Feynmann and Gell-Mann [8].

The X equation is, for example, as follows

$$\{[(\partial_\mu - ieA_\mu)^2 - e\boldsymbol{\sigma}(\boldsymbol{B} - i\boldsymbol{E})] + m^2\} X \begin{pmatrix} \dfrac{1+\sigma_3}{2} \\ \end{pmatrix} + \{\partial_\mu^2 + m^2\} X \begin{pmatrix} \dfrac{1-\sigma_3}{2} \\ \end{pmatrix} = 0 .$$

All the previous remarks are still valid not only for the (p, n) doublet, but also for (Σ^+, Y_0) and, after a suitable change of sign in (2), for (Z^0, Σ^-) and (Ξ^0, Ξ^-).

In a further note we shall treat the case of non-reducible equations related to π, and eventually K-meson interactions.

* * *

We wish to express our thanks to Prof. L. M. Brown and Prof. P. Caldirola for their kind interest and especially to Prof. F. Duimio for the very useful discussions and suggestions.

---

(7) K. Nishijima: *Nuovo Cimento*, **5**, 1349 (1957).

(8) H. A. Kramers: *Vesh. Zeeman Jubil.*, 403 (1935); R. P. Feynmann and M. Gell-Mann: *Phys. Rev.*, **109**, 193 (1958); L. M. Brown: *Phys. Rev.*, **111**, 957 (1958).

IL NUOVO CIMENTO Vol. XIII. N. 6 16 Settembre 1959

Interactions of 1.15 GeV/c K^- Mesons in Emulsions.

Preliminary Results.

C. M. Garelli, B. Quassiati, L. Tallone and M. Vigone

Istituto di Fisica dell'Università - Torino
Istituto Nazionale di Fisica Nucleare - Sezione di Torino

(ricevuto il 1° Agosto 1959)

We want here expose the results of a preliminary scanning of a large stack of G-5 emulsions, exposed to the 1.15 GeV/c K^- beam at the Berkeley bevatron. This beam has been developed by Good and Ticho [1] and the average composition is expected to be: 1.5 K^-; 4.5 μ^-; 0.2 π^-. The actual composition during our exposure is not known at present and probably the ratio π^-/K^- is higher than the quoted value. We hope to be able to check this ratio in the near future.

A total of 400 interactions have been studied till now. Hundred of these have been found by track following, the remaining ones by area scanning. The first method of scanning gives unbiased results, the second one can give a loss of small stars. Actually, this is not the case, as proved by the mean number of prongs per star that results to be:

5.6 ± 0.6 in the stars found by track following;

6.2 ± 0.4 in the stars found by area scanning.

(1) L. W. Alvarez, Ph. Eberhard, M. L. Good, W. Graziano, H. K. Ticho and S. G. Wojcicki: *Phys. Rev. Lett.*, **2**, 215 (1959).

In the 400 stars, all the prongs with ionization $\geqslant 1.5$ the minimum, have been followed until they came to rest, or interacted, or decayed, or left the stack. The results are the following:

stable prongs	2223
π^- mesons	22
π^+ mesons	8
K^- re-emitted	6
hyperfragments . . .	5
charged Σ hyperons .	40

Among the 2223 stable prongs we include 11 stops in flight, 19 interacting tracks and 49 tracks leaving the stack. On the tracks that did not come to rest, measurements were performed every time the geometrical conditions were suitable, and the analysis ruled out the possibility that they can be π or K mesons.

The 6 K^- re-emitted have kinetic energy lower that 20 MeV, and give a capture star at rest.

One of the 5 hyperfragments undergoes a mesonic decay; the emitted meson is a π^- of 30 MeV kinetic energy.

The total number of charged Σ hyperons observed among the prongs of the 400 stars is 40. Of these, 18 are certainly

Σ^- (14 giving stars at rest and 4 decaying in flight in a π^- that comes to rest in the emulsion); 7 are certainly Σ^+ (3 cases of $\Sigma^+ \to p + \pi^0$ decaying at rest, 3 cases of $\Sigma^+ \to p + \pi^0$ decaying in flight and 1 case of $\Sigma^+ \to n + \pi^+$ decaying at rest). In the remaining 15 cases it is not possible to determine the charge of the hyperon because the decay product is a $\pi^\pm$ that leaves the stack (13 cases) or because the hyperon interacts in flight (2 cases). One of the Σ's interacting in flight produces a star from which an hyperfragment is emitted. The absorption stars of the Σ^- captured at rest have two or more prongs.

We looked very carefully for the double production of hyperons, and we found one star that probably is an example of this phenomenon. One prong of the star is certainly a Σ^- captured at rest; an other prong can be interpreted as a Σ^+. The kinematics of the event is compatible with the decay $\Sigma^+ \to p + \pi^0$, although we cannot exclude the inelastic scattering of a proton. This event could therefore give an indication for the reaction:

$$K^- + n + p \to \Sigma^+ + \Sigma^- + K^0 .$$

In the 400 analysed stars a total of 181 relativistic prongs have been observed; their distribution is the following:

no. of stars with one relativistic prong . . .	139
no. of stars with two relativistic prongs . . .	20

At present, 50 relativistic tracks have been followed through the stack. Only one of these tracks came to rest, and gave a $\pi \to \mu \to e$ decay; among the other tracks we could recognize 2 K mesons interacting in flight and 18 $\pi^\pm$ mesons. A more detailed analysis is in progress.

Although the statistics now available is poor, we can give a rough evaluation of the percentage of the charged Σ hyperons. The 40 cases reported here, represent only a part of the Σ hyperons actually emitted because of the scanning and geometrical losses. Correcting only for the greatest bias, arising from the fact that we detect only those Σ^- absorptions at rest which have two or more prongs, the number of charged hyperons rises to 70. The corrections have been made using the same criteria of EISENBERG *et al.* ([2]).

Moreover the number of analysed stars (400) has to be corrected according to the value of the ratio π^-/K^- of the beam. This value is not exactly known, but it is at least the one given by ALVAREZ *et al.* ([1]), *i.e.* $\pi^-/K^- = 0.2/1.5$. We can say that the maximum number of observed stars produced by K^- mesons is 350. Therefore the percentage of charged hyperons produced by 1.15 GeV/c K^- mesons is probably higher than 20%.

* * *

We are very grateful to Prof. E. J. LOFGREN, Dr. W. WENZEL, Dr. P. EBERHARD, Dr. M. L. GOOD, Dr. H. K. TICHO for having permitted the use of the magnetically focused K^--beam and for excel- support and co-operation.

We are very indebted to Prof. G. GOLDHABER and S. GOLDHABER for the generous help and valuable advices during the exposure and for having put at our disposal their processing equipment.

Our thanks are also due to Prof. BARKAS and his co-workers for having sent us their preliminary results on this subject. (*Interactions of* 1.15 GeV/c K^- *mesons in emulsions*: W. H. BARKAS, N. N. BISWAS, D. A. DE LISE, J. N. DYER, H. H. HECKMAN and F. M. SMITH (preprint)).

([2]) Y. EISEMBERG, W. KOCH, E. LOHRMANN, M. NICOLIC, M. SCHEEBERGER and H. WINZELER: *Nuovo Cimento*, **9**, 745 (1958).

IL NUOVO CIMENTO Vol. XIII, N. 6 16 Settembre 1959

Measurement of the Refractive Index of a Plasma in the Optical Region.

U. Ascoli-Bartoli (*) and F. Rasetti (**)

Laboratorio Gas Ionizzati del C.N.R.N. - Roma

(ricevuto il 3 Agosto 1959)

The refractive index of an electron gas in the optical region is expected to be accurately represented by the classical dispersion formula:

$$(1) \qquad n - 1 = -\frac{2\pi N_e e^2}{m\omega^2},$$

where N is the electron density and the other symbols have the usual meaning.

For the noble gases in the visible region, $n - 1$ is positive and considerably smaller in magnitude than for free electrons, owing to the short wavelength (Schumann region) of the absorption lines. For example, for argon of density N_a at the wavelength of the green mercury line λ 5460, $n - 1 = +1.05 \cdot 10^{-23} N_a$ whereas for free electrons, $n - 1 = -1.3 \cdot 10^{-22} N_e$. These circumstances suggest the possibility of measuring the electron density in a plasma by observing a decrease in refractive index when the gas is electrically excited. Of course, the application of this principle is well known in the radiofrequency and microwave regions.

This preliminary note describes the effects observed on an argon plasma excited by a radiofrequency field.

Light from a high-pressure mercury arc formed interference fringes through a Jamin interferometer giving a 2 cm separation between the beams. The fringes were focused on the wide slit of a small spectrograph. In the spectrum the fringe systems due to the single Hg lines appeared well separated. One of the beams (the strong one, reflected by the back surface of the first interferometer plate) passed through the discharge tube, the other through an open, air-filled tube whose function was to prevent strong thermal convection currents being formed in the vicinity of the heated discharge tube. A better solution would be to evacuate this side tube; however, we had no time yet to overcome the slight technical difficulties connected with this procedure. The fringe shift due to the refractive index difference between the low-pressure argon in the discharge tube and the air at atmospheric pressure in the side tube was compensated by adjusting the interferometer plates, so that fringes of orders near zero appeared through the spectrum. An interference filter was usually employed to eliminate light of unwanted wavelenghts.

(*) Istituto Sperimentale delle Ferrovie dello Stato, Roma.

(**) Johns Hopkins University, Baltimore, Maryland.

The tubes were made of Pyrex glass or fused quartz of 20 to 30 mm diameter and 30 cm length. The tubes were closed at both ends with optical glass plates cemented with silver chloride. The plates extended beyond the tube on one side to cover both interfering beams. The tubes were evacuated by a diffusion pump, degassed, filled with argon at the desired pressure (of the order of one Tor), and sealed off through a short, narrow side tube. It was important to use a tube of uniform diameter with but little « dead » volume, since otherwise the expected effect (a decrease in refractive index) might be simulated by a density decrease of the gas due to heating by the discharge. In a cylindrical tube no such effect exists regardless of the longitudinal density distribution.

To minimize and practically eliminate the bothersome overlapping of the strong light from the discharge with the fringe system, a lens focused an image of the mercury arc source (covered by a diaphragm with a 3 mm circular aperture) on the collimator lens of the spectrometer. The aperture of the collimator was made wide enough to pass this image, thereby reducing by a factor of about 100 the parasitic light from the plasma. The resolving power of the spectrograph was thereby decreased, still being amply sufficient for the purpose.

In order to measure small fringe shifts, a quartz fiber was placed across the slit, so that its image would appear as a dark streak parallel to the fringes and serve as a reference line.

The discharge was excited by placing the tube coaxially with a coil of 8 cm diameter and 20 cm length, consisting of 6 turns of wire and operated by a 20 MHz oscillator. The R.F. source consists of a self-excited oscillator employing a pair of 450TH tubes in push-pull. At an anode potential of 3000 V the circuit delivers about 1 kW R.F. power output.

Feeding of R.F. power to the discharge tube was carefully checked and several different coupling circuits were tried, the most successful being the one described by MINNHAGEN and STIGMARK [1]. The R.F. power delivered with this coupling was estimated to be about 1 kW.

Visual observations effected by alternately turning the discharge on and off for short periods, of less than a second, showed a small but clearly observable fringe shift in the proper direction. The shift appeared and disappeared instantaneously with the discharge, within the resolving time of the eye of about 1/10 s, thus enabling one to distinguish the effect unambiguously from the slow, continuous drift that set in soon after beginning the operation of the discharge tube. The drift, in the opposite direction of that of the discharge effect, is due to heating of the side tube and consequent density decrease of the air contained therein.

To perform quantitative measurements, the following procedure was adopted. The fringe system was adjusted so that the reference line fell in the center of an intensity maximum and was observed to be stable. A photograph with a $\frac{1}{2}$ second to 1 second exposure was taken, with the discharge off. About 2 seconds later, a similar exposure, was taken by simultaneously turning on the discharge. Visual observations had shown that no appreciable drift of the fringes sets in during the first few seconds of operation. The tubes were allowed to attain room temperature before taking the next pair of exposures. The fringe shift between the two exposures of each pair was measured by scanning the plates under a Hilger microphotometer and recording the abscissae of the fringe positions at half-maximum transmission. Shifts several times smaller than those observed could have been measured.

---

[1] L. MINNHAGEN and L. STIGMARK: *Ark. f. Fys.*, **8**, 481 (1954).

The appearance of the discharge was found to be sensitive to small changes in radiofrequency excitation. Sometimes the plasma appeared strongly luminous and was mainly confined to the portion of the tube surrounded by the coil; at other times the luminosity, though less intense, extended through most of the length of the tube. The latter type of discharge predominated at lower pressures. The preliminary measurements here reported were performed with a quartz tube 20 mm in diameter and 32 cm in length filled at 0.5 Tor pressure (measured at room temperature). With this tube, the fringe shifts observed ranged from -0.03 to -0.06 fringes, the higher values obtaining when the discharge took the more luminous, concentrated aspect.

Fig. 1 shows the aspect of a pair of photographs. To evaluate the elctron density, we note that the fringe shift expressed in number of fringes is:

$$s = (n-1)\,L/\lambda\,, \tag{2}$$

where L is the length of the gas column. Assuming (incorrectly) uniform conditions throughout the length of the tube, we find that to $s = -0.06$ corresponds $n-1 = -1.03\cdot10^{-7}$ which, according to (1), yields an electron density $N_e = 7.6\cdot10^{14}$. If, as it is more likely, the dense electron gas occupies about half the length of the tube, the electron density in this region is twice as large.

We may express the result in another manner which is independent of the longitudinal electron density distribution. When the tube is uniformly filled the density of argon atoms is $N_a = 1.8\cdot10^{16}$, hence we can state that 4.2 percent of the argon atoms had been ionized. This conclusion rests on the assumption that the refractivities of argon ions and atoms are the same, which certainly is not true; however, the result is insensitive to the small differences to be expected, owing to the large effect of an electron compared with a neutral atom and certainly also with an ion. The total argon in the tube produces a fringe shift $s = +0.11$ and hence the ionized fraction a much smaller one.

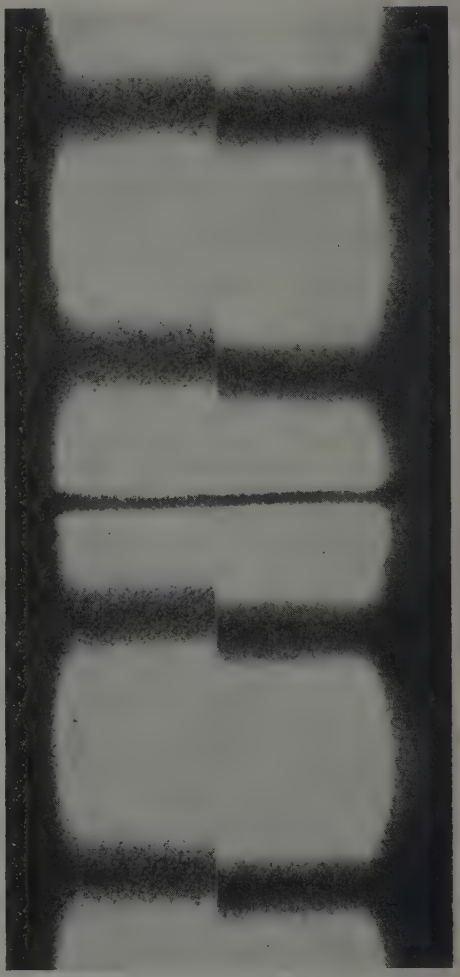

Fig. 1. – Fringes of the green mercury line with the discharge off (left) and on (right). The reference line was brought to concidence in the two photographs. The shift is -0.06 fringes. Magnified $\times 18$.

We can exclude the possibility that we are observing a spurious effect due to thermal expansion of the quartz tube during the discharge with consequent

shortening of the air path on the interfering beam. While this effect would produce a fringe shift in the same direction as observed, it would show an appreciable time lag and would appear in greatly different magnitudes for Pyrex and quartz tubes, whereas we observed essentially identical shifts in both cases. Furthermore, from the small expansion coefficient of fused quartz, one may evaluate that improbably large temperature changes in short times would be required to produce the observed shifts.

It thus appears that the observed decrease in refractive index can only be attributed to the free electrons, unless it be due to the anomalous dispersion connected with a transition starting from some excited state of argon. This alternative interpretation seems unlikely, especially in view of the fact that preliminary observations on the yellow mercury lines showed effects of the same sign and order of magnitude as those measured on the green line. The presence of properly placed absorption lines of excited argon to produce a decrease of the refractive index for both mercury lines is highly improbable. Nevertheless, it is planned to check the predicted wavelength dependence over an extended spectral region to determine with absolute certainty that the effects are due to free electrons. Also studies on other gases at various pressures and excitation frequency are in project.

Observations on the free electron refractive index in shock waves were recently reported by ALPHER and WHITE[2]. However, to our knowledge no similar measurements on electrically excited plasmas have been published.

The present method of determining electron densities seems to afford a valuable tool in plasma studies, as it gives absolute electron densities on the basis of a simple theory, and the measurements do not affect the plasma. Furthermore, the method is unaffected by the strong electric and magnetic fields in which the plasma is often produced. The main shortcoming is the low sensitivity, requiring high electron densities and thick plasma layers for accurate measurements. It will be advantageous to use the method in the extreme red or near infrared, on account of the decrease of $n - 1$ proportional to λ^2 and of the lesser sensitivity of the fringes to the quality of the optical medium and to various disturbances in the longer wavelength region.

* * *

We are greatly indebted to Dr. A. DE ANGELIS and Mr. S. MARTELLUCCI for valuable help rendered during this investigation. One of us (F. RASETTI) is also indebted to the John Simon Guggenheim Memorial Foundation for a fellowship.

---

(2) R. A. ALPHER and D. R. WHITE: *Phys. Fluids*, **2**, 162 (1959).

IL NUOVO CIMENTO Vol. XIII, N. 6 16 Settembre 1959

Preliminary Remarks on a Consequence of the Two-Centers Model of Multiple Meson Production.

V. Petržílka

Faculty of Technical and Nuclear Physics of Charles University - Praha

(ricevuto il 12 Agosto 1959)

H. W. Meier shows in his paper (1) that it is not necessary to fulfil the equations for γ_1 and γ_2

$$\gamma_1 = \bar{\gamma}\gamma_c + \sqrt{\bar{\gamma}^2 - 1}\sqrt{\gamma_c^2 - 1}\cos\bar{\Theta}\,, \tag{1}$$

$$\gamma_2 = \bar{\gamma}\gamma_c - \sqrt{\bar{\gamma}^2 - 1}\sqrt{\gamma_c^2 - 1}\cos\bar{\Theta}\,, \tag{2}$$

in the two-center model by putting $\bar{\Theta}_1 = \bar{\Theta}_2 = \bar{\Theta} = 0$ and by calculating $\gamma_c = \sqrt{\gamma_1\gamma_2}$, as it was done in papers (2) and (3), but that it is possible to obtain Θ by determining the value for γ_c on a basis of the isobar model and by estimating the value of γ_1 and γ_2 for the narrow and diffuse cone of secondary particles.

The present preliminary report will mention the fact, that it is possible to determine the values of $\bar{\Theta}$ and $\bar{\gamma}$ from the equations (1) and (2) by using for the evaluation of γ_c, γ_1 and γ_2 the relations given in the paper (4). By the application of this procedure the $\bar{\Theta}$ and $\bar{\gamma}$ in the C.M.S. and the corresponding angles ϑ_1 and ϑ_2 in the L.S. were calculated for jets Be 2 (5) and P 27 (4), which are used as an example in the paper of H. W. Meier (1). Our results for these two jets together with the results for other two jets P 61 and P 115 (4,6,7), obtained in the same way, are given in the following Table I.

---

(1) H. W. Meier: *Nuovo Cimento*, **11**, 307 (1959).

(2) P. Ciok, T. Coghen, J. Gierula, R. Hołyński, A. Jurak, M. Mięsowicz and T. Saniewska: *Nuovo Cimento*, **10**, 741 (1958).

(3) G. Cocconi: *Phys. Rev.*, **111**, 1699 (1958), and preprint.

(4) V. Petržílka: *Nuovo Cimento*, **10**, 490 (1958).

(5) G. Bozoki, F. Domokos, E. Fenyves, E. Gombosi, K. Lanius and H. W. Meier: *Padua-Venice Conference* (1957), Report XIII-20.

(6) P. Ciok, M. Danysz, J. Gierula, A. Jurak, M. Mięsowicz and J. Pernegr: *Nuovo Cimento*, **6**, 1409 (1957).

(7) J. Pernegr, V. Petržílka and J. Vrána: *Czechosl. Journ. Phys.*, **8**, 137 (1958).

TABLE I.

Jet no.	γ_1	γ_2	γ_0	$\bar{\gamma}$	$\bar{\Theta}=\bar{\Theta}_1=\bar{\Theta}_2$	ϑ_1	ϑ_2	$\vartheta_1+\vartheta_2$
P 115	2875	65.2	309	4.76	17° 50′	0° 2′	0° 49′	0° 51′
P 27	164	14.5	33.4	3.20	23° 5′	0° 5′	7° 8′	7° 13′
Be 2	236	6.0	20.3	5.97	16° 3′	0° 23′	13° 56′	14° 19′
P 61	25.9	5.81	8.41	1.89	51° 10′	2° 57′	9° 40′	12° 37′

The values obtained by this procedure for $\vartheta_1+\vartheta_2$ do not differ essentially from those determined by H. W. MEIER. However, they show quite clearly, that it is not possible to make the supposition that $\bar{\Theta}=0$.

IL NUOVO CIMENTO Vol. XIII, N. 6 16 Settembre 1959

On Large Angle Pair Production and the Limits of Validity of Electrodynamics.

G. Poiani and I. Reina

Istituto di Fisica dell'Università - Trieste
Istituto Nazionale di Fisica Nucleare - Sottosezione di Trieste

(ricevuto il 13 Agosto 1959)

It is known [1] that information on the limits of validity of electrodynamics can be obtained by measuring the cross-section for large angle pair creation by photons in the field of the proton. In the methods mentioned above the charge distribution of the proton had to be deduced from electron elastic scattering experiments.

In this note we want to point out that by comparing the results of experiments in different kinematic situations one could both lower considerably the uncertainty coming from the non perfectly known charge distribution of the target proton and increase the effect of an eventual breakdown of electrodynamics at small distances.

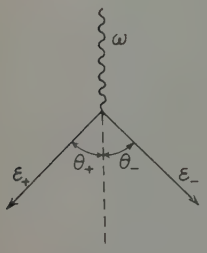

Fig. 1.

In fact let

$$\mathrm{d}\sigma_{\mathrm{L}} = |F(q^2)|\,\sigma'_{\mathrm{L}}(\omega, \varepsilon_+, \varepsilon_-, \theta_+, \theta_-, \varphi)\,\mathrm{d}\varepsilon_+\,\mathrm{d}\Omega_+\,\mathrm{d}\Omega_-\,,$$

be the pair production cross-section (in the first Born approximation) for local electrodynamics, where $F(q^2)$ represents the proton form factor and the other symbols have the usual meaning [1].

Let also

$$\mathrm{d}\sigma_{\mathrm{NL}} = |F(q^2)|\,\sigma'_{\mathrm{NL}}(\omega, \varepsilon_+, \varepsilon_-, \theta_+, \theta_-, \varphi, A, A', B, B')\,\mathrm{d}\varepsilon_+\,\mathrm{d}\Omega_+\,\mathrm{d}\Omega_-\,,$$

be the corresponding cross-section for non-local electrodynamics, where A, A', B, B', represent the electrodynamical vertex form factors.

One can easily show that for given ω, ε_+, φ and $|q|$ (transferred impulse) one obtains two (or one, in the limiting case) values of θ_- for every θ_+, compatible with momentum-energy conservation.

---

[1] P. Budini, G. Poiani and I. Reina: *Intern. Conf. on Mesons* (Padua-Venice, 1957), IX, 17 S. Drell: *Ann. Phys.*, **4**, 75 (1958); G. Poiani and I. Reina: *Nuovo Cimento*, **13**, 19 (1959).

Consider now the ratio

$$r(\theta_+, \theta_-) = \frac{\mathrm{d}\sigma_{\mathrm{NL}}}{\mathrm{d}\sigma_{\mathrm{L}}} = \frac{\mathrm{d}\sigma_{\mathrm{NL}}}{|F(q^2)|\,\sigma'_{\mathrm{L}}} = \frac{\sigma'_{\mathrm{NL}}(\omega, \varepsilon_+, \varepsilon_-, \theta_+, \theta_-, \varphi, A, A', B, B')}{\sigma'_{\mathrm{L}}(\omega, \varepsilon_+, \varepsilon_-, \theta_+, \theta_-)} ,$$

where ω, ε_+, φ, $|q|$ have been fixed. In this way the ratio depends only on θ_+ (or θ_-).

The value of r can be obtained by measuring experimentally $\mathrm{d}\sigma_{\mathrm{NL}}$, by calculating σ'_{L}, and by using the $F(q^2)$ values which can be deduced from the electron-proton scattering experiments [2]. The calculation of the pair production cross-section in a local theory, taking into account all the corrections, can be carried to a high accuracy [3], so that no difficulty arises in the evaluation of σ'_{L} for the determination of r. The values of the square form factor F^2 for the proton are known from the experiments of CHAMBERS and HOFSTADTER [4] with a good accuracy up to an energy of 550 MeV.

Suppose now to consider the same ratio corresponding to another value of the angles θ'_+, θ'_-, but obtained in such a way that the transferred impulse, $|q|$, be the same as above.

Then the ratio

$$R = \frac{r(\theta_+, \theta_-)}{r(\theta'_+, \theta'_-)} ,$$

depends only on measurable quantities and on the electrodynamic form factors. This means that by comparing the measured cross-sections at two values of θ_+, θ_- for which q^2 is the same, one does not need the knowledge of the target charge distribution to obtain information on the limit of validity of electrodynamics. In fact the value of R is obtained now from the expression

$$R = \frac{\mathrm{d}\sigma_{\mathrm{NL}}(\theta_+, \theta_-)}{\mathrm{d}\sigma_{\mathrm{NL}}(\theta'_+, \theta'_-)} \cdot \frac{\sigma'_{\mathrm{L}}(\theta'_+, \theta'_-)}{\sigma'_{\mathrm{L}}(\theta_+, \theta_-)} ,$$

that is, from the measurements of the pair production cross-section, $\mathrm{d}\sigma_{\mathrm{NL}}$, at two different angles, with $|q|$ constant, and from the calculation of the same cross-sections, σ'_{L}, with the local formalism. In this way the influence of the proton form factor for the evaluation of the electrodynamical effects is eliminated.

As an example we have calculated $r(\theta_+, \theta_-)$ for the plane case ($\varphi = \pi$), with the electrodynamical form factor used by DRELL, $\Lambda^{-1} = 7 \cdot 10^{-14} f$.

We have chosen

$$\omega = 1000 \text{ GeV}; \qquad \varepsilon_+ = \varepsilon_- \cong 500 \text{ MeV} \qquad |q| = \omega(1 - \cos\theta) ,$$

that is the q value corresponding to the pair emerging symmetrically at 30°.

---

(2) R. HOFSTADTER: *Ann. Rev. Nucl. Sc.*, **7**, 231 (1957).
(3) J. D. BJORKEN, S. D. DRELL and S. C. FRAUTSCHI: *Phys. Rev.*, **111**, 1409 (1958).
(4) E. E. CHAMBERS and R. HOFSTADTER: *Phys. Rev.*, **103**, 1354 (1956).

The curve reported in Fig. 2 gives the results obtained by plotting the values of $r(\theta_+, \theta_-)$ as a function of the angles θ_+. The corresponding values of θ_- are reported on the curve. The two values of θ_- that are obtained for every θ_+ are reprinted: the first on the solid line and the second on the dashed one. Then to each value

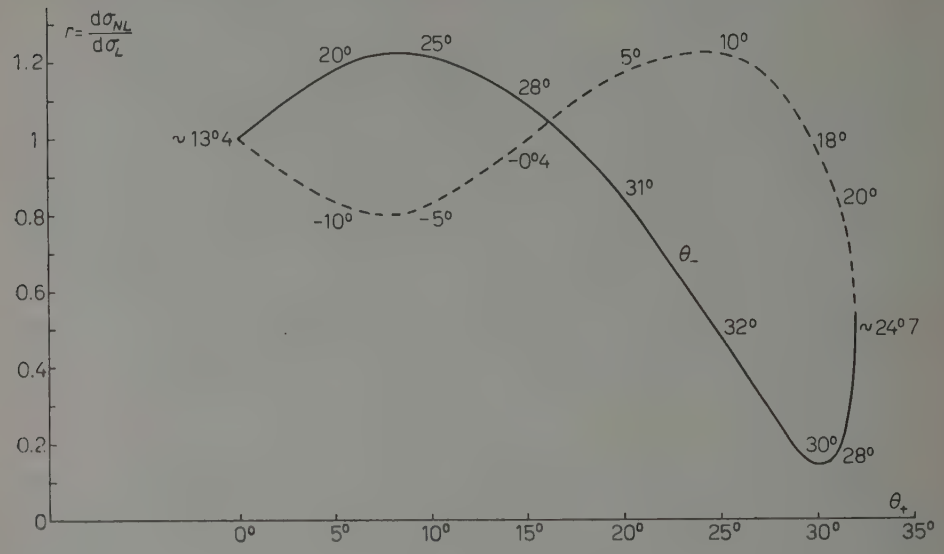

Fig. 2.

of θ_+ correspond two values of the ratio r. The negative θ_-'s, that are seen on the left side of the dashed line, indicate that both electron and positron are lying on the same side with respect of the direction of the incoming photon.

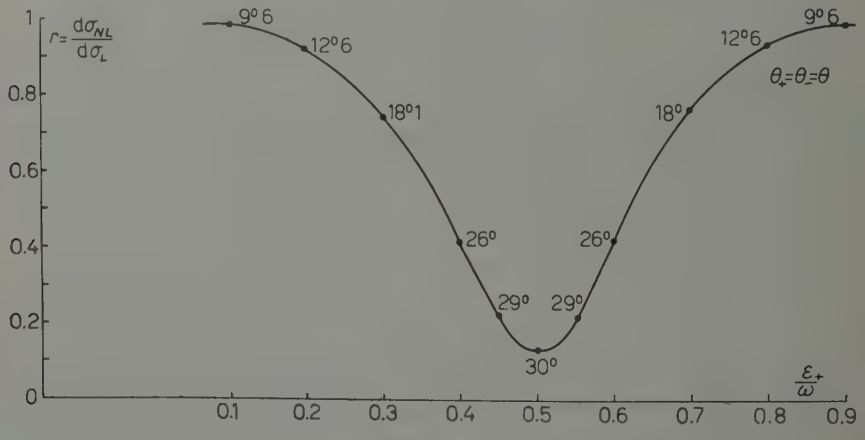

Fig. 3.

Due to interference effects of the two matrix elements contributing to the cross-section, the value of r may exceed one in some cases. This happens for instance

when $\theta_+ = 25°$ and $\theta_- = 10°$. In this way a more favorable situation for the evaluation of an eventual breakdown of electrodynamics is established, because the effect will be appreciably enhanced.

In the curve of Fig. 3 the values of r are plotted as a function of the fractional energy of the positron, when $|q|$ is maintained constant and equal to the value that it assumes when the pair is emerging symmetrically at 30°, and $\theta_+ = \theta_- = \theta$ throughout. Values of θ are reported on the curve.

Similar considerations can be extended also to bremsstrahlung.

* * *

Thanks are due to prof. P. BUDINI for helpful comments.

IL NUOVO CIMENTO Vol. XIII, N. 6 16 Settembre 1959

On the Radiation of Mesons with a Constant Transverse Momentum P_T in Cosmic Ray Jets (*).

G. YEKUTIELI

Department of Physics, The Weizmann Institute of Science - Rehovoth

(*Nuovo Cimento*, **13**, 646 (1959))

ERRATA CORRIGE

pag. 646, 2nd column:

5th line from top:

$n = \cos\varphi$ $1/n = \cos\varphi$.

5th line from bottom till the end of column:

In this case, we shall write

$$-4\pi\nu f(0) = k_T^2\,,$$

and

$$n^2 = 1 - \frac{k_T^2}{k^2} = \cos^2\varphi \quad \text{or} \quad p = \frac{P_T}{\sin\varphi}\,,$$

$(p = \hbar k)$;

In this case we shall write

$$4\pi\nu f(0) = k_T^2\,,$$

and for $k \gg k$

$$\frac{1}{n^2} = 1 - \frac{k_T^2}{k^2} = \cos^2\varphi \quad \text{or} \quad p = \frac{P_T}{\sin\varphi}\,,$$

$(p = \hbar k)$;

IL NUOVO CIMENTO

INDICI

DEL VOLUME XIII - SERIE X

1959

PRINTED IN ITALY